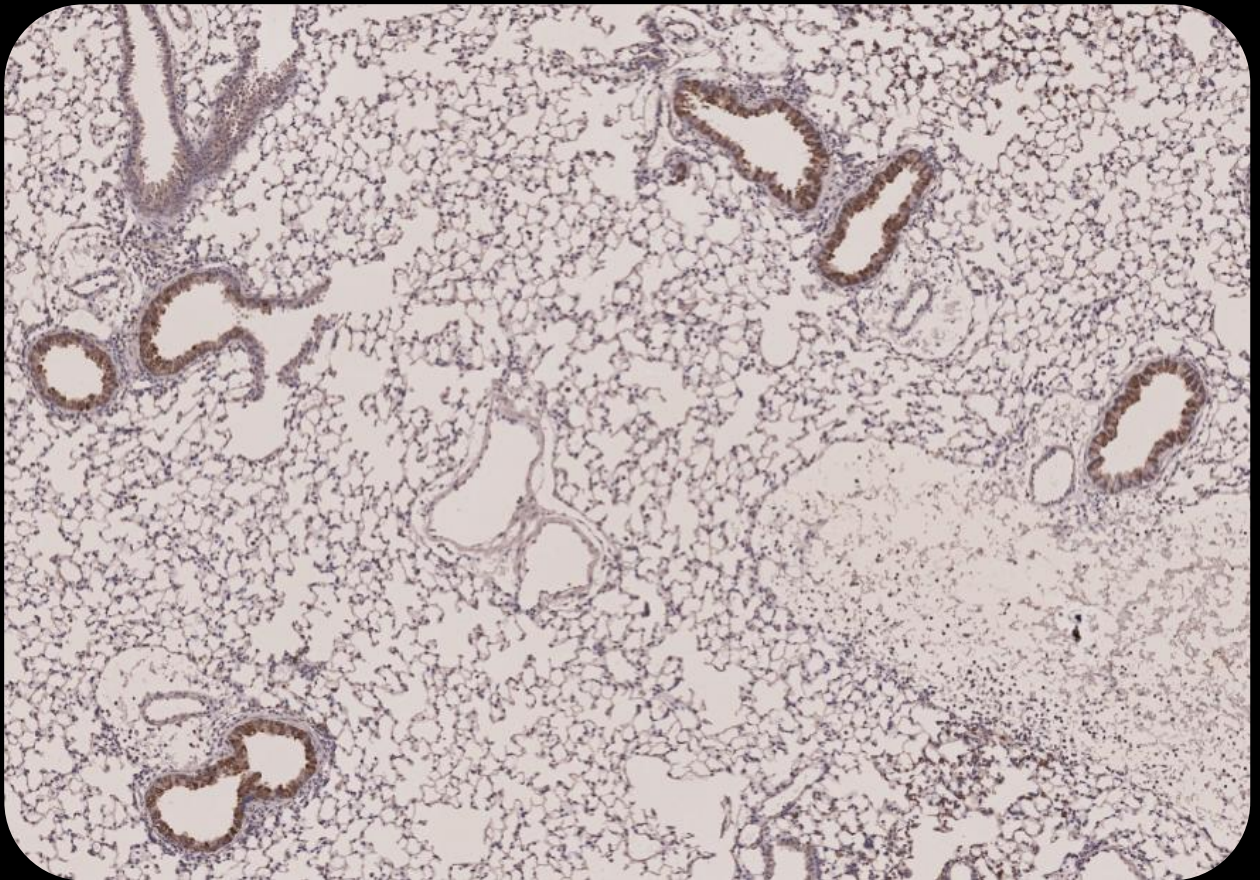


Interplay between DAF and viral proteins HA and NA modulates viral pathogenesis

Nuno Filipe Brito Pais dos Santos



Dissertation presented to obtain the Ph.D degree in Molecular Biosciences
Instituto de Tecnologia Química e Biológica António Xavier | Universidade Nova de Lisboa

Oeiras,
March, 2021




UNIVERSIDADE
NOVA
DE LISBOA

Interplay between DAF and viral proteins HA and NA modulates viral pathogenesis

Nuno Filipe Brito Pais dos Santos

Dissertation presented to obtain the Ph.D degree in Molecular Biosciences
Instituto de Tecnologia Química e Biológica António Xavier | Universidade Nova de Lisboa

Research work coordinated by:  INSTITUTO
GULBENKIAN
DE CIÊNCIA

Oeiras, March, 2021

Acknowledgements

“If you wanna take the hard road, you gotta cherish the ride”

Michael Wayne Atha

Experienced people usually tell you that a PhD is a demanding journey, full of obstacles to overcome. However, I had never imagined those obstacles might include a pandemic of a competing virus.

I have to start by acknowledging my mother who selflessly supported me in pursuing what I love to do.

Living with someone doing a PhD is an enormous challenge too. Thank you, Joana, for your huge patience and to keep me (kind of) sane throughout. And with a healthy smile.

I realized I loved research when I had the opportunity to do my Master's thesis with Carlos São-José and Sofia Fernandes. Your influence was truly life-changing.

I was extremely concerned about choosing the right PhD supervisor. Fortunately, Maria João was the best I could have asked for. I am deeply thankful for the opportunity to actually enjoy my PhD. I am grateful to have shared the lab with Ana Vinagre, Catarina C, Chris, Diogo, Daniela, Etibor, Joana P, João D, and the interns Bruna and Rahaf, all of you contributed to this journey. To the Postdocs Filipe, who deserved the MacGyver award, Marta, who does everything you do but better and faster and Sílvia, who is the ultimate perfectionist, thank you for your guidance. Finally, a special thank you to Zoé. It was a pleasure working with you and an honor finishing what you have started. You were an inspiration due to your resilience throughout and I cannot thank you enough for your precious time spent teaching me, and for your trust, kind words and advice.

I want to acknowledge my thesis committee, Mónica and Vera, for your availability to support me with whatever, and whenever needed.

Eduardo, Francisco and Hugo, when we first met in 2008, who would have imagined we would all become PhDs? Now it is the time to update the Whatsapp group. Cris, thank you for your constant examples of determination. Andreia, even 1000km away, you have been supporting me in every situation in my life. My Vimeiro/beach friends who have been around since the beginning: António, Ed, Fred, Freire, Gonçalo, Henrique, Heytor, Miguel, Rodrigo, Ruizinho and Vasco.

PGCD was one of the best things that happened to me. I want to thank Joana Sá, Patrícia, Carla, Inês, Leonor and all the volunteer teachers for materializing that. I want to acknowledge my colleagues: Cláudia, Danilo, Dete, Dizi, Hamilton, Hélio, Irina, Jacky, Kapitão, Joe, Valdir and Valéria. We are not together, but you still are an inspiration.

I am indebted to the IBB class of 2016 who adopted us: Abdul, Alba, Ana Catarina, Catarina, Chandra, Filipe, Gabri, Gonçalo, Rafael P and Sónia. I was lucky to meet the previous PGCD students Edison, Elves, Pâmela and Yara who set the bar really high. I also want to thank Alex, Andreia T, Diogo, Jernej, Mattia, Paulo NC, Renato and Vítor. I want to highlight the “invisible” work of João at Quarantine, the caretakers at the Animal House, Marta and Mariana at Flow cytometry, Andreia, Cláudia, Joana, Mafalda and Pedro at Histopathology, Ana Regalado at Antibodies, the PhD delegates, Élio, Jorge Carneiro and Ana Aranda. I also thank Gabriel Nuñez for the scientific input, and a renowned scientist for the motivational advice to “publish this it in a sh*tty journal and get rid of this project as soon as possible”.

I want to specially thank the #nonotioncrew: André, Catarina, Filipe, Gonçalo, Henrique, Luís, Yash and Rafael.

Finally, I want to pay tribute to AJ, BB, ES and MC, who were gone too soon and I was not there to say one last goodbye.

Table of contents

Acknowledgements	i
Table of contents	iii
List of figures	vii
List of tables	x
Abbreviations	xi
Summary	xviii
Título e resumo	xix
Chapter 1 – General introduction	1
1.1 Influenza A virus	2
1.1.1 The flu.....	2
1.1.2 Taxonomy.....	3
1.1.3 Structure and life cycle	4
1.1.4 Ecology.....	10
1.1.5 Antigenic drift and shift	11
1.1.6 HA.....	12
1.1.7 NA.....	14
1.1.8 Host restriction and HA/NA balance.....	16
1.2 Host defenses	18
1.2.1 The airways	18
1.2.2 Physical barrier.....	23
1.2.3 Interferon (IFN).....	26
1.2.4 Neutrophils	30
1.2.5 Monocytes and macrophages	32
1.2.6 NK cells	33
1.2.7 Eosinophils, $\gamma\delta$ T, MAIT, ILC and platelets	33
1.2.8 Adaptive immunity	36
1.2.9 Complement system.....	39
1.2.10 Complement decay-accelerating factor (DAF)	42
1.2.11 Sialic acid	45
1.3 Final remarks	46
1.4 Aims and general objectives	49
1.4.1 Aims and general objectives	49
1.4.2 Chapter 2 – Complement decay-accelerating factor increases immunopathology via complement activation and immune cell recruitment.....	50

1.4.3 Chapter 3 – Influenza A virus neuraminidase cleaves sialic acid from the complement decay-accelerating factor and activates complement	50
1.4.4 Chapter 4 – Mutation S110L of H1N1 influenza A virus hemagglutinin: a potent determinant of attenuation	51
1.4 References	52
Chapter 2 – Complement decay-accelerating factor increases immunopathology via complement activation and immune cell recruitment	84
2.1 Author contributions	85
2.2 Summary	86
2.3 Introduction	87
2.4 Results	95
2.4.1 DAF-induced immunopathology relies on elevated complement activation, immune cell recruitment and levels of IFN- γ	95
2.4.2 DAF-HA interaction modulates adaptive immune cell recruitment.	100
2.4.3 DAF-NA interaction modulates innate immune cell recruitment.	104
2.5 Discussion	110
2.6 Materials and methods	114
2.6.1 Statistical analyses	114
2.6.2 Ethics statement	114
2.6.3 Mice infection	115
2.6.4 Viral loads	115
2.6.5 Histology and Immunohistochemistry (IHC)	116
2.6.6 Bronchoalveolar lavage (BAL)	116
2.6.7 ELISA	117
2.6.8 Flow cytometry	117
2.6.9 Immune cell depletion	118
2.6.10 Primary mouse embryo fibroblasts (MEF) isolation	118
2.6.11 Primary mouse lung cells isolation	118
2.6.12 Cell culture	119
2.6.13 Influenza A virus strains	119
2.6.14 Reverse genetics	120
2.6.15 Virus titration by Plaque Assay	120
2.6.16 Infections	121
2.6.17 Complement-dependent cytotoxicity (CDC)	121
2.7 References	122
2.8 Acknowledgements	128
2.9 Supplementary material	129

Chapter 3 – Influenza A virus neuraminidase cleaves sialic acid from the complement decay-accelerating factor and activates complement	133
3.1 Author contributions.....	134
3.2 Summary.....	135
3.3 Introduction	136
3.4 Results	140
3.4.1 IAV decreases DAF molecular weight in the timecourse of infection.	140
3.4.2 NA removes DAF sialic acid, partially inside the cell.	142
3.4.3 NA removes DAF α 2,6-linked sialic acid and increases complement activation.	145
3.5 Discussion	152
3.6 Materials and methods.....	157
3.6.1 Statistical analyses	157
3.6.2 Ethics statement.....	157
3.6.3 Cell culture.....	157
3.6.4 Primary MEF isolation	158
3.6.5 Primary mouse lung cells isolation	158
3.6.6 Influenza A virus strains	159
3.6.7 Reverse genetics.....	160
3.6.8 Infections	160
3.6.9 Bacteria and cloning.....	160
3.6.10 Transfections	161
3.6.11 Lentivirus production	161
3.6.12 C5b-9 deposition	162
3.6.13 Complement-dependent cytotoxicity (CDC)	162
3.6.14 DAF glycosylation.....	163
3.6.15 Western blotting	164
3.6.16 Immunofluorescence	165
3.7 References.....	166
3.8 Acknowledgements.....	172
3.9 Supplementary material.....	173
Chapter 4 – Mutation S110L of H1N1 influenza A virus hemagglutinin: a potent determinant of attenuation.....	176
4.1 Author contributions.....	177
4.2 Summary.....	177
4.3 Introduction	179

4.4 Results	184
4.4.1 HA S110L induces lower lung histological damage than CAL	184
4.4.2 HA mut infection affects a lower proportion of lung epithelial cells and leukocytes.....	188
4.5 Discussion	191
4.6 Materials and methods.....	196
4.6.1 Statistical analyses	196
4.6.2 Ethics statement	196
4.6.3 Mice infection.....	196
4.6.4 Histology	196
4.6.5 Immunohistochemistry	197
4.6.6 Flow cytometry	198
4.6.7 Influenza A virus strains	198
4.7 References.....	200
4.8 Acknowledgements.....	204
4.9 Supplementary material.....	205
Chapter 5 – General discussion.....	208
5.1 General discussion	209
5.2 Future perspectives	218
5.3 References.....	220
5.4 Supplementary material.....	225

List of figures

Fig. 1.1 – Representation of IAV structure.	5
Fig. 1.2 – Summarized representation of IAV lifecycle.	10
Fig. 1.3 – HA structure and domains	13
Fig. 1.4 – NA structure and domains	15
Fig. 1.5 – Schematic representation of the respiratory tract.	20
Fig. 1.6 – Representation of immune cells involved in response to IAV infection.	22
Fig. 1.7 – Representation of airway mucosal barrier	24
Fig. 1.8 – Interferon (IFN) activation pathways and mechanisms of IAV evasion.	28
Fig. 1.9 – Components of the innate and adaptive immune system.	34
Fig. 1.10 – Adaptive immune response to IAV.	37
Fig. 1.11 – Simplified representation of complement pathway.	41
Fig. 1.12 – Regulators of complement activation	43
Fig. 1.13 – Sialic acid structure.	45
Fig. 1.14 – Representation of possible infection outcomes.	48
Fig. 1.15 – Objectives proposed for this thesis.	50
Fig. 2.1 – Complement decay-accelerating factor (DAF) aggravates IAV infection in vivo.	90
Fig. 2.2 – <i>Daf</i>^{-/-} mice are protected against PR8-HK4,6, but not PR8, and protection is specific of this RCA.	92
Fig. 2.3 – DAF does not affect viral replication, clearance, or tissue penetration, but is an immunopathology instigator.	93
Fig. 2.4 – <i>Daf</i>^{-/-} mice have reduced complement activation and recruitment of innate immune cells.	100
Fig. 2.5 – DAF interaction with HA worsens disease outcome, without increasing immunopathology.	102

Fig. 2.6 – Daf^{-/-} mice have reduced complement activation and T cell recruitment upon PR8-HK6 infection.....	104
Fig. 2.7 – DAF interaction with NA modulates immunopathology.	107
Fig. 2.8 – Daf^{-/-} mice present lower complement activation and neutrophil recruitment at 3 d.p.i. upon PR8-HK4 infection.	109
Fig. 2.9 – Proposed model for DAF as a virulence factor upon IAV infection.....	113
Fig. 2.10 – Experimental setup of mice infection.....	115
Fig. 2.S1 – NK cell depletion does not alter disease outcome....	129
Fig. 2.S2 – DAF does not affect replication of PR8, PR8-HK4,6, PR8-HK4 and PR8-HK6.....	130
Fig. 2.S3 – Representative flow cytometry gating strategy	131
Fig. 3.1 – Sialic acid structure.....	137
Fig. 3.2 – Influenza A virus sialic acid preference.	139
Fig. 3.3 – Influenza A virus decreases DAF molecular weight (MW) in the timecourse of the infection.....	142
Fig. 3.4 – Influenza A virus neuraminidase cleaves DAF through its sialidase activity.	143
Fig. 3.5 – Influenza A virus neuraminidase cleaves DAF partially inside the cell.....	145
Fig. 3.6 – NA removes α2,6-linked sialic acid from DAF O-glycans.	146
Fig. 3.7 – NA removes DAF α2,6-linked sialic acid and increases complement activation.	148
Fig. 3.8 – DAF protects from complement-dependent toxicity, but NA-mediated desialylation increases complement activation....	150
Fig. 3.9 – Proposed model for DAF-mediated immunopathology.	155
Fig. 3.10 – Summary of Chapters 2 and 3 contribution to viral pathogenesis.....	156
Fig. 3.S1 – vRNPs are not involved in DAF cleavage.	173
Fig. 3.S2 – Influenza A viruses with avian NA promptly adapt to cleave DAF.	174

Fig. 4.1 – HA S110L mutation increases neutralization, but does not affect glycosylation and acid stability	181
Fig. 4.2 – HA S110L mutation does not affect cell entry nor replication	182
Fig. 4.3 – HA S110L confers protection from infection in vivo ...	183
Fig. 4.4 – HA S110L mutation decreases lung histological damage	185
Fig. 4.5 – HA S110L mutation decreases NP expression in the airways	187
Fig. 4.6 – Lung cells are differentially infected by CAL and HA mut viruses	189
Fig. 4.7 – Proposed model for HA mut attenuation	195
Fig. 4.S1 – Immunological damage in lungs of CAL and HA mut-infected mice.....	205
Fig. 4.S2 – NP expression in lungs of CAL and HA mut-infected mice	206
Fig. 5.1 – Summary of the contribution of host and viral factors to pathogenesis.....	210
Fig. 5.2 – Proposed model for DAF-mediated immunopathology.	217
Fig. 5.S1 – Complement decay-accelerating factor is required for dose-dependent pathology.	225

List of tables

Table 1.1 – IAV segments and respective encoded polypeptides.	.6
Table 1.2 – Immune cells patrolling the airways.....	21
Table 1.3 – Mucins studied upon infection.	25
Table 2.S1 –Histological scoring parameters.	131
Table 2.S2 – Antibodies used in flow cytometry.....	132
Table 3.S1 – Primers used in cloning and site-directed mutagenesis.....	174
Table 3.S2 – Antibodies used in western blot.....	175

Abbreviations

AEC	Alveolar epithelial cell
AM	Alveolar macrophage
AMP	Antimicrobial peptide
AP	Alternative pathway
APC	Antigen-presenting cell
ARDS	Acute respiratory distress syndrome
BAL	Bronchoalveolar lavage
BCA	Bicinchoninic acid protein assay
BCR	B cell receptor
BS ³	Bis(sulfosuccinimidyl)suberate
BSA	Bovine serum albumin
C/EBP β	CCAAT/enhancer binding protein beta
Cal	A/California/7/09
CAL	A/California/04/2009
CALCOCO2	Calcium-binding and coiled-coil domain 2
CARD	Caspase associated recruitment domain
CDC	Complement-dependent cytotoxicity
COVID-19	Coronavirus disease 2019
CP	Classical pathway
CPSF30	30-kDa cleavage and polyadenylation specificity factor 30
CR1	Complement receptor type 1; CD35
CRM1	Chromosomal region maintenance 1
cRNA	Complementary RNA
Crry	Complement receptor 1-related gene/protein Y
CT	Cytoplasmic tail
CTL	Cytotoxic T lymphocyte
CXCL12	C-X-C motif chemokine ligand 12

cysLT	Cysteinyl leukotriene
d.p.i.	Days post-infection
DAF	Complement decay-accelerating factor; CD55
DAMP	Damage-associated molecular pattern
DC	Dendritic cell
DMEM	Dulbecco's Modified Eagle Medium
dsRNA	Double stranded RNA
Eng	A/England/195/2009
EpCAM	Epithelial cell adhesion molecule; CD326
ER	Endoplasmic reticulum
ERES	Endoplasmic reticulum exit sites
ESCRT	Endosomal sorting complex required for transport
F-IAV	Viral isolate from a fatal case patient
FBS	Fetal bovine serum
fH	Factor H
fI	Factor I
Gal	Galactose
GAPDH	Glyceraldehyde 3-phosphate dehydrogenase
GFP	Green fluorescence protein
GlcNAc	N-acetylglucosamine
GPI-AP	Glycosylphosphatidylinositol-anchored protein
H&E	Hematoxylin and eosin
h.p.i.	Hours post-infection
HA	Hemagglutinin
HA mut	A/California/04/2009 HA S110L
HAT	Human airway trypsin-like protease
HDAC6	Histone deacetylase 6
HEK293T	Human embryonic kidney 293 cells, transformed with large T antigen
HI	Heat-inactivated

HIF	Hypoxia-inducible factor
HK68	A/Hong Kong/1/68
HNP-1	Human neutrophil peptide 1
HRP	Horseradish peroxidase
IAV	Influenza A virus
IBV	Influenza B virus
ICV	Influenza C virus
ICTV	International Committee on Taxonomy of Viruses
IDV	Influenza D virus
IFN	Interferon
IFNAR1	Interferon-alpha/beta receptor alpha chain
IFNGR	Interferon-gamma receptor
IHC	Immunohistochemistry
IL-28R α /IL-10R β	Interleukin-28 receptor α /interleukin-10 receptor β
ILC	Innate lymphoid cell
IRF-3	Interferon regulatory factor 3
ISG	Interferon-stimulated gene
ISG15	Interferon-stimulated gene 15
JAK/STAT	Janus kinase/signal transducers and activators of transcription
kDa	Kilodalton
LAP-TGF- β	Latency-associated peptide-TGF- β
LP	Lectin pathway
M-IAV	Viral isolate from a patient with mild symptoms
M.F.I.	Median fluorescence intensity
m.o.i.	Multiplicity of infection
M1	Matrix protein 1
M2	Matrix protein 2
MAC	Membrane attack complex; C5b-9

MAIT	Mucosal-associated invariant T cell
MAL	<i>Maackia amurensis</i> lectin
Man	Mannose
MASP	MBL-associated serine protease
MAVS	Mitochondrial antiviral signaling protein
MBL	Mannose-binding lectin
MCC	Mucociliary clearance
MCP	Membrane cofactor protein; CD46
MDCK	Madin-Darby canine kidney cells
MEF	Mouse embryo fibroblast
MERS-CoV	Middle eastern respiratory syndrome coronavirus
MHC	Major histocompatibility complex
mRNA	Messenger RNA
Muc1-ED	Mucin1 extracellular domain
mvRNA	Mini viral RNA
MW	Molecular weight
NA	Neuraminidase
Mx1	Myxovirus resistance protein 1
MxA	Human myxovirus resistance protein 1
NCS	Newborn calf serum
NCZ	Nucleozin
NEP	Nuclear export protein (alternative name of NS2)
NET	Neutrophil extracellular trap
Neu5Ac	N-acetylneuraminic acid
Neu5GC	N-glycolylneuraminic acid
NF- κ B	Nuclear factor- κ B
NK	Natural killer
NKT	Natural killer T
NLS	Nuclear localizing signals
NP	Nucleoprotein

NS1	Non-structural protein 1
NS2	Non-structural protein 2 (alternative name of NEP)
OAS	Oligoadenylate synthase
PA	Polymerase acidic protein
PAGE	Polyacrylamide gel electrophoresis
PAMP	Pathogen-associated molecular pattern
PB1	Polymerase basic protein 1
PB2	Polymerase basic protein 2
PBS	Phosphate buffered saline
PCR	Polymerase chain reaction
PFA	Paraformaldehyde
PFU	Plaque forming units
PKR	Proteinase kinase R
Pol II	RNA polymerase II
PKR	dsRNA-activated protein kinase
PR8	A/Puerto Rico/8/34
PR8-HK4	A/Puerto Rico/8/34 containing segment 4 from HK68
PR8-HK4,6	A/Puerto Rico/8/34 containing segments 4 and 6 from HK68 (alternative name of X31)
PR8-HK6	A/Puerto Rico/8/34 containing segment 6 from HK68
PRR	Pattern-recognition receptor
PVP	Polyvinylpyrrolidone
RANTES	Regulated on activation, normal T cells expressed and secreted
RCA	Regulator of complement activation
RdRp	RNA-dependent-RNA-polymerase
RG	Reverse genetics
RIG-I	Retinoic acid-inducible gene I
RIPLET	E3 Ubiquitin-Protein Ligase RNF135
RNS	Reactive nitrogen species

ROS	Reactive oxygen species
RSV	Respiratory syncytial virus
SARS-CoV	Severe acute respiratory syndrome coronavirus
SARS-CoV-2	Severe acute respiratory syndrome coronavirus 2
SCR	Short consensus repeat
sd	Standard deviation
SDS	Sodium dodecyl sulfate
SHM	Somatic hypermutation
SEM	Standard error of the mean
Sia	Sialic acid
Siglec	Sialic acid-binding immunoglobulin-type lectin
SNA	<i>Sambucus nigra</i> agglutinin
ssRNA	Single-stranded RNA
STING	Stimulator of IFN genes
TCR	T cell receptor
Tfh	Follicular helper T cell
TGF- β	Transforming growth factor- β
TGN	Trans Golgi network
TLR	Toll-like receptor
TMD	Transmembrane domain
TMPRSS2	Transmembrane serine protease 2
Th	T helper cell
Treg	Regulatory T cells
TRIM25	Tripartite motif containing 25
UPR	Unfolded protein response
VLP	Virus-like particle
vRNA	Viral RNA
vRNP	Viral ribonucleoprotein
VSV	Vesicular stomatitis virus
WHO	World Health Organization

WT	Wild-type
X31	A/X-31
Zan	Zanamivir

Summary

Host and viral factors contribute to define viral pathology. In this work, we explore the role of complement decay-accelerating factor (DAF) in activating complement and in modulating influenza A virus (IAV) infection via an interplay with the antigenic viral proteins hemagglutinin (HA) and neuraminidase (NA). We observed that DAF, contrary to what could be expected, potentiates complement activation upon IAV infection. Particularly, we describe that the viral sialidase NA acts on DAF, in a strain-specific manner, removing α -2,6-linked sialic acids and propose that this may regulate pathogenicity. Given that the recognition of different conformations of sialic acid by the virus is a key driver in IAV intra- and interspecies transmission, our findings may have implications for zoonotic events.

Our results also showed that besides DAF increasing complement activation, it exacerbates immune cell recruitment, especially of neutrophils and monocytes, which promote lung immunopathology without altering viral loads. Therefore, upon infection, DAF reveals a novel mechanism of virulence, as well as immune evasion.

Additionally, we show an alternative mechanism of controlling pathology, based on a mutation in viral HA that attenuates the virus. We observed that this mutation prevented viral replication and penetration in the lung tissue, conferring protection associated with decreased viral loads.

Taken together, our results add to the understanding of how host and viral factors may contribute in distinct ways to viral-mediated pathology.

Título e resumo

Interação entre DAF e as proteínas virais HA e NA modelam a patogênese viral

Neste trabalho exploramos o papel do fator acelerador de decaimento do complemento (DAF) na ativação do complemento, e consequentemente da modelação da infecção pelo vírus da gripe A (IAV), através da interação com as proteínas virais hemaglutinina (HA) e neuraminidase (NA). Observámos que, ao contrário do previsto, o DAF potencia a ativação do complemento durante a infecção por IAV. Adicionalmente, descrevemos que a sialidase NA, dependendo da estirpe, atua no DAF removendo os seus ácidos siálicos com ligação $\alpha 2,6$, e propomos que isto pode controlar a patogenicidade. O reconhecimento de diferentes conformações de ácido siálico pelo vírus é um fator determinante na transmissão intra e interespecífica, logo as nossas observações poderão ter implicações na compreensão de zoonoses.

Os nossos resultados mostraram que o DAF além de ativar o complemento, aumenta o recrutamento de células do sistema imunitário, especialmente neutrófilos e monócitos, promovendo imunopatologia nos pulmões, sem alterar a carga viral. Assim, revelámos um novo mecanismo de virulência, através do DAF.

Adicionalmente, descrevemos um mecanismo alternativo, baseado na atenuação de um vírus com uma mutação na HA, em que observámos uma inibição da replicação viral e penetração no tecido pulmonar, sem influenciar a carga viral.

Resumidamente, este trabalho ajuda a compreender em maior detalhe como interações entre fatores virais e do hospedeiro podem contribuir de formas distintas para a severidade da patologia.

Chapter 1 – General introduction

1.1 Influenza A virus

1.1.1 The flu

Influenza A virus (IAV) is the causal agent of the flu, a respiratory infection with variable severity. The first reports of flu-like symptoms date back to Hippocrates in ancient Greece around 5-4 b.C. (1), while disease outbreaks that could be attributed to IAV were described by historians even earlier (2). However, it was only in the 14th century that the name *Influenza* was widespread, originated from the fact that sick people were thought to be under detrimental astral influence (2).

IAV was identified as the etiological agent of the flu after being first isolated from pigs (3) and shortly after from humans (4) in the early 1930s. Despite being around for numerous centuries, IAV still provokes 3 to 5 million severe infections yearly that result in up to 650.000 annual deaths (5). Seasonal influenza constitutes an important burden to economics and to society (6–8). More so, if we consider the burden of recurrent deadly pandemics with devastating consequences (2,9–11). The deadliest one recorded was the Spanish Flu in 1918, when up to 50 million people were killed (2,10), while the most recent was in 2009 and still provoked up to 500.000 fatalities (12,13). Despite the availability of two antiviral drugs approved by the Food and Drug Administrations (FDA, USA), at the moment, vaccination is the best existing protection against IAV. However, it needs constant update to overcome viral evolution and escape immune protection and therefore its effectiveness varies widely (7,8,14). Hence, deeper understanding of IAV is indispensable to unveil new means of preventing and/or fighting infectious diseases. An infectious disease results from a complex interaction of the pathogen with its host. Influenza provokes severe complications and deaths resultant from excess inflammation (7,15–17). Underpinning prolonged inflammation is the host immune response to viral or secondary bacterial infections (18–20). As a consequence,

understanding how the host mounts an excessive inflammatory response will lead to a better control of viral infections.

1.1.2 Taxonomy

Influenza is a member of the *Orthomyxoviridae* family (21,22), which loosely translates as “virus from the mucus”. According to the International Committee on Taxonomy of Viruses (ICTV), there are 4 genus of influenza virus: *Alphainfluenzavirus*, *Betainfluenzavirus*, *Gammainfluenzavirus* and *Deltainfluenzavirus*, respectively including the species *Influenza A virus*, *Influenza B virus*, *Influenza C virus* and *Influenza D virus* (23). Influenza A and B are associated with seasonal flu epidemics and influenza A to pandemic outbreaks. IAV is considered to be responsible for most serious human infections. *Influenza B virus* (IBV) infects humans, however it is restricted to a considerably narrower host range (humans and seals) and presents a decreased mutation rate when compared to IAV (21,24). The two conserved lineages of human IBV, Yamagata and Victoria (21,22,25), are included in the recommended vaccine formulations (26). *Influenza C virus* (ICV) was isolated from infected humans more than 70 years ago (27). ICV predominantly infects children, usually resulting in upper airway infections with mild symptoms (22,28,29). Nevertheless, severe infections have been reported, and its actual incidence and disease burden remains elusive. (28,29).

Recently, the new species *Influenza D virus* (IDV) was defined, when at least two distinct lineages with only 50% homology to known human ICVs were isolated from cattle (30,31). IDV mainly affects cattle, with most human infections resulting from occupational exposure (32,33). Additionally, IDV has a wider cell tropism when compared to ICV, however both genera appear to be antigenically stable, and hence do not represent a serious danger to humans (34). Conversely, IAV is the only genus that poses a substantial threat to human health due to

risk of zoonosis, host switch, and generation of pandemics, and therefore is the focus of this work.

1.1.3 Structure and life cycle

IAV is an enveloped virus, containing the surface proteins Hemagglutinin (HA), Neuraminidase (NA) and Matrix protein 2 (M2) (Fig. 1.1-A). As the viral membrane derives from the infected cell, it may also include host proteins (35,36). Beneath the membrane, is a layer of Matrix protein 1 (M1), and the core contains IAV segmented genome composed of eight distinct negative sense, single stranded (ss) RNA segments, in the form of viral ribonucleoproteins (vRNPs) (Fig. 1.1-A). vRNPs are constituted by a copy of the RNA-dependent-RNA-polymerase (RdRp), formed by polymerase basic protein 1 (PB1), polymerase basic protein 2 (PB2) and polymerase acidic protein (PA) (37–39), nucleoprotein (NP) and viral RNA (vRNA). The 5' and 3' extremities of vRNA comprise conserved sequences with partial inverted complementarity, which maintain an anti-parallel base-pairing, establishing an approximately 15-base pair-long panhandle structure, where the RdRp connects (40,41). Consequently, a double-helical hairpin is formed, with one end folding back on itself (42,43). NP oligomerization forms a string of positive residues, which enables the binding of vRNA to the outside of the complex, yet not protecting vRNA from RNase digestion (44–46). Additionally, Non-structural protein 2/nuclear export protein (NS2/NEP) was initially included in the list of non-structural proteins, but is now a well-established component of virions (36,47–49).

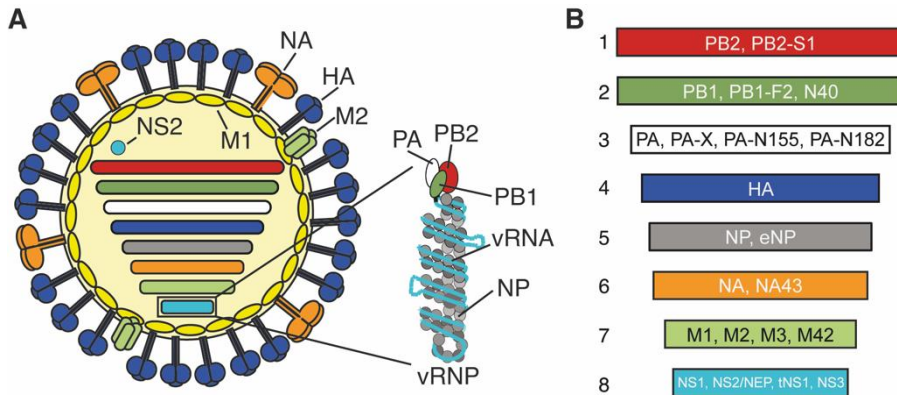


Fig. 1.1 – Representation of IAV structure.

Virion organization, with vRNP structure highlighted (**A**). Genome segments, including all known encoded polypeptides (their function is detailed in Table 1) (**B**). PB2 – Polymerase basic protein 2; PB1 – Polymerase basic protein 1; PA – Polymerase acidic protein; HA – Hemagglutinin; NP – Nucleoprotein; NA – Neuraminidase; M – Matrix protein 1/2; NS – Non-structural protein 1/2; vRNA – Viral RNA; vRNP – Viral ribonucleoprotein.

IAV eight-partite genome encodes 10 main proteins, but up to 22 may be expressed in infected cells in a viral strain/cell type-specific manner (Table 1.1) (50). The genome of the virus encodes for several non-structural proteins, being the most well studied the Non-structural protein 1 (NS1). NS1 is encoded by segment 8, and is a multifunctional protein (47). It stimulates viral translation (51–56), promotes nuclear export (54,57), and inhibits cell autonomous immune response (58–60). The splicing product of the same segment is Non-structural protein 2/Nuclear export protein (NS2/NEP) which has a pivotal role in vRNP nuclear export (61). Furthermore, other roles for NS2 have been elucidated, as control of replication, transcription and recruitment of host factors to promote budding (62–64).

Depending on the strain, additional accessory polypeptides may be expressed (50), namely PB2-S1 (65), PB1-F2 (66), PB1-N40 (67,68),

PA-N155 (67,69), PA-N182 (67,69), PA-X (70–72), eNP (73), NA43 (74), M3 (75) M42 (76), tNS1 (77) and NS3 (78), as well as defective ribosomal products (DRiPs) (79) and chimeric viral-host hybrid proteins (80). However, their specific contributions to infection are still unclear.

Table 1.1 – IAV segments and respective encoded polypeptides.

Seg	Polypeptide	Function	Ref
1	PB2	Component of RNA transcriptase - 7m GpppNm recognition	(47)
	PB2-S1	Mitochondrial, inhibits RIG-I/MAVS	(65)
2	PB1	Component of RNA transcriptase - catalyzes nucleotide addition	(47)
	PB1-F2	Mitochondrial, apoptosis induction and virulence factor	(66)
	PB1-N40	Unclear - suggested role in replication	(67,68)
3	PA	Component of RNA transcriptase - endonuclease, involved in cap snatching	(47)
	PA-X	Non-specific mRNA endonuclease, involved in host shut-off	(70,71)
	PA-N155	Unclear - suggested role in replication	(67,69)
	PA-N182	Unclear - suggested role in replication	(67,69)
4	HA	Sialic acid binding, fusion activity and antigenic determinant	(81)
5	NP	vRNP formation, nuclear import and export and transcription	(82)
	eNP	Unclear - suggested role in gene expression	(73)
6	NA	Sialidase activity, budding, cell exit and antigenic determinant	(81)
	NA43	Unclear	(74)
7	M1	vRNP nuclear export, virus assembly and major virion protein	(75)
	M2	Ion channel, HA maturation and virus uncoating and budding	(75)
	M3	Unclear - suggested to downregulate early segment 7 expression	(75)
	M42	Functionally replaces M2 upon its depletion	(76)
8	NS1	Inhibits host pre-mRNA processing and maturation and antiviral IFN responses	(83)
	tNS1	Cytoplasmic, inhibits IRF3 and IFN- β	(77)
	NS2/NEP	vRNP nuclear export	(83)
	NS3	Unclear - suggested role in replication	(78)

IAV life cycle has been widely studied (reviewed in (8,22,84–87)), nevertheless not all steps are yet fully understood. The viral protein HA recognizes and binds to receptors at the membrane of host cells that contain sialic acids with specific ligations to galactose (88–90). Human adapted IAVs have preference for α 2,6 ligations whilst avian adapted

strains bind to $\alpha 2,3$ (21,91–94). Binding to sialylated receptors leads to IAV internalization by clathrin-mediated (95,96) or clathrin- and caveolin-independent endocytosis (97,98). Macropinocytosis has also been proposed as an unconventional entry pathway (99). Recently, an alternative sialic acid-independent entry mechanism has also been reported (100). Upon internalization, as endosomes mature, their pH drops (101), which induces a conformational change in HA that exposes its fusion peptide (102), promoting the fusion of the viral and endosome membranes (103–106). Also in the endosome, M2, a transmembrane tetramer that works as an ion channel, promotes the acidification of the interior of the virion and the import of K^+ ions, which weakens the interactions between M1 and the vRNP bundle (75,107–109).

Then, the E3 ubiquitin ligase Itch (110), CUL3-SPOPL E3 ubiquitin ligase complex (111), histone deacetylase 6 (HDAC6)-dependent pathways (112,113) and the member of importin- β family transportin 1 (114) contribute to disassemble the viral core and release vRNPs in the cytoplasm.

Unlike most RNA viruses, IAV messenger RNA (mRNA) is synthesized in the host cell nucleus (115–117). It has been shown that vRNPs, devoid of M1, can enter the nucleus by the nuclear pore, in an ATP-dependent process (118). For this, after viral uncoating, NP and PB2 nuclear localizing signals (NLS) contribute to sort vRNPs to the nucleus (119–121). Recently, it has been shown that subsequent from interaction of M1 with transportin 1, vRNPs are bound to importin- α/β and transported to the nucleus (114).

In the nucleus, the viral RdRp is responsible for replication and transcription of the eight separate segments of the viral RNA genome (122–124). The RdRp synthesizes viral mRNA using short capped primers derived from cellular transcripts by a unique 'cap-snatching' mechanism (125). The PB2 subunit binds the 5' cap of host pre-mRNAs, which are subsequently cleaved after 10–13 nucleotides by the

endonuclease PA (38,126–128). Viral replication occurs via a positive sense intermediary, complementary RNA (cRNA), that is a full-length copy of the vRNA (122,126,129). cRNA is produced 5% relative to the positive sense mRNA, and serves to amplify genome production (116,130). Both c- and vRNA production requires *de novo* synthesis of the viral proteins NP, PB1, PB2 and PA, as they form ribonucleoprotein complexes (131). After genome replication, vRNPs are exported from the nucleus in an active process mediated by NS2, M1 and the host protein chromosomal region maintenance 1 (CRM1) forming a daisy chain complex (61,132,133).

Due to its segmented nature, IAV genome assembly is a very sophisticated and not yet fully understood process. Nevertheless, available evidence favors a model of selective packaging, over that of random assembly, based in flexible sequence-specific RNA-RNA interactions (134–138). Upon nuclear export, vRNPs associate with Rab11 vesicles, in a process that impairs the endocytic recycling compartment by outcompeting molecular motor adaptors (87,139–142). Alternatively, vRNPs were also shown to associate with the ER and proposed to use this route as an alternative before being loaded in Rab11 vesicles (143). Recently, it has been demonstrated that vRNPs form viral inclusions (aggregates) that display the properties of liquid organelles close to ER exit sites (ERES) (144). Furthermore, as one vRNP is enough to induce the formation of these liquid inclusions, it has been suggested that the viral inclusions were sites dedicated to IAV genome assembly (144). The delivery of IAV genomic complex to sites of virion assembly at the plasma membrane has been proposed to occur on Rab11 vesicles. However, in the light of recent reports, viral inclusions and Rab11 may be a way station and a distinct pathway may promote IAV genomic complex delivery to the plasma membrane (87).

HA and NA are transmembrane proteins, both synthesized and glycosylated in the ER, and then transported through the classical

secretory pathway, to cholesterol-rich domains (lipid rafts) at the plasma membrane where they accumulate and recruit M1 to initiate virion assembly and budding (145–152). However, this process is apparently inefficient and not fully understood (87,148). It was suggested that expression of M1 in cells was sufficient to release virus-like particles (VLPs) (153). However, this was observed upon M1 overexpression and might not represent physiological conditions, as it was later reported that expression of HA and NA was enough to release VLPs, independently of M1 (146). Interestingly, M1 incorporation in VLPs was dependent on HA and NA cytoplasmic tails, which supports a sequential a model of HA and NA localizing to lipid rafts and initiating the budding, and then recruiting M1 and vRNPs for viral assembly (146). Subsequent studies proposed that NA expression alone was sufficient to induce budding of VLPs with correct morphology and enzymatic activity (149,154). Remarkably, some NAs were only able to induce budding but not release in the presence of tetherin, suggesting that budding-competent NAs possess a redundant function in virion release (149). However, following findings reported M2 to be in the neck of budding virions, and the depletion of its amphipathic helix enough to prevent membrane fission and virion release (155). Furthermore, HA was able to induce budding, but in the absence of M2 virion release was prevented (155). Therefore, it suggests that M2 bypasses the need of host factors, namely the Endosomal Sorting Complex Required for Transport (ESCRT), to release progeny virions (155–158).

Viral release requires NA-mediated cleavage of sialic acids attaching progeny virions to the cell surface or to glycan side-chains in other nascent virions, and thus insufficient sialidase activity results in viral aggregation in the form of beads on a string (81,159). In order to proceed to a new cycle of infection, HA synthesized as the inactive precursor HA0 needs to be cleaved into HA1 and HA2 by host proteases

in order to present fusion capability (104,160–162). A simplified scheme of the viral lifecycle is provided in Fig. 1.2.

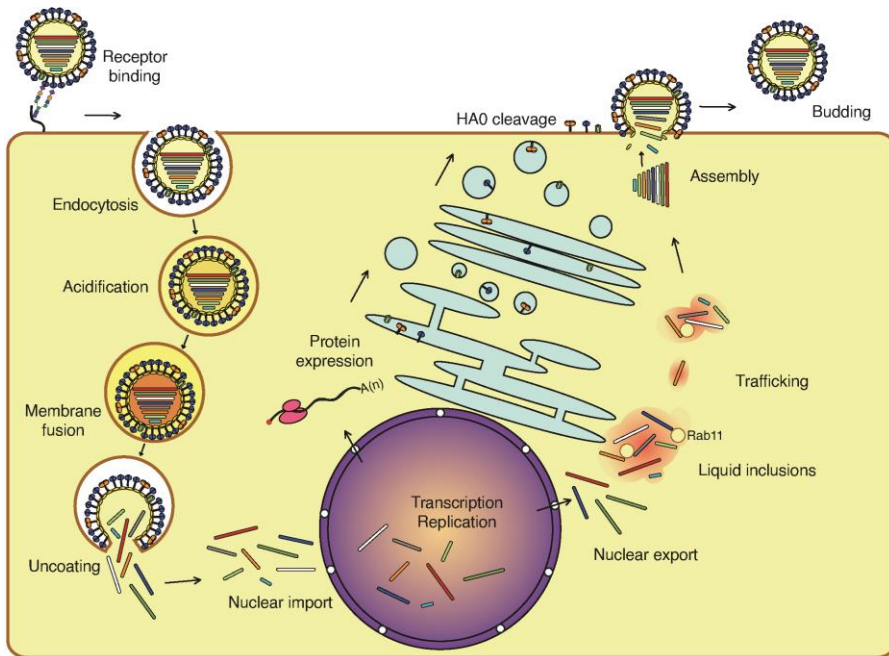


Fig. 1.2 – Summarized representation of IAV lifecycle.

1.1.4 Ecology

IAVs are spread across many species. Most IAV strains can be found in aquatic fowl, their major reservoir, where they are usually not pathogenic (21,91,163,164). IAVs have been isolated from a vast ecological niche, including human, pigs, horses, dogs, cats, marine animals, and both wild and domestic birds (21,91). IAV are subtyped on the basis of the 2 virus surface glycoproteins, HA and NA, into 16 HA and 9 NA subtypes. More recently, additional virus subtypes have been discovered in bats, but their impact for the ecology, epidemiology and circulation of IAV is uncertain (165–167). IAV of 3 subtypes – H1N1, H2N2, and H3N2 – have been endemic in humans, with H1N1 and H3N2 being the subtypes currently circulating. These are thought to have originated from aquatic birds directly or through complex genome

reassortment events involving intermediate hosts (9,21,168). Since 1997, several cases of human infections with different subtypes (H5N1, H5N6, H6N1, H7N2, H7N3, H7N7, H7N9, H9N2, H10N7 and H10N8) of avian influenza viruses have been identified in humans, with H5N1, H5N6, H7N9 and H10N8 associated with high mortality (94,169–172). Overall, at least five HA subtypes (H5, H6, H7, H9 and H10) of avian IAVs have been identified in humans in conjunction with a multitude of NAs, which raised concerns for their pandemic potential (94,173,174). It is well-described that IAVs are zoonotic pathogens, able to jump across species and establish in avian and mammalian hosts (91,94), but this requires sophisticated adaptation processes. For example, in aquatic birds where the body temperature is 42°C, influenza viruses replicate predominantly in the intestinal tract (175), the HA recognizes preferentially α 2,3-linked sialic acid receptors and PB2 contains glutamic acids at position 627 (21,91,175,176). In humans, endemic IAV have adapted to replicating at 35–37 °C in the upper respiratory tract with an HA preferring α 2,6-linked sialic acid receptors and a lysine occupies the 627 position of PB2 (21,91,176). Therefore, there is a lot of interest to understand the IAV mechanisms of adaptation.

1.1.5 Antigenic drift and shift

IAV exhibits a rapid evolution (8,21,22,91,92). IAV possesses an error-prone polymerase, which promotes low-fidelity replication (177). Recent measurements in the model strain A/Puerto Rico/8/1934 (PR8, H1N1) estimate an overall mutation rate of 0.92 to 1.8×10^{-4} substitutions per nucleotide per strand copied, meaning 1.2 to 2.4 mutations per replicated genome (177–179). At a first glimpse, this may seem detrimental to the virus. However, these mutations may produce viruses that are more fit to replicate in a different host and thus contribute to viral adaptation to new environments. In addition, it can lead to changes in the surface antigenic proteins HA and NA, in a

process called antigenic drift (8,21,22). Consequently, this heterogeneity may also result in novel antigenic variants able to evade the host immune system and cause infection (8,21,22,180). Moreover, mutations in the targets of the available antiviral drugs are readily selected. Therefore, the low-fidelity replication process also contributes to the emergence of drug resistant viruses (8,13,181,182), even to the most recent therapies pimodivir (183), favipiravir (184) and baloxavir (185), that target the polymerase complex.

The segmented nature of IAV genome requires an intricate packaging process, however it sets the stage for evolution leaps by interchanging segments between dissimilar viruses infecting the same cell in a process called antigenic shift (8,9,21). Although direct transmission between avian and human viruses is thought to have occurred in the 1918 Spanish flu, avian-adapted viruses with zoonotic potential are often inefficient in transmitting between humans, owing to host-restriction mechanisms (detailed in the next section) (21,91,92,94). However, co-infection in a permissive host, like swine (168,186), of human- and avian-adapted IAVs may constitute suitable mixing vessels that produce reassortant IAVs with pandemic potential (2,9,21,94).

1.1.6 HA

The ability of HA to agglutinate erythrocytes has been well-known for a long time, and it was a pioneering way to quantify viruses (187). HA gene was identified in 1976 (81) and its structure was resolved in the 1980s, revealing a trimer whose subunits contain two different domains, the stalk and the globular head, encompassing the conserved receptor binding site where sialic acid is bound (Fig. 1.3) (93,188–190).

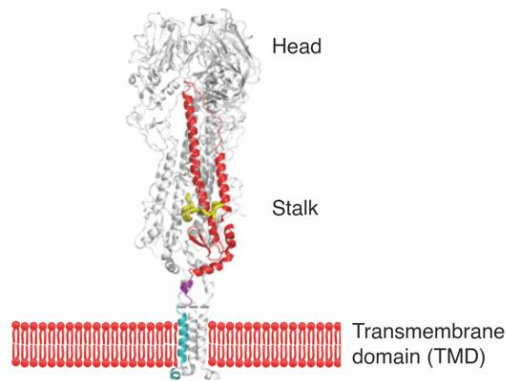


Fig. 1.3 – HA structure and domains (adapted from (190)).

HA is a glycosylated protein and, remarkably, its glycosylation levels result from a balance between escape from lectin recognition and adaptive immunity, while maintaining viral fitness (191–193). Furthermore, it can directly modulate virulence, as addition of two N-linked glycosylation sites to the HA from 1918 H1N1 resulted in decreased virulence (194). After proper folding, HA traffics with NA from the trans Golgi network (TGN) to lipid rafts, where they promote the initiation of viral budding (145,148,150,151,195).

HA has two major roles in the viral lifecycle. First, in order to enter a cell, HA binds to sialic acid receptors when a virion reaches the cell surface (8,93). Initially, the cell receptor was suggested to be a polysaccharide (196), however, later it was identified as being sialic acids attached to glycoproteins, whose recognition by viral HA depended on the species of origin (197). Depending on the receptor preference, HA may bind N-glycolylneuraminic acid (Neu5Gc) or N-acetylneuraminic acid (Neu5Ac) linked to galactose (88,89,198,199). Furthermore, linkage orientation is important, as avian hosts express α 2,3- while human airways express α 2,6-linked sialic acid moieties (21,91–93,200). Thus, adaptation of a virus to a new host requires the adjustment of HA to bind to a new receptor. Additionally, HA adaptation has been described as a limiting step for droplet transmission in ferrets

(201,202). However, there are still unanswered questions. New types of receptors have been recently identified, such as the sialylated Ca^{2+} channel Cav1.2 (203) and non-sialylated phosphorylated receptors (93,204). Furthermore, the contribution of HA to incorporation of host proteins in the virion, as well as to viral budding and shape is still largely unknown (87).

The other major role of HA in infection is mediating the fusion between the viral and endosome membranes to allow release of the viral genome into the cytoplasm (93,205). In order to be in its active conformation, HA needs to be cleaved by host proteases (93,103,160,161), which represent an additional host restriction factor. Interestingly, HA cleavage site is directly associated with higher or lower pathogenicity of a virus (15,206). While low-pathogenicity HAs possess a monobasic cleavage site which can only be cleaved by trypsin-like proteases, highly-pathogenic HAs present a polybasic site that can be cleaved by other proteases, such as furin, which facilitates virus tropism (206,207). Despite no definite identification of the involved proteases in human airways, the serine proteases transmembrane serine protease 2 (TMPRSS2) and human airway trypsin-like protease (HAT), have been proposed to activate HA (162,208).

As HA is the most abundant protein at the viral surface, its antigenic potential has been acknowledged, and therefore, it has been the major component used in vaccine development (8,14,209). Thus, interactions between HA and the host immune system are an attractive subject that deserves further research.

1.1.7 NA

NA, initially called “receptor-destroying enzyme”, is a homotetrameric sialidase which is indispensable to a productive infection (8,22,159,210). NA gene was identified in 1976 (81) and its structure including catalytic and antigenic sites was resolved in 1983

(211,212). Each of the NA monomers is composed of a highly conserved cytoplasmic tail (CT), a transmembrane domain (TMD), a stalk and a catalytic head (Fig. 1.4) (159).

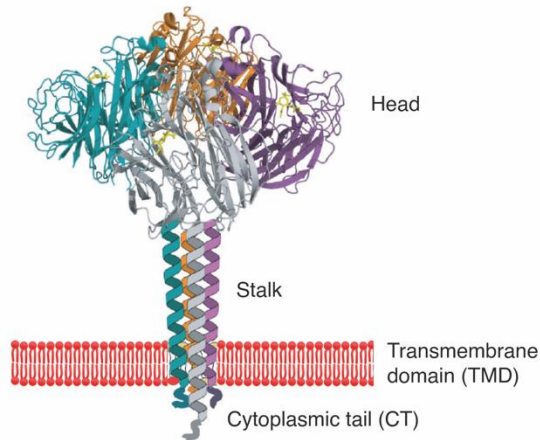


Fig. 1.4 – NA structure and domains (adapted from (159)).

NA does not contain a cleavable signal sequence, however its NH₂-terminal hydrophobic domain functions both as an anchor and as a signal for ER translocation, where it is matured until tetramerization (147,213,214). As HA, NA is glycosylated, with repercussions in immune evasion and host adaptation (191,193,215). Remarkably, adaptation to new hosts and pandemic events have been associated with glycosylation site shifts (193). NA co-traffics with HA from the TGN to lipid rafts mediated by Rab17 and then Rab23 (150,151). The TMD and the highly conserved cytoplasmic NA tail (Fig. 1.4) are essential for correct lipid raft accumulation and efficient budding (146,149,152,154).

NA enzymatic activity in the mucus was observed for the first time in 1947 (216). In recent times it was also acknowledged that in order to infect a new host, both in humans and swine, NA is required for viral invasion, making its way through the mucus layer, as it contains sialic acid decoys that are bound by HA and trap incoming virions (217–223).

Additionally, efficient aerosol transmission has been suggested to be dependent on NA sialidase activity (224). Recently, unconventional roles for NA have been proposed. It has been suggested that NA participates in cell entry, being involved in a viral motility mechanism that allows the virus to roll through the elongated sialylated mucins until reaching the cell surface, as well as scanning it for a region of higher receptor density (225–228). Additionally, avian- but not human-derived NAs possess a second sialic acid-binding site, which improves the accessibility of the sialidase catalytic site to α 2,3-linked sialic acid receptors (229–231). Despite being an antigenic protein, NA content has been somehow neglected in vaccines. However, a recent study reported that NA promotes the selection of escape mutations to cope with HA-targeted immunity and hence should be included in vaccination strategies (215,232,233). Due to its preponderant role in viral lifecycle, NA is the target for the recommended antivirals zanamivir, oseltamivir and most recently peramivir. Oseltamivir is the current standard for IAV treatment, however it is not effective against IBV (234,235). Recently, novel non-sialic acid analogues NA inhibitors have been proposed as lead compounds to develop (236).

NA is a relatively unspecific sialidase able to use many substrates. In a system of viral co-infection of IAV with vesicular stomatitis virus (VSV), NA was shown to cleave the sialic acid content of VSV-G within the cell (237). Remarkably, purified virions have been shown to cleave the precursor protein LAP-TGF- β , activating it, with direct implications in host immune response (238,239). As IAV recurrently interacts with sialic acid, this raises the prospect that by acting on these moieties, NA may modify their function. Therefore, determining which host proteins may be substrates of NA, may reveal new aspects of how NA is implicated in the regulation of viral-induced pathogenesis.

1.1.8 Host restriction and HA/NA balance

IAV is spread amongst many species, but inter-species transmission is restricted by many factors, being the host receptor preference one of the best described (91,93,94,164,240). Due to increased surveillance, there has been the recurrent identification of mutations associated with human adaptation in avian-derived IAVs (241–243).

As previously mentioned, in avian-adapted IAV strains, HA and NA have preference for α 2,3-linked sialic acid receptors, while human-adapted IAVs bind and cleave α 2,6-sialic acid, being this the most abundant type of receptor in the human upper airways (93,94,164,240). Therefore, for productive infection, HA and NA must be matched to their substrate preference. Not surprisingly, changes in the receptor-destroying NA have been described to accompany HA changes for sialic acid linkage preference in receptor host adaptation, while alterations in HA have been shown to follow mutations in NA (91,159,193,230,244).

The complementary functions of HA and NA require both proteins to feature well-adjusted activities. HA/NA balance has been defined as the balance between HA and NA activities on the complex environment comprising cells and mucus (245). Briefly, upon infection, HA binds sialic acid moieties, while NA needs to cleave them in order to release the newly formed virions. Thus, besides sialic acid preference, both proteins must have a balanced strength and substrate accessibility, in order to allow a productive infection (159,229,240,246–248). If NA has suboptimal activity, budding virions may be clumped together and/or stuck to decoy receptors in the mucus layer; conversely, if NA outpowers HA, it may cleave sialic acid receptors before the virus is able to trigger endocytosis, with both scenarios eventually resulting in virus inability to replicate (159,240,248). Recently, the balance between HA and NA has also been shown to be required for viral motility (229,245). Interestingly, imbalanced HA-NA may reach a productive equilibrium by decreasing

protein activity, as illustrated by the increase of pandemic H1N1 severity in mice, upon treatment with the NA inhibitor oseltamivir (249).

Thus, HA and NA ultimately control virulence, as they are the viral proteins directly interacting with the host immune system, either innate or adaptive (detailed in next section), and they are responsible for selecting which cells to infect, due to their roles in cell entry and progeny release, respectively. Of note, virulence and flu-derived pathology result from a complex interplay between the host immune system, viral factors, and also, on occasion, secondary bacterial infections (7,18,250,251). Therefore, interaction between HA, NA and host proteins, and how they modulate the immune response and disease severity, is a topic that needs to be explored.

1.2 Host defenses

1.2.1 The airways

Human airways cope with approximately 10,000L of air every day, which implicates constant exposure to dangerous particles and pathogens (252). Recent measurements of air particles estimate that we inhale 6×10^6 virus-like particles daily, 5×10^6 indoors and 1×10^6 outdoors (253). Therefore, the immune system in the airways needs to be vigilant and quick to respond to any threats, yet tightly restricted to prevent unnecessary immunopathology (252,254–256).

The complex architecture of the respiratory tract is illustrated in Fig. 1.5. Throughout the airways, secretory cells such as goblet and club cells produce mucins that compose the mucus layer (detailed in next section). This layer covers the epithelium, in order to prevent pathogen adherence and promote clearance. Ciliated cells enforce the clearance, maintaining a continuous flow by synchronously beating their cilia, in a process called mucociliary clearance (MCC) (221,222). Inhaled air is conducted until the alveoli, where gas exchanges occur. The alveolar

epithelium represents 99% of the lung surface, and is mainly composed of alveolar epithelial cells (AEC) which ensure gas exchange, cell renewal and immunomodulation (257).

AECs are divided in type 1 (AECI) and type 2 (AECII), in similar numbers, but disproportionate surface areas (257,258). AECI occupy approximately 95% of the alveolar surface, as they form a thin flat layer to allow gas exchange with the surrounding capillaries (257,259). It has been proposed that, due to their larger area, AECI promote inflammatory responses by detecting invading pathogens and interacting directly with macrophages (257,259). On the other hand, AECII are “defenders” of the alveoli, as they secrete surfactant, proliferate to renew AECI, control alveolar lining fluid levels, take part in innate immunity and minimize inflammation (257,258). Besides the physical barrier, airways are patrolled by immune cells that quickly respond to challenges.

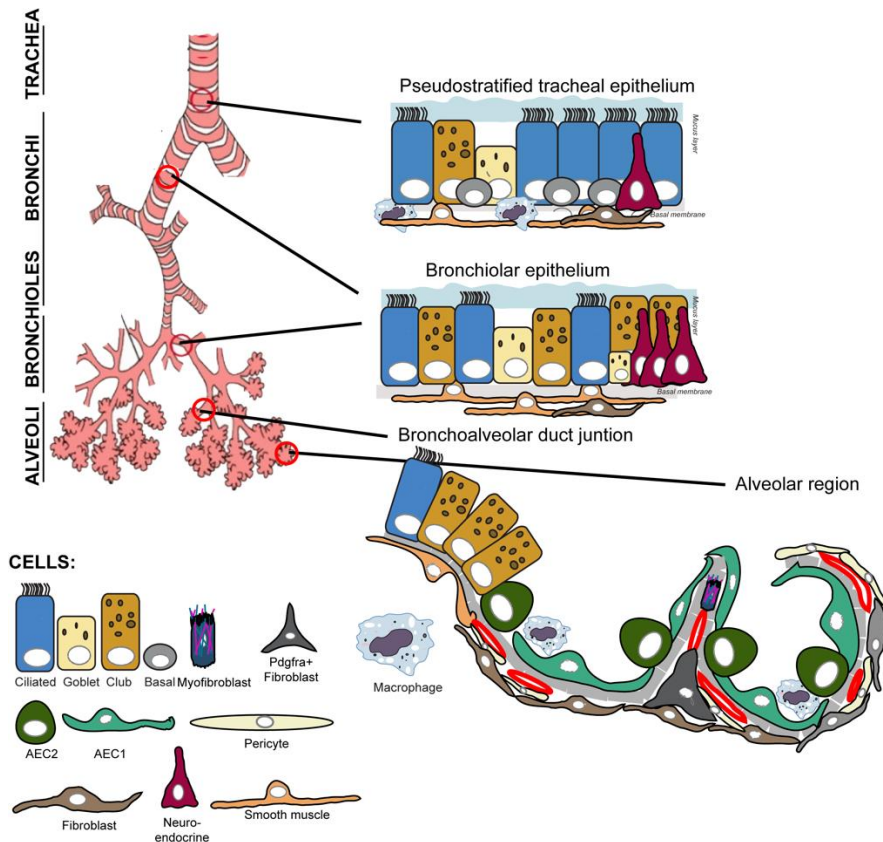


Fig. 1.5 – Schematic representation of the respiratory tract (kind gift from MJ Amorim).

The immune system deals with each pathogen by using and building specific defenses, whilst pathogens evolve mechanisms to circumvent them, giving rise to a constant host-pathogen tug-of-war that promotes host and pathogen co-evolution. This interaction is complex and is underpinned by physical barriers that hinder the access of pathogens to cells. In addition, a series of immune related cells, listed in Table 1.2 and illustrated in Fig. 1.6, which reside in the respiratory tract or are recruited to sites of infection once an insult has been detected, also regulate this interaction and this will be explored in the next sections. We will also explore their involvement in IAV infection as well as the mechanisms that the virus has developed (if any) to elude them.

Table 1.2 – Immune cells patrolling the airways.

Resident cells

Dendritic cells

Innate lymphoid cells

Monocytes

Macrophages

Natural killer cells

Neutrophils

Recruited upon IAV infection

B cells

CD4⁺ T cells

CD8⁺ T cells

Eosinophils

Monocytes

Monocytes-derived dendritic cells

Monocyte-derived macrophages

Mucosal-associated invariant T cells

Natural killer cells

Neutrophils

γδ T cells

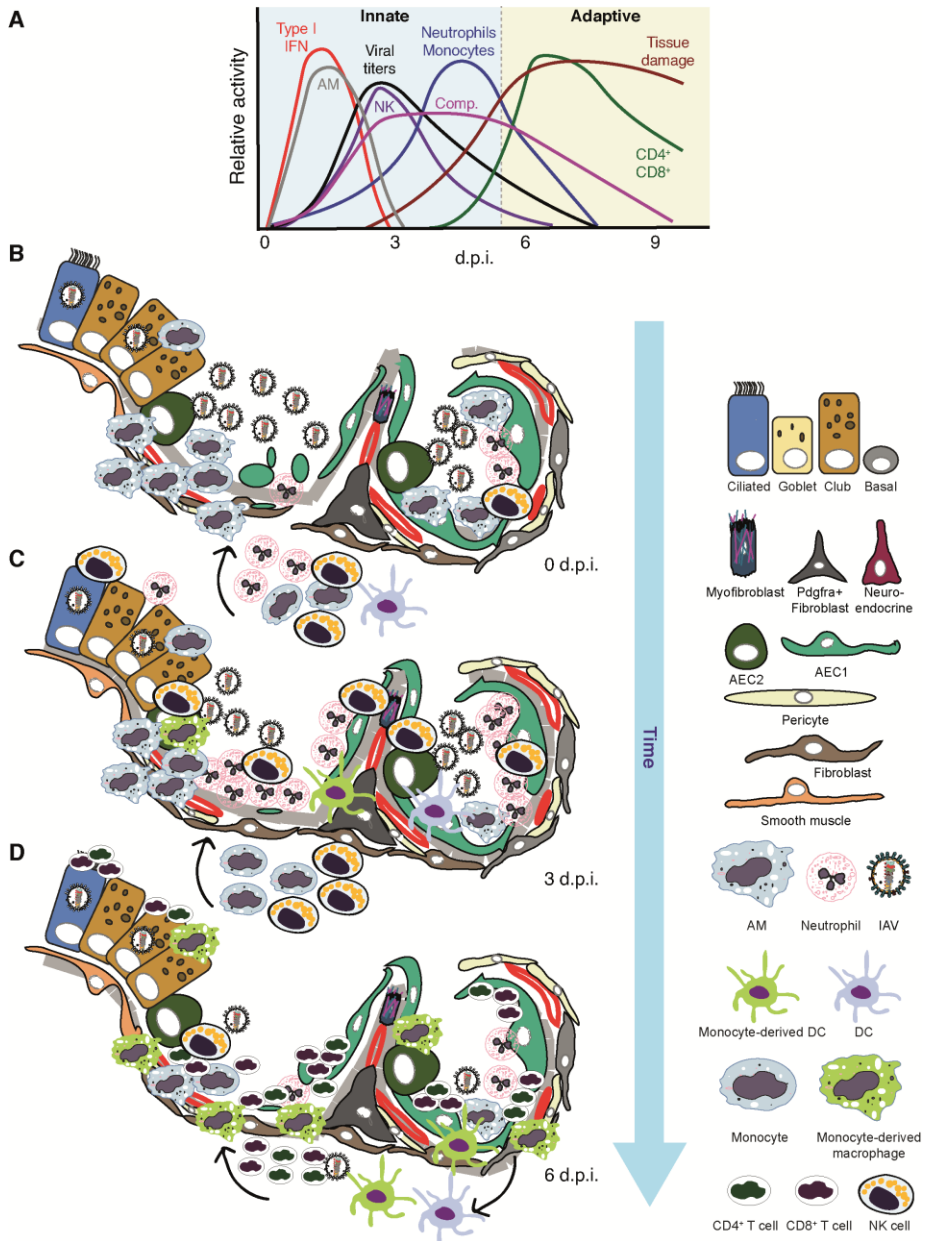


Fig. 1.6 – Representation of immune cells involved in response to IAV infection (adapted from a scheme by MJ Amorim).

A: Simplified timeline of the immune response to IAV. Upon infection, the innate immune system provides a rapid response to limit initial viral replication until the setting of the slower, but more effective adaptive response. **B:** The interferon (IFN) response promotes the production of

factors that block viral replication in the infected and adjacent cells. Alveolar macrophages (AM) patrol the airways detect the infection via pattern-recognition receptors (PRR) and respond by activating phagocytosis and secreting cytokines that promote an influx of neutrophils, monocytes and natural killer (NK) cells. **C:** These immune cells limit viral replication by directly killing infected cells, as well as secreting cytokines. Furthermore, monocyte-derived dendritic cells (DCs) contribute to antigen presentation and adaptive immune recruitment. However, an excessive response may result in tissue damage, without contributing to improve viral clearance. **D:** Later in infection, T cells are recruited to the airways. CD8⁺ T cells differentiate into cytotoxic T lymphocytes (CTLs) which eliminate infected cells, while CD4⁺ T cells participate in B cell priming. An optimal immune response will clear the virus, without inflicting unnecessary damage to the lung tissue. AM – alveolar macrophage; Comp. – complement; DC – dendritic cell; IFN – interferon; NK – natural killer cell.

1.2.2 Physical barrier

In the airways, the first line of defense against a pathogen such as IAV is the mucosal barrier, a multifaceted environment sealed by epithelial cells that contains antimicrobial peptides (AMPs), reactive oxygen species (ROS), immune cells, complement peptides and sialic acid decoys (Fig. 1.5; 1.7) (222,260–263). The mucosal barrier is robust and even when challenged by pathogens such as IAV, that dramatically affect the airways, destroying ciliated cells and reducing epithelial thickness, remains integral (255,264).

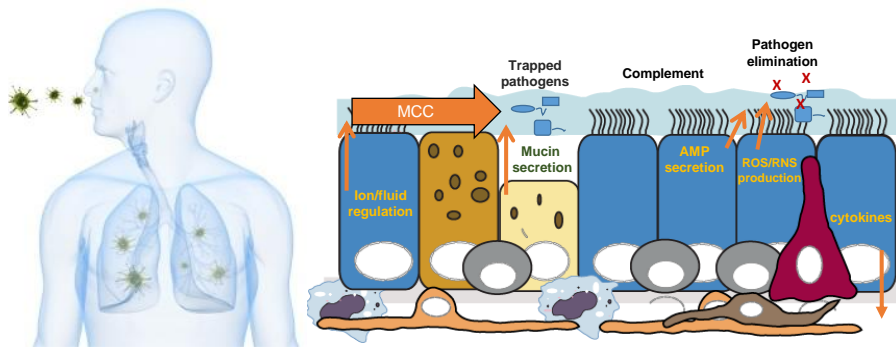


Fig. 1.7 – Representation of airway mucosal barrier (kind gift from MJ Amorim).

AMP – antimicrobial peptide; MCC – mucociliary clearance; RNS – reactive nitrogen species; ROS – reactive oxygen species.

The mucus layer is a complex structure. It is composed of mucins, highly sialylated proteins, that form a structure composed of a periciliary and a gel layer (221,222,265,266). The upper thicker layer, composed of mucins Muc5ac and Muc5b physically traps the particles or pathogens, while the periciliary layer composed of Muc1, Muc4, Muc16 and Muc20 acts as a lubricant that allows cilia to beat, ensuring the mucociliary clearance (MCC) (221,222,265–267).

There are several mucins, being the most studied upon infection the membrane-associated mucin Muc1 and the secreted mucins Muc5ac and Muc5b (Table 1.3) (221,268). Besides being part of the periciliary layer, the membrane-bound mucin Muc1 also has immunomodulatory properties, as its depletion resulted in increased inflammation upon *Pseudomonas aeruginosa* infection (269,270). Furthermore, it may act as a decoy-receptor, as its sialylated extracellular domain (Muc1-ED) is shed upon IAV binding (271). Interestingly, a similar mechanism based on the human sialidase NEU1 promotes the shedding of Muc1-ED as a decoy for *P. aeruginosa*, revealing the flexibility of this mechanism (272). The secreted mucin

Muc5ac overexpression protected from IAV infection, resulting in lower viral loads and neutrophil recruitment, probably due to a thicker mucus layer that prevents the virions to reach the epithelial cells (223). Additionally, its depletion did not affect MCC nor host survival (273). However, Muc5b, another component of the gel layer, is required for efficient MCC and consequently general airway defense, with mice genetically deficient in Muc5b presenting increased mortality either in steady-state or upon *Staphylococcus aureus* challenge (273). Moreover, inhalation of dry air, which alters mucus rheological properties, also impairs MCC and tissue repair (274).

Table 1.3 – Mucins studied upon infection.

Strain	Phenotype	Ref
	Increased inflammation and <i>P. aeruginosa</i> clearance	(269)
<i>Muc1^{-/-}</i>	Increased inflammation and <i>P. aeruginosa</i> susceptibility upon repeated challenge	(270)
	Increased IAV replication and susceptibility	(271)
<i>Muc5ac^{+/+}</i>	Decreased IAV replication	(223)
<i>Muc5ac^{-/-}</i>	No alterations in MCC or <i>S. aureus</i> susceptibility	(273)
<i>Muc5b^{-/-}</i>	Impaired MCC, increased mortality in steady-state and upon <i>S. aureus</i> challenge	(273)

Additionally to mucins, broad spectrum AMPs that reside in the gel layer protect the airways from pathogen invasion, via direct inhibition and/or by immunomodulation (275–277). Pre-treatment of mice with β -defensin (Defb4, Bpifa1, Camp) decreased IAV viral loads in a strain specific manner, through its immunomodulating activity (276). As an example of a direct inhibition, human neutrophil peptide 1 (HNP-1), another defensin, inactivates a broad spectrum of viruses, including IAV (278). The cathelicidins LL-37 and mCRAMP (human and murine, respectively) have been shown to protect mice from IAV infection by

directly associating with the virion and by modulating neutrophil response when in complex with IAV (279,280). In a similar fashion, neutrophil-derived ROS may directly inactivate IAV or modulate the innate immune response through mitochondrial-mediated expression of interferon-stimulated genes (ISGs) (281,282).

1.2.3 Interferon (IFN)

Detection of pathogens by host cells is enforced by the presence of pattern-recognition receptors (PRR) which recognize pathogen- or danger-associated molecular patterns (PAMPs and DAMPs, respectively) (60,261,283,284). There are several described cell autonomous mechanisms of defense such as stress granules (72,285), inflammasomes (284,286), unfolded protein response (UPR) (287,288) and MHC-I (289,290), being IFN response the most studied upon IAV infection (60,261,291).

Interferons were discovered in 1957 while studying viral interference, and are class 2 α -helical cytokines acting early in the immune response (292,293). Due to its efficacy against viral infections, IFN has been used to treat chronic hepatitis B and C viruses infections (292,294). However it causes severe side-effects such as flu-like symptoms, lymphopenia, depression and autoimmune complications, and therefore patients cannot tolerate high doses (292,294).

Once IAV enters the cells, the main sensor is the retinoic acid-inducible gene-I (RIG-I) in the cytoplasm, which detects the 5'-triphosphate motifs in the viral genetic material (60,291,295–297). Upon binding, RIG-I caspase associated recruitment domains (CARDs) are ubiquitinated, which promotes the interaction with mitochondrial antiviral signaling protein (MAVS) and subsequent nuclear translocation of interferon regulatory factor 3 (IRF-3) and nuclear factor- κ B (NF- κ B) to induce type I IFN (IFN- α/β) production (60,261,291,298–300). Consequently, type I IFN binding to its receptor interferon-alpha/beta

receptor alpha chain (IFNAR1) triggers the Janus kinase/signal transducers and activators of transcription (JAK/STAT) pathway and stimulates the expression of ISGs such as myxovirus resistance protein 1 (Mx1/MxA), proteinase kinase R (PKR), oligoadenylate synthase (OAS) and interferon-stimulated gene 15 (ISG15), which ultimately lead to an antiviral state (60,261,291). In addition, endosomal Toll-like receptors (TLR)3/7/8 may perceive viruses that fail to escape the endosome (261,291,301,302).

Alternatively, the production of type II IFN (IFN- γ), mainly by NK and T cells, activates its receptor interferon-gamma receptor (IFNGR) in epithelial cells, which induces the expression of overlapping but distinct ISGs from type I IFNs (261,303,304). Remarkably, depletion of both type I and II IFNs led to a detrimental proinflammatory response in IAV-infected mice that exacerbated disease severity (303).

Type III IFNs (IFN- λ) act mainly in epithelial cells, where they bind the heterodimeric receptor interleukin-28 receptor α /interleukin-10 receptor β (IL-28R α /IL-10R β), which induces similar ISGs to type I IFNs (305–307). *In vivo*, Type III IFNs are the first being expressed upon IAV infection, and prevent uncontrolled initial viral replication (305,308). Furthermore, IFN- λ prevents IAV spreading from the upper airways to the lungs, which limits disease severity and transmission (309). Remarkably, mice depleted of IFN- λ receptors were only moderately more susceptible to IAV infection, but mice depleted of both type I and III IFN receptors were highly susceptible, even to IAV lacking the antagonist NS1, which suggests complementary roles for type I and III IFNs (261,305).

In addition to the cell autonomous response, the multifaceted IFN response also modulates immune cell recruitment, as IFN- α inhibition led to increased immune cell recruitment, without altering viral loads (303). Furthermore, IFN- α treatment of neutrophils increased cytokines and chemokines expression (308). Of note, in a strain-specific manner,

IAV infection suppressed IFN- α production, and therefore downregulated NK cell-mediated IFN- γ secretion (310). In order to evade IFN signaling, IAV evolved several mechanisms (60,291,311), which are illustrated in Fig. 1.8.

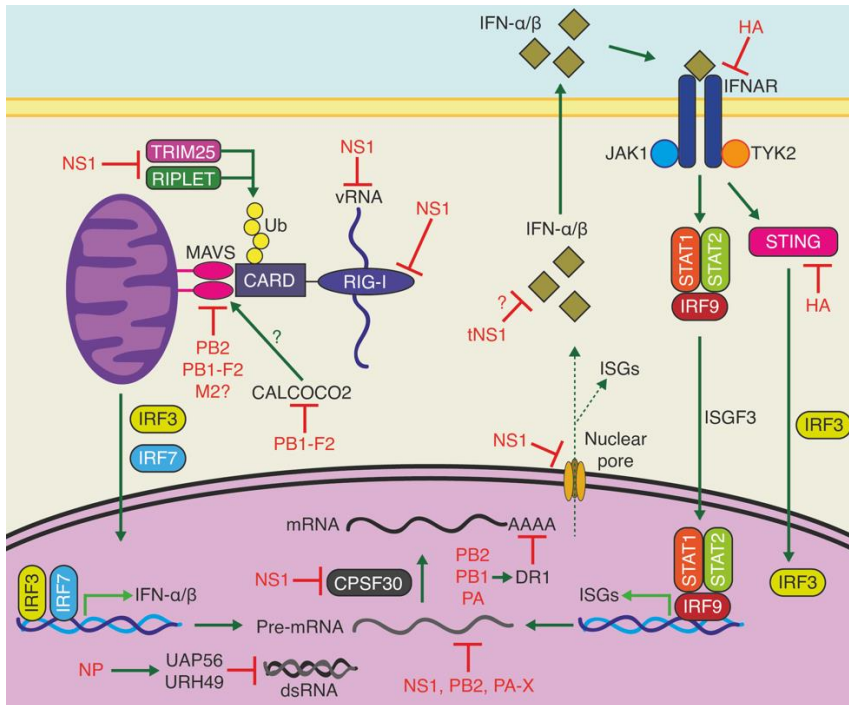


Fig. 1.8 – Interferon (IFN) activation pathways and mechanisms of IAV evasion.

NS1 is a multifunctional protein which has been considered a major IFN antagonist, since infection by IAV lacking NS1 correlates with an increase in IFN promoter activity (58). NS1 is able to directly bind double-stranded RNA (dsRNA), which suggests that NS1 prevents its recognition by cellular sensors (312). Remarkably, NS1 is able to directly bind and inhibit RIG-I (313,314) and dsRNA-activated protein kinase (PKR) (59). Besides, NS1 targets tripartite motif containing 25 (TRIM25) and E3 Ubiquitin-Protein Ligase RNF135 (RIPLET), which counteracts RIG-I CARD ubiquitination and hinders further pathway

activation (299,315). Interestingly, the cytoplasmic truncated polypeptide tNS1 was also reported to counteract IFN- β transcription (77). In the nucleus, NS1 binds the polyadenylation factor 30-kDa cleavage and polyadenylation specificity factor 30 (CPSF30), which avoids host mRNA processing and eventually blocks the host immune response (54). Recently it was shown that NS1 binds to host pre-mRNAs, including RIG-I, suggesting a specific posttranscriptional inhibition of IFN activation (316). Furthermore, NS1 promotes phosphorylation of the repressor element CCAAT/Enhancer Binding Protein beta (C/EBP β) and thus its association to RIG-I promoter region (317). Finally, NS1 has recently been shown to inhibit nuclear export, thus preventing the translation of host mRNAs (318).

Besides NS1, other proteins have been reported to be involved in IFN evasion (291,311). IAV associates with host RNA polymerase II (Pol II) and decreases polymerase occupancy, as well as promotes termination failure, independently of NS1, which contributes to host shut-off (319).

NP structural role likely prevents vRNA accessibility to host sensors. Nevertheless, NP was shown to recruit the host helicases UAP56 and URH49 to unwind any dsRNA generated upon viral genome replication (320).

The components of IAV polymerase complex (PB1, PB2, and PA), besides capping vRNPs, also interact with the cellular transcriptional repressor DR1, which suppresses the ISGs (321). Individually, PB2 cap-snatching from host mRNA promotes general inhibition of transcription (291) and, in a strain-specific manner, PB2 may localize to mitochondria where it is thought to counteract MAVS signaling (322,323). The other polypeptide from segment 1, PB1-F2, has also been shown to localize to mitochondria and likely hinders MAVS signaling (324,325). Furthermore PB1-F2 also interacts with the cytoplasmic protein calcium-binding and coiled-coil domain 2 (CALCOCO2), which has been

proposed to participate in MAVS signaling network (326). PA-X, through its endonuclease activity, degrades host mRNA contributing to general transcriptional shut-off and thus decreasing IFN activation (72,327).

M2 contribution to immune evasion remains elusive. However, recently it has been shown that M2 associates with mitochondria and promotes MAVS self-association and aggregation (328). The major surface protein HA has also been shown to contribute to cell autonomous immune evasion through its subunits which target stimulator of IFN genes (STING) and IFNAR1 (329,330).

However, uncontrolled IFN activation may be detrimental. Despite its inherent protection, type I IFN is also involved in pathogenicity *in vitro* and *in vivo* (331). This is reinforced by the observation that excessive type I IFN signaling promotes epithelial cell death and therefore increases IAV-induced immunopathology in mice (332), which is in agreement with the described side-effects of IFN therapy (292).

Therefore, a robust but controlled early IFN activation is crucial to mount an adequate immune response, and further understanding of how host and viral factors interact to generate it is of major importance.

1.2.4 Neutrophils

Neutrophils are polymorphonuclear phagocytic leukocytes that promptly respond to danger signals and their associated inflammatory mechanisms, accumulating rapidly at the inflammatory sites after being recruited from the peripheral blood (16,252,333,334). Recruitment is a response to surface TLRs, complement receptors and thrombin-activated receptors (252,261,335). Importantly, neutrophil deficiency increases susceptibility to microbial and fungal infections (336–339).

At the infection site, neutrophils kill microorganisms and clear infections via a series of mechanisms including phagocytosis and release of ROS, granular proteins and cytokines. Additionally, several studies demonstrated the importance of neutrophil extracellular traps

(NETs), a secretion product consisting in DNA, histones, elastase and myeloperoxidase, which traps and kills the pathogens, preventing their spreading (252,339–342).

Additionally, a large body of evidence highlights the importance of neutrophils in the modulation of the adaptive immune response (333,343–345). Upon activation, neutrophils interact with and recruit macrophages and NK cells, but also B and T cells, making them crucial to the outcome of infection (252,334). Interestingly, neutrophils have been shown to leave C-X-C motif chemokine ligand 12 (CXCL12) trails for CD8⁺ T cell recruitment (346), which has been reported as an immunopathology driver upon IAV (347) and respiratory syncytial virus (RSV) infection (348). Neutrophils have been associated with acute respiratory distress syndrome (ARDS), suggesting their deregulated response may be deleterious upon viral infection (16,252,349,350).

Neutrophil heterogeneity has been long described, but only recently many subtypes of neutrophils have been classified (333,351–353). This can be elucidated upon IAV infection, where lung-recruited neutrophils express numerous chemokine receptors that are absent in circulating neutrophils, suggesting an activation mechanism (354). Regardless of these advances, the role of neutrophils in IAV infection is still controversial.

A protective role for neutrophils has been observed upon A/X-31 (X31; H3N2) infection, as their depletion in mice resulted in exacerbated viral loads and lung damage, as well as decreased host survival (355,356). Conversely, many studies with other viral strains identified neutrophils as promoters of immunopathology, by the fact that neutrophil ablation prevented tissue damage without affecting viral loads (17,357–359). Overall, these studies suggest that neutrophil response must be fine-tuned, and any deviation from the equilibrium may be detrimental for disease outcome. Therefore, neutrophils appear to be an appealing target to modulate immunopathology.

1.2.5 Monocytes and macrophages

Monocytes are circulating mononuclear phagocytes (360). Additionally, monocytes and macrophages are present in human airways in steady state, exhibiting a lower inflammatory profile (361,362). Upon IAV challenge, infected AECs recruit monocytes through the secretion of Regulated on Activation, Normal T cells Expressed and Secreted (RANTES)/CCL5 and CCL2/MCP-1 (363–366), which then differentiate in DCs or macrophages (16,360,367). Monocyte-derived DCs and macrophages share intrinsic properties with their conventional counterparts and have been studied upon IAV infection (362,367). Remarkably, IAV can directly infect macrophages (16,368). Regardless of abortive infection in some viral strains (369), monocyte-derived macrophages function is modulated by IAV, illustrated by the increase in cytokine secretion and phagocytic activity (364,370,371).

As for neutrophils, the protective role of monocytes and macrophages upon IAV infection is ambiguous. Tissue resident alveolar macrophages (AMs) are necessary to prevent uncontrolled viral replication, independently of B and T cells (369,372). A proposed mechanism involves the prevention of type I AECs infection, by suppressing the cysteinyl leukotriene (cysLT) pathway (373). Additionally, IAV-induced monocyte-derived macrophages have been shown to confer protection from secondary bacterial infections, after infection by the mildly virulent strain A/X-31 (X31) (374). Conversely, upon challenge with the more virulent strain A/Puerto Rico/8/34 (PR8), CCR2⁺ monocyte and monocyte-derived cells contribute to immunopathology, as their depletion decreased disease severity without altering viral loads (375). Furthermore, this detrimental effect was amplified by IFNAR1, as delayed viral clearance promoted type I IFN

secretion and CCR2⁺ monocyte recruitment, which was correlated with strain virulence and consequently disease severity (376).

1.2.6 NK cells

Natural Killer (NK) cells are essential for a rapid immune response in the lungs (377,378). This is promptly elucidated in mice, where NK cells represent around 10% of all lung lymphocytes, the highest frequency of all organs (379). NK cells can be activated by anomalous cells lacking inhibitory ligands and/or presenting activation ligands (378). Activated NK cells promote cytolysis through the release of perforin and granzyme, as well as cytokine secretion, mainly IFN- γ (310,377,378). Not surprisingly, NK cells are involved in the response to viral challenges, including IAV (377,378), both in humans (380) and mice (381).

In a strain-specific manner, IAV triggers NK cells to produce IFN- γ , which contributes to mount the immune response (310,378). Interestingly, NK cell depletion may lead to contradictory outcomes, depending on the viral dose (382,383). In infected cells, HA exposed at surface binds sialylated NK cell receptors (384–387), which stimulates direct cell elimination (388,389). However, IAV is able to counteract detection through NA-mediated desialylation of NK cell receptors (388,389). Other immune evasion strategies include the direct infection of NK cells, promoting apoptosis (390,391) and the HA-induced downregulation of granule exocytosis (392). Besides killing infected cells, NK cells also promote cell proliferation and tissue regeneration, through the production of IL-22 (393).

In summary, contradictory roles for NK cells in the outcome of IAV infection highlight the need of further studies.

1.2.7 Eosinophils, $\gamma\delta$ T, MAIT, ILC and platelets

The immune system encompasses an astonishing complexity of cells and features (344,394) (Fig. 1.9), with distinct contributions to the host response.

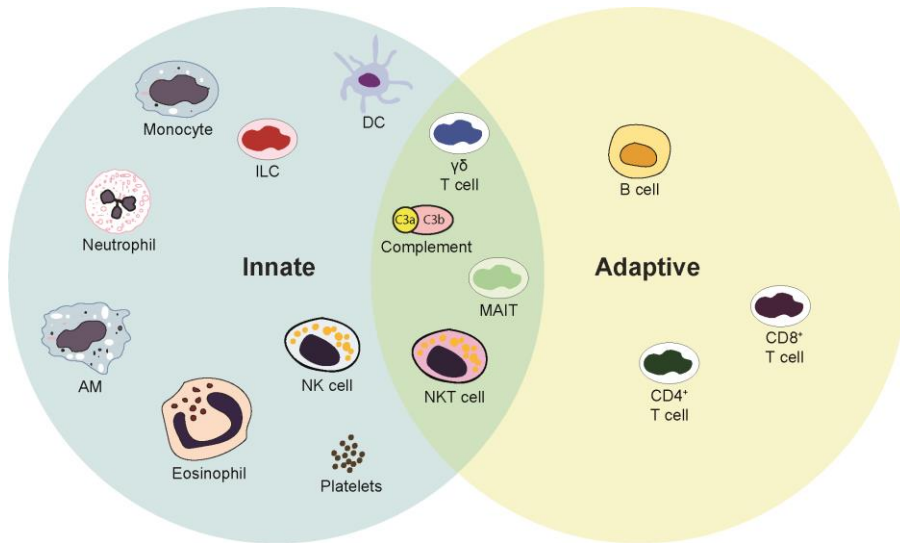


Fig. 1.9 – Components of the innate and adaptive immune system.

Innate immune system is characterized by a rapid response to infection, however not specific. Adaptive immune system provides a specific and efficient response, however slower. Some immune elements, such as the complement system, share properties of both innate and adaptive immunity, and bridge them together. Efficient protection against a pathogen challenge requires effective communication between the branches of the immune system. AM – alveolar macrophage; DC – dendritic cell; ILC – innate lymphoid cell; MAIT – mucosal-associated invariant T cell; NK – natural killer cell; NKT – natural killer T cell.

Eosinophils are granulocytes characterized by their ability to release granular cationic proteins and cytokines (395). In steady state, eosinophils circulate in reduced numbers, however upon stimuli they are quickly mobilized to the site of infection (395). Despite their contribution to IAV protection being usually disregarded, recently it has been shown

that eosinophils specifically upregulate antiviral genes upon IAV challenge (396). Furthermore, it has been suggested their recruitment is important for efficient CD8⁺-mediated immunity, tissue reparation and AMPs release (377,395–397).

$\gamma\delta$ T cells are a specific subset of innate-like T cells which express γ and δ chains as receptors (398). Upon signaling from DCs and macrophages, $\gamma\delta$ T cells are recruited during the early stage of IAV infection, and are involved in direct killing of infected cells and IFN- γ secretion (377,399,400). Similarly to NK cells, HA can directly activate $\gamma\delta$ T cells upon binding to sialylated receptors (401) (Lu 13).

Mucosal-associated invariant T cells (MAITs) are innate-like T lymphocytes that release cytokines, perforin and granzyme when activated (252,399). MAITs are activated after signaling from IAV-exposed monocytes and contribute to antiviral immunity early in infection (402,403). These cells exhibit rapid effector responses upon IAV challenge, however are scarce in mice (252,404).

Innate lymphoid cells (ILCs) encompass three types of cells of lymphoid lineage which do not present antigen receptors (252,399,405). Following IAV infection, ILCs are essential to maintain respiratory function and promote airway remodeling (406). Specifically, ILC2 confer protection against pandemic H1N1 by promoting tissue repair mechanisms (407).

Dysfunctional coagulation is often observed upon highly pathogenic IAV infection, being an important immunopathology driver (408,409). In human patients, platelets have been shown to be activated through TLR7 and internalize IAV, however not being infected (410,411). Interestingly, HA has been shown to directly bind platelets and promote their lysis by antibodies and complement (412). Recently, it has also been elucidated the presence of megakaryocytes residing in the lung, which display antigen presenting properties, besides platelet production (413).

1.2.8 Adaptive immunity

Innate immunity provides an expeditious broad-spectrum mechanism to control the infection while the host mounts the specific adaptive immune response to clear the pathogen (344,394,398). Furthermore, host adaptive immunity confers long-term protection to a pathogen. A brief illustration of the adaptive immune response to IAV is depicted in Fig. 1.10.

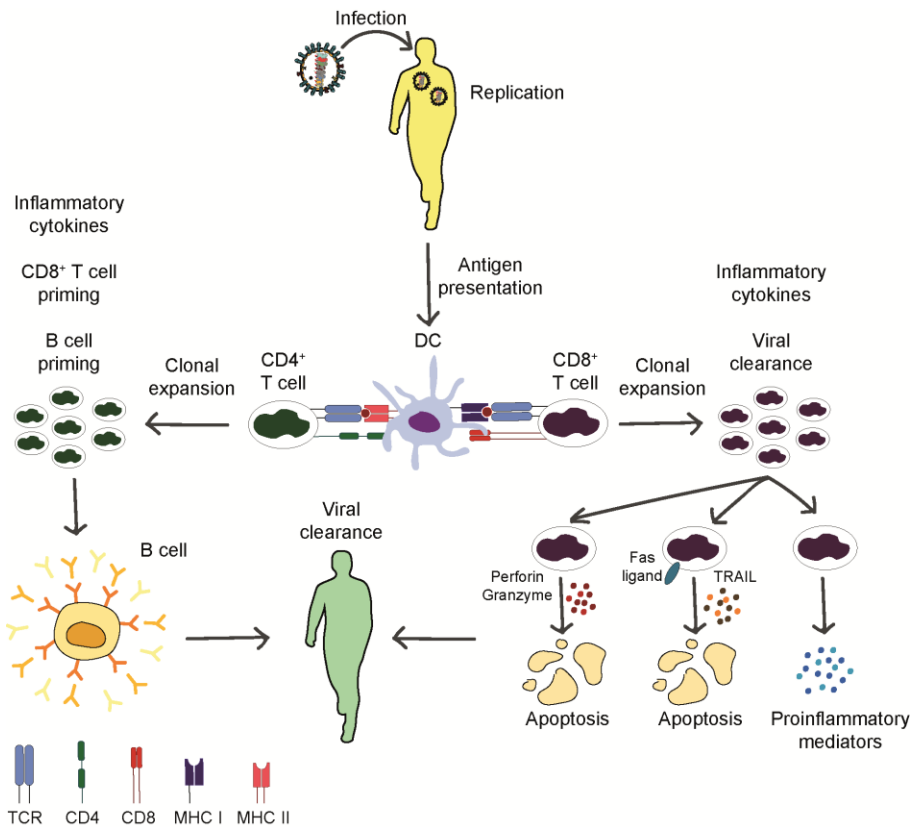


Fig. 1.10 – Adaptive immune response to IAV.

Upon IAV infection, dendritic cells (DCs) recruit CD8⁺ and CD4⁺ T cells, and present them viral antigens via MHC class I (MHC I) or MHC class II (MHC II), respectively. CD8⁺ undergo clonal expansion, and differentiate into cytotoxic T lymphocytes (CTLs), which release antiviral molecules and directly kill infected cells. In parallel, CD4⁺ T cells prime B cells, which produce antibodies to target the virus. Both pathways contribute to viral clearance. MHC – major histocompatibility complex; TCR – T cell receptor.

T and B cells are the major players in adaptive immunity, and have been described during the course of IAV infection (8,209,263,399,414).

Briefly, conventional mature T cells are divided into CD4⁺ and CD8⁺ cell subsets (263,394,398,399). CD4⁺ T cells interact with major histocompatibility complex (MHC) class II, expressed in antigen-presenting cells (APCs), while CD8⁺ T cells recognize peptides from within the cell exposed in MHC class I (263,394,398,399).

The largest group are the CD4⁺ T cells, enrolling in different functions depending on their subset. T helper (Th)1 effector CD4⁺ T cells express cytokines such as IL-2 and IFN- γ and promote CD8⁺ T cell growth (263,394,398,415). Alternatively, Th2 secrete IL-4, IL-5, IL-10 and IL-13 and drive antibody production (263,398,415). More recently, other subsets have been proposed, such as Th17 and Th9, based on differential cytokine secretion patterns (263,398,416,417). Additionally, other members of CD4⁺ T cells are the follicular helper T cells (Tfh), which trigger activation of B cells and regulatory T cells (Treg) (263,394,398).

Upon detection of viral-originated peptides loaded in MHC class I, CD8⁺ T cells differentiate into cytotoxic T lymphocytes (CTLs), which release antiviral molecules and directly kill infected cells through granzyme and perforin (263,344,394,398).

B cells recognize signals from T cells or APCs and respond by producing antibodies (398). Concisely, B cells can be divided in B-1, which quickly produce low affinity IgM and B-2, providing a slower but more specific response (398). B cell activation can be T cell-independent, mainly induced by PRR signaling, and result in early IgM response to viruses, such as IAV (344,398,418). T cell-dependent antibody response requires engagement of the B cell receptor (BCR) by an antigen, as well as signaling from Tfh cells and additional cytokines to induce class-switch after entering the germinal center (344,394,398). Furthermore, associated with class-switch is somatic hypermutation (SHM), which promotes the selection of antibodies with higher affinity for the antigen, and thus allows the response to a secondary challenge to be quicker and more specific (394,398).

In naive mice, the initial response to IAV is an innate-like B-1 response (419). Next, the early extrafollicular response of B-2 cells assists in clearing the infection, through differentiation of plasmablasts secreting specific anti-IAV IgM, IgA and IgG. Interestingly, IgG was shown to protect from pathogenesis but IgA was required to prevent transmission (420). Finally, the later germinal center response, which only peaks around the resolution of the infection, confers long term memory (419).

B and T cell priming is dependent on IAV-activated macrophages and DCs migration to lymph nodes (377). DCs recruited to the lungs are in tight communication with AECs and contribute to define the immune response (421). In fact, an association was found between DC depletion and hospitalization upon pandemic H1N1 infection (422). Increased disease severity likely resulted from impaired subsequent CD4⁺ and CD8⁺ T cell recruitment (422). Additionally, DCs may be directly infected with IAV, with the level of viral replication modulating antigen presentation activity (423). Infected DCs also secrete type I IFNs, which then limit the spread of infection (423,424). Alternatively, plasmacytoid

DCs with poor endocytic capacity may take up antigens from infected cells and expose them to CD8⁺ T cells (424). Nevertheless, DC-mediated protection is strain and site specific (425,426).

Besides their innate roles, neutrophils can also directly present antigens acquired by infection or by phagocytosis to CD8⁺ T cells (427). NK cells also contribute to adaptive immunity, by regulating CD8⁺ cell priming and DC migration depending on IFN- γ and perforin (428). Additionally, IL-15 supports the generation of lung resident memory CD4⁺ T cells after IAV infection (429).

Type I and II IFNs are also involved in the regulation of adaptive immunity. B cells sense type I IFN before antigen presentation, which modulates their response (344,419). The generation of IAV-specific CTLs requires the production of IFN- α and IFN- γ (344,430). The switch from innate to adaptive immunity depends on IFN- γ producing CD4⁺ T cells in the lungs, illustrated in toddler mice (431).

In summary, an efficient adaptive immune response to control the infection greatly depends on the preceding innate response. Therefore, it is critical to understand how viral factors may contribute to modulate these networks.

1.2.9 Complement system

The complement system consists of a cascade of proteolytic interactions that lead to the direct killing of the pathogen or infected cell, as well as to the recruitment of proinflammatory immune cells (Fig. 11) (335,432,433). Remarkably, the central component of this system (C3) has been found within the mucus barrier (Fig. 1.5; 1.7) (260), which elucidates the role of complement in early immune response in the airways.

There are three pathways of complement activation. The classical pathway (CP) is activated by the binding of C1q to IgG or IgM bound to the antigen. On the other hand, the lectin pathway (LP) is activated by

the binding of mannose-binding lectin (MBL) or ficolins to pathogen sugars, and subsequent activation of MBL-associated serine protease 1 (MASP-1) and 2 (MASP-2). The alternative pathway (AP) is activated upon the spontaneous hydrolysis of C3 and ensures a basal level of complement activation. Moreover, when needed, it provides a positive feedback loop to amplify complement activation. The three pathways converge in the cleavage of C3, making it the central piece in the complement system (335,432).

The C3 convertases (CP/LP – C4b2a; AP – C3bBb) cleave C3 in C3a and C3b. C3a is a chemoattractant for neutrophils, monocytes and T cells (434–436). C3b is an opsonin, promoting the opsonization and phagocytosis of the pathogen (335,432). The C5 convertases (CP/LP – C4b2aC3b; AP – C3bBbC3b) are formed by the binding of a C3b molecule to a C3 convertase and, when assembled, they cleave C5 in C5a and C5b (335,432). C5a is an anaphylatoxin (434,435,437,438), while C5b deposits on the surface of the target membrane and recruits C6, C7, C8 and C9 to form the membrane attack complex (MAC) C5b-9 (335,432). Considering its hybrid nature, the complement system bridges innate and adaptive immune systems.

Complement has been shown to be activated upon IAV infection (435,436,439,440), and is able to directly neutralize virions by the deposition of C3 and C4 on their surface (441). Furthermore, C3 is required for efficient viral clearance *in vivo* (440,442). However, complement has been described to exacerbate lung injury by C5a-mediated recruitment of monocytes, neutrophils and T cells (434,437,438,443). Recent reports also link IAV-induced excessive complement activation to systemic effects, such as increased risk of myocardial infarction (408,410,444). Therefore, further studies are required to dissect complement-induced modulation of the immune response.

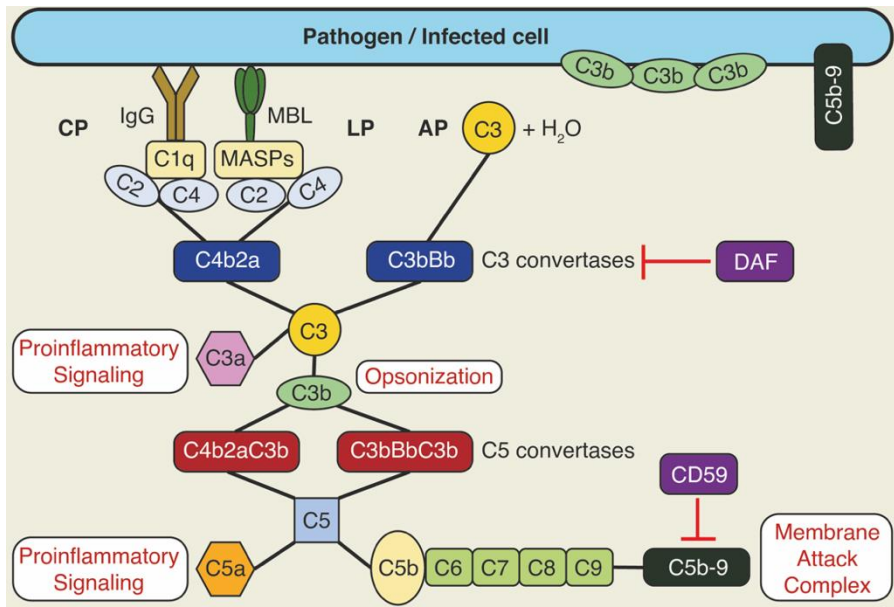


Fig. 1.11 – Simplified representation of complement pathway.

Complement system bridges the innate and adaptive immune system. There are three pathways of activation. In classical pathway (CP), C1q binds to IgG at the surface of the pathogen or infected cell. Similarly, in the lectin pathway (LP), lectins such as mannose-binding lectin (MBL) bind danger- or pathogen-associated molecular patterns (DAMPs or PAMPs, respectively). Both pathways meet in the formation of C4b2a C3 convertase, which will then cleave C3. The alternative pathway (AP) is activated by the spontaneous cleavage of C3, and forms the AP C3 convertase C3bBb. The three pathways converge in C3, making it the central molecule in the complement pathway. C4b2a and C3bBb cleave C3 into C3a and C3b. C3a is an anaphylatoxin, which promotes inflammation. A C3b molecule associates with a C3 convertase, forming the C5 convertases C4b2aC3b (CP, LP) or C3bBbC3b (AP). Additionally, C3b directly inhibits the pathogen by promoting opsonization. C5 convertases break C5 into C5a and C5b. As C3a, C5a is an anaphylatoxin. C5b instead, recruits C6 and initiates a chain of associated molecules that results in the formation of the membrane attack complex (MAC) C5b-9, a cytolytic pore that deposits at the surface of the infected cell or pathogen. As complement is not specific, the host has regulators of complement activation (RCAs) which prevent activation in

steady state. The two RCAs addressed in this work are the complement decay accelerating factor (DAF) and CD59, which inhibit the C3 convertases and the assembly of C5b-9, respectively.

1.2.10 Complement decay-accelerating factor (DAF)

The complement system is a potent yet nonspecific mechanism that needs tight regulation. Membrane-bound or soluble regulators of complement activation (RCAs) prevent excessive complement activation by inhibiting specific steps of the pathway, thus protecting healthy host cells (Fig. 1.12) (445,446). RCAs inhibit different steps of the complement cascade. The membrane-bound complement decay-accelerating factor (DAF or CD55), membrane cofactor protein (MCP, CD46), human complement receptor type 1 (CR1, CD35) and murine complement receptor 1-related gene/protein Y (Crry) possess a variable number of short consensus repeats (SCRs), which inhibit convertase activity (445,446). On the other hand, CD59 structure does not resemble the remaining membrane-bound RCAs, and it hinders the assembly of the MAC C5b-9, the same target of the soluble RCAs clusterin and vitronectin (445,446). Complement factor H (fH) blocks complement activation by binding to specific glycans at cell surface. Factor I (fI) is a plasma serine protease that cleaves complement C3b and C4b into the inactive or less reactive forms iC3b, C3c and C3d or iC4b, C3c and C3d, respectively.

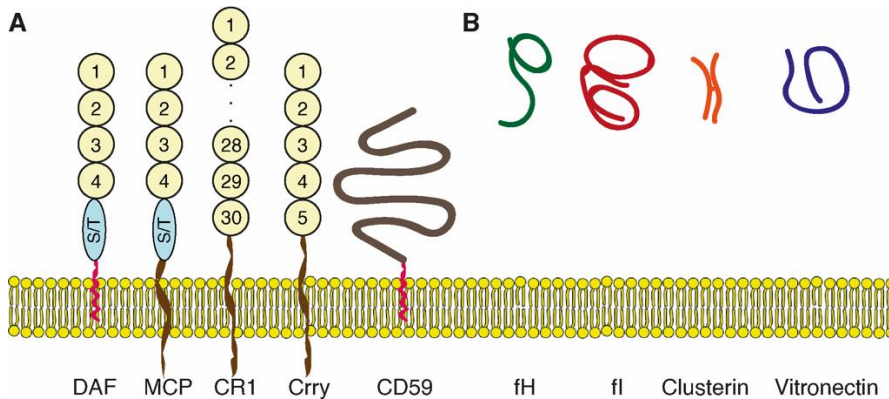


Fig. 1.12 – Regulators of complement activation (adapted from (445)).

As complement is a non-specific mechanism, regulators of complement activation (RCAs) prevent complement attack in steady state. **A:** Membrane-bound RCAs complement decay-accelerating factor (DAF, CD55), membrane cofactor protein (MCP, CD46), complement receptor type 1 (CR1, CD35; human), complement receptor 1-related gene/protein Y (Crry; murine) and CD59. DAF, MCP, CR1 and Crry have a variable number of short consensus repeats (SCRs) that inhibit complement C3 convertases. CD59 presents a unique structure upon the membrane-bound RCAs, and prevents the formation of the membrane attack complex C5b-9. DAF and CD59 possess a GPI anchor, while MCP, CR1 and Crry are transmembrane proteins. **B:** Soluble RCAs factor H (fH), factor I (fI), clusterin and vitronectin. fH binds host specific glycans and blocks complement activation. fI is a protease, that cleaves C3b and C4b in inactive subproducts. Clusterin and vitronectin prevent the assembly of C5b-9.

One of the membrane-bound RCAs is DAF, which inhibits the assembly of C3 convertases through the action of its modular complement regulation domains (Fig. 6) (447–450). In humans, it has been observed that DAF deficiency increased complement activation with severe systemic implications (451–454). Furthermore, DAF deregulation may also impact immune cell recruitment by increased C3b and C5a release, resulting in augmented neutrophil infiltration (455).

Besides its role in regulating complement activity, DAF performs alternative functions (454), as evidenced by its ability to bind immune cells expressing the adhesion G protein-coupled receptor CD97 (456–459). Remarkably, DAF was shown to maintain its RCA activity while bound to CD97 (459), thus suggesting that DAF may decrease complement activation while increasing leukocyte recruitment (456,459). This model is attractive, as macrophages and neutrophils express CD97 (460,461). In fact, neutrophil migration in the lungs requires CD97, as mice treated with α -CD97 and challenged with *S. pneumoniae* presented lower neutrophil levels in the lungs (460).

However, as DAF-CD97 is a low affinity ligation (462), DAF is able to perform beyond CD97. In the apical side of epithelial cells, DAF helps neutrophils transmigrate from the endothelial to the luminal site, independently of CD97 (463). Remarkably, the level of transmigration correlates with the severity of the inflammatory disease (463). On the other hand, DAF is induced upon hypoxia by hypoxia-inducible factors (HIFs) and promotes neutrophil transmigration and clearance, suggesting a mechanism of protection of the mucosae from excessive inflammation (464). However, it has also been shown that the HIF-1 α downregulates DAF expression in mice lungs, promoting locally increased complement activation (465). Taken together, these results suggest a feedback mechanism of DAF regulation upon hypoxia in the airways, which should be further explored.

In summary, these studies elucidate DAF potential in modulating the immune response to invading pathogens. Further supporting this, genomics studies in the aftermath of the 2009 IAV pandemic identified DAF downregulation as a putative contributor to poor disease outcome, associated with increased complement activation (466–468). As DAF is a heavily sialylated glycosylphosphatidylinositol-anchored protein (GPI-AP), being exposed at the surface of most cell types, including the

human and murine airways (465,469–474), it makes it a particularly interesting factor upon IAV infection.

1.2.11 Sialic acid

Sialic acid is an ubiquitous terminal nine-carbon monosaccharide modification in proteins with multiple functional implications in biological events both in health and disease, including signaling in cell proliferation, differentiation and immune response (Fig. 1.13) (475,476).

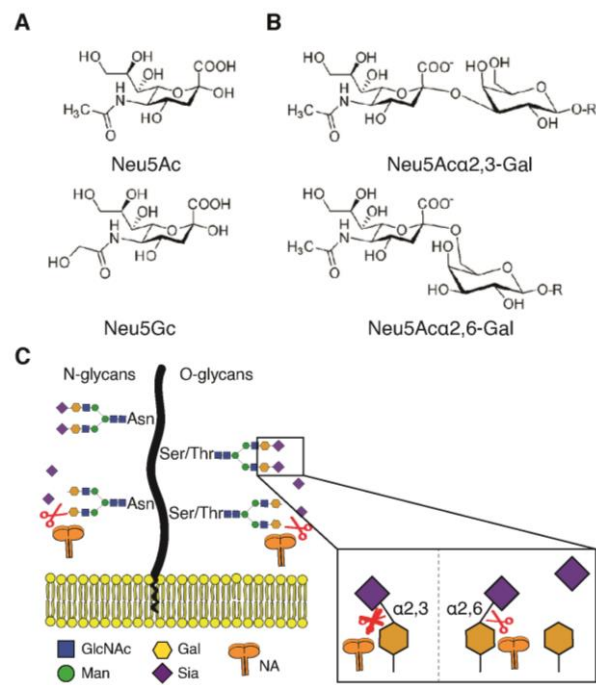


Fig. 1.13 – Sialic acid structure.

A: Sialic acid is a nine-carbon monosaccharide modification, being the most abundant N-acetylneuraminic acid (Neu5Ac) and N-glycolylneuraminic acid (Neu5Gc). Remarkably, humans do not express Neu5Gc. **B:** Sialic acid residues are connected to glycan chains by α 2,6- or α 2,3-linkages. **C:** NAs exhibit preference for sialic acid linkages. Avian-adapted strains cleave α 2,3-linked sialic acid, while human-adapted cleave α 2,6-linkages.

In immunity regulation, it has been shown that sialic acid is involved in complement activation (477–479), sialic acid-binding immunoglobulin-type lectin (Siglec)-mediated self- vs. non self-recognition by masking specific epitopes (480,481), as well as in IgG regulation at Fc or Fab domains (482,483). Furthermore, desialylation by host or microbial sialidases has been reported to activate neutrophils and monocytes (484–486).

The role of sialic acid has also been reported in secondary infection by *S. pneumoniae*, as it utilizes sialic acid released upon IAV infection to proliferate (487). It has also been proposed that IAV may cause localized immunodeficiency in the airways by altering IgA clearance kinetics through sialic acid cleavage (488).

Recently, it has been shown that high mannose at the surface of IAV infected cells activates the complement via the LP (489), demonstrating the role of sugars in cell recognition. Thus, viral-induced alterations in sialic acid levels may pose relevant functional implications in immune response.

1.3 Final remarks

Host-pathogen interactions are very complex and ultimately the progression and outcome of viral infections results from viral and host factors. Viruses are equipped with PAMPs that alert the host of their presence. The host possesses PRRs that detect the pathogen and initiate the immune response. It is generally accepted that for viral infections an aggressive initial innate immune activation favors the host, whilst mechanisms that prolong inflammation are detrimental, and associated with severe outcomes. This paradigm underpins for example the sex differences observed for coronavirus disease 2019 (COVID-19) that leads to reduced number of deaths in women, despite similar incidence of infection in both sexes (490,491).

On the other hand, evidence suggests that the host response to a pathogen challenge needs to be fine-tuned, with any deviations from such equilibrium being detrimental. Damage may be inflicted by the pathogen itself, or by an excessive immune attack resulting in immunopathology (492).

The ultimate outcome of infection is either host survival or death (Fig. 1.14-A). Host protection may be conceded by one of two distinct mechanisms: disease resistance or disease tolerance (261,493). Disease resistance consists in eliminating the pathogen with an adequate immune response, and is illustrated by lower pathogen loads when compared to a control (Fig. 1.14-B). On the other hand, disease tolerance entails host resilience to infection that is achieved by preventing immunopathology. It is characterized by lower tissue damage despite unaltered pathogen loads (Fig. 1.14-C). Therefore, the threshold of the immune response needed to clear the pathogen without provoking immunopathology is very subtle.

In respiratory viral infections, including IAV, severe complications usually derive from an exacerbated immune response that provokes tissue damage (Fig. 1.14-D) (494,495).

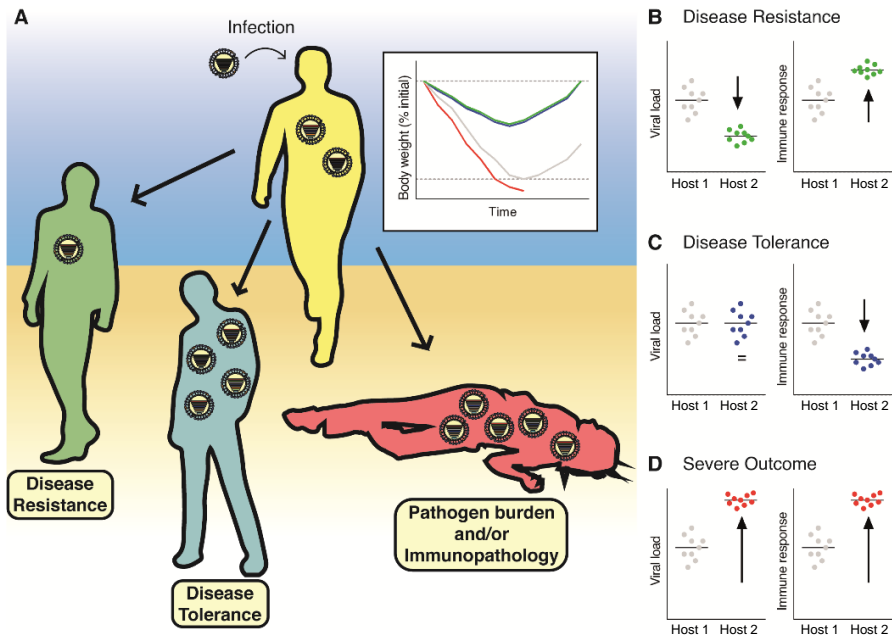


Fig. 1.14 – Representation of possible infection outcomes.

A: Upon infection with a pathogen such as IAV, disease may progress differently, as illustrated by body weight loss. **B:** Disease resistance occurs when a host immune system efficiently clears the pathogen, thus preventing a severe outcome. **C:** Disease tolerance arises when, while sustaining similar pathogen loads, a host immune response is regulated and prevents unnecessary tissue damage. **D:** Severe or fatal outcomes result from uncontrolled pathogen loads and/or immunopathology from a disproportionate immune response.

Remarkably, tissue damage poses the opportunity for secondary bacterial infections, increasing morbidity and mortality after viral infections (18,19,487,496). Therefore, minimizing immunopathology in the lungs is of utmost importance.

Pandemic viral infections caused by IAV and the recent severe acute respiratory coronavirus 2 (SARS-CoV-2) exhibit a very heterogeneous and non-linear disease progression (497). Identifying intrinsic risk factors, understanding how host and viral determinants

work in concert and contribute to this heterogeneity may uncover new therapeutic targets with decreased proneness to develop resistance.

Recently, defects in type I IFN response have been associated with the more severe cases of COVID-19 (498,499), suggesting that the initial immune response defines the disease outcome. Nevertheless, there are other players involved in mounting the immune response, such as the complement system. Disease severity and mortality have been associated with excessive complement activation in several viral infections such as severe acute respiratory syndrome coronavirus (SARS-CoV) (443,500), middle eastern respiratory syndrome coronavirus (MERS-CoV) (501), SARS-CoV-2 (502,503) and IAV (434,437,438). However, it is still unclear how fine-tuning complement activation may impact in the development of disease severity. One way to address this is by targeting complement regulators.

1.4 Aims and general objectives

1.4.1 Aims and general objectives

It is well accepted that viral pathogenesis results from the interaction of host and viral factors. Several host factors contributing to pathology have been identified, however more factors likely remain to be elucidated. Moreover, how these factors interact is still poorly understood. In this work, we aim to explore host and viral factors that contribute to IAV-induced pathogenesis. Specifically, we focus on the host sialylated complement regulator DAF, and the viral proteins that bind and cleave sialic acid, HA and NA, respectively (Fig. 1.15).

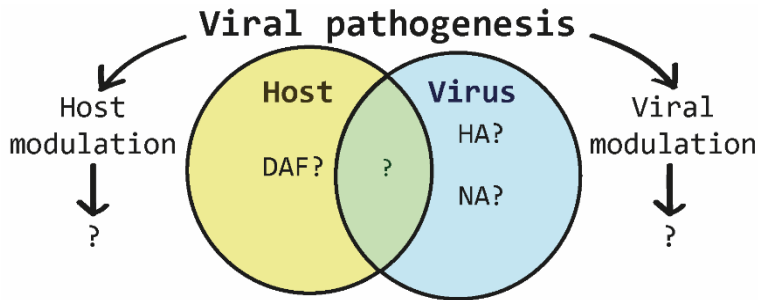


Fig. 1.15 – Objectives proposed for this thesis.

In this work we aim to dissect host and viral factors that could modulate viral pathogenesis. Particularly, we will focus on the interplay between the host protein DAF, with the viral proteins HA and NA.

1.4.2 Chapter 2 – Complement decay-accelerating factor increases immunopathology via complement activation and immune cell recruitment

DAF inhibits complement attack, hence we would expect increased complement activation in DAF depleted mice, with consequences to tissue damage and/or viral clearance. Preliminary data indicated that DAF contributed to IAV pathology, without altering viral loads. We dissected the immune response in the absence of DAF, and its role in complement activation. Furthermore, we studied the detrimental role of DAF upon infection with different reassortant viruses, defining the role of DAF-HA and DAF-NA interactions to the immune response.

1.4.3 Chapter 3 – Influenza A virus neuraminidase cleaves sialic acid from the complement decay-accelerating factor and activates complement

In the previous chapter we observed that DAF-NA interactions modulate the innate immune response. DAF is a sialylated protein, and it has been proposed that NA could cleave sialic acid from host proteins, with impact in the immune response. Here we tested the ability of NA to

cleave DAF sialic acid moieties, and explored a mechanism that may link to exacerbation of *in vivo* pathology.

1.4.4 Chapter 4 – Mutation S110L of H1N1 influenza A virus hemagglutinin: a potent determinant of attenuation

In the previous chapters we focused on how the interaction between a host and viral factors contributes to pathology, without affecting viral loads. Here, we assessed the role of a mutation in viral protein HA in conferring attenuation, thus providing an alternative mechanism of modulating viral-induced pathogenesis.

1.4 References

1. Pappas G, Kiriaze IJ, Falagas ME. Insights into infectious disease in the era of Hippocrates. *Int J Infect Dis*. 2008 Jul;12(4):347–50.
2. Morens DM, Taubenberger JK. Pandemic influenza: certain uncertainties. *Rev Med Virol*. 2011 Sep;21(5):262–84.
3. Shope RE. THE ETIOLOGY OF SWINE INFLUENZA. *Science*. 1931 Feb 20;73(1886):214–5.
4. Smith W, Andrewes CH, Laidlaw PP. A VIRUS OBTAINED FROM INFLUENZA PATIENTS. *The Lancet*. 1933 Jul;222(5732):66–8.
5. WHO. Influenza (Seasonal) [Internet]. [cited 2021 Feb 9]. Available from: [https://www.who.int/en/news-room/fact-sheets/detail/influenza-\(seasonal\)](https://www.who.int/en/news-room/fact-sheets/detail/influenza-(seasonal))
6. Iuliano AD, Roguski KM, Chang HH, Muscatello DJ, Palekar R, Tempia S, et al. Estimates of global seasonal influenza-associated respiratory mortality: a modelling study. *Lancet*. 2018 Mar 31;391(10127):1285–300.
7. Mettelman RC, Thomas PG. Human Susceptibility to Influenza Infection and Severe Disease. *Cold Spring Harb Perspect Med*. 2020 Jan 21;
8. Krammer F, Smith GJD, Fouchier RAM, Peiris M, Kedzierska K, Doherty PC, et al. Influenza. *Nat Rev Dis Primers*. 2018 Jun 28;4(1):3.
9. Taubenberger JK, Kash JC. Influenza virus evolution, host adaptation, and pandemic formation. *Cell Host Microbe*. 2010 Jun 25;7(6):440–51.
10. Taubenberger JK, Morens DM. 1918 Influenza: the mother of all pandemics. *Emerg Infect Dis*. 2006 Jan;12(1):15–22.
11. Neumann G, Noda T, Kawaoka Y. Emergence and pandemic potential of swine-origin H1N1 influenza virus. *Nature*. 2009 Jun 18;459(7249):931–9.
12. Dawood FS, Iuliano AD, Reed C, Meltzer MI, Shay DK, Cheng P-Y, et al. Estimated global mortality associated with the first 12 months of 2009 pandemic influenza A H1N1 virus circulation: a modelling study. *Lancet Infect Dis*. 2012 Sep;12(9):687–95.
13. Hurt AC, Chotpitayasunondh T, Cox NJ, Daniels R, Fry AM, Gubareva LV, et al. Antiviral resistance during the 2009 influenza A H1N1 pandemic: public health, laboratory, and clinical perspectives. *Lancet Infect Dis*. 2012 Mar;12(3):240–8.
14. Krammer F. The human antibody response to influenza A virus infection and vaccination. *Nat Rev Immunol*. 2019 Jun;19(6):383–97.
15. Taubenberger JK, Morens DM. The pathology of influenza virus infections. *Annu Rev Pathol*. 2008;3:499–522.
16. Short KR, Kroeze EJBV, Fouchier RAM, Kuiken T. Pathogenesis of influenza-induced acute respiratory distress syndrome. *Lancet Infect Dis*. 2014 Jan;14(1):57–69.
17. Perrone LA, Plowden JK, García-Sastre A, Katz JM, Tumpey TM. H5N1 and 1918 pandemic influenza virus infection results in early and excessive infiltration of macrophages and neutrophils in the lungs of mice. *PLoS Pathog*. 2008 Aug 1;4(8):e1000115.

18. Kash JC, Taubenberger JK. The role of viral, host, and secondary bacterial factors in influenza pathogenesis. *Am J Pathol.* 2015 Jun;185(6):1528–36.
19. Melvin JA, Bomberger JM. Compromised Defenses: Exploitation of Epithelial Responses During Viral-Bacterial Co-Infection of the Respiratory Tract. *PLoS Pathog.* 2016 Sep;12(9):e1005797.
20. Morens DM, Taubenberger JK, Fauci AS. Predominant role of bacterial pneumonia as a cause of death in pandemic influenza: implications for pandemic influenza preparedness. *J Infect Dis.* 2008 Oct 1;198(7):962–70.
21. Wille M, Holmes EC. The Ecology and Evolution of Influenza Viruses. *Cold Spring Harb Perspect Med.* 2020 Jul 1;10(7).
22. Hutchinson EC, Yamauchi Y. Understanding Influenza. *Methods Mol Biol.* 2018;1836:1–21.
23. International Committee on Taxonomy of Viruses. Taxonomy [Internet]. [cited 2021 Feb 27]. Available from: <https://talk.ictvonline.org/taxonomy/>
24. Nobusawa E, Sato K. Comparison of the mutation rates of human influenza A and B viruses. *J Virol.* 2006 Apr;80(7):3675–8.
25. Caini S, Kuszniierz G, Garate VV, Wangchuk S, Thapa B, de Paula Júnior FJ, et al. The epidemiological signature of influenza B virus and its B/Victoria and B/Yamagata lineages in the 21st century. *PLoS One.* 2019;14(9):e0222381.
26. WHO. Recommended composition of influenza virus vaccines for use in the 2021 southern hemisphere influenza season [Internet]. [cited 2021 Feb 9]. Available from: https://www.who.int/influenza/vaccines/virus/recommendations/2021_south/en/
27. Taylor RM. Studies on survival of influenza virus between epidemics and antigenic variants of the virus. *Am J Public Health Nations Health.* 1949 Feb;39(2):171–8.
28. Fritsch A, Schweiger B, Biere B. Influenza C virus in pre-school children with respiratory infections: retrospective analysis of data from the national influenza surveillance system in Germany, 2012 to 2014. *Euro Surveill.* 2019 Mar;24(10).
29. Sederdahl BK, Williams JV. Epidemiology and Clinical Characteristics of Influenza C Virus. *Viruses.* 2020 Jan 13;12(1).
30. Hause BM, Ducatez M, Collin EA, Ran Z, Liu R, Sheng Z, et al. Isolation of a novel swine influenza virus from Oklahoma in 2011 which is distantly related to human influenza C viruses. *PLoS Pathog.* 2013 Feb;9(2):e1003176.
31. Collin EA, Sheng Z, Lang Y, Ma W, Hause BM, Li F. Cocirculation of two distinct genetic and antigenic lineages of proposed influenza D virus in cattle. *J Virol.* 2015 Jan 15;89(2):1036–42.
32. Liu R, Sheng Z, Huang C, Wang D, Li F. Influenza D virus. *Curr Opin Virol.* 2020 Oct;44:154–61.
33. Asha K, Kumar B. Emerging Influenza D Virus Threat: What We Know so Far! *J Clin Med.* 2019 Feb 5;8(2).
34. Su S, Fu X, Li G, Kerlin F, Veit M. Novel Influenza D virus: Epidemiology, pathology, evolution and biological characteristics. *Virulence.* 2017 Nov 17;8(8):1580–91.

35. Shaw ML, Stone KL, Colangelo CM, Gulcicek EE, Palese P. Cellular proteins in influenza virus particles. *PLoS Pathog*. 2008 Jun 6;4(6):e1000085.
36. Hutchinson EC, Charles PD, Hester SS, Thomas B, Trudgian D, Martínez-Alonso M, et al. Conserved and host-specific features of influenza virion architecture. *Nat Commun*. 2014 Sep 16;5:4816.
37. Horisberger MA. The large P proteins of influenza A viruses are composed of one acidic and two basic polypeptides. *Virology*. 1980 Nov;107(1):302–5.
38. Guilligay D, Tarendeau F, Resa-Infante P, Coloma R, Crepin T, Sehr P, et al. The structural basis for cap binding by influenza virus polymerase subunit PB2. *Nat Struct Mol Biol*. 2008 May;15(5):500–6.
39. Honda A, Mukaigawa J, Yokoiyama A, Kato A, Ueda S, Nagata K, et al. Purification and molecular structure of RNA polymerase from influenza virus A/PR8. *J Biochem*. 1990 Apr;107(4):624–8.
40. Murti KG, Webster RG, Jones IM. Localization of RNA polymerases on influenza viral ribonucleoproteins by immunogold labeling. *Virology*. 1988 Jun;164(2):562–6.
41. Detjen BM, St Angelo C, Katze MG, Krug RM. The three influenza virus polymerase (P) proteins not associated with viral nucleocapsids in the infected cell are in the form of a complex. *J Virol*. 1987 Jan;61(1):16–22.
42. Hsu MT, Parvin JD, Gupta S, Krystal M, Palese P. Genomic RNAs of influenza viruses are held in a circular conformation in virions and in infected cells by a terminal panhandle. *Proc Natl Acad Sci U S A*. 1987 Nov;84(22):8140–4.
43. Pons MW, Schulze IT, Hirst GK, Hauser R. Isolation and characterization of the ribonucleoprotein of influenza virus. *Virology*. 1969 Oct;39(2):250–9.
44. Arranz R, Coloma R, Chichón FJ, Conesa JJ, Carrascosa JL, Valpuesta JM, et al. The structure of native influenza virion ribonucleoproteins. *Science*. 2012 Dec 21;338(6114):1634–7.
45. Moeller A, Kirchdoerfer RN, Potter CS, Carragher B, Wilson IA. Organization of the influenza virus replication machinery. *Science*. 2012 Dec 21;338(6114):1631–4.
46. Yamanaka K, Ishihama A, Nagata K. Reconstitution of influenza virus RNA-nucleoprotein complexes structurally resembling native viral ribonucleoprotein cores. *J Biol Chem*. 1990 Jul 5;265(19):11151–5.
47. Inglis SC, Carroll AR, Lamb RA, Mahy BW. Polypeptides specified by the influenza virus genome I. Evidence for eight distinct gene products specified by fowl plague virus. *Virology*. 1976 Oct 15;74(2):489–503.
48. Richardson JC, Akkina RK. NS2 protein of influenza virus is found in purified virus and phosphorylated in infected cells. *Arch Virol*. 1991;116(1–4):69–80.
49. Yasuda J, Nakada S, Kato A, Toyoda T, Ishihama A. Molecular assembly of influenza virus: association of the NS2 protein with virion matrix. *Virology*. 1993 Sep;196(1):249–55.
50. Pinto RM, Lycett S, Gaunt E, Digard P. Accessory Gene Products of Influenza A Virus. *Cold Spring Harb Perspect Med*. 2020 Sep 28;
51. Enami K, Sato TA, Nakada S, Enami M. Influenza virus NS1 protein stimulates translation of the M1 protein. *J Virol*. 1994 Mar;68(3):1432–7.

52. Panthu B, Terrier O, Carron C, Traversier A, Corbin A, Balvay L, et al. The NS1 Protein from Influenza Virus Stimulates Translation Initiation by Enhancing Ribosome Recruitment to mRNAs. *J Mol Biol.* 2017 Oct 27;429(21):3334–52.
53. Trapp S, Soubieux D, Lidove A, Esnault E, Lion A, Guillory V, et al. Major contribution of the RNA-binding domain of NS1 in the pathogenicity and replication potential of an avian H7N1 influenza virus in chickens. *Virology.* 2018 Mar 27;15(1):55.
54. Nemeroff ME, Barabino SM, Li Y, Keller W, Krug RM. Influenza virus NS1 protein interacts with the cellular 30 kDa subunit of CPSF and inhibits 3' end formation of cellular pre-mRNAs. *Mol Cell.* 1998 Jun;1(7):991–1000.
55. Aragón T, de la Luna S, Novoa I, Carrasco L, Ortín J, Nieto A. Eukaryotic translation initiation factor 4GI is a cellular target for NS1 protein, a translational activator of influenza virus. *Mol Cell Biol.* 2000 Sep;20(17):6259–68.
56. Garaigorta U, Falcón AM, Ortín J. Genetic analysis of influenza virus NS1 gene: a temperature-sensitive mutant shows defective formation of virus particles. *J Virol.* 2005 Dec;79(24):15246–57.
57. Mor A, White A, Zhang K, Thompson M, Esparza M, Muñoz-Moreno R, et al. Influenza virus mRNA trafficking through host nuclear speckles. *Nat Microbiol.* 2016 May 27;1(7):16069.
58. García-Sastre A, Egorov A, Matasov D, Brandt S, Levy DE, Durbin JE, et al. Influenza A virus lacking the NS1 gene replicates in interferon-deficient systems. *Virology.* 1998 Dec 20;252(2):324–30.
59. Bergmann M, Garcia-Sastre A, Carnero E, Pehamberger H, Wolff K, Palese P, et al. Influenza virus NS1 protein counteracts PKR-mediated inhibition of replication. *J Virol.* 2000 Jul;74(13):6203–6.
60. Muñoz-Moreno R, Martínez-Romero C, García-Sastre A. Induction and Evasion of Type-I Interferon Responses during Influenza A Virus Infection. *Cold Spring Harb Perspect Med.* 2020 Jul 6;
61. O'Neill RE, Talon J, Palese P. The influenza virus NEP (NS2 protein) mediates the nuclear export of viral ribonucleoproteins. *EMBO J.* 1998 Jan 2;17(1):288–96.
62. Robb NC, Smith M, Vreede FT, Fodor E. NS2/NEP protein regulates transcription and replication of the influenza virus RNA genome. *J Gen Virol.* 2009 Jun;90(Pt 6):1398–407.
63. Gorai T, Goto H, Noda T, Watanabe T, Kozuka-Hata H, Oyama M, et al. F1Fo-ATPase, F-type proton-translocating ATPase, at the plasma membrane is critical for efficient influenza virus budding. *Proc Natl Acad Sci U S A.* 2012 Mar 20;109(12):4615–20.
64. Paterson D, Fodor E. Emerging roles for the influenza A virus nuclear export protein (NEP). *PLoS Pathog.* 2012;8(12):e1003019.
65. Yamayoshi S, Watanabe M, Goto H, Kawaoka Y. Identification of a Novel Viral Protein Expressed from the PB2 Segment of Influenza A Virus. *J Virol.* 2016 Jan 1;90(1):444–56.
66. Chen W, Calvo PA, Malide D, Gibbs J, Schubert U, Bacik I, et al. A novel influenza A virus mitochondrial protein that induces cell death. *Nat Med.* 2001 Dec;7(12):1306–12.
67. Akkina RK, Richardson JC, Aguilera MC, Yang CM. Heterogeneous forms of

polymerase proteins exist in influenza A virus-infected cells. *Virus Res.* 1991 Mar;19(1):17–30.

68. Wise HM, Foeglein A, Sun J, Dalton RM, Patel S, Howard W, et al. A complicated message: Identification of a novel PB1-related protein translated from influenza A virus segment 2 mRNA. *J Virol.* 2009 Aug;83(16):8021–31.

69. Muramoto Y, Noda T, Kawakami E, Akkina R, Kawaoka Y. Identification of novel influenza A virus proteins translated from PA mRNA. *J Virol.* 2013 Mar;87(5):2455–62.

70. Firth AE, Jagger BW, Wise HM, Nelson CC, Parsawar K, Wills NM, et al. Ribosomal frameshifting used in influenza A virus expression occurs within the sequence UCC_UUU_CGU and is in the +1 direction. *Open Biol.* 2012 Oct;2(10):120109.

71. Jagger BW, Wise HM, Kash JC, Walters K-A, Wills NM, Xiao Y-L, et al. An overlapping protein-coding region in influenza A virus segment 3 modulates the host response. *Science.* 2012 Jul 13;337(6091):199–204.

72. Khapersky DA, Emara MM, Johnston BP, Anderson P, Hatchette TF, McCormick C. Influenza A virus host shutoff disables antiviral stress-induced translation arrest. *PLoS Pathog.* 2014 Jul;10(7):e1004217.

73. Wanitchang A, Patarasirin P, Jengarn J, Jongkaewwattana A. Atypical characteristics of nucleoprotein of pandemic influenza virus H1N1 and their roles in reassortment restriction. *Arch Virol.* 2011 Jun;156(6):1031–40.

74. Machkovech HM, Bloom JD, Subramaniam AR. Comprehensive profiling of translation initiation in influenza virus infected cells. *PLoS Pathog.* 2019 Jan;15(1):e1007518.

75. Lamb RA, Lai CJ. Conservation of the influenza virus membrane protein (M1) amino acid sequence and an open reading frame of RNA segment 7 encoding a second protein (M2) in H1N1 and H3N2 strains. *Virology.* 1981 Jul 30;112(2):746–51.

76. Wise HM, Hutchinson EC, Jagger BW, Stuart AD, Kang ZH, Robb N, et al. Identification of a novel splice variant form of the influenza A virus M2 ion channel with an antigenically distinct ectodomain. *PLoS Pathog.* 2012;8(11):e1002998.

77. Kuo R-L, Li L-H, Lin S-J, Li Z-H, Chen G-W, Chang C-K, et al. Role of N Terminus-Truncated NS1 Proteins of Influenza A Virus in Inhibiting IRF3 Activation. *J Virol.* 2016 May;90(9):4696–705.

78. Selman M, Dankar SK, Forbes NE, Jia J-J, Brown EG. Adaptive mutation in influenza A virus non-structural gene is linked to host switching and induces a novel protein by alternative splicing. *Emerg Microbes Infect.* 2012 Nov;1(11):e42.

79. Yewdell JW, Antón LC, Bennink JR. Defective ribosomal products (DRiPs): a major source of antigenic peptides for MHC class I molecules? *J Immunol.* 1996 Sep 1;157(5):1823–6.

80. Ho JSY, Angel M, Ma Y, Sloan E, Wang G, Martinez-Romero C, et al. Hybrid Gene Origination Creates Human-Virus Chimeric Proteins during Infection. *Cell.* 2020 Jun 25;181(7):1502-1517.e23.

81. Palese P, Schulman JL. Mapping of the influenza virus genome: identification of the hemagglutinin and the neuraminidase genes. *Proc Natl Acad Sci U S A.* 1976 Jun;73(6):2142–6.

82. Compans RW, Content J, Duesberg PH. Structure of the ribonucleoprotein of influenza virus. *J Virol.* 1972 Oct;10(4):795–800.
83. Lamb RA, Etkind PR, Choppin PW. Evidence for a ninth influenza viral polypeptide. *Virology.* 1978 Nov;91(1):60–78.
84. Einfeld AJ, Neumann G, Kawaoka Y. At the centre: influenza A virus ribonucleoproteins. *Nat Rev Microbiol.* 2015 Jan;13(1):28–41.
85. Dou D, Revol R, Östbye H, Wang H, Daniels R. Influenza A Virus Cell Entry, Replication, Virion Assembly and Movement. *Front Immunol.* 2018;9:1581.
86. Watanabe T, Watanabe S, Kawaoka Y. Cellular networks involved in the influenza virus life cycle. *Cell Host Microbe.* 2010 Jun 25;7(6):427–39.
87. Amorim MJ. A Comprehensive Review on the Interaction Between the Host GTPase Rab11 and Influenza A Virus. *Front Cell Dev Biol.* 2018;6:176.
88. Ito T, Suzuki Y, Suzuki T, Takada A, Horimoto T, Wells K, et al. Recognition of N-glycolylneuraminic acid linked to galactose by the alpha2,3 linkage is associated with intestinal replication of influenza A virus in ducks. *J Virol.* 2000 Oct;74(19):9300–5.
89. Suzuki Y, Ito T, Suzuki T, Holland RE, Chambers TM, Kiso M, et al. Sialic acid species as a determinant of the host range of influenza A viruses. *J Virol.* 2000 Dec;74(24):11825–31.
90. Kuchipudi SV, Nelli RK, Gontu A, Satyakumar R, Surendran Nair M, Subbiah M. Sialic Acid Receptors: The Key to Solving the Enigma of Zoonotic Virus Spillover. *Viruses.* 2021 Feb 8;13(2).
91. Yoon S-W, Webby RJ, Webster RG. Evolution and ecology of influenza A viruses. *Curr Top Microbiol Immunol.* 2014;385:359–75.
92. Joseph U, Su YCF, Vijaykrishna D, Smith GJD. The ecology and adaptive evolution of influenza A interspecies transmission. *Influenza Other Respir Viruses.* 2017 Jan;11(1):74–84.
93. Gamblin SJ, Vachieri SG, Xiong X, Zhang J, Martin SR, Skehel JJ. Hemagglutinin Structure and Activities. *Cold Spring Harb Perspect Med.* 2020 Jun 8;
94. Wang D, Zhu W, Yang L, Shu Y. The Epidemiology, Virology, and Pathogenicity of Human Infections with Avian Influenza Viruses. *Cold Spring Harb Perspect Med.* 2020 Jan 21;
95. Roy AM, Parker JS, Parrish CR, Whittaker GR. Early stages of influenza virus entry into Mv-1 lung cells: involvement of dynamin. *Virology.* 2000 Feb 1;267(1):17–28.
96. Chen C, Zhuang X. Epsin 1 is a cargo-specific adaptor for the clathrin-mediated endocytosis of the influenza virus. *Proc Natl Acad Sci U S A.* 2008 Aug 19;105(33):11790–5.
97. Sieczkarski SB, Whittaker GR. Influenza virus can enter and infect cells in the absence of clathrin-mediated endocytosis. *J Virol.* 2002 Oct;76(20):10455–64.
98. Rust MJ, Lakadamyali M, Zhang F, Zhuang X. Assembly of endocytic machinery around individual influenza viruses during viral entry. *Nat Struct Mol Biol.* 2004 Jun;11(6):567–73.
99. de Vries E, Tscherne DM, Wienholts MJ, Cobos-Jiménez V, Scholte F, García-Sastre A, et al. Dissection of the influenza A virus endocytic routes reveals

macropinocytosis as an alternative entry pathway. *PLoS Pathog.* 2011 Mar;7(3):e1001329.

100. Kajiwara N, Nomura N, Ukaji M, Yamamoto N, Kohara M, Yasui F, et al. Cell-penetrating peptide-mediated cell entry of H5N1 highly pathogenic avian influenza virus. *Sci Rep.* 2020 Oct 22;10(1):18008.

101. Huotari J, Helenius A. Endosome maturation. *EMBO J.* 2011 Aug 31;30(17):3481–500.

102. Bullough PA, Hughson FM, Skehel JJ, Wiley DC. Structure of influenza haemagglutinin at the pH of membrane fusion. *Nature.* 1994 Sep 1;371(6492):37–43.

103. Maeda T, Ohnishi S. Activation of influenza virus by acidic media causes hemolysis and fusion of erythrocytes. *FEBS Lett.* 1980 Dec 29;122(2):283–7.

104. Maeda T, Kawasaki K, Ohnishi S. Interaction of influenza virus hemagglutinin with target membrane lipids is a key step in virus-induced hemolysis and fusion at pH 5.2. *Proc Natl Acad Sci U S A.* 1981 Jul;78(7):4133–7.

105. White J, Helenius A, Gething MJ. Haemagglutinin of influenza virus expressed from a cloned gene promotes membrane fusion. *Nature.* 1982 Dec 16;300(5893):658–9.

106. Yoshimura A, Ohnishi S. Uncoating of influenza virus in endosomes. *J Virol.* 1984 Aug;51(2):497–504.

107. Lamb RA, Zebedee SL, Richardson CD. Influenza virus M2 protein is an integral membrane protein expressed on the infected-cell surface. *Cell.* 1985 Mar;40(3):627–33.

108. Holsinger LJ, Lamb RA. Influenza virus M2 integral membrane protein is a homotetramer stabilized by formation of disulfide bonds. *Virology.* 1991 Jul;183(1):32–43.

109. Stauffer S, Feng Y, Nebioglu F, Heilig R, Picotti P, Helenius A. Stepwise priming by acidic pH and a high K⁺ concentration is required for efficient uncoating of influenza A virus cores after penetration. *J Virol.* 2014 Nov;88(22):13029–46.

110. Su W-C, Chen Y-C, Tseng C-H, Hsu PW-C, Tung K-F, Jeng K-S, et al. Pooled RNAi screen identifies ubiquitin ligase Itch as crucial for influenza A virus release from the endosome during virus entry. *Proc Natl Acad Sci U S A.* 2013 Oct 22;110(43):17516–21.

111. Gschweil M, Ulbricht A, Barnes CA, Enchev RI, Stoffel-Studer I, Meyer-Schaller N, et al. A SPOPL/Cullin-3 ubiquitin ligase complex regulates endocytic trafficking by targeting EPS15 at endosomes. *Elife.* 2016 Mar 23;5:e13841.

112. Banerjee I, Miyake Y, Nobs SP, Schneider C, Horvath P, Kopf M, et al. Influenza A virus uses the aggresome processing machinery for host cell entry. *Science.* 2014 Oct 24;346(6208):473–7.

113. Rudnicka A, Yamauchi Y. Ubiquitin in Influenza Virus Entry and Innate Immunity. *Viruses.* 2016 Oct 24;8(10).

114. Miyake Y, Keusch JJ, Decamps L, Ho-Xuan H, Iketani S, Gut H, et al. Influenza virus uses transportin 1 for vRNP debundling during cell entry. *Nat Microbiol.* 2019 Apr;4(4):578–86.

115. Herz C, Stavnezer E, Krug R, Gurney T. Influenza virus, an RNA virus,

synthesizes its messenger RNA in the nucleus of infected cells. *Cell*. 1981 Nov;26(3 Pt 1):391–400.

116. Shapiro GI, Gurney T, Krug RM. Influenza virus gene expression: control mechanisms at early and late times of infection and nuclear-cytoplasmic transport of virus-specific RNAs. *J Virol*. 1987 Mar;61(3):764–73.

117. Amorim MJ, Digard P. Influenza A virus and the cell nucleus. *Vaccine*. 2006 Nov 10;24(44–46):6651–5.

118. Kemler I, Whittaker G, Helenius A. Nuclear import of microinjected influenza virus ribonucleoproteins. *Virology*. 1994 Aug 1;202(2):1028–33.

119. Lin BC, Lai CJ. The influenza virus nucleoprotein synthesized from cloned DNA in a simian virus 40 vector is detected in the nucleus. *J Virol*. 1983 Jan;45(1):434–8.

120. Jones IM, Reay PA, Philpott KL. Nuclear location of all three influenza polymerase proteins and a nuclear signal in polymerase PB2. *EMBO J*. 1986 Sep;5(9):2371–6.

121. Martin K, Helenius A. Transport of incoming influenza virus nucleocapsids into the nucleus. *J Virol*. 1991 Jan;65(1):232–44.

122. Fodor E. The RNA polymerase of influenza a virus: mechanisms of viral transcription and replication. *Acta Virol*. 2013;57(2):113–22.

123. Fodor E, Te Velthuis AJW. Structure and Function of the Influenza Virus Transcription and Replication Machinery. *Cold Spring Harb Perspect Med*. 2020 Sep 1;10(9).

124. Wandzik JM, Kouba T, Cusack S. Structure and Function of Influenza Polymerase. *Cold Spring Harb Perspect Med*. 2020 Apr 27;

125. Plotch SJ, Bouloy M, Ulmanen I, Krug RM. A unique cap(m7GpppXm)-dependent influenza virion endonuclease cleaves capped RNAs to generate the primers that initiate viral RNA transcription. *Cell*. 1981 Mar;23(3):847–58.

126. Reich S, Guilligay D, Pflug A, Malet H, Berger I, Crépin T, et al. Structural insight into cap-snatching and RNA synthesis by influenza polymerase. *Nature*. 2014 Dec 18;516(7531):361–6.

127. Fechter P, Mingay L, Sharps J, Chambers A, Fodor E, Brownlee GG. Two aromatic residues in the PB2 subunit of influenza A RNA polymerase are crucial for cap binding. *J Biol Chem*. 2003 May 30;278(22):20381–8.

128. Li ML, Rao P, Krug RM. The active sites of the influenza cap-dependent endonuclease are on different polymerase subunits. *EMBO J*. 2001 Apr 17;20(8):2078–86.

129. Etkind PR, Krug RM. Purification of influenza viral complementary RNA: its genetic content and activity in wheat germ cell-free extracts. *J Virol*. 1975 Dec;16(6):1464–75.

130. Kawakami E, Watanabe T, Fujii K, Goto H, Watanabe S, Noda T, et al. Strand-specific real-time RT-PCR for distinguishing influenza vRNA, cRNA, and mRNA. *J Virol Methods*. 2011 Apr;173(1):1–6.

131. Pflug A, Lukarska M, Resa-Infante P, Reich S, Cusack S. Structural insights into RNA synthesis by the influenza virus transcription-replication machine. *Virus Res*. 2017 Apr 15;234:103–17.

132. Neumann G, Hughes MT, Kawaoka Y. Influenza A virus NS2 protein mediates vRNP nuclear export through NES-independent interaction with hCRM1. *EMBO J.* 2000 Dec 15;19(24):6751–8.
133. Huang S, Chen J, Chen Q, Wang H, Yao Y, Chen J, et al. A second CRM1-dependent nuclear export signal in the influenza A virus NS2 protein contributes to the nuclear export of viral ribonucleoproteins. *J Virol.* 2013 Jan;87(2):767–78.
134. Hutchinson EC, von Kirchbach JC, Gog JR, Digard P. Genome packaging in influenza A virus. *J Gen Virol.* 2010 Feb;91(Pt 2):313–28.
135. Gavazzi C, Yver M, Isel C, Smyth RP, Rosa-Calatrava M, Lina B, et al. A functional sequence-specific interaction between influenza A virus genomic RNA segments. *Proc Natl Acad Sci U S A.* 2013 Oct 8;110(41):16604–9.
136. Le Sage V, Kanarek JP, Snyder DJ, Cooper VS, Lakdawala SS, Lee N. Mapping of Influenza Virus RNA-RNA Interactions Reveals a Flexible Network. *Cell Rep.* 2020 Jun 30;31(13):107823.
137. Dadonaite B, Gilbertson B, Knight ML, Trifkovic S, Rockman S, Laederach A, et al. The structure of the influenza A virus genome. *Nat Microbiol.* 2019 Nov;4(11):1781–9.
138. Lakdawala SS, Wu Y, Wawrzusin P, Kabat J, Broadbent AJ, Lamirande EW, et al. Influenza A virus assembly intermediates fuse in the cytoplasm. *PLoS Pathog.* 2014 Mar;10(3):e1003971.
139. Amorim MJ, Bruce EA, Read EKC, Foeglein A, Mahen R, Stuart AD, et al. A Rab11- and microtubule-dependent mechanism for cytoplasmic transport of influenza A virus viral RNA. *J Virol.* 2011 May;85(9):4143–56.
140. Momose F, Sekimoto T, Ohkura T, Jo S, Kawaguchi A, Nagata K, et al. Apical transport of influenza A virus ribonucleoprotein requires Rab11-positive recycling endosome. *PLoS One.* 2011;6(6):e21123.
141. Eisfeld AJ, Kawakami E, Watanabe T, Neumann G, Kawaoka Y. RAB11A is essential for transport of the influenza virus genome to the plasma membrane. *J Virol.* 2011 Jul;85(13):6117–26.
142. Vale-Costa S, Alenquer M, Sousa AL, Kellen B, Ramalho J, Tranfield EM, et al. Influenza A virus ribonucleoproteins modulate host recycling by competing with Rab11 effectors. *J Cell Sci.* 2016 Apr 15;129(8):1697–710.
143. de Castro Martin IF, Fournier G, Sachse M, Pizarro-Cerda J, Risco C, Naffakh N. Influenza virus genome reaches the plasma membrane via a modified endoplasmic reticulum and Rab11-dependent vesicles. *Nat Commun.* 2017 Nov 9;8(1):1396.
144. Alenquer M, Vale-Costa S, Etibor TA, Ferreira F, Sousa AL, Amorim MJ. Influenza A virus ribonucleoproteins form liquid organelles at endoplasmic reticulum exit sites. *Nat Commun.* 2019 Apr 9;10(1):1629.
145. Takeda M, Leser GP, Russell CJ, Lamb RA. Influenza virus hemagglutinin concentrates in lipid raft microdomains for efficient viral fusion. *Proc Natl Acad Sci U S A.* 2003 Dec 9;100(25):14610–7.
146. Chen BJ, Leser GP, Morita E, Lamb RA. Influenza virus hemagglutinin and neuraminidase, but not the matrix protein, are required for assembly and budding of plasmid-derived virus-like particles. *J Virol.* 2007 Jul;81(13):7111–23.
147. Wang N, Glidden EJ, Murphy SR, Pearse BR, Hebert DN. The cotranslational

maturation program for the type II membrane glycoprotein influenza neuraminidase. *J Biol Chem*. 2008 Dec 5;283(49):33826–37.

148. Nayak DP, Balogun RA, Yamada H, Zhou ZH, Barman S. Influenza virus morphogenesis and budding. *Virus Res*. 2009 Aug;143(2):147–61.

149. Yondola MA, Fernandes F, Belicha-Villanueva A, Uccellini M, Gao Q, Carter C, et al. Budding capability of the influenza virus neuraminidase can be modulated by tetherin. *J Virol*. 2011 Mar;85(6):2480–91.

150. Ohkura T, Momose F, Ichikawa R, Takeuchi K, Morikawa Y. Influenza A virus hemagglutinin and neuraminidase mutually accelerate their apical targeting through clustering of lipid rafts. *J Virol*. 2014 Sep 1;88(17):10039–55.

151. Sato R, Okura T, Kawahara M, Takizawa N, Momose F, Morikawa Y. Apical Trafficking Pathways of Influenza A Virus HA and NA via Rab17- and Rab23-Positive Compartments. *Front Microbiol*. 2019;10:1857.

152. Barman S, Adhikary L, Chakrabarti AK, Bernas C, Kawaoka Y, Nayak DP. Role of transmembrane domain and cytoplasmic tail amino acid sequences of influenza a virus neuraminidase in raft association and virus budding. *J Virol*. 2004 May;78(10):5258–69.

153. Gómez-Puertas P, Albo C, Pérez-Pastrana E, Vivo A, Portela A. Influenza virus matrix protein is the major driving force in virus budding. *J Virol*. 2000 Dec;74(24):11538–47.

154. Lai JCC, Chan WWL, Kien F, Nicholls JM, Peiris JSM, Garcia J-M. Formation of virus-like particles from human cell lines exclusively expressing influenza neuraminidase. *J Gen Virol*. 2010 Sep;91(Pt 9):2322–30.

155. Rossman JS, Jing X, Leser GP, Lamb RA. Influenza virus M2 protein mediates ESCRT-independent membrane scission. *Cell*. 2010 Sep 17;142(6):902–13.

156. Lamb RA. The Structure, Function, and Pathobiology of the Influenza A and B Virus Ion Channels. *Cold Spring Harb Perspect Med*. 2020 Nov 2;10(11).

157. Yondola M, Carter C. Un-“ESCRT”-ed budding. *Viruses*. 2011 Jan;3(1):26–31.

158. Rossman JS, Lamb RA. Influenza virus assembly and budding. *Virology*. 2011 Mar 15;411(2):229–36.

159. McAuley JL, Gilbertson BP, Trifkovic S, Brown LE, McKimm-Breschkin JL. Influenza Virus Neuraminidase Structure and Functions. *Front Microbiol*. 2019;10:39.

160. Huang RT, Rott R, Klenk HD. Influenza viruses cause hemolysis and fusion of cells. *Virology*. 1981 Apr 15;110(1):243–7.

161. Zhirnov OP, Ikizler MR, Wright PF. Cleavage of influenza a virus hemagglutinin in human respiratory epithelium is cell associated and sensitive to exogenous antiproteases. *J Virol*. 2002 Sep;76(17):8682–9.

162. Böttcher E, Matrosovich T, Beyerle M, Klenk H-D, Garten W, Matrosovich M. Proteolytic activation of influenza viruses by serine proteases TMPRSS2 and HAT from human airway epithelium. *J Virol*. 2006 Oct;80(19):9896–8.

163. Olsen B, Munster VJ, Wallensten A, Waldenström J, Osterhaus ADME, Fouchier RAM. Global patterns of influenza a virus in wild birds. *Science*. 2006 Apr 21;312(5772):384–8.

164. Long JS, Mistry B, Haslam SM, Barclay WS. Host and viral determinants of influenza A virus species specificity. *Nat Rev Microbiol*. 2019 Jan;17(2):67–81.
165. Ciminski K, Schwemmler M. Bat-Borne Influenza A Viruses: An Awakening. *Cold Spring Harb Perspect Med*. 2019 Dec 30;
166. Tong S, Li Y, Rivaller P, Conrardy C, Castillo DAA, Chen L-M, et al. A distinct lineage of influenza A virus from bats. *Proc Natl Acad Sci U S A*. 2012 Mar 13;109(11):4269–74.
167. Tong S, Zhu X, Li Y, Shi M, Zhang J, Bourgeois M, et al. New world bats harbor diverse influenza A viruses. *PLoS Pathog*. 2013;9(10):e1003657.
168. Ito T, Couceiro JN, Kelm S, Baum LG, Krauss S, Castrucci MR, et al. Molecular basis for the generation in pigs of influenza A viruses with pandemic potential. *J Virol*. 1998 Sep;72(9):7367–73.
169. Zhou J, Wang D, Gao R, Zhao B, Song J, Qi X, et al. Biological features of novel avian influenza A (H7N9) virus. *Nature*. 2013 Jul 25;499(7459):500–3.
170. Bi Y, Tan S, Yang Y, Wong G, Zhao M, Zhang Q, et al. Clinical and Immunological Characteristics of Human Infections With H5N6 Avian Influenza Virus. *Clin Infect Dis*. 2019 Mar 19;68(7):1100–9.
171. Chang P, Sealy JE, Sadeyen J-R, Bhat S, Lukosaityte D, Sun Y, et al. Immune Escape Adaptive Mutations in the H7N9 Avian Influenza Hemagglutinin Protein Increase Virus Replication Fitness and Decrease Pandemic Potential. *J Virol*. 2020 Sep 15;94(19).
172. Bonilla-Aldana DK, Aguirre-Florez M, Villamizar-Peña R, Gutiérrez-Ocampo E, Henao-Martínez JF, Cvetkovic-Vega A, et al. After SARS-CoV-2, will H5N6 and other influenza viruses follow the pandemic path? *Infez Med*. 2020 Dec 1;28(4):475–85.
173. Ren H, Jin Y, Hu M, Zhou J, Song T, Huang Z, et al. Ecological dynamics of influenza A viruses: cross-species transmission and global migration. *Sci Rep*. 2016 Nov 9;6:36839.
174. WHO. Influenza (Avian and other zoonotic) [Internet]. [cited 2021 Feb 9]. Available from: [https://www.who.int/news-room/fact-sheets/detail/influenza-\(avian-and-other-zoonotic\)](https://www.who.int/news-room/fact-sheets/detail/influenza-(avian-and-other-zoonotic))
175. Webster RG, Yakhno M, Hinshaw VS, Bean WJ, Murti KG. Intestinal influenza: replication and characterization of influenza viruses in ducks. *Virology*. 1978 Feb;84(2):268–78.
176. Jonges M, Welkers MRA, Jeeninga RE, Meijer A, Schneeberger P, Fouchier RAM, et al. Emergence of the virulence-associated PB2 E627K substitution in a fatal human case of highly pathogenic avian influenza virus A(H7N7) infection as determined by Illumina ultra-deep sequencing. *J Virol*. 2014 Feb;88(3):1694–702.
177. Lin R-W, Chen G-W, Sung H-H, Lin R-J, Yen L-C, Tseng Y-L, et al. Naturally occurring mutations in PB1 affect influenza A virus replication fidelity, virulence, and adaptability. *J Biomed Sci*. 2019 Jul 31;26(1):55.
178. Pauly MD, Procaro MC, Lauring AS. A novel twelve class fluctuation test reveals higher than expected mutation rates for influenza A viruses. *Elife*. 2017 Jun 9;6.
179. Naito T, Shirai K, Mori K, Muratsu H, Ushirogawa H, Ohniwa RL, et al. Tyr82 Amino Acid Mutation in PB1 Polymerase Induces an Influenza Virus Mutator Phenotype. *J Virol*. 2019 Nov 15;93(22).

180. Jones JE, Le Sage V, Lakdawala SS. Viral and host heterogeneity and their effects on the viral life cycle. *Nat Rev Microbiol.* 2020 Oct 6;
181. Whitley RJ, Boucher CA, Lina B, Nguyen-Van-Tam JS, Osterhaus A, Schutten M, et al. Global assessment of resistance to neuraminidase inhibitors, 2008-2011: the Influenza Resistance Information Study (IRIS). *Clin Infect Dis.* 2013 May;56(9):1197–205.
182. Vahey MD, Fletcher DA. Low-Fidelity Assembly of Influenza A Virus Promotes Escape from Host Cells. *Cell.* 2019 Jan 10;176(1–2):281-294.e19.
183. Finberg RW, Lanno R, Anderson D, Fleischhackl R, van Duijnhoven W, Kauffman RS, et al. Phase 2b Study of Pimodivir (JNJ-63623872) as Monotherapy or in Combination With Oseltamivir for Treatment of Acute Uncomplicated Seasonal Influenza A: TOPAZ Trial. *J Infect Dis.* 2019 Mar 15;219(7):1026–34.
184. Goldhill DH, Te Velthuis AJW, Fletcher RA, Langat P, Zambon M, Lackenby A, et al. The mechanism of resistance to favipiravir in influenza. *Proc Natl Acad Sci U S A.* 2018 Nov 6;115(45):11613–8.
185. Ikematsu H, Hayden FG, Kawaguchi K, Kinoshita M, de Jong MD, Lee N, et al. Baloxavir Marboxil for Prophylaxis against Influenza in Household Contacts. *N Engl J Med.* 2020 Jul 23;383(4):309–20.
186. Eriksson P, Lindskog C, Engholm E, Blixt O, Waldenström J, Munster V, et al. Characterization of avian influenza virus attachment patterns to human and pig tissues. *Sci Rep.* 2018 Aug 15;8(1):12215.
187. Hirst GK. THE QUANTITATIVE DETERMINATION OF INFLUENZA VIRUS AND ANTIBODIES BY MEANS OF RED CELL AGGLUTINATION. *J Exp Med.* 1942 Jan 1;75(1):49–64.
188. Wilson IA, Skehel JJ, Wiley DC. Structure of the haemagglutinin membrane glycoprotein of influenza virus at 3 Å resolution. *Nature.* 1981 Jan 29;289(5796):366–73.
189. Weis W, Brown JH, Cusack S, Paulson JC, Skehel JJ, Wiley DC. Structure of the influenza virus haemagglutinin complexed with its receptor, sialic acid. *Nature.* 1988 Jun 2;333(6172):426–31.
190. Benton DJ, Nans A, Calder LJ, Turner J, Neu U, Lin YP, et al. Influenza hemagglutinin membrane anchor. *Proc Natl Acad Sci U S A.* 2018 Oct 2;115(40):10112–7.
191. York IA, Stevens J, Alymova IV. Influenza virus N-linked glycosylation and innate immunity. *Biosci Rep.* 2019 Jan 31;39(1).
192. Tate MD, Job ER, Deng Y-M, Gunalan V, Maurer-Stroh S, Reading PC. Playing hide and seek: how glycosylation of the influenza virus hemagglutinin can modulate the immune response to infection. *Viruses.* 2014 Mar 14;6(3):1294–316.
193. Kim P, Jang YH, Kwon SB, Lee CM, Han G, Seong BL. Glycosylation of Hemagglutinin and Neuraminidase of Influenza A Virus as Signature for Ecological Spillover and Adaptation among Influenza Reservoirs. *Viruses.* 2018 Apr 7;10(4).
194. Sun X, Jayaraman A, Mani Prasad P, Raman R, Houser KV, Pappas C, et al. N-linked glycosylation of the hemagglutinin protein influences virulence and antigenicity of the 1918 pandemic and seasonal H1N1 influenza A viruses. *J Virol.* 2013 Aug;87(15):8756–66.

195. Keller P, Simons K. Cholesterol is required for surface transport of influenza virus hemagglutinin. *J Cell Biol.* 1998 Mar 23;140(6):1357–67.
196. Hirst GK. The nature of the virus receptors of red cells; evidence on the chemical nature of the virus receptors of red cells and of the existence of a closely analogous substance in normal serum. *J Exp Med.* 1948 Apr 1;87(4):301–14.
197. Rogers GN, Paulson JC. Receptor determinants of human and animal influenza virus isolates: differences in receptor specificity of the H3 hemagglutinin based on species of origin. *Virology.* 1983 Jun;127(2):361–73.
198. Springer SA, Diaz SL, Gagneux P. Parallel evolution of a self-signal: humans and new world monkeys independently lost the cell surface sugar Neu5Gc. *Immunogenetics.* 2014 Nov;66(11):671–4.
199. Broszeit F, Tzarum N, Zhu X, Nemanichvili N, Eggink D, Leenders T, et al. N-Glycolylneuraminic Acid as a Receptor for Influenza A Viruses. *Cell Rep.* 2019 Jun 11;27(11):3284-3294.e6.
200. Matrosovich M, Tuzikov A, Bovin N, Gambaryan A, Klimov A, Castrucci MR, et al. Early alterations of the receptor-binding properties of H1, H2, and H3 avian influenza virus hemagglutinins after their introduction into mammals. *J Virol.* 2000 Sep;74(18):8502–12.
201. Imai M, Watanabe T, Hatta M, Das SC, Ozawa M, Shinya K, et al. Experimental adaptation of an influenza H5 HA confers respiratory droplet transmission to a reassortant H5 HA/H1N1 virus in ferrets. *Nature.* 2012 May 2;486(7403):420–8.
202. de Vries RP, Zhu X, McBride R, Rigter A, Hanson A, Zhong G, et al. Hemagglutinin receptor specificity and structural analyses of respiratory droplet-transmissible H5N1 viruses. *J Virol.* 2014 Jan;88(1):768–73.
203. Fujioka Y, Nishide S, Ose T, Suzuki T, Kato I, Fukuhara H, et al. A Sialylated Voltage-Dependent Ca²⁺ Channel Binds Hemagglutinin and Mediates Influenza A Virus Entry into Mammalian Cells. *Cell Host Microbe.* 2018 Jun 13;23(6):809-818.e5.
204. Byrd-Leotis L, Jia N, Dutta S, Trost JF, Gao C, Cummings SF, et al. Influenza binds phosphorylated glycans from human lung. *Sci Adv.* 2019 Feb;5(2):eaav2554.
205. Hamilton BS, Whittaker GR, Daniel S. Influenza virus-mediated membrane fusion: determinants of hemagglutinin fusogenic activity and experimental approaches for assessing virus fusion. *Viruses.* 2012 Jul;4(7):1144–68.
206. Kawaoka Y, Webster RG. Sequence requirements for cleavage activation of influenza virus hemagglutinin expressed in mammalian cells. *Proc Natl Acad Sci U S A.* 1988 Jan;85(2):324–8.
207. Sun X, Tse LV, Ferguson AD, Whittaker GR. Modifications to the hemagglutinin cleavage site control the virulence of a neurotropic H1N1 influenza virus. *J Virol.* 2010 Sep;84(17):8683–90.
208. Bertram S, Heurich A, Lavender H, Gierer S, Danisch S, Perin P, et al. Influenza and SARS-coronavirus activating proteases TMPRSS2 and HAT are expressed at multiple sites in human respiratory and gastrointestinal tracts. *PLoS One.* 2012;7(4):e35876.
209. Aljurayyan A, Puksuriwong S, Ahmed M, Sharma R, Krishnan M, Sood S, et al. Activation and Induction of Antigen-Specific T Follicular Helper Cells Play a Critical Role in Live-Attenuated Influenza Vaccine-Induced Human Mucosal Anti-influenza

Antibody Response. *J Virol.* 2018 Jun 1;92(11).

210. Hirst GK. ADSORPTION OF INFLUENZA VIRUS ON CELLS OF THE RESPIRATORY TRACT. *J Exp Med.* 1943 Aug 1;78(2):99–109.

211. Varghese JN, Laver WG, Colman PM. Structure of the influenza virus glycoprotein antigen neuraminidase at 2.9 Å resolution. *Nature.* 1983 May 5;303(5912):35–40.

212. Colman PM, Varghese JN, Laver WG. Structure of the catalytic and antigenic sites in influenza virus neuraminidase. *Nature.* 1983 May 5;303(5912):41–4.

213. Bos TJ, Davis AR, Nayak DP. NH₂-terminal hydrophobic region of influenza virus neuraminidase provides the signal function in translocation. *Proc Natl Acad Sci U S A.* 1984 Apr;81(8):2327–31.

214. Saito T, Taylor G, Webster RG. Steps in maturation of influenza A virus neuraminidase. *J Virol.* 1995 Aug;69(8):5011–7.

215. Zhu X, Turner HL, Lang S, McBride R, Bangaru S, Gilchuk IM, et al. Structural Basis of Protection against H7N9 Influenza Virus by Human Anti-N9 Neuraminidase Antibodies. *Cell Host Microbe.* 2019 Dec 11;26(6):729–738.e4.

216. Burnet FM, McCREA JF, Anderson SG. Mucin as substrate of enzyme action by viruses of the mumps influenza group. *Nature.* 1947 Sep 20;160(4064):404.

217. Matrosovich MN, Matrosovich TY, Gray T, Roberts NA, Klenk H-D. Neuraminidase is important for the initiation of influenza virus infection in human airway epithelium. *J Virol.* 2004 Nov;78(22):12665–7.

218. Cohen M, Zhang X-Q, Senaati HP, Chen H-W, Varki NM, Schooley RT, et al. Influenza A penetrates host mucus by cleaving sialic acids with neuraminidase. *Virol J.* 2013 Nov 22;10:321.

219. Yang X, Steukers L, Forier K, Xiong R, Braeckmans K, Van Reeth K, et al. A beneficiary role for neuraminidase in influenza virus penetration through the respiratory mucus. *PLoS One.* 2014;9(10):e110026.

220. Vahey MD, Fletcher DA. Influenza A virus surface proteins are organized to help penetrate host mucus. *Elife.* 2019 May 14;8.

221. Zanin M, Baviskar P, Webster R, Webby R. The Interaction between Respiratory Pathogens and Mucus. *Cell Host Microbe.* 2016 Feb 10;19(2):159–68.

222. Williams OW, Sharafkhaneh A, Kim V, Dickey BF, Evans CM. Airway mucus: From production to secretion. *Am J Respir Cell Mol Biol.* 2006 May;34(5):527–36.

223. Ehre C, Worthington EN, Liesman RM, Grubb BR, Barbier D, O'Neal WK, et al. Overexpressing mouse model demonstrates the protective role of Muc5ac in the lungs. *Proc Natl Acad Sci U S A.* 2012 Oct 9;109(41):16528–33.

224. Zanin M, Marathe B, Wong S-S, Yoon S-W, Collin E, Oshansky C, et al. Pandemic Swine H1N1 Influenza Viruses with Almost Undetectable Neuraminidase Activity Are Not Transmitted via Aerosols in Ferrets and Are Inhibited by Human Mucus but Not Swine Mucus. *J Virol.* 2015 Jun;89(11):5935–48.

225. Ohuchi M, Asaoka N, Sakai T, Ohuchi R. Roles of neuraminidase in the initial stage of influenza virus infection. *Microbes Infect.* 2006 Apr;8(5):1287–93.

226. Yang J, Liu S, Du L, Jiang S. A new role of neuraminidase (NA) in the influenza

virus life cycle: implication for developing NA inhibitors with novel mechanism of action. *Rev Med Virol.* 2016 Jul;26(4):242–50.

227. Sakai T, Nishimura SI, Naito T, Saito M. Influenza A virus hemagglutinin and neuraminidase act as novel motile machinery. *Sci Rep.* 2017 Mar 27;7:45043.

228. Guo H, Rabouw H, Slomp A, Dai M, van der Vegt F, van Lent JWM, et al. Kinetic analysis of the influenza A virus HA/NA balance reveals contribution of NA to virus-receptor binding and NA-dependent rolling on receptor-containing surfaces. *PLoS Pathog.* 2018 Aug;14(8):e1007233.

229. Du W, Guo H, Nijman VS, Doedt J, van der Vries E, van der Lee J, et al. The 2nd sialic acid-binding site of influenza A virus neuraminidase is an important determinant of the hemagglutinin-neuraminidase-receptor balance. *PLoS Pathog.* 2019 Jun;15(6):e1007860.

230. Du W, Wolfert MA, Peeters B, van Kuppeveld FJM, Boons G-J, de Vries E, et al. Mutation of the second sialic acid-binding site of influenza A virus neuraminidase drives compensatory mutations in hemagglutinin. *PLoS Pathog.* 2020 Aug;16(8):e1008816.

231. Du W, de Vries E, van Kuppeveld FJM, Matrosovich M, de Haan CAM. Second sialic acid-binding site of influenza A virus neuraminidase: binding receptors for efficient release. *FEBS J.* 2020 Dec 14;

232. Krammer F, Li L, Wilson PC. Emerging from the Shadow of Hemagglutinin: Neuraminidase Is an Important Target for Influenza Vaccination. *Cell Host Microbe.* 2019 Dec 11;26(6):712–3.

233. Fox A, Carolan L. Neuraminidase escape attempts. *Nat Microbiol.* 2019 Dec;4(12):2031–2.

234. Muthuri SG, Venkatesan S, Myles PR, Leonardi-Bee J, Al Khuwaitir TSA, Al Mamun A, et al. Effectiveness of neuraminidase inhibitors in reducing mortality in patients admitted to hospital with influenza A H1N1pdm09 virus infection: a meta-analysis of individual participant data. *Lancet Respir Med.* 2014 May;2(5):395–404.

235. Ison MG, Portsmouth S, Yoshida Y, Shishido T, Mitchener M, Tsuchiya K, et al. Early treatment with baloxavir marboxil in high-risk adolescent and adult outpatients with uncomplicated influenza (CAPSTONE-2): a randomised, placebo-controlled, phase 3 trial. *Lancet Infect Dis.* 2020 Oct;20(10):1204–14.

236. Márquez-Domínguez L, Reyes-Leyva J, Herrera-Camacho I, Santos-López G, Scior T. Five Novel Non-Sialic Acid-Like Scaffolds Inhibit In Vitro H1N1 and H5N2 Neuraminidase Activity of Influenza A Virus. *Molecules.* 2020 Sep 16;25(18).

237. Fuller SD, Bravo R, Simons K. An enzymatic assay reveals that proteins destined for the apical or basolateral domains of an epithelial cell line share the same late Golgi compartments. *EMBO J.* 1985 Feb;4(2):297–307.

238. Schultz-Cherry S, Hinshaw VS. Influenza virus neuraminidase activates latent transforming growth factor beta. *J Virol.* 1996 Dec;70(12):8624–9.

239. Carlson CM, Turpin EA, Moser LA, O'Brien KB, Cline TD, Jones JC, et al. Transforming growth factor- β : activation by neuraminidase and role in highly pathogenic H5N1 influenza pathogenesis. *PLoS Pathog.* 2010 Oct 7;6(10):e1001136.

240. Byrd-Leotis L, Cummings RD, Steinhauer DA. The Interplay between the Host Receptor and Influenza Virus Hemagglutinin and Neuraminidase. *Int J Mol Sci.* 2017 Jul

17;18(7).

241. Zeng H, Belser JA, Goldsmith CS, Gustin KM, Veguilla V, Katz JM, et al. A(H7N9) virus results in early induction of proinflammatory cytokine responses in both human lung epithelial and endothelial cells and shows increased human adaptation compared with avian H5N1 virus. *J Virol*. 2015 Apr;89(8):4655–67.
242. Chrzastek K, Lee D-H, Gharaibeh S, Zsak A, Kapczynski DR. Characterization of H9N2 avian influenza viruses from the Middle East demonstrates heterogeneity at amino acid position 226 in the hemagglutinin and potential for transmission to mammals. *Virology*. 2018 May;518:195–201.
243. Vachieri SG, Xiong X, Collins PJ, Walker PA, Martin SR, Haire LF, et al. Receptor binding by H10 influenza viruses. *Nature*. 2014 Jul 24;511(7510):475–7.
244. Gaymard A, Le Briand N, Frobert E, Lina B, Escuret V. Functional balance between neuraminidase and haemagglutinin in influenza viruses. *Clin Microbiol Infect*. 2016 Dec;22(12):975–83.
245. de Vries E, Du W, Guo H, de Haan CAM. Influenza A Virus Hemagglutinin-Neuraminidase-Receptor Balance: Preserving Virus Motility. *Trends Microbiol*. 2020 Jan;28(1):57–67.
246. Kaverin NV, Gambaryan AS, Bovin NV, Rudneva IA, Shilov AA, Khodova OM, et al. Postreassortment changes in influenza A virus hemagglutinin restoring HA-NA functional match. *Virology*. 1998 May 10;244(2):315–21.
247. Zanin M, Duan S, Wong S-S, Kumar G, Baviskar P, Collin E, et al. An Amino Acid in the Stalk Domain of N1 Neuraminidase Is Critical for Enzymatic Activity. *J Virol*. 2017 Jan 15;91(2).
248. Mitnaul LJ, Matrosovich MN, Castrucci MR, Tuzikov AB, Bovin NV, Kobasa D, et al. Balanced hemagglutinin and neuraminidase activities are critical for efficient replication of influenza A virus. *J Virol*. 2000 Jul;74(13):6015–20.
249. Ranadheera C, Hagan MW, Leung A, Collignon B, Cutts T, Theriault S, et al. Reduction of Neuraminidase Activity Exacerbates Disease in 2009 Pandemic Influenza Virus-Infected Mice. *J Virol*. 2016 Nov 1;90(21):9931–41.
250. Tscherne DM, García-Sastre A. Virulence determinants of pandemic influenza viruses. *J Clin Invest*. 2011 Jan;121(1):6–13.
251. McCullers JA. Insights into the interaction between influenza virus and pneumococcus. *Clin Microbiol Rev*. 2006 Jul;19(3):571–82.
252. Hartl D, Tirouvanziam R, Laval J, Greene CM, Habel D, Sharma L, et al. Innate Immunity of the Lung: From Basic Mechanisms to Translational Medicine. *J Innate Immun*. 2018;10(5–6):487–501.
253. Prussin AJ, Garcia EB, Marr LC. Total Virus and Bacteria Concentrations in Indoor and Outdoor Air. *Environ Sci Technol Lett*. 2015;2(4):84–8.
254. Iwasaki A, Foxman EF, Molony RD. Early local immune defences in the respiratory tract. *Nat Rev Immunol*. 2017 Jan;17(1):7–20.
255. LeMessurier KS, Tiwary M, Morin NP, Samarasinghe AE. Respiratory Barrier as a Safeguard and Regulator of Defense Against Influenza A Virus and *Streptococcus pneumoniae*. *Front Immunol*. 2020;11:3.
256. Riches DWH, Martin TR. Overview of Innate Lung Immunity and Inflammation.

Methods Mol Biol. 2018;1809:17–30.

257. Guillot L, Nathan N, Tabary O, Thouvenin G, Le Rouzic P, Corvol H, et al. Alveolar epithelial cells: master regulators of lung homeostasis. *Int J Biochem Cell Biol*. 2013 Nov;45(11):2568–73.

258. Mason RJ. Biology of alveolar type II cells. *Respirology*. 2006 Jan;11 Suppl:S12-15.

259. Yamamoto K, Ferrari JD, Cao Y, Ramirez MI, Jones MR, Quinton LJ, et al. Type I alveolar epithelial cells mount innate immune responses during pneumococcal pneumonia. *J Immunol*. 2012 Sep 1;189(5):2450–9.

260. Radicioni G, Cao R, Carpenter J, Ford AA, Wang T, Li L, et al. The innate immune properties of airway mucosal surfaces are regulated by dynamic interactions between mucins and interacting proteins: the mucin interactome. *Mucosal Immunol*. 2016 Nov;9(6):1442–54.

261. Iwasaki A, Pillai PS. Innate immunity to influenza virus infection. *Nat Rev Immunol*. 2014 May;14(5):315–28.

262. Hariri BM, Cohen NA. New insights into upper airway innate immunity. *Am J Rhinol Allergy*. 2016 Sep;30(5):319–23.

263. Chen X, Liu S, Goraya MU, Maarouf M, Huang S, Chen J-L. Host Immune Response to Influenza A Virus Infection. *Front Immunol*. 2018;9:320.

264. Wu N-H, Yang W, Beineke A, Dijkman R, Matrosovich M, Baumgärtner W, et al. The differentiated airway epithelium infected by influenza viruses maintains the barrier function despite a dramatic loss of ciliated cells. *Sci Rep*. 2016 Dec 22;6:39668.

265. Button B, Cai L-H, Ehre C, Kesimer M, Hill DB, Sheehan JK, et al. A periciliary brush promotes the lung health by separating the mucus layer from airway epithelia. *Science*. 2012 Aug 24;337(6097):937–41.

266. Witten J, Samad T, Ribbeck K. Selective permeability of mucus barriers. *Curr Opin Biotechnol*. 2018 Aug;52:124–33.

267. Okuda K, Chen G, Subramani DB, Wolf M, Gilmore RC, Kato T, et al. Localization of Secretory Mucins MUC5AC and MUC5B in Normal/Healthy Human Airways. *Am J Respir Crit Care Med*. 2019 Mar 15;199(6):715–27.

268. Dhar P, McAuley J. The Role of the Cell Surface Mucin MUC1 as a Barrier to Infection and Regulator of Inflammation. *Front Cell Infect Microbiol*. 2019;9:117.

269. Lu W, Hisatsune A, Koga T, Kato K, Kuwahara I, Lillehoj EP, et al. Cutting edge: enhanced pulmonary clearance of *Pseudomonas aeruginosa* by Muc1 knockout mice. *J Immunol*. 2006 Apr 1;176(7):3890–4.

270. Umehara T, Kato K, Park YS, Lillehoj EP, Kawauchi H, Kim KC. Prevention of lung injury by Muc1 mucin in a mouse model of repetitive *Pseudomonas aeruginosa* infection. *Inflamm Res*. 2012 Sep;61(9):1013–20.

271. McAuley JL, Corcilius L, Tan H-X, Payne RJ, McGuckin MA, Brown LE. The cell surface mucin MUC1 limits the severity of influenza A virus infection. *Mucosal Immunol*. 2017 Nov;10(6):1581–93.

272. Lillehoj EP, Guang W, Hyun SW, Liu A, Hegerle N, Simon R, et al. Neuraminidase 1-mediated desialylation of the mucin 1 ectodomain releases a decoy receptor that protects against *Pseudomonas aeruginosa* lung infection. *J Biol Chem*.

2019 Jan 11;294(2):662–78.

273. Roy MG, Livraghi-Butrico A, Fletcher AA, McElwee MM, Evans SE, Boerner RM, et al. Muc5b is required for airway defence. *Nature*. 2014 Jan;505(7483):412–6.

274. Kudo E, Song E, Yockey LJ, Rakib T, Wong PW, Homer RJ, et al. Low ambient humidity impairs barrier function and innate resistance against influenza infection. *Proc Natl Acad Sci U S A*. 2019 May 28;116(22):10905–10.

275. Hsieh I-N, Hartshorn KL. The Role of Antimicrobial Peptides in Influenza Virus Infection and Their Potential as Antiviral and Immunomodulatory Therapy. *Pharmaceuticals (Basel)*. 2016 Sep 6;9(3).

276. LeMessurier KS, Lin Y, McCullers JA, Samarasinghe AE. Antimicrobial peptides alter early immune response to influenza A virus infection in C57BL/6 mice. *Antiviral Res*. 2016 Sep;133:208–17.

277. Hsieh I-N, De Luna X, White MR, Hartshorn KL. The Role and Molecular Mechanism of Action of Surfactant Protein D in Innate Host Defense Against Influenza A Virus. *Front Immunol*. 2018;9:1368.

278. Daher KA, Selsted ME, Lehrer RI. Direct inactivation of viruses by human granulocyte defensins. *J Virol*. 1986 Dec;60(3):1068–74.

279. Tripathi S, Verma A, Kim E-J, White MR, Hartshorn KL. LL-37 modulates human neutrophil responses to influenza A virus. *J Leukoc Biol*. 2014 Nov;96(5):931–8.

280. Barlow PG, Svoboda P, Mackellar A, Nash AA, York IA, Pohl J, et al. Antiviral activity and increased host defense against influenza infection elicited by the human cathelicidin LL-37. *PLoS One*. 2011;6(10):e25333.

281. Kim S, Kim M-J, Park DY, Chung HJ, Kim C-H, Yoon J-H, et al. Mitochondrial reactive oxygen species modulate innate immune response to influenza A virus in human nasal epithelium. *Antiviral Res*. 2015 Jul;119:78–83.

282. Gingerich A, Pang L, Hanson J, Dlugolenski D, Streich R, Lafontaine ER, et al. Hypothiocyanite produced by human and rat respiratory epithelial cells inactivates extracellular H1N2 influenza A virus. *Inflamm Res*. 2016 Jan;65(1):71–80.

283. Saito T, Gale M. Principles of intracellular viral recognition. *Curr Opin Immunol*. 2007 Feb;19(1):17–23.

284. Spel L, Martinon F. Detection of viruses by inflammasomes. *Curr Opin Virol*. 2020 Nov 8;46:59–64.

285. Kikkert M. Innate Immune Evasion by Human Respiratory RNA Viruses. *J Innate Immun*. 2020;12(1):4–20.

286. Lee S, Ishitsuka A, Noguchi M, Hirohama M, Fujiyasu Y, Petric PP, et al. Influenza restriction factor MxA functions as inflammasome sensor in the respiratory epithelium. *Sci Immunol*. 2019 Oct 25;4(40).

287. Mehrbod P, Ande SR, Alizadeh J, Rahimizadeh S, Shariati A, Malek H, et al. The roles of apoptosis, autophagy and unfolded protein response in arbovirus, influenza virus, and HIV infections. *Virulence*. 2019 Dec;10(1):376–413.

288. Frabutt DA, Wang B, Riaz S, Schwartz RC, Zheng Y-H. Innate Sensing of Influenza A Virus Hemagglutinin Glycoproteins by the Host Endoplasmic Reticulum (ER) Stress Pathway Triggers a Potent Antiviral Response via ER-Associated Protein Degradation. *J Virol*. 2018 Jan 1;92(1).

289. Blumberg RS, van de Wal Y, Claypool S, Corazza N, Dickinson B, Nieuwenhuis E, et al. The multiple roles of major histocompatibility complex class-I-like molecules in mucosal immune function. *Acta Odontol Scand*. 2001 Jun;59(3):139–44.
290. Wei J, Kishton RJ, Angel M, Conn CS, Dalla-Venezia N, Marcel V, et al. Ribosomal Proteins Regulate MHC Class I Peptide Generation for Immunosurveillance. *Mol Cell*. 2019 Mar 21;73(6):1162-1173.e5.
291. García-Sastre A. Induction and evasion of type I interferon responses by influenza viruses. *Virus Res*. 2011 Dec;162(1–2):12–8.
292. Pestka S. The interferons: 50 years after their discovery, there is much more to learn. *J Biol Chem*. 2007 Jul 13;282(28):20047–51.
293. Isaacs A, Lindenmann J. Virus interference. I. The interferon. *Proc R Soc Lond B Biol Sci*. 1957 Sep 12;147(927):258–67.
294. Dusheiko G. Side effects of alpha interferon in chronic hepatitis C. *Hepatology*. 1997 Sep;26(3 Suppl 1):112S-121S.
295. Hornung V, Ellegast J, Kim S, Brzózka K, Jung A, Kato H, et al. 5'-Triphosphate RNA is the ligand for RIG-I. *Science*. 2006 Nov 10;314(5801):994–7.
296. Pichlmair A, Schulz O, Tan CP, Näslund TI, Liljeström P, Weber F, et al. RIG-I-mediated antiviral responses to single-stranded RNA bearing 5'-phosphates. *Science*. 2006 Nov 10;314(5801):997–1001.
297. Kato H, Takeuchi O, Sato S, Yoneyama M, Yamamoto M, Matsui K, et al. Differential roles of MDA5 and RIG-I helicases in the recognition of RNA viruses. *Nature*. 2006 May 4;441(7089):101–5.
298. Yoneyama M, Kikuchi M, Natsukawa T, Shinobu N, Imaizumi T, Miyagishi M, et al. The RNA helicase RIG-I has an essential function in double-stranded RNA-induced innate antiviral responses. *Nat Immunol*. 2004 Jul;5(7):730–7.
299. Gack MU, Kirchhofer A, Shin YC, Inn K-S, Liang C, Cui S, et al. Roles of RIG-I N-terminal tandem CARD and splice variant in TRIM25-mediated antiviral signal transduction. *Proc Natl Acad Sci U S A*. 2008 Oct 28;105(43):16743–8.
300. Oshiumi H, Miyashita M, Inoue N, Okabe M, Matsumoto M, Seya T. The ubiquitin ligase Riplet is essential for RIG-I-dependent innate immune responses to RNA virus infection. *Cell Host Microbe*. 2010 Dec 16;8(6):496–509.
301. Blasius AL, Beutler B. Intracellular toll-like receptors. *Immunity*. 2010 Mar 26;32(3):305–15.
302. Patel MC, Shirey KA, Boukhvalova MS, Vogel SN, Blanco JCG. Serum High-Mobility-Group Box 1 as a Biomarker and a Therapeutic Target during Respiratory Virus Infections. *mBio*. 2018 Mar 13;9(2).
303. Durbin JE, Fernandez-Sesma A, Lee CK, Rao TD, Frey AB, Moran TM, et al. Type I IFN modulates innate and specific antiviral immunity. *J Immunol*. 2000 Apr 15;164(8):4220–8.
304. Der SD, Zhou A, Williams BR, Silverman RH. Identification of genes differentially regulated by interferon alpha, beta, or gamma using oligonucleotide arrays. *Proc Natl Acad Sci U S A*. 1998 Dec 22;95(26):15623–8.
305. Mordstein M, Kochs G, Dumoutier L, Renaud J-C, Paludan SR, Klucher K, et al. Interferon-lambda contributes to innate immunity of mice against influenza A virus

- but not against hepatotropic viruses. *PLoS Pathog.* 2008 Sep 12;4(9):e1000151.
306. Sommereyns C, Paul S, Staeheli P, Michiels T. IFN- λ (IFN- λ) is expressed in a tissue-dependent fashion and primarily acts on epithelial cells in vivo. *PLoS Pathog.* 2008 Mar 14;4(3):e1000017.
307. Lazear HM, Schoggins JW, Diamond MS. Shared and Distinct Functions of Type I and Type III Interferons. *Immunity.* 2019 Apr 16;50(4):907–23.
308. Galani IE, Triantafyllia V, Eleminiadou E-E, Koltsida O, Stavropoulos A, Manioudaki M, et al. Interferon- λ Mediates Non-redundant Front-Line Antiviral Protection against Influenza Virus Infection without Compromising Host Fitness. *Immunity.* 2017 May 16;46(5):875-890.e6.
309. Klinkhammer J, Schnepf D, Ye L, Schwaderlapp M, Gad HH, Hartmann R, et al. IFN- λ prevents influenza virus spread from the upper airways to the lungs and limits virus transmission. *Elife.* 2018 Apr 13;7.
310. Kronstad LM, Seiler C, Vergara R, Holmes SP, Blish CA. Differential Induction of IFN- α and Modulation of CD112 and CD54 Expression Govern the Magnitude of NK Cell IFN- γ Response to Influenza A Viruses. *J Immunol.* 2018 Oct 1;201(7):2117–31.
311. Weber-Gerlach M, Weber F. To Conquer the Host, Influenza Virus Is Packing It In: Interferon-Antagonistic Strategies beyond NS1. *J Virol.* 2016 Oct 1;90(19):8389–94.
312. Liu J, Lynch PA, Chien CY, Montelione GT, Krug RM, Berman HM. Crystal structure of the unique RNA-binding domain of the influenza virus NS1 protein. *Nat Struct Biol.* 1997 Nov;4(11):896–9.
313. Mibayashi M, Martínez-Sobrido L, Loo Y-M, Cárdenas WB, Gale M, García-Sastre A. Inhibition of retinoic acid-inducible gene I-mediated induction of beta interferon by the NS1 protein of influenza A virus. *J Virol.* 2007 Jan;81(2):514–24.
314. Jureka AS, Kleinpeter AB, Cornilescu G, Cornilescu CC, Petit CM. Structural Basis for a Novel Interaction between the NS1 Protein Derived from the 1918 Influenza Virus and RIG-I. *Structure.* 2015 Nov 3;23(11):2001–10.
315. Rajsbaum R, Albrecht RA, Wang MK, Maharaj NP, Versteeg GA, Nistal-Villán E, et al. Species-specific inhibition of RIG-I ubiquitination and IFN induction by the influenza A virus NS1 protein. *PLoS Pathog.* 2012;8(11):e1003059.
316. Zhang L, Wang J, Muñoz-Moreno R, Kim M, Sakthivel R, Mo W, et al. Influenza Virus NS1 Protein-RNA Interactome Reveals Intron Targeting. *J Virol.* 2018 Dec 15;92(24).
317. Kumari R, Guo Z, Kumar A, Wiens M, Gangappa S, Katz JM, et al. Influenza virus NS1- C/EBP β gene regulatory complex inhibits RIG-I transcription. *Antiviral Res.* 2020 Apr;176:104747.
318. Zhang K, Xie Y, Muñoz-Moreno R, Wang J, Zhang L, Esparza M, et al. Structural basis for influenza virus NS1 protein block of mRNA nuclear export. *Nat Microbiol.* 2019 Oct;4(10):1671–9.
319. Bauer DLV, Tellier M, Martínez-Alonso M, Nojima T, Proudfoot NJ, Murphy S, et al. Influenza Virus Mounts a Two-Pronged Attack on Host RNA Polymerase II Transcription. *Cell Rep.* 2018 May 15;23(7):2119-2129.e3.
320. Wisskirchen C, Ludersdorfer TH, Müller DA, Moritz E, Pavlovic J. The cellular RNA helicase UAP56 is required for prevention of double-stranded RNA formation

- during influenza A virus infection. *J Virol.* 2011 Sep;85(17):8646–55.
321. Hsu S-F, Su W-C, Jeng K-S, Lai MMC. A host susceptibility gene, DR1, facilitates influenza A virus replication by suppressing host innate immunity and enhancing viral RNA replication. *J Virol.* 2015 Apr;89(7):3671–82.
322. Graef KM, Vreede FT, Lau Y-F, McCall AW, Carr SM, Subbarao K, et al. The PB2 subunit of the influenza virus RNA polymerase affects virulence by interacting with the mitochondrial antiviral signaling protein and inhibiting expression of beta interferon. *J Virol.* 2010 Sep;84(17):8433–45.
323. Iwai A, Shiozaki T, Kawai T, Akira S, Kawaoka Y, Takada A, et al. Influenza A virus polymerase inhibits type I interferon induction by binding to interferon beta promoter stimulator 1. *J Biol Chem.* 2010 Oct 15;285(42):32064–74.
324. Dudek SE, Wixler L, Nordhoff C, Nordmann A, Anhlan D, Wixler V, et al. The influenza virus PB1-F2 protein has interferon antagonistic activity. *Biol Chem.* 2011 Dec;392(12):1135–44.
325. Varga ZT, Ramos I, Hai R, Schmolke M, García-Sastre A, Fernandez-Sesma A, et al. The influenza virus protein PB1-F2 inhibits the induction of type I interferon at the level of the MAVS adaptor protein. *PLoS Pathog.* 2011 Jun;7(6):e1002067.
326. Leymarie O, Meyer L, Tafforeau L, Lotteau V, Costa BD, Delmas B, et al. Influenza virus protein PB1-F2 interacts with CALCOCO2 (NDP52) to modulate innate immune response. *J Gen Virol.* 2017 Jun;98(6):1196–208.
327. Hayashi T, MacDonald LA, Takimoto T. Influenza A Virus Protein PA-X Contributes to Viral Growth and Suppression of the Host Antiviral and Immune Responses. *J Virol.* 2015 Jun;89(12):6442–52.
328. Wang R, Zhu Y, Lin X, Ren C, Zhao J, Wang F, et al. Influenza M2 protein regulates MAVS-mediated signaling pathway through interacting with MAVS and increasing ROS production. *Autophagy.* 2019 Jul;15(7):1163–81.
329. Holm CK, Rahbek SH, Gad HH, Bak RO, Jakobsen MR, Jiang Z, et al. Influenza A virus targets a cGAS-independent STING pathway that controls enveloped RNA viruses. *Nat Commun.* 2016 Feb 19;7:10680.
330. Xia C, Vijayan M, Pritzl CJ, Fuchs SY, McDermott AB, Hahm B. Hemagglutinin of Influenza A Virus Antagonizes Type I Interferon (IFN) Responses by Inducing Degradation of Type I IFN Receptor 1. *J Virol.* 2015 Dec 16;90(5):2403–17.
331. García-Sastre A, Durbin RK, Zheng H, Palese P, Gertner R, Levy DE, et al. The role of interferon in influenza virus tissue tropism. *J Virol.* 1998 Nov;72(11):8550–8.
332. Davidson S, Crotta S, McCabe TM, Wack A. Pathogenic potential of interferon $\alpha\beta$ in acute influenza infection. *Nat Commun.* 2014 May 21;5:3864.
333. Kolaczkowska E, Kubes P. Neutrophil recruitment and function in health and inflammation. *Nat Rev Immunol.* 2013 Mar;13(3):159–75.
334. Nicolás-Ávila JÁ, Adrover JM, Hidalgo A. Neutrophils in Homeostasis, Immunity, and Cancer. *Immunity.* 2017 Jan 17;46(1):15–28.
335. Gadjeva M. The complement system. Overview. *Methods Mol Biol.* 2014;1100:1–9.
336. Gerson SL, Talbot GH, Hurwitz S, Strom BL, Lusk EJ, Cassileth PA. Prolonged granulocytopenia: the major risk factor for invasive pulmonary aspergillosis in patients

- with acute leukemia. *Ann Intern Med.* 1984 Mar;100(3):345–51.
337. Feldmesser M. Role of neutrophils in invasive aspergillosis. *Infect Immun.* 2006 Dec;74(12):6514–6.
338. Eichelberger KR, Goldman WE. Human Neutrophil Isolation and Degranulation Responses to *Yersinia pestis* Infection. *Methods Mol Biol.* 2019;2010:197–209.
339. Urban CF, Nett JE. Neutrophil extracellular traps in fungal infection. *Semin Cell Dev Biol.* 2019 May;89:47–57.
340. Brinkmann V, Reichard U, Goosmann C, Fauler B, Uhlemann Y, Weiss DS, et al. Neutrophil extracellular traps kill bacteria. *Science.* 2004 Mar 5;303(5663):1532–5.
341. Cortjens B, de Boer OJ, de Jong R, Antonis AF, Sabogal Piñeros YS, Lutter R, et al. Neutrophil extracellular traps cause airway obstruction during respiratory syncytial virus disease. *J Pathol.* 2016 Feb;238(3):401–11.
342. Papayannopoulos V. Neutrophil extracellular traps in immunity and disease. *Nat Rev Immunol.* 2018 Feb;18(2):134–47.
343. Mantovani A, Cassatella MA, Costantini C, Jaillon S. Neutrophils in the activation and regulation of innate and adaptive immunity. *Nat Rev Immunol.* 2011 Jul 25;11(8):519–31.
344. Iwasaki A, Medzhitov R. Control of adaptive immunity by the innate immune system. *Nat Immunol.* 2015 Apr;16(4):343–53.
345. Rosales C. Neutrophils at the crossroads of innate and adaptive immunity. *J Leukoc Biol.* 2020 Jul;108(1):377–96.
346. Lim K, Hyun Y-M, Lambert-Emo K, Capece T, Bae S, Miller R, et al. Neutrophil trails guide influenza-specific CD8⁺ T cells in the airways. *Science.* 2015 Sep 4;349(6252):aaa4352.
347. Nakamura R, Maeda N, Shibata K, Yamada H, Kase T, Yoshikai Y. Interleukin-15 is critical in the pathogenesis of influenza a virus-induced acute lung injury. *J Virol.* 2010 Jun;84(11):5574–82.
348. Habibi MS, Thwaites RS, Chang M, Jozwik A, Paras A, Kirsebom F, et al. Neutrophilic inflammation in the respiratory mucosa predisposes to RSV infection. *Science.* 2020 Oct 9;370(6513).
349. Weiland JE, Davis WB, Holter JF, Mohammed JR, Dorinsky PM, Gadek JE. Lung neutrophils in the adult respiratory distress syndrome. Clinical and pathophysiologic significance. *Am Rev Respir Dis.* 1986 Feb;133(2):218–25.
350. Barnes BJ, Adrover JM, Baxter-Stoltzfus A, Borczuk A, Cools-Lartigue J, Crawford JM, et al. Targeting potential drivers of COVID-19: Neutrophil extracellular traps. *J Exp Med.* 2020 Jun 1;217(6).
351. Gallin JI. Human neutrophil heterogeneity exists, but is it meaningful? *Blood.* 1984 May;63(5):977–83.
352. Tak T, Wijten P, Heeres M, Pickkers P, Scholten A, Heck AJR, et al. Human CD62Ldim neutrophils identified as a separate subset by proteome profiling and in vivo pulse-chase labeling. *Blood.* 2017 Jun 29;129(26):3476–85.
353. Silvestre-Roig C, Fridlender ZG, Glogauer M, Scapini P. Neutrophil Diversity in Health and Disease. *Trends Immunol.* 2019 Jul;40(7):565–83.

354. Rudd JM, Pulavendran S, Ashar HK, Ritchey JW, Snider TA, Malayer JR, et al. Neutrophils Induce a Novel Chemokine Receptors Repertoire During Influenza Pneumonia. *Front Cell Infect Microbiol*. 2019 Apr 16;9:108.
355. Tate MD, Deng Y-M, Jones JE, Anderson GP, Brooks AG, Reading PC. Neutrophils ameliorate lung injury and the development of severe disease during influenza infection. *J Immunol*. 2009 Dec 1;183(11):7441–50.
356. Tate MD, Ioannidis LJ, Croker B, Brown LE, Brooks AG, Reading PC. The role of neutrophils during mild and severe influenza virus infections of mice. *PLoS One*. 2011 Mar 14;6(3):e17618.
357. Narasaraju T, Yang E, Samy RP, Ng HH, Poh WP, Liew A-A, et al. Excessive neutrophils and neutrophil extracellular traps contribute to acute lung injury of influenza pneumonitis. *Am J Pathol*. 2011 Jul;179(1):199–210.
358. Bradley LM, Douglass MF, Chatterjee D, Akira S, Baaten BJJ. Matrix metalloprotease 9 mediates neutrophil migration into the airways in response to influenza virus-induced toll-like receptor signaling. *PLoS Pathog*. 2012;8(4):e1002641.
359. Zhu B, Zhang R, Li C, Jiang L, Xiang M, Ye Z, et al. BCL6 modulates tissue neutrophil survival and exacerbates pulmonary inflammation following influenza virus infection. *Proc Natl Acad Sci U S A*. 2019 Jun 11;116(24):11888–93.
360. Williams M, Mildner A, Yona S. Developmental and Functional Heterogeneity of Monocytes. *Immunity*. 2018 Oct 16;49(4):595–613.
361. Baharom F, Thomas S, Rankin G, Lepzien R, Pourazar J, Behndig AF, et al. Dendritic Cells and Monocytes with Distinct Inflammatory Responses Reside in Lung Mucosa of Healthy Humans. *J Immunol*. 2016 Jun 1;196(11):4498–509.
362. Duan M, Hibbs ML, Chen W. The contributions of lung macrophage and monocyte heterogeneity to influenza pathogenesis. *Immunol Cell Biol*. 2017 Mar;95(3):225–35.
363. Matsukura S, Kokubu F, Kubo H, Tomita T, Tokunaga H, Kadokura M, et al. Expression of RANTES by normal airway epithelial cells after influenza virus A infection. *Am J Respir Cell Mol Biol*. 1998 Feb;18(2):255–64.
364. Herold S, von Wulffen W, Steinmueller M, Pleschka S, Kuziel WA, Mack M, et al. Alveolar epithelial cells direct monocyte transepithelial migration upon influenza virus infection: impact of chemokines and adhesion molecules. *J Immunol*. 2006 Aug 1;177(3):1817–24.
365. Gill MA, Long K, Kwon T, Muniz L, Mejias A, Connolly J, et al. Differential recruitment of dendritic cells and monocytes to respiratory mucosal sites in children with influenza virus or respiratory syncytial virus infection. *J Infect Dis*. 2008 Dec 1;198(11):1667–76.
366. Rosseau S, Selhorst J, Wiechmann K, Leissner K, Maus U, Mayer K, et al. Monocyte Migration Through the Alveolar Epithelial Barrier: Adhesion Molecule Mechanisms and Impact of Chemokines. *J Immunol*. 2000 Jan 1;164(1):427–35.
367. Coillard A, Segura E. In vivo Differentiation of Human Monocytes. *Front Immunol*. 2019;10:1907.
368. Meischel T, Villalon-Letelier F, Saunders PM, Reading PC, Londrigan SL. Influenza A virus interactions with macrophages: Lessons from epithelial cells. *Cell Microbiol*. 2020 May;22(5):e13170.

369. Tate MD, Pickett DL, van Rooijen N, Brooks AG, Reading PC. Critical role of airway macrophages in modulating disease severity during influenza virus infection of mice. *J Virol*. 2010 Aug;84(15):7569–80.
370. Hoeve MA, Nash AA, Jackson D, Randall RE, Dransfield I. Influenza virus A infection of human monocyte and macrophage subpopulations reveals increased susceptibility associated with cell differentiation. *PLoS One*. 2012;7(1):e29443.
371. Sprenger H, Meyer RG, Kaufmann A, Bussfeld D, Rischkowsky E, Gemsa D. Selective induction of monocyte and not neutrophil-attracting chemokines after influenza A virus infection. *J Exp Med*. 1996 Sep 1;184(3):1191–6.
372. Schneider C, Nobs SP, Heer AK, Kurrer M, Klinke G, van Rooijen N, et al. Alveolar macrophages are essential for protection from respiratory failure and associated morbidity following influenza virus infection. *PLoS Pathog*. 2014 Apr;10(4):e1004053.
373. Cardani A, Boulton A, Kim TS, Braciale TJ. Alveolar Macrophages Prevent Lethal Influenza Pneumonia By Inhibiting Infection Of Type-1 Alveolar Epithelial Cells. *PLoS Pathog*. 2017 Jan;13(1):e1006140.
374. Aegerter H, Kulikauskaite J, Crotta S, Patel H, Kelly G, Hessel EM, et al. Influenza-induced monocyte-derived alveolar macrophages confer prolonged antibacterial protection. *Nat Immunol*. 2020 Feb;21(2):145–57.
375. Lin KL, Suzuki Y, Nakano H, Ramsburg E, Gunn MD. CCR2+ monocyte-derived dendritic cells and exudate macrophages produce influenza-induced pulmonary immune pathology and mortality. *J Immunol*. 2008 Feb 15;180(4):2562–72.
376. Lin S-J, Lo M, Kuo R-L, Shih S-R, Ojcius DM, Lu J, et al. The pathological effects of CCR2+ inflammatory monocytes are amplified by an IFNAR1-triggered chemokine feedback loop in highly pathogenic influenza infection. *J Biomed Sci*. 2014 Nov 18;21:99.
377. Lamichhane PP, Samarasinghe AE. The Role of Innate Leukocytes during Influenza Virus Infection. *J Immunol Res*. 2019;2019:8028725.
378. Cong J, Wei H. Natural Killer Cells in the Lungs. *Front Immunol*. 2019 Jun 25;10:1416.
379. Wang J, Li F, Zheng M, Sun R, Wei H, Tian Z. Lung natural killer cells in mice: phenotype and response to respiratory infection. *Immunology*. 2012 Sep;137(1):37–47.
380. Ennis FA, Meager A, Beare AS, Qi YH, Riley D, Schwarz G, et al. Interferon induction and increased natural killer-cell activity in influenza infections in man. *Lancet*. 1981 Oct 24;2(8252):891–3.
381. Stein-Streilein J, Bennett M, Mann D, Kumar V. Natural killer cells in mouse lung: surface phenotype, target preference, and response to local influenza virus infection. *J Immunol*. 1983 Dec;131(6):2699–704.
382. Abdul-Careem MF, Mian MF, Yue G, Gillgrass A, Chenoweth MJ, Barra NG, et al. Critical Role of Natural Killer Cells in Lung Immunopathology During Influenza Infection in Mice. *The Journal of Infectious Diseases*. 2012 Jul 15;206(2):167–77.
383. Zhou G, Juang SWW, Kane KP. NK cells exacerbate the pathology of influenza virus infection in mice. *Eur J Immunol*. 2013 Apr;43(4):929–38.
384. Mandelboim O, Lieberman N, Lev M, Paul L, Arnon TI, Bushkin Y, et al. Recognition of haemagglutinins on virus-infected cells by NKp46 activates lysis by

- human NK cells. *Nature*. 2001 Feb 22;409(6823):1055–60.
385. Arnon TI, Lev M, Katz G, Chernobrov Y, Porgador A, Mandelboim O. Recognition of viral hemagglutinins by NKp44 but not by NKp30. *Eur J Immunol*. 2001 Sep;31(9):2680–9.
386. Ho JW, Hershkovitz O, Peiris M, Zilka A, Bar-Ilan A, Nal B, et al. H5-Type Influenza Virus Hemagglutinin Is Functionally Recognized by the Natural Killer-Activating Receptor NKp44. *JVI*. 2008 Feb 15;82(4):2028–32.
387. Ali SA, Rees RC, Oxford J. Modulation of human natural killer cytotoxicity by influenza virus and its subunit protein. *Immunology*. 1984 Aug;52(4):687–95.
388. Bar-On Y, Seidel E, Tsukerman P, Mandelboim M, Mandelboim O. Influenza virus uses its neuraminidase protein to evade the recognition of two activating NK cell receptors. *J Infect Dis*. 2014 Aug 1;210(3):410–8.
389. Duev-Cohen A, Bar-On Y, Glasner A, Berhani O, Ophir Y, Levi-Schaffer F, et al. The human 2B4 and NTB-A receptors bind the influenza viral hemagglutinin and co-stimulate NK cell cytotoxicity. *Oncotarget*. 2016 Mar 15;7(11):13093–105.
390. Mao H, Tu W, Qin G, Law HKW, Sia SF, Chan P-L, et al. Influenza Virus Directly Infects Human Natural Killer Cells and Induces Cell Apoptosis. *JVI*. 2009 Sep 15;83(18):9215–22.
391. van Erp E, van Kampen M, van Kasteren P, de Wit J. Viral Infection of Human Natural Killer Cells. *Viruses*. 2019 Mar 12;11(3):243.
392. Mao H, Tu W, Liu Y, Qin G, Zheng J, Chan P-L, et al. Inhibition of human natural killer cell activity by influenza virions and hemagglutinin. *J Virol*. 2010 May;84(9):4148–57.
393. Kumar P, Thakar MS, Ouyang W, Malarkannan S. IL-22 from conventional NK cells is epithelial regenerative and inflammation protective during influenza infection. *Mucosal Immunol*. 2013 Jan;6(1):69–82.
394. Parkin J, Cohen B. An overview of the immune system. *Lancet*. 2001 Jun 2;357(9270):1777–89.
395. Flores-Torres AS, Salinas-Carmona MC, Salinas E, Rosas-Taraco AG. Eosinophils and Respiratory Viruses. *Viral Immunol*. 2019 Jun;32(5):198–207.
396. LeMessurier KS, Rooney R, Ghoneim HE, Liu B, Li K, Smallwood HS, et al. Influenza A virus directly modulates mouse eosinophil responses. *J Leukoc Biol*. 2020 Jul;108(1):151–68.
397. Samarasinghe AE, Melo RCN, Duan S, LeMessurier KS, Liedmann S, Surman SL, et al. Eosinophils Promote Antiviral Immunity in Mice Infected with Influenza A Virus. *Jl*. 2017 Apr 15;198(8):3214–26.
398. Bonilla FA, Oettgen HC. Adaptive immunity. *J Allergy Clin Immunol*. 2010 Feb;125(2 Suppl 2):S33-40.
399. Nüssing S, Sant S, Koutsakos M, Subbarao K, Nguyen THO, Kedzierska K. Innate and adaptive T cells in influenza disease. *Front Med*. 2018 Feb;12(1):34–47.
400. Li H, Xiang Z, Feng T, Li J, Liu Y, Fan Y, et al. Human V γ 9V δ 2-T cells efficiently kill influenza virus-infected lung alveolar epithelial cells. *Cell Mol Immunol*. 2013 Mar;10(2):159–64.

401. Lu Y, Li Z, Ma C, Wang H, Zheng J, Cui L, et al. The interaction of influenza H5N1 viral hemagglutinin with sialic acid receptors leads to the activation of human $\gamma\delta$ T cells. *Cell Mol Immunol*. 2013 Nov;10(6):463–70.
402. Loh L, Wang Z, Sant S, Koutsakos M, Jegaskanda S, Corbett AJ, et al. Human mucosal-associated invariant T cells contribute to antiviral influenza immunity via IL-18-dependent activation. *Proc Natl Acad Sci U S A*. 2016 Sep 6;113(36):10133–8.
403. van Wilgenburg B, Loh L, Chen Z, Pediongco TJ, Wang H, Shi M, et al. MAIT cells contribute to protection against lethal influenza infection in vivo. *Nat Commun*. 2018 Dec;9(1):4706.
404. Godfrey DI, Koay H-F, McCluskey J, Gherardin NA. The biology and functional importance of MAIT cells. *Nat Immunol*. 2019 Sep;20(9):1110–28.
405. Sonnenberg GF, Hepworth MR. Functional interactions between innate lymphoid cells and adaptive immunity. *Nat Rev Immunol*. 2019 Oct;19(10):599–613.
406. Monticelli LA, Sonnenberg GF, Abt MC, Alenghat T, Ziegler CGK, Doering TA, et al. Innate lymphoid cells promote lung-tissue homeostasis after infection with influenza virus. *Nat Immunol*. 2011 Nov;12(11):1045–54.
407. Califano D, Furuya Y, Roberts S, Avram D, McKenzie ANJ, Metzger DW. IFN- γ increases susceptibility to influenza A infection through suppression of group II innate lymphoid cells. *Mucosal Immunol*. 2018 Jan;11(1):209–19.
408. Yang Y, Tang H. Aberrant coagulation causes a hyper-inflammatory response in severe influenza pneumonia. *Cell Mol Immunol*. 2016 Jul;13(4):432–42.
409. Lê VB, Schneider JG, Boergeling Y, Berri F, Ducatez M, Guerin J-L, et al. Platelet Activation and Aggregation Promote Lung Inflammation and Influenza Virus Pathogenesis. *Am J Respir Crit Care Med*. 2015 Apr;191(7):804–19.
410. Koupenova M, Corkrey HA, Vitseva O, Manni G, Pang CJ, Clancy L, et al. The role of platelets in mediating a response to human influenza infection. *Nat Commun*. 2019 Apr 16;10(1):1780.
411. Boilard E, Paré G, Rousseau M, Cloutier N, Dubuc I, Lévesque T, et al. Influenza virus H1N1 activates platelets through Fc γ RIIA signaling and thrombin generation. *Blood*. 2014 May 1;123(18):2854–63.
412. Kazatchkine MD, Lambré CR, Kieffer N, Maillet F, Nurden AT. Membrane-bound hemagglutinin mediates antibody and complement-dependent lysis of influenza virus-treated human platelets in autologous serum. *J Clin Invest*. 1984 Sep;74(3):976–84.
413. Pariser DN, Hilt ZT, Ture SK, Blick-Nitko SK, Looney MR, Cleary SJ, et al. Lung megakaryocytes are immune modulatory cells. *Journal of Clinical Investigation*. 2021 Jan 4;131(1):e137377.
414. Jansen JM, Gerlach T, Elbahesh H, Rimmelzwaan GF, Saletti G. Influenza virus-specific CD4 $^{+}$ and CD8 $^{+}$ T cell-mediated immunity induced by infection and vaccination. *J Clin Virol*. 2019 Oct;119:44–52.
415. Mosmann TR, Cherwinski H, Bond MW, Giedlin MA, Coffman RL. Two types of murine helper T cell clone. I. Definition according to profiles of lymphokine activities and secreted proteins. *J Immunol*. 1986 Apr 1;136(7):2348–57.
416. Steinman L. A brief history of T(H)17, the first major revision in the T(H)1/T(H)2 hypothesis of T cell-mediated tissue damage. *Nat Med*. 2007 Feb;13(2):139–45.

417. Veldhoen M, Uyttenhove C, van Snick J, Helmby H, Westendorf A, Buer J, et al. Transforming growth factor-beta "reprograms" the differentiation of T helper 2 cells and promotes an interleukin 9-producing subset. *Nat Immunol*. 2008 Dec;9(12):1341–6.
418. Baumgarth N, Herman OC, Jager GC, Brown LE, Herzenberg LA, Chen J. B-1 and B-2 cell-derived immunoglobulin M antibodies are nonredundant components of the protective response to influenza virus infection. *J Exp Med*. 2000 Jul 17;192(2):271–80.
419. Lam JH, Baumgarth N. The Multifaceted B Cell Response to Influenza Virus. *J Immunol*. 2019 Jan 15;202(2):351–9.
420. Seibert CW, Rahmat S, Krause JC, Eggink D, Albrecht RA, Goff PH, et al. Recombinant IgA Is Sufficient To Prevent Influenza Virus Transmission in Guinea Pigs. *Journal of Virology*. 2013 Jul 15;87(14):7793–804.
421. Kopf M, Schneider C, Nobs SP. The development and function of lung-resident macrophages and dendritic cells. *Nat Immunol*. 2015 Jan;16(1):36–44.
422. Lichtner M, Mastroianni CM, Rossi R, Russo G, Belvisi V, Marocco R, et al. Severe and persistent depletion of circulating plasmacytoid dendritic cells in patients with 2009 pandemic H1N1 infection. *PLoS One*. 2011;6(5):e19872.
423. Moltedo B, Li W, Yount JS, Moran TM. Unique Type I Interferon Responses Determine the Functional Fate of Migratory Lung Dendritic Cells during Influenza Virus Infection. Mossman KL, editor. *PLoS Pathog*. 2011 Nov 3;7(11):e1002345.
424. Lui G, Manches O, Angel J, Molens J-P, Chaperot L, Plumas J. Plasmacytoid dendritic cells capture and cross-present viral antigens from influenza-virus exposed cells. *PLoS One*. 2009 Sep 22;4(9):e7111.
425. Wolf AI, Buehler D, Hensley SE, Cavanagh LL, Wherry EJ, Kastner P, et al. Plasmacytoid Dendritic Cells Are Dispensable during Primary Influenza Virus Infection. *J Immunol*. 2009 Jan 15;182(2):871–9.
426. Vangeti S, Gertow J, Yu M, Liu S, Baharom F, Scholz S, et al. Human Blood and Tonsil Plasmacytoid Dendritic Cells Display Similar Gene Expression Profiles but Exhibit Differential Type I IFN Responses to Influenza A Virus Infection. *J Immunol*. 2019 Apr 1;202(7):2069–81.
427. Hufford MM, Richardson G, Zhou H, Manicassamy B, Garcia-Sastre A, Enelow RI, et al. Influenza-infected neutrophils within the infected lungs act as antigen presenting cells for anti-viral CD8(+) T cells. *PLoS One*. 2012;7(10):e46581.
428. Ge MQ, Ho AWS, Tang Y, Wong KHS, Chua BYL, Gasser S, et al. NK cells regulate CD8+ T cell priming and dendritic cell migration during influenza A infection by IFN- γ and perforin-dependent mechanisms. *J Immunol*. 2012 Sep 1;189(5):2099–109.
429. Strutt TM, Dhume K, Finn CM, Hwang JH, Castonguay C, Swain SL, et al. IL-15 supports the generation of protective lung-resident memory CD4 T cells. *Mucosal Immunol*. 2018 May;11(3):668–80.
430. Yamada YK, Meager A, Yamada A, Ennis FA. Human interferon alpha and gamma production by lymphocytes during the generation of influenza virus-specific cytotoxic T lymphocytes. *J Gen Virol*. 1986 Nov;67 (Pt 11):2325–34.
431. Verhoeven D, Perry S. Differential mucosal IL-10-induced immunoregulation of innate immune responses occurs in influenza infected infants/toddlers and adults. *Immunol Cell Biol*. 2017 Mar;95(3):252–60.

432. Sarma JV, Ward PA. The complement system. *Cell Tissue Res.* 2011 Jan;343(1):227–35.
433. Merle NS, Church SE, Fremeaux-Bacchi V, Roumenina LT. Complement System Part I - Molecular Mechanisms of Activation and Regulation. *Front Immunol.* 2015;6:262.
434. Sun S, Zhao G, Liu C, Wu X, Guo Y, Yu H, et al. Inhibition of complement activation alleviates acute lung injury induced by highly pathogenic avian influenza H5N1 virus infection. *Am J Respir Cell Mol Biol.* 2013 Aug;49(2):221–30.
435. Kandasamy M, Ying PC, Ho AWS, Sumatoh HR, Schlitzer A, Hughes TR, et al. Complement mediated signaling on pulmonary CD103(+) dendritic cells is critical for their migratory function in response to influenza infection. *PLoS Pathog.* 2013 Jan;9(1):e1003115.
436. Kulkarni HS, Liszewski MK, Brody SL, Atkinson JP. The complement system in the airway epithelium: An overlooked host defense mechanism and therapeutic target? *J Allergy Clin Immunol.* 2018 May;141(5):1582-1586.e1.
437. Garcia CC, Weston-Davies W, Russo RC, Tavares LP, Rachid MA, Alves-Filho JC, et al. Complement C5 activation during influenza A infection in mice contributes to neutrophil recruitment and lung injury. *PLoS One.* 2013;8(5):e64443.
438. Song N, Li P, Jiang Y, Sun H, Cui J, Zhao G, et al. C5a receptor1 inhibition alleviates influenza virus-induced acute lung injury. *Int Immunopharmacol.* 2018 Jun;59:12–20.
439. Bjornson AB, Mellencamp MA, Schiff GM. Complement is activated in the upper respiratory tract during influenza virus infection. *Am Rev Respir Dis.* 1991 May;143(5 Pt 1):1062–6.
440. O'Brien KB, Morrison TE, Dundore DY, Heise MT, Schultz-Cherry S. A protective role for complement C3 protein during pandemic 2009 H1N1 and H5N1 influenza A virus infection. *PLoS One.* 2011 Mar 9;6(3):e17377.
441. Beebe DP, Schreiber RD, Cooper NR. Neutralization of influenza virus by normal human sera: mechanisms involving antibody and complement. *J Immunol.* 1983 Mar;130(3):1317–22.
442. Kopf M, Abel B, Gallimore A, Carroll M, Bachmann MF. Complement component C3 promotes T-cell priming and lung migration to control acute influenza virus infection. *Nat Med.* 2002 Apr;8(4):373–8.
443. Wang R, Xiao H, Guo R, Li Y, Shen B. The role of C5a in acute lung injury induced by highly pathogenic viral infections. *Emerg Microbes Infect.* 2015 May;4(5):e28.
444. Kwong JC, Schwartz KL, Campitelli MA, Chung H, Crowcroft NS, Karnauchov T, et al. Acute Myocardial Infarction after Laboratory-Confirmed Influenza Infection. *N Engl J Med.* 2018 Jan 25;378(4):345–53.
445. Kim DD, Song W-C. Membrane complement regulatory proteins. *Clin Immunol.* 2006 Mar;118(2–3):127–36.
446. Miwa T, Song WC. Membrane complement regulatory proteins: insight from animal studies and relevance to human diseases. *Int Immunopharmacol.* 2001 Mar;1(3):445–59.
447. Hoffmann EM. Inhibition of complement by a substance isolated from human

erythrocytes. II. Studies on the site and mechanism of action. *Immunochemistry*. 1969 May;6(3):405–19.

448. Medof ME, Kinoshita T, Nussenzweig V. Inhibition of complement activation on the surface of cells after incorporation of decay-accelerating factor (DAF) into their membranes. *J Exp Med*. 1984 Nov 1;160(5):1558–78.

449. Harris CL, Pettigrew DM, Lea SM, Morgan BP. Decay-accelerating factor must bind both components of the complement alternative pathway C3 convertase to mediate efficient decay. *J Immunol*. 2007 Jan 1;178(1):352–9.

450. Panwar HS, Ojha H, Ghosh P, Barage SH, Raut S, Sahu A. Molecular engineering of an efficient four-domain DAF-MCP chimera reveals the presence of functional modularity in RCA proteins. *Proc Natl Acad Sci U S A*. 2019 May 14;116(20):9953–8.

451. Alegretti AP, Mucenic T, Merzoni J, Faulhaber GA, Silla LM, Xavier RM. Expression of CD55 and CD59 on peripheral blood cells from systemic lupus erythematosus (SLE) patients. *Cell Immunol*. 2010;265(2):127–32.

452. Ozen A, Comrie WA, Ardy RC, Domínguez Conde C, Dalgic B, Beser ÖF, et al. CD55 Deficiency, Early-Onset Protein-Losing Enteropathy, and Thrombosis. *N Engl J Med*. 2017 Jul 6;377(1):52–61.

453. Hill A, DeZern AE, Kinoshita T, Brodsky RA. Paroxysmal nocturnal haemoglobinuria. *Nat Rev Dis Primers*. 2017 May 18;3:17028.

454. Dho SH, Lim JC, Kim LK. Beyond the Role of CD55 as a Complement Component. *Immune Netw*. 2018 Feb;18(1):e11.

455. Li B, Allendorf DJ, Hansen R, Marroquin J, Cramer DE, Harris CL, et al. Combined yeast β -glucan and antitumor monoclonal antibody therapy requires C5a-mediated neutrophil chemotaxis via regulation of decay-accelerating factor CD55. *Cancer Res*. 2007 Aug 1;67(15):7421–30.

456. Hamann J, Vogel B, van Schijndel GM, van Lier RA. The seven-span transmembrane receptor CD97 has a cellular ligand (CD55, DAF). *J Exp Med*. 1996 Sep 1;184(3):1185–9.

457. Qian YM, Haino M, Kelly K, Song WC. Structural characterization of mouse CD97 and study of its specific interaction with the murine decay-accelerating factor (DAF, CD55). *Immunology*. 1999 Oct;98(2):303–11.

458. Hamann J, van Zeventer C, Bijl A, Molenaar C, Tesselaar K, van Lier RA. Molecular cloning and characterization of mouse CD97. *Int Immunol*. 2000 Apr;12(4):439–48.

459. Abbott RJM, Spendlove I, Roversi P, Fitzgibbon H, Knott V, Teriete P, et al. Structural and Functional Characterization of a Novel T Cell Receptor Co-regulatory Protein Complex, CD97-CD55. *Journal of Biological Chemistry*. 2007 Jul;282(30):22023–32.

460. Leemans JC, te Velde AA, Florquin S, Bennink RJ, de Bruin K, van Lier RAW, et al. The Epidermal Growth Factor-Seven Transmembrane (EGF-TM7) Receptor CD97 Is Required for Neutrophil Migration and Host Defense. *J Immunol*. 2004 Jan 15;172(2):1125–31.

461. Hsiao C-C, van der Poel M, van Ham TJ, Hamann J. Macrophages Do Not Express the Phagocytic Receptor BAI1/ADGRB1. *Front Immunol*. 2019 May 3;10:962.

462. Lin HH, Stacey M, Saxby C, Knott V, Chaudhry Y, Evans D, et al. Molecular analysis of the epidermal growth factor-like short consensus repeat domain-mediated protein-protein interactions: dissection of the CD97-CD55 complex. *J Biol Chem*. 2001 Jun 29;276(26):24160–9.
463. Lawrence DW, Bruyninckx WJ, Louis NA, Lublin DM, Stahl GL, Parkos CA, et al. Antiadhesive Role of Apical Decay-accelerating Factor (CD55) in Human Neutrophil Transmigration across Mucosal Epithelia. *Journal of Experimental Medicine*. 2003 Oct 6;198(7):999–1010.
464. Louis NA, Hamilton KE, Kong T, Colgan SP. HIF-dependent induction of apical CD55 coordinates epithelial clearance of neutrophils. *FASEB J*. 2005 Jun;19(8):950–9.
465. Pandya PH, Fisher AJ, Mickler EA, Temm CJ, Lipking KP, Gracon A, et al. Hypoxia-Inducible Factor-1 α Regulates CD55 in Airway Epithelium. *Am J Respir Cell Mol Biol*. 2016 Dec;55(6):889–98.
466. Zhou J, To KK-W, Dong H, Cheng Z-S, Lau CC-Y, Poon VKM, et al. A functional variation in CD55 increases the severity of 2009 pandemic H1N1 influenza A virus infection. *J Infect Dis*. 2012 Aug 15;206(4):495–503.
467. Garcia-Etxebarria K, Bracho MA, Galán JC, Pumarola T, Castilla J, Ortiz de Lejarazu R, et al. No Major Host Genetic Risk Factor Contributed to A(H1N1)2009 Influenza Severity. *PLoS One*. 2015;10(9):e0135983.
468. Lee N, Cao B, Ke C, Lu H, Hu Y, Tam CHT, et al. IFITM3, TLR3, and CD55 Gene SNPs and Cumulative Genetic Risks for Severe Outcomes in Chinese Patients With H7N9/H1N1pdm09 Influenza. *J Infect Dis*. 2017 Jul 1;216(1):97–104.
469. Lublin DM, Krsek-Staples J, Pangburn MK, Atkinson JP. Biosynthesis and glycosylation of the human complement regulatory protein decay-accelerating factor. *J Immunol*. 1986 Sep 1;137(5):1629–35.
470. Medof ME, Walter EI, Rutgers JL, Knowles DM, Nussenzweig V. Identification of the complement decay-accelerating factor (DAF) on epithelium and glandular cells and in body fluids. *J Exp Med*. 1987 Mar 1;165(3):848–64.
471. Reddy P, Caras I, Krieger M. Effects of O-linked glycosylation on the cell surface expression and stability of decay-accelerating factor, a glycopospholipid-anchored membrane protein. *J Biol Chem*. 1989 Oct 15;264(29):17329–36.
472. Coyne KE, Hall SE, Thompson S, Arce MA, Kinoshita T, Fujita T, et al. Mapping of epitopes, glycosylation sites, and complement regulatory domains in human decay accelerating factor. *J Immunol*. 1992 Nov 1;149(9):2906–13.
473. Varsano S, Frolkis I, Ophir D. Expression and distribution of cell-membrane complement regulatory glycoproteins along the human respiratory tract. *Am J Respir Crit Care Med*. 1995 Sep;152(3):1087–93.
474. Lukacik P, Roversi P, White J, Esser D, Smith GP, Billington J, et al. Complement regulation at the molecular level: the structure of decay-accelerating factor. *Proc Natl Acad Sci U S A*. 2004 Feb 3;101(5):1279–84.
475. Varki A. Sialic acids in human health and disease. *Trends Mol Med*. 2008 Aug;14(8):351–60.
476. Varki A, Gagneux P. Multifarious roles of sialic acids in immunity. *Ann N Y Acad Sci*. 2012 Apr;1253:16–36.
477. Langford-Smith A, Day AJ, Bishop PN, Clark SJ. Complementing the Sugar

Code: Role of GAGs and Sialic Acid in Complement Regulation. *Front Immunol.* 2015;6:25.

478. Oerlemans MMP, Moons SJ, Heming JJA, Boltje TJ, de Jonge MI, Langereis JD. Uptake of Sialic Acid by Nontypeable *Haemophilus influenzae* Increases Complement Resistance through Decreasing IgM-Dependent Complement Activation. *Infect Immun.* 2019 Jun;87(6).

479. Abeln M, Albers I, Peters-Bernard U, Flächsig-Schulz K, Kats E, Kispert A, et al. Sialic acid is a critical fetal defense against maternal complement attack. *J Clin Invest.* 2019 Jan 2;129(1):422–36.

480. Khan N, de Manuel M, Peyregne S, Do R, Prufer K, Marques-Bonet T, et al. Multiple Genomic Events Altering Hominin SIGLEC Biology and Innate Immunity Predated the Common Ancestor of Humans and Archaic Hominins. *Genome Biol Evol.* 2020 Jul 1;12(7):1040–50.

481. Macauley MS, Crocker PR, Paulson JC. Siglec-mediated regulation of immune cell function in disease. *Nat Rev Immunol.* 2014 Oct;14(10):653–66.

482. Pagan JD, Kitaoka M, Anthony RM. Engineered Sialylation of Pathogenic Antibodies In Vivo Attenuates Autoimmune Disease. *Cell.* 2018 Jan 25;172(3):564-577.e13.

483. van de Bovenkamp FS, Derksen NIL, Ooijevaar-de Heer P, van Schie KA, Kruithof S, Berkowska MA, et al. Adaptive antibody diversification through N-linked glycosylation of the immunoglobulin variable region. *Proc Natl Acad Sci U S A.* 2018 Feb 20;115(8):1901–6.

484. Formiga RO, Amaral FC, Souza CF, Mendes DAGB, Wanderley CWS, Lorenzini CB, et al. Neuraminidase inhibitors rewire neutrophil function in murine sepsis and COVID-19 patient cells. *bioRxiv.* 2020 Nov 12;

485. Suzuki H, Kurita T, Kakinuma K. Effects of neuraminidase on O₂ consumption and release of O₂ and H₂O₂ from phagocytosing human polymorphonuclear leukocytes. *Blood.* 1982 Aug;60(2):446–53.

486. Chang Y-C, Uchiyama S, Varki A, Nizet V. Leukocyte inflammatory responses provoked by pneumococcal sialidase. *mBio.* 2012;3(1).

487. Siegel SJ, Roche AM, Weiser JN. Influenza promotes pneumococcal growth during coinfection by providing host sialylated substrates as a nutrient source. *Cell Host Microbe.* 2014 Jul 9;16(1):55–67.

488. Bhatia A, Kast R. How influenza's neuraminidase promotes virulence and creates localized lung mucosa immunodeficiency. *Cellular and Molecular Biology Letters [Internet].* 2007 Jan 1 [cited 2021 Feb 25];12(1). Available from: <https://www.degruyter.com/doi/10.2478/s11658-006-0055-x>

489. Heindel DW, Koppolu S, Zhang Y, Kasper B, Meche L, Vaiana CA, et al. Glycomic analysis of host response reveals high mannose as a key mediator of influenza severity. *Proc Natl Acad Sci U S A.* 2020 Oct 27;117(43):26926–35.

490. Gargaglioni LH, Marques DA. Let's talk about sex in the context of COVID-19. *J Appl Physiol (1985).* 2020 Jun 1;128(6):1533–8.

491. Gebhard C, Regitz-Zagrosek V, Neuhauser HK, Morgan R, Klein SL. Impact of sex and gender on COVID-19 outcomes in Europe. *Biol Sex Differ.* 2020 May 25;11(1):29.

492. Sell S. Immunopathology. *Am J Pathol*. 1978 Jan;90(1):211–80.
493. Medzhitov R, Schneider DS, Soares MP. Disease tolerance as a defense strategy. *Science*. 2012 Feb 24;335(6071):936–41.
494. Newton AH, Cardani A, Braciale TJ. The host immune response in respiratory virus infection: balancing virus clearance and immunopathology. *Semin Immunopathol*. 2016 Jul;38(4):471–82.
495. Damjanovic D, Small C-L, Jeyanathan M, Jeyananthan M, McCormick S, Xing Z. Immunopathology in influenza virus infection: uncoupling the friend from foe. *Clin Immunol*. 2012 Jul;144(1):57–69.
496. Talmi-Frank D, Altboum Z, Solomonov I, Udi Y, Jaitin DA, Klepfish M, et al. Extracellular Matrix Proteolysis by MT1-MMP Contributes to Influenza-Related Tissue Damage and Mortality. *Cell Host Microbe*. 2016 Oct 12;20(4):458–70.
497. Wu Z, McGoogan JM. Characteristics of and Important Lessons From the Coronavirus Disease 2019 (COVID-19) Outbreak in China: Summary of a Report of 72 314 Cases From the Chinese Center for Disease Control and Prevention. *JAMA*. 2020 Apr 7;323(13):1239–42.
498. Arunachalam PS, Wimmers F, Mok CKP, Perera RAPM, Scott M, Hagan T, et al. Systems biological assessment of immunity to mild versus severe COVID-19 infection in humans. *Science*. 2020 Sep 4;369(6508):1210–20.
499. Hadjadj J, Yatim N, Barnabei L, Corneau A, Boussier J, Smith N, et al. Impaired type I interferon activity and inflammatory responses in severe COVID-19 patients. *Science*. 2020 Aug 7;369(6504):718–24.
500. Gralinski LE, Sheahan TP, Morrison TE, Menachery VD, Jensen K, Leist SR, et al. Complement Activation Contributes to Severe Acute Respiratory Syndrome Coronavirus Pathogenesis. *mBio*. 2018 Oct 9;9(5).
501. Jiang Y, Zhao G, Song N, Li P, Chen Y, Guo Y, et al. Blockade of the C5a-C5aR axis alleviates lung damage in hDPP4-transgenic mice infected with MERS-CoV. *Emerg Microbes Infect*. 2018 Apr 24;7(1):77.
502. Fletcher-Sandersjö A, Bellander B-M. Is COVID-19 associated thrombosis caused by overactivation of the complement cascade? A literature review. *Thromb Res*. 2020 Oct;194:36–41.
503. Lo MW, Kemper C, Woodruff TM. COVID-19: Complement, Coagulation, and Collateral Damage. *J Immunol*. 2020 Sep 15;205(6):1488–95.

**Chapter 2 – Complement decay-accelerating factor
increases immunopathology via complement activation and
immune cell recruitment**

2.1 Author contributions

The experiments presented in this chapter were designed and planned by Nuno B Santos, Zoé E. Vaz da Silva and Maria João Amorim. Experiments and data generated for Fig. 1, Fig. 2 and part of Fig. 3 and Table S1 were performed by Zoé E Vaz da Silva. Primary mouse embryo fibroblasts (MEF) used for Fig. S2-B-E were collected by Zoé E Vaz da Silva. All the remaining experiments were performed by Nuno B Santos. Nuno B Santos, Zoé E Vaz da Silva and Maria João Amorim wrote the manuscript. This chapter is part of a submitted manuscript, which can be assessed as a preprint: Santos NB, Vaz da Silva ZE, Gomes C, Reis CA, Amorim MJ. Complement Decay-Accelerating Factor is a modulator of influenza A virus lung immunopathology. *bioRxiv* **2021**, 10.1101/2021.02.16.431406, 2021.2002.2016.431406, doi:10.1101/2021.02.16.431406.

2.2 Summary

Clearance of viral infections, such as influenza A virus (IAV), must be fine-tuned to eliminate the pathogen without causing immunopathology. As such, an aggressive initial innate immune response favors the host in contrast to a detrimental prolonged inflammation. The complement pathway bridges the innate and adaptive immune system and contributes to the response by directly clearing pathogens or infected cells, as well as recruiting proinflammatory immune cells and regulating inflammation. However, the impact of modulating complement activation in viral infections is still unclear.

In this work, we targeted the complement decay-accelerating factor (DAF/CD55), a surface protein that protects cells from non-specific complement attack, and analyzed its role in IAV infections. We found that DAF modulates IAV infection in vivo, via an interplay with the antigenic viral proteins hemagglutinin (HA) and neuraminidase (NA), in a strain specific manner.

Our results reveal that, contrary to what could be expected, DAF potentiates complement activation, increasing the recruitment of neutrophils, monocytes and T cells. Remarkably, this mechanism has no impact on viral loads but rather on the host resilience to infection.

2.3 Introduction

Host-pathogen interactions are very complex with both parts contributing to the progression and outcome of infections. In the case of viruses, pathogen- and damage-associated molecular patterns (PAMP and DAMP, respectively) are detected by pattern recognition receptors (PRR) alerting the host of their presence, and triggering the immune response to clear the infection (1,2). It is generally accepted that for viral infections, an aggressive initial activation of innate immunity favors the host, whilst mechanisms that originate prolonged inflammation are associated with severe outcomes. This paradigm underpins for example the sex differences observed for coronavirus disease 19 (COVID-19), that results in lower death rate in women, despite similar incidence of infection in both sexes (3–5). However, an excessive immune response activation might destabilize the equilibrium needed to eliminate the pathogen without causing tissue damage, and lead to immunopathology (6,7). It is therefore important to determine the host factors and viral characteristics that result in an efficient immune response for clearing the pathogen without provoking immunopathology.

Influenza A virus (IAV) is the prevalent cause of seasonal flu, a relevant health problem as it kills up to 600,000 people worldwide yearly (8). IAV replication occurs in the upper and lower respiratory tracts, peaks normally 2 days after infection, and in most cases little virus shed can be detected after 6 days (9). Usually, symptoms (fever, cough, acute viral nasopharyngitis, headache) clear after 7-10 days, with fatigue enduring for weeks, without serious outcomes (8,10,11). In a proportion of people, however, severe complications occur, with the elderly, immunosuppressed, pregnant women, and people with associated comorbidities being at higher risk (12). IAV can also provoke pandemic outbreaks, associated with zoonotic events, which lead to significant higher mortality than seasonal epidemics. The 1918 Spanish influenza,

for example, caused up to 50 million deaths (13). Complications may include hemorrhagic bronchitis, pneumonia (primary viral or secondary bacterial), and death (14–17). They usually derive from an exacerbated immune response leading to tissue damage (18,19). Identifying intrinsic risk factors that contribute to severe disease outcomes may minimize immunopathology in the lungs and uncover new therapeutic targets with decreased proneness to develop resistance.

Defects in type I IFN response have been associated with the more severe cases of COVID-19 (20,21), suggesting that the initial steps in immune activation define disease outcome. However, there are other players involved in mounting immune responses, such as the complement system. The complement system has been extensively reviewed (22–24) and consists in a cascade of proteolytic interactions that lead to the direct killing of the pathogen or infected cell, as well as proinflammatory immune cell recruitment. Remarkably, C3 has been found within the mucus barrier (25), which elucidates complement role in early immune response upon pathogen infection in the airways. Disease severity and mortality have been associated with both lack or excess of complement activation in several viral infections such as severe acute respiratory syndrome coronavirus (SARS-CoV) (26,27), middle eastern respiratory syndrome coronavirus (MERS-CoV) (28), severe acute respiratory syndrome coronavirus 2 (SARS-CoV-2) (29–31), and IAV (32–34). However, it is still unclear how fine-tuning complement activation may impact in the development of disease severity.

One strategy to tune complement activation in infection is to target its regulators. Complement decay-accelerating factor (DAF/CD55) is a membrane-bound regulator of complement activation (RCA) exposed at the surface of most cell types, including human and murine airways (35–37). DAF promotes the decay of C3 convertases, thus protecting healthy cells from non-specific complement attack, and inhibiting the release of

anaphylatoxins that would recruit and activate the immune response (38–40). In humans, it has been reported that DAF deficiency leads to excess complement activation with systemic implications such as hemolysis, in a condition named paroxysmal nocturnal haemoglobinuria (PNH) (41–43). In order to improve their life condition, PNH patients take complement inhibitors, which increase proneness to infections, being 11.2% of viral origin (43,44). Within those, 21.7% are caused by IAV (44). Furthermore, higher risk of severity upon infection with pandemic and avian IAV strains has been associated with SNPs in DAF promoter region decreasing protein expression (45,46).

Previously in our lab, we observed that mice depleted of DAF were protected from human circulating strains of IAV, A/California/7/2009 (Cal) and A/England/195/2009 (Eng), elucidated by decreased bodyweight loss and mortality (Fig. 2.1-A, B).

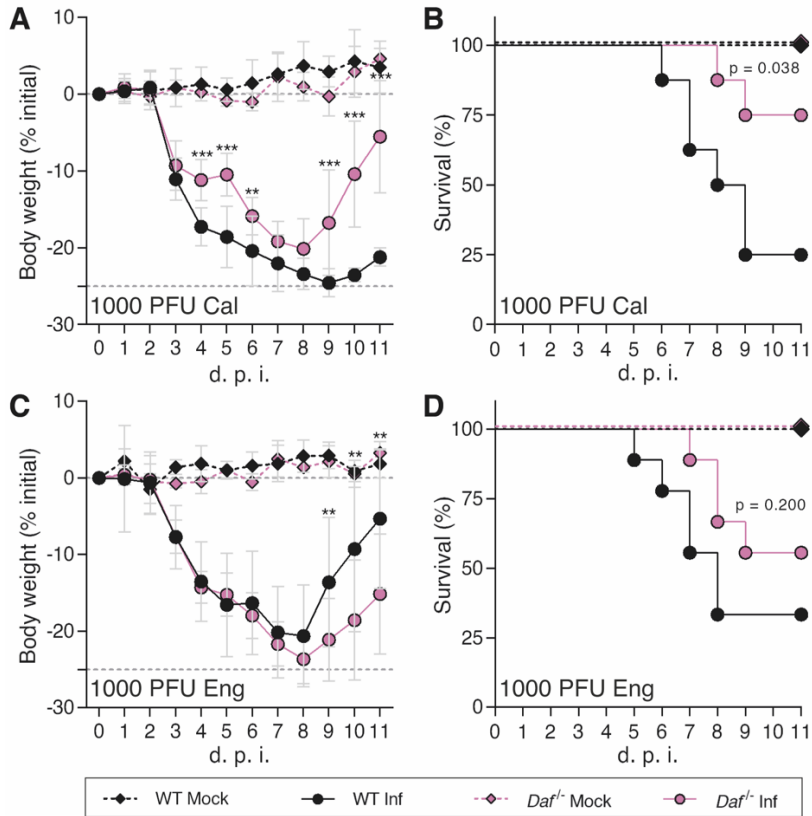


Fig. 2.1 – Complement decay-accelerating factor (DAF) aggravates IAV infection in vivo.
A, B: Bodyweight loss (**A**) and mortality (**B**) of C57BL/6J WT or *Daf*^{-/-} mice infected with 1000 PFU of A/California/7/2009 (Cal) (Inf n = 8; mock n = 3 for per group) **C, D:** Bodyweight loss (**C**) and mortality (**D**) of C57BL/6J WT or *Daf*^{-/-} mice infected with 1000 PFU of A/England/195/2009 (Eng) (Inf n = 9 per group; mock n = 5 and n = 4 for WT and *Daf*^{-/-} respectively). Results are expressed as mean±sd, statistical analysis detailed in materials and methods.

Additionally, *Daf*^{-/-} mice were protected upon challenge with the lower virulence lab-adapted strain A/X-31 (X31 is a reassortant strain of PR8 containing segments 4 and 6 from A/Hong Kong/1/68 (HK68) (47) and for clarity purposes, the X31 strain will be mentioned as PR8-HK4,6 throughout this work), but not from the more virulent A/Puerto

Rico/8/1934 (PR8) (Fig. 2.2-A, D). This protection was conferred specifically by DAF absence, but not the terminal RCA CD59 (40) (Fig. 2.2-E, F).

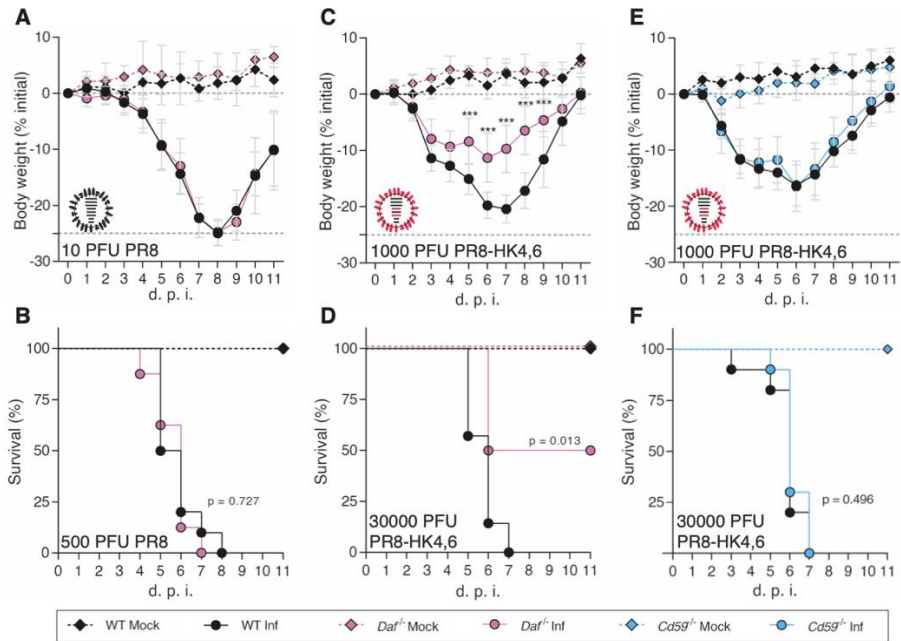


Fig. 2.2 – *Daf*^{-/-} mice are protected against PR8-HK4,6, but not PR8, and protection is specific of this RCA.

A, B: Bodyweight loss (**A**) and mortality (**B**) of C57BL/6J WT or *Daf*^{-/-} mice infected with the indicated doses of A/Puerto Rico/8/1934 (PR8) (**A:** Inf n = 8 per group; mock n = 7 and n = 4 for WT and *Daf*^{-/-} respectively; **B:** Inf n = 9 and n = 10, mock n = 8 and n = 4 for WT and *Daf*^{-/-} respectively). **C, D:** Bodyweight loss (**C**) and mortality (**D**) of C57BL/6J WT or *Daf*^{-/-} mice infected with the indicated doses of A/X-31 (PR8-HK4,6) (**C:** Inf n = 9 and n = 10, mock n = 8 and n = 4 for WT and *Daf*^{-/-} respectively; **D:** Inf n = 7 and n = 8, mock n = 3 and n = 2 for WT and *Daf*^{-/-} respectively). **E, F:** Bodyweight loss (**E**) and mortality (**F**) of C57BL/6J WT or *Cd59*^{-/-} mice infected with the indicated doses of PR8-HK4,6 (**E:** Inf n = 10 and n = 11 for WT and *Daf*^{-/-} respectively, mock = 7 per group; **F:** Inf n = 10 per group, mock n = 4 and n = 7 for WT and *Daf*^{-/-} respectively). Results are expressed as mean±sd, statistical analysis detailed in materials and methods.

Interestingly, upon PR8-HK4,6 infection, DAF did not alter viral replication, clearance (Fig. 2.3-A, B) or tissue penetration (Fig. 2.3-C, D), however its presence increased lung tissue damage (Fig. 2.3-E, F).

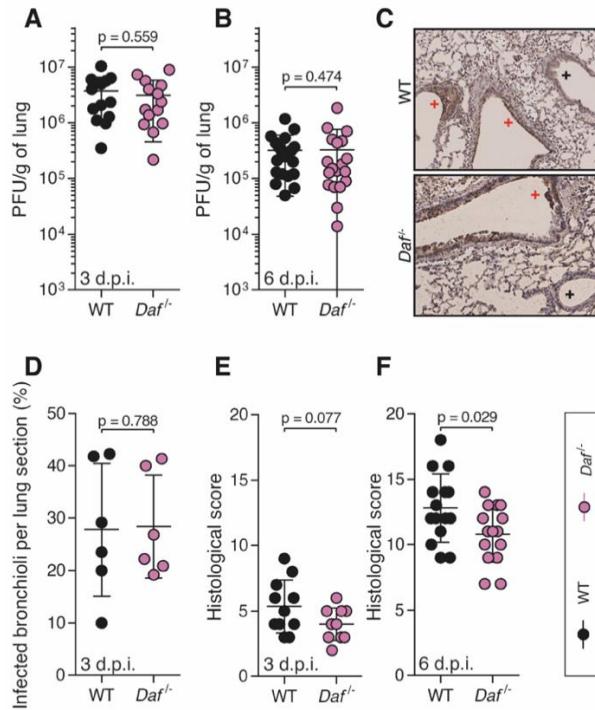


Fig. 2.3 – DAF does not affect viral replication, clearance, or tissue penetration, but is an immunopathology instigator.

A, B: Lung viral titers of C57BL/6J WT or *Daf*^{-/-} mice infected with 1000 PFU of A/X-31 (PR8HK4,6). Samples collected at 3 d.p.i. (**A**, n = 13 and n = 14 for WT and *Daf*^{-/-} respectively) and 6 d.p.i. (**B**, n = 18 and n = 19 for WT and *Daf*^{-/-} respectively). **C:** Immunohistochemistry detection of IAV nucleoprotein (NP) in WT or *Daf*^{-/-} mice 3 d.p.i. with 1000 PFU of PR8HK4,6 (+ healthy; + infected). **D:** Quantification of infected bronchioli (n = 6 per group). **E, F:** Histological score of C57BL/6J WT or *Daf*^{-/-} mice infected with 1000 PFU of PR8HK4,6 was assessed blindly. Evaluated parameters detailed in Table S1. Samples collected at 3 d.p.i. (**E**, n = 11 and n = 10 for WT and *Daf*^{-/-} respectively) and 6 d.p.i. (**F**, n = 15 per group). Results are expressed as mean±sd. Statistical analysis detailed in materials and methods.

The severity of viral infections is not homogeneous, with both viral and host factors contributing to viral pathology (48). Importantly, the host immune response may dictate the infection outcome, independently of

pathogen clearance (2,6). In this chapter, we explore the role of a host protein, DAF, in activating complement and modulating IAV infection via an interplay with the antigenic viral proteins hemagglutinin (HA) and neuraminidase (NA).

We observed that DAF, contrary to what could be expected, potentiates complement activation upon IAV infection. Furthermore, DAF leads to increased immune cell recruitment, especially of neutrophils, monocytes and T cells, increasing lung immunopathology without altering viral loads, therefore revealing a novel mechanism of virulence in infection. These results help to understand how a host factor could define the outcome of a viral infection, without affecting viral elimination.

2.4 Results

2.4.1 DAF-induced immunopathology relies on elevated complement activation, immune cell recruitment and levels of IFN- γ .

Immune response to viral infections such as IAV must be tightly regulated in order to clear the pathogen without causing immunopathology. The complement system is at the frontline of the immune response, recognizing pathogens, and activating and recruiting immune cells. The absence of a regulator of this system, such as DAF, is expected to increase complement activation, resulting in more efficient viral clearance and/or increased tissue damage. Preliminary data indicated that DAF exerts a detrimental effect for the host during mildly virulent IAV infection, without altering viral loads. As DAF is a complement regulator, these results suggest an important role for complement in modulating disease outcome. To further dissect the mechanisms behind such role, we focused on infections with PR8-HK4,6 as it is a well-described laboratorial model, with a virulence resembling circulating strains (Fig. 2.1-A-D; 2.2-C, D).

We first focused on determining the role of the complement pathway upon IAV infection. For that purpose, C57BL/6J $C3^{-/-}$ ($C3^{-/-}$) and C57BL/6J $C3^{-/-} / Daf^{-/-}$ ($C3^{-/-} / Daf^{-/-}$) mice were infected with 500 PFU of PR8-HK4,6 or mock infected with PBS and bodyweight loss monitored over the course of infection. As expected (49,50), mock infected mice did not exhibit bodyweight loss during the 11 days of monitoring for all the conditions (Fig. 2.4-A). Conversely, infected mice lost significant weight, with $C3^{-/-}$ mice losing significantly more bodyweight than the WT. In fact, $C3^{-/-}$ mice lost up to 20.8% of the initial bodyweight, when WT mice lost only 9.8%. However, upon infection, the double knocked-out mice $C3^{-/-} / Daf^{-/-}$ mice, lost the weight loss difference, presenting a bodyweight loss comparable to that observed for $C3^{-/-}$ mice, losing up to 20.5% of the initial bodyweight (Fig. 2.4-A). These results show that the

protection of *Daf^{-/-}* mice is C3-dependent, and thus complement mediated.

DAF regulates complement activation by accelerating the decay of C3 convertases, reducing the levels of C3a. Hence, we proceeded by analyzing the levels of C3a in the bronchoalveolar lavages (BALs) of PR8-HK4,6 infected WT or *Daf^{-/-}* mice. The main differences in tissue damage occurred at 6 d.p.i., and therefore we limited our analysis to that time point. Quite surprisingly, in PR8-HK4,6 infected *Daf^{-/-}* mice the levels of C3a were of 439.8 ± 474.6 ng/ml, and in WT mice of 1425.0 ± 899.5 ng/ml (Fig. 2.4-B). Thus, IAV infection induced lower complement activation in *Daf^{-/-}* mice than in WT mice, indicating that complement activation may play a role in increased tissue damage of WT mice. Taken together, these results highlight the equilibrium needed to clear the disease without causing damage and the important role of complement in both these processes.

The complement pathway is a cascade of reactions that will release cytokines for recruitment and activation of the immune system, and culminating in the formation of a cytolytic pore (C5b-9). Our results showed that depletion of CD59, inhibitor of C5b-9, does not impact disease outcome in the context of IAV infection (Fig. 2.2-E, F), suggesting that the protection observed in *Daf^{-/-}* mice does not rely on complement-dependent cytotoxicity (CDC). To confirm this hypothesis, WT and *Daf^{-/-}* murine primary lung cells were infected with PR8-HK4,6, treated with serum collected from naïve WT mice, and cell viability assessed as a measurement of CDC. *Daf^{-/-}*-derived lung cells were more prone to CDC than WT-derived ones, both at steady state ($57.7 \pm 2.1\%$ vs. $25.4 \pm 1.5\%$) and upon PR8-HK4,6 infection ($72.6 \pm 2.3\%$ vs. $38.5 \pm 5.1\%$). This effect is specific of complement attack, as heat-inactivated serum did not increase cell death (Fig. 2.4-C), and confirms that *Daf^{-/-}* mice protection is not dependent on complement cytolytic attack.

Given that *Daf^{-/-}* mice have lower complement activation but that protection does not depend on CDC, it should rely on the release of anaphylatoxins leading to an alteration of immune cell recruitment and/or activation. To assess this, WT and *Daf^{-/-}* mice were infected with 1000 PFU of PR8-HK4,6 and the recruitment of specific immune cell types measured in BALs. Analyses were carried at 3 and 6 d.p.i. in order to uncouple the first rapid response from a more mature later one. At 3 d.p.i. we observed that *Daf^{-/-}* mice had similar numbers of natural killer (NK) cells and neutrophils recruited to the lungs, when compared to WT mice (84.4±16.8% vs. 100±71.0% NK cells; 79.7±47.4% vs. 100±59.3% neutrophils), but lower numbers of monocytes (66.3±30.3% vs. 100±25.6%) (Fig. 2.4-D-F). At 6 d.p.i., *Daf^{-/-}* mice maintained the lower number of monocytes when compared to WT mice (58.1±30.3% vs. 100±35.8%), and also had reduced levels of neutrophils (69.1±28.8% vs. 100±27.5%) (Fig. 2.4-G, H). Levels of NK cells were not analyzed at this time point, nor in following analysis, as depletion of NK cells in PR8-HK4,6 infected WT mice did not alter disease outcome (Fig. 2.S1-A, B). Additionally, we analyzed recruitment of adaptive immune cells, namely CD4⁺ and CD8⁺ T cells that have been shown to play an important role in IAV infection (51). Interestingly, there was no difference in recruitment of both CD4⁺ and CD8⁺ T cells (Fig. 2.4-I, J), indicating that the protection observed in *Daf^{-/-}* mice is likely dependent on lower immunopathology mediated by the innate immune response.

Cytokines are also key players in the recruitment and activation of the immune system. IFN- γ , in particular, is an essential player in viral responses, and, like all members of the immune system, can cause tissue damage. Indeed, it has recently been shown that IFN- γ , which is produced upon IAV infection, is detrimental to the host by suppressing the protective effect of group II innate lymphoid cells (ILC2) (52). Therefore, levels of IFN- γ were measured in BALs of PR8-HK4,6-infected WT and *Daf^{-/-}* mice at 6 d.p.i.. *Daf^{-/-}* mice had significantly lower

levels of IFN- γ than WT (22.9 ± 24.3 pg/mL vs. 44.4 ± 32.5 pg/mL) (Fig. 2.4-K), which is in accordance with the reduced immunopathology and tissue damage in this context.

Taken together these results suggest that lower complement activation leads to a reduced immune response and recruitment of innate immune cells, such as neutrophils and monocytes. This will allow a reduction in tissue damage, ameliorating disease outcome. Interestingly, and counter-intuitively, the decrease in complement activation is a consequence of the absence of a major complement regulator, DAF.

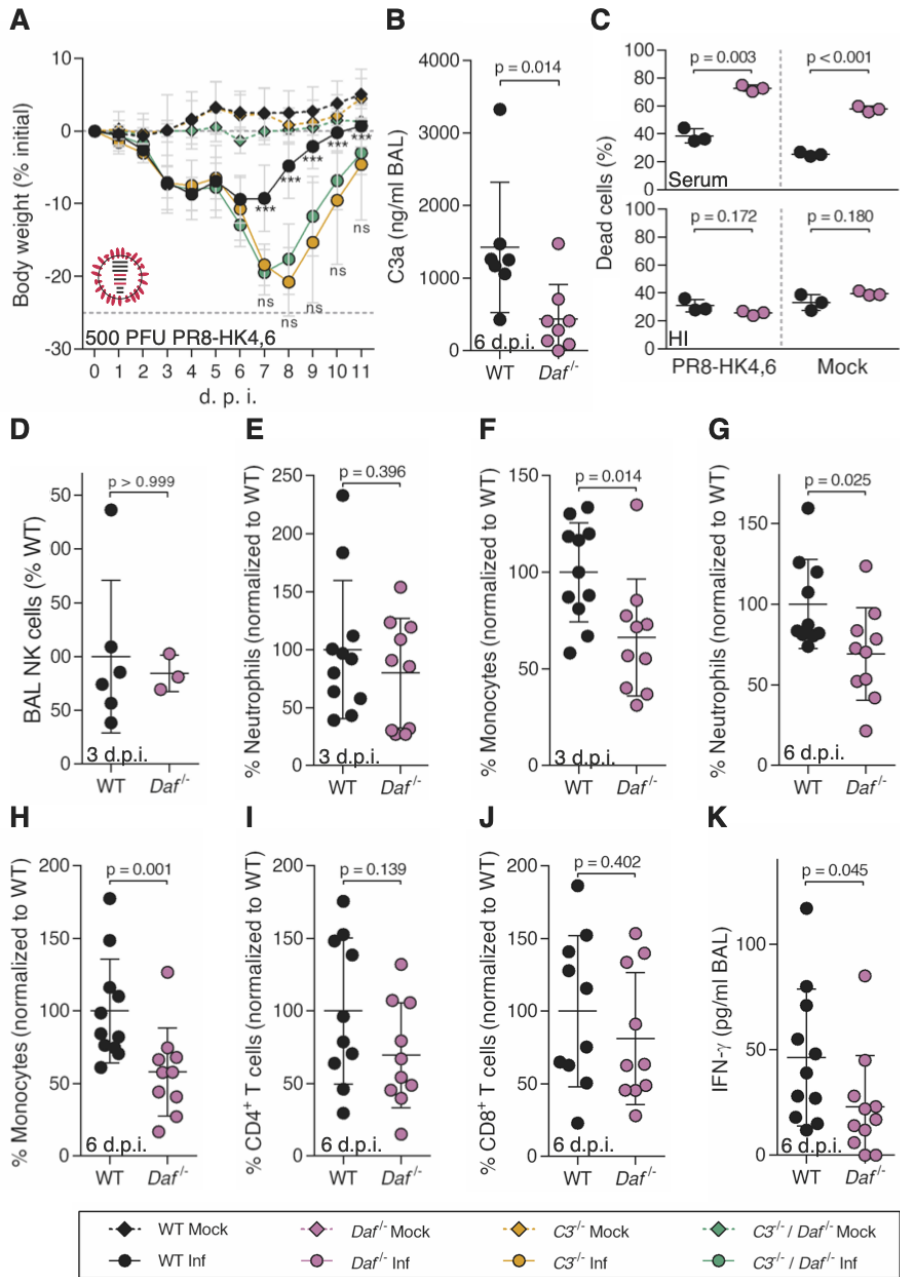


Fig. 2.4 – *Daf*^{-/-} mice have reduced complement activation and recruitment of innate immune cells.

A: Bodyweight loss of C57BL/6J WT, *C3*^{-/-} or *C3*^{-/-} / *Daf*^{-/-} mice infected with 500 PFU of A/X-31 (PR8-HK4,6) (Inf n = 10, n = 6 and n = 10, mock n = 5, n = 5 and n = 7 for WT, *C3*^{-/-} and *C3*^{-/-} / *Daf*^{-/-} respectively). Results are expressed as mean±sd. **B:** C3a levels in BALs of C57BL/6J WT (n = 7) or *Daf*^{-/-} (n = 8) mice 6 d.p.i. with 1000 PFU of PR8-HK4,6. Results are expressed as mean±sd. **C:** Cell death of primary lung cells derived from WT or *Daf*^{-/-} mice infected or mock-infected with PR8-HK4,6 and treated with serum. Results are expressed as mean±sd from 3 replicates from 2 independent experiments. **D, E, F:** Analysis of NK cells (**D**, n = 6 and n = 3 for WT and *Daf*^{-/-} respectively), neutrophils (**E**, n = 11 and n = 10 for WT and *Daf*^{-/-} respectively) and monocytes (**F**, n = 11 and n = 10 for WT and *Daf*^{-/-} respectively) levels in BALs of WT or *Daf*^{-/-} mice, 3 d.p.i. with 1000 PFU PR8-HK4,6. Results are expressed as mean±sd. **G, H, I, J, K:** Analysis of neutrophils (**G**), monocytes (**H**), CD4⁺ T cells (**I**), CD8⁺ T cells (**J**) and IFN-γ (**K**) levels in BALs of WT or *Daf*^{-/-} mice, 6 d.p.i. with 1000 PFU PR8-HK4,6 (n = 10 per group). Results are expressed as mean±sd. Statistical analysis detailed in materials and methods.

2.4.2 DAF-HA interaction modulates adaptive immune cell recruitment.

We observed that lack of DAF protected mice from infection with PR8-HK4,6, but not with PR8 (Fig. 2.2-A-D). These strains differ only in haemagglutinin (HA) and neuraminidase (NA) (47). To investigate the individual role of these proteins in the resilience to infection, we constructed chimeric viruses in PR8 background containing either HA (PR8-HK4) or NA (PR8-HK6) from HK68. It is important to note that analyses are performed in comparison with PR8-HK4,6 infections and not PR8. Therefore, it is the removal of HK6 in PR8-HK4 that will allow investigating the contributions of different NAs, and the removal of HK4 in PR8-HK6 that will enable assessment of the contributions of HAs.

On a first step, *Daf*^{-/-} and WT mice were infected with PR8-HK6, hence highlighting the role of HA. Infection with a sublethal dose of PR8-HK6 resulted in a modest amelioration of bodyweight loss in *Daf*^{-/-} mice, reaching -16.8% of the initial bodyweight, when compared to WT mice that lost up to 20.1% of the initial bodyweight (Fig. 2.5-A). When infected with lethal doses of this strain, both *Daf*^{-/-} and WT mice had a mortality of 100% (Fig. 2.5-B). *In vitro* and *ex vivo* experiments had shown that this strain had increased replication levels when compared to PR8, PR8-HK4,6 or PR8-HK4 (Fig. 2.S2-A-E). Therefore, we hypothesized that the increased mortality of *Daf*^{-/-} mice, when compared to infection with the other strains, could be due to increased viral titers. Interestingly, analysis of lung viral loads showed no difference between *Daf*^{-/-} and WT mice both at 3 and 6 d.p.i. (Fig. 2.5-C, D) and titers were not higher than those observed for the infection with PR8-HK4,6 (Fig. 2.3-A, B). Therefore, HA-DAF interaction modulates virulence, without impacting in viral replication or clearance *in vivo*.

As HA is involved in adhesion of viral particles to host cells, we asked if differences in HA would impact tissue penetration. As observed in PR8-HK4,6 infected mice, IHC of NP and quantification of infected bronchioli showed no difference in infection levels and patterns between *Daf*^{-/-} and WT mice (Fig. 2.5-E, F), indicating that HA-DAF interaction has no role in this context. Additionally, analysis of tissue damage showed that histological scores between *Daf*^{-/-} and WT mice were similar at 3 d.p.i. (4.7±3.5 vs. 4.1±2.8) (Fig. 2.5-G), but significantly reduced in *Daf*^{-/-} mice when compared to WT at 6 d.p.i. (7.4±3.7 vs. 10.9±2.8) (Fig. 2.5-H). These results show that HA-DAF interaction contributes to disease severity and worse disease outcome observed in WT mice, but does not impact lung tissue damage and hence does not completely explain the protective effect of DAF absence.

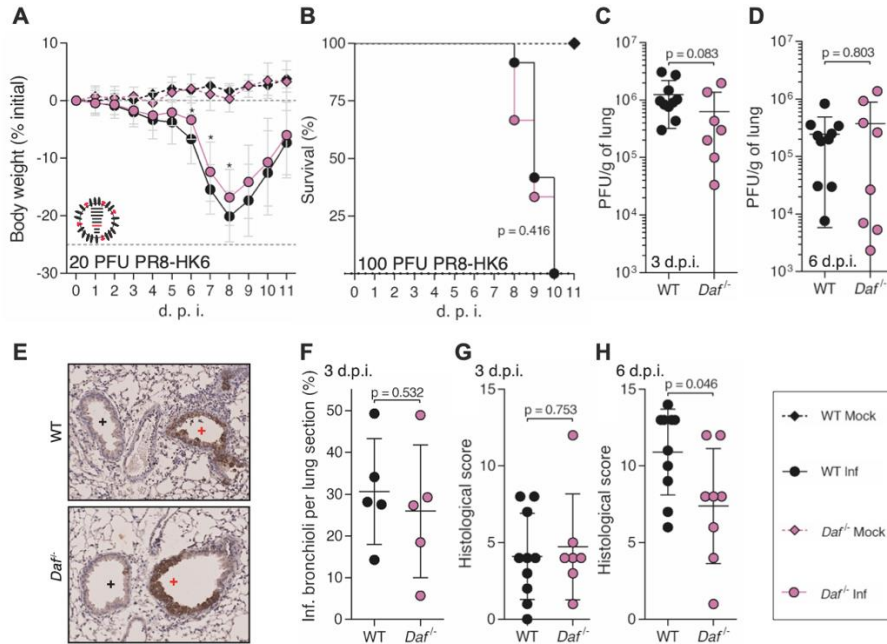


Fig. 2.5 – DAF interaction with HA worsens disease outcome, without increasing immunopathology.

A, B: Bodyweight loss (**A**) and mortality (**B**) of C57BL/6J WT or *Daf*^{-/-} mice infected with the indicated doses of A/Puerto Rico/8/1934 with segment 6 from A/Hong Kong/1/68 (PR8-HK6). (**A:** Inf n = 16 and n = 18, mock n = 6 and n = 7 for WT and *Daf*^{-/-} respectively; **B:** Inf n = 12 and n = 9, mock n = 4 and n = 2 for WT and *Daf*^{-/-} respectively). Results are expressed as mean±sd. **C, D:** Lung viral titers of C57BL/6J WT or *Daf*^{-/-} mice infected with 20 PFU of PR8-HK6. Samples collected at 3 d.p.i. (**C**) and 6 d.p.i. (**D**) (n = 10 and n = 7 for WT and *Daf*^{-/-} respectively). **E:** Immunohistochemistry detection of IAV nucleoprotein (NP) in WT or *Daf*^{-/-} 3 d.p.i. with 20 PFU of PR8-HK6 (+ healthy; + infected). **F:** Quantification of infected bronchioli (n = 5 per group). **G, H:** Histological score of C57BL/6J WT or *Daf*^{-/-} mice infected with 20 PFU of PR8-HK6. Samples collected at 3 d.p.i. (**E**, n = 10 and n = 7 for WT and *Daf*^{-/-} respectively) and 6 d.p.i. (**F**, n = 10 and n = 8 for WT and *Daf*^{-/-} respectively). Results are expressed as mean±sd. Statistical analysis detailed in materials and methods.

To better understand the role of HA-DAF interaction in disease outcome, we analyzed complement and immune cell recruitment in the lungs of PR8-HK6 infected mice. Interestingly $C3^{-/-}$ and $C3^{-/-} / Daf^{-/-}$ mice had similar bodyweight loss when infected with PR8-HK6 (Fig. 2.6-A), and the levels of C3a were reduced in BALs of $Daf^{-/-}$ mice when compared to their WT counterparts ($178.4 \pm 36.8 \text{ ng/mL}$ vs. $405.8 \pm 99.2 \text{ ng/mL}$) (Fig. 2.6-B). These observations correspond to what was seen in PR8-HK4,6 infection and indicate that different HA-DAF interactions do not elicit different complement responses.

Analysis of lung immune cell recruitment in PR8-HK6 infected mice showed that at 3 d.p.i. levels of neutrophils and monocytes were identical between $Daf^{-/-}$ and WT mice (Fig. 2.6-C, D). At 6 d.p.i, however, $Daf^{-/-}$ mice had lower numbers of neutrophils and monocytes when compared to their WT counterparts ($58.6 \pm 21.3\%$ vs. $100 \pm 36.41\%$ neutrophils; $61.4 \pm 19.6\%$ vs. $100 \pm 41.45\%$ monocytes) (Fig. 2.6-E, F) showing that a change in HA does not alter the innate immune cell recruitment observed in PR8-HK4,6. Of note, the levels of $CD4^{+}$ and $CD8^{+}$ T cells were decreased in PR8-HK6 infected $Daf^{-/-}$ mice when compared to their WT counterparts ($57.5 \pm 26.2\%$ vs. $100 \pm 35.9\%$ $CD4^{+}$ T cells and $49.3 \pm 36.7\%$ vs. $100 \pm 50.5\%$ $CD8^{+}$ T cells) (Fig. 2.6-G, H), contrarily to what was seen in PR8-HK4,6 infection (Fig. 2.4-I, J) and showing that HA-DAF interaction modulates the adaptive immune response.

Taken together these results show that HA-DAF interaction controls disease severity, without impacting complement or innate immune responses leading to immunopathology. It does, however, impact the recruitment of T cells. The decreased activation of the adaptive immune response, together with the higher virulence of this strain may exceed the beneficial effect of reduced tissue damage and explain the similar mortality in $Daf^{-/-}$ and WT mice.

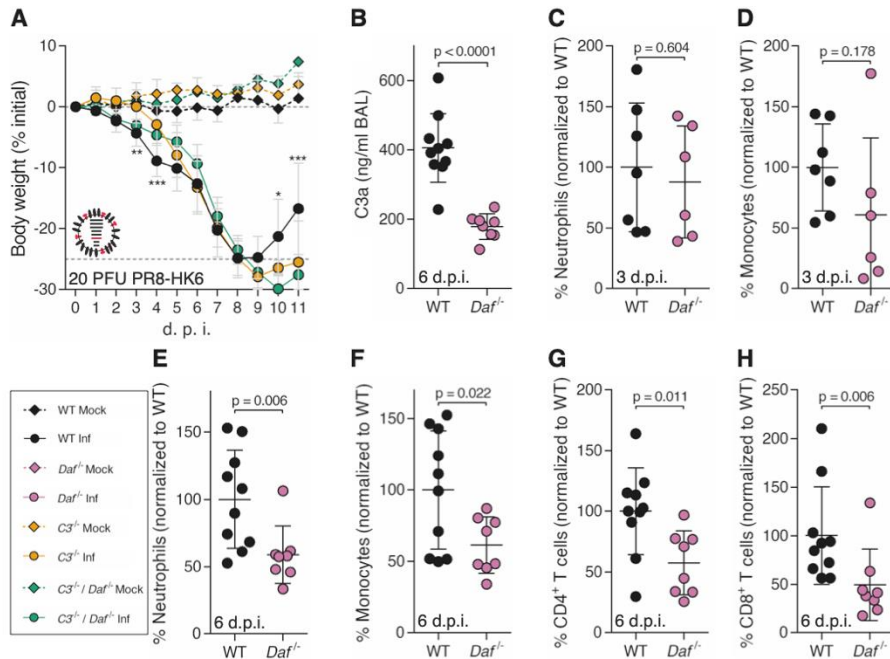


Fig. 2.6 – $Daf^{-/-}$ mice have reduced complement activation and T cell recruitment upon PR8-HK6 infection.

A: Bodyweight loss of C57BL/6J WT $C3^{-/-}$ or $C3^{-/-} / Daf^{-/-}$ mice infected with 20 PFU of A/Puerto Rico/8/1934 with segment 6 from A/Hong Kong/1/68 (PR8-HK6) (Inf n = 10, n = 10 and n = 4, mock n = 4, n = 3 and n = 1, for WT, $C3^{-/-}$ and $C3^{-/-} / Daf^{-/-}$ respectively). Results are expressed as mean \pm sd. **B:** C3a levels in BALs of C57BL/6J WT (n = 10) or $Daf^{-/-}$ (n = 8) mice 6 d.p.i. with 20 PFU of PR8-HK6. Results are expressed as mean \pm sd. **C, D:** Analysis of neutrophils (**C**) and monocytes (**D**) levels in BALs of WT (n = 7) or $Daf^{-/-}$ (n = 6) mice, 3 d.p.i. with 10 PFU PR8-HK6. Results are expressed as mean \pm sd. **E, F, G, H:** Analysis of neutrophils (**E**), monocyte (**F**), CD4⁺ T cells (**G**) and CD8⁺ T cells (**H**) levels in BALs of WT (n = 10) or $Daf^{-/-}$ (n = 8) mice, 6 d.p.i. with 20 PFU PR8-HK6. Results are expressed as mean \pm sd. Statistical analysis detailed in materials and methods.

2.4.3 DAF-NA interaction modulates innate immune cell recruitment.

As HA-DAF interaction did not impact complement nor innate immune responses, we proceeded with analysis of NA-DAF

interactions. Following the principle stated above, analyses were done in comparison with PR8-HK4,6 and not PR8 and thus the removal of HK6 from PR8-HK4,6 allowed assessing the role of different NAs. Therefore, to understand the contribution of NA in the protection conferred by DAF depletion, *Daf^{f/-}* and WT mice were infected with sublethal and lethal doses of PR8-HK4. Upon infection with this strain, *Daf^{f/-}* mice showed a reduced bodyweight loss when compared to the WT mice (17.7% vs. 21.8% maximum bodyweight loss) (Fig. 2.7-A). The detrimental effect of DAF was more evident when mice were challenged with lethal doses. Indeed, 87.5% of WT mice succumbed to infection with 250 PFU of PR8-HK4, whereas all of *Daf^{f/-}* mice survived (Fig. 2.7-B). As these results correspond to what was observed with PR8-HK4,6, NA-DAF interaction does not directly impact disease severity.

Similarly, lung viral loads were identical in *Daf^{f/-}* and WT mice infected with PR8-HK4 both at 3 ($2.2 \pm 1.9 \times 10^6$ PFU/g vs. $4.1 \pm 5.5 \times 10^6$ PFU/g) and 6 d.p.i. ($8.8 \pm 9.9 \times 10^4$ PFU/g vs. $6.1 \pm 4.1 \times 10^4$ PFU/g). Also, PR8-HK4 infection foci were mainly restricted to the alveoli with no difference at the level of infected bronchioli in *Daf^{f/-}* and WT mice lung sections ($25.8 \pm 8.3\%$ vs. $24.2 \pm 13.6\%$) (Fig. 2.7-E, F). These results show that NA-DAF interaction does not impact viral replication, clearance or tissue penetration. Interestingly, further analysis of PR8-HK4 infected lungs showed that the lungs of *Daf^{f/-}* mice were more damaged at 3 d.p.i. with a histological score of 4.3 ± 0.9 , when compared to lungs from WT mice that had a score of 2.9 ± 1.5 . At 6 d.p.i. this difference was no longer present, *Daf^{f/-}* lungs having a score of 8.3 ± 3.8 , and WT of 9.2 ± 3.1 . Hence PR8-HK4 infected *Daf^{f/-}* mice have more lung tissue damage at an early time point in infection, when compared to WT mice, and oppositely to what was observed in PR8-HK4,6 infection. NA-DAF interaction would then control lung immunopathology in this context, but with no real consequence in disease outcome, as *Daf^{f/-}* still

had decreased bodyweight loss and mortality when compared to the WT.

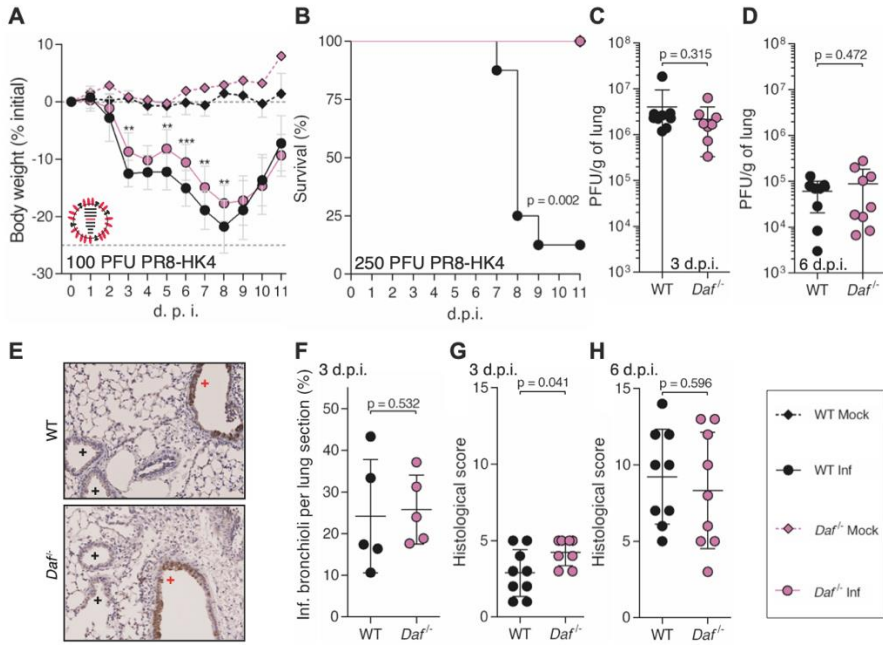


Fig. 2.7 – DAF interaction with NA modulates immunopathology.

A, B: Bodyweight loss (**A**) and mortality (**B**) of C57BL/6J WT or *Daf*^{-/-} mice infected with the indicated doses of A/Puerto Rico/8/1934 with segment 4 from A/Hong Kong/1/68 (PR8-HK4). (**A:** Inf n = 14 and n = 10, mock n = 4 and n = 1 for WT and *Daf*^{-/-} respectively; **B:** Inf n = 8 per group, mock n = 4 and n = 1 for WT and *Daf*^{-/-} respectively). Results are expressed as mean±sd. **C, D:** Lung viral titers of C57BL/6J WT or *Daf*^{-/-} mice infected with 100 PFU of PR8-HK4. Samples collected at 3 d.p.i. (**C**, n = 9 and n = 8 for WT and *Daf*^{-/-} respectively) and 6 d.p.i. (**D**, n = 9 per group). Results are expressed as mean±sd. **E:** Immunohistochemistry detection of IAV nucleoprotein (NP) in WT or *Daf*^{-/-} 3 d.p.i. with 100 PFU of PR8-HK4 (+ healthy; + infected). **F:** Quantification of infected bronchioli (n = 5 per group). **G, H:** Histological score of C57BL/6J WT or *Daf*^{-/-} mice infected with 100 PFU of PR8-HK4. Samples collected at 3 d.p.i. (**G**, Inf n = 16 and n = 18, mock n = 6 and n = 7 for WT and *Daf*^{-/-} respectively) and 6 d.p.i. (**H**, Inf n = 13 and n = 9, mock n = 4 and n = 2 for WT and *Daf*^{-/-} respectively). Results are expressed as mean±sd. Statistical analysis detailed in materials and methods.

To better understand the mechanism behind this observation, we started by assessing the role of complement. *C3*^{-/-} / *Daf*^{-/-} and *C3*^{-/-} mice had a similar bodyweight loss upon PR8-HK4 infection (Fig. 2.8-A), and *Daf*^{-/-} mice had significantly lower levels of C3a detected in BALs at 6 d.p.i. when compared to their WT counterparts (194.4±115.6 ng/mL vs. 506.4±180.2 ng/mL) (Fig. 2.8-B). These results confirm that, similarly to what was observed in PR8-HK4,6 and PR8-HK6 infections, the protection of *Daf*^{-/-} mice upon PR8-HK4 infection is complement mediated, and *Daf*^{-/-} mice might be protected via lower levels of complement activation.

We then proceeded with analysis of immune cell recruitment to the lungs at 3 and 6 d.p.i.. At 3 d.p.i., *Daf*^{-/-} mice had reduced levels of neutrophils but not monocytes when compared to their WT counterparts (16.2±8.6% vs. 100±112.1% neutrophils; 38.1±21.1% vs. 100±79.5%

monocytes) (Fig. 2.8-C, D). Then, at 6 d.p.i., *Daf^{-/-}* and WT mice had comparable levels of both neutrophils and monocytes, and CD4⁺ and CD8⁺ T cells (Fig. 2.8-E-J) (105.0±62.9% vs. 100±49.2% neutrophils; 104.5±54.0% vs. 100±49.1% monocytes; 106±67.0% vs. 100±61.7% CD4⁺ T cells; 104.3±60.6% vs. 100±52.6% CD8⁺ T cells). These results do not correspond to what was observed in infections with PR8-HK4,6, where the main differences between *Daf^{-/-}* and WT mice resided in reduced numbers of monocytes at 3 d.p.i., and reduced numbers of both neutrophils and monocytes at 6 d.p.i. (Fig. 2.4-E-H). We can therefore conclude that different NA elicit different innate immune responses, and that NA-DAF interaction is responsible for the recruitment of innate immune cells.

In summary, *Daf^{-/-}* mice are protected from PR8-HK4 infection with decreased complement levels and reduced neutrophil recruitment but increased immunopathology early in infection. At later time points we did not observe differences between WT and *Daf^{-/-}* mice regarding both lung tissue damage and immune cell recruitment. The reduction in neutrophil recruitment reflects what was observed in PR8-HK4,6 infection, albeit at an earlier time point. One might then suggest that NA-DAF interaction is important in regulation of neutrophil recruitment, and that these cells play an important role in modulating disease outcome.

Taken together, our results demonstrate that both HA and NA play a role in disease severity, and that the cumulative effect of both HA- and NA-DAF interactions results in the mechanism worsening the outcome observed upon Cal, Eng and PR8-HK4,6 infections.

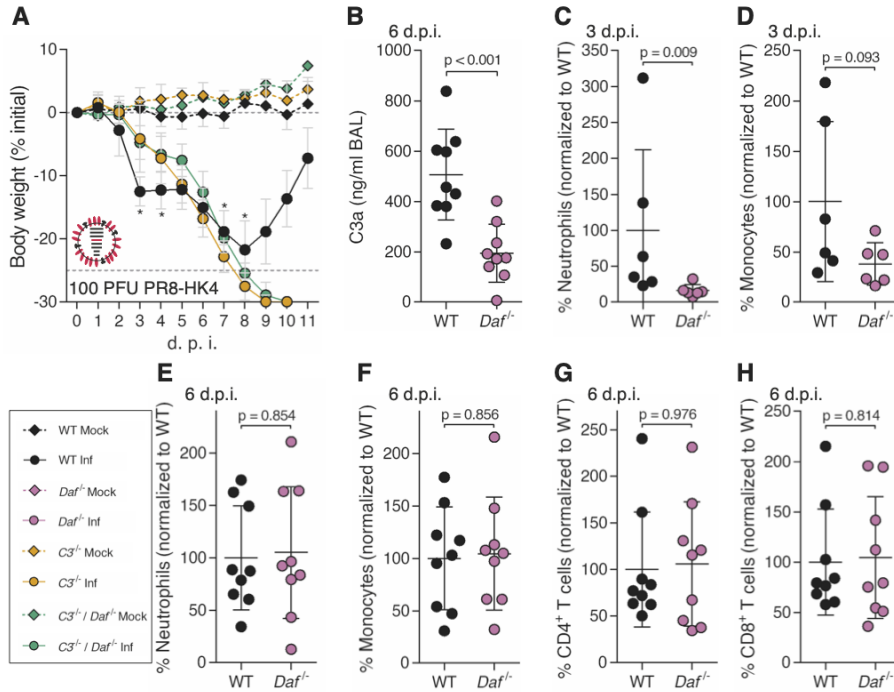


Fig. 2.8 – *Daf*^{-/-} mice present lower complement activation and neutrophil recruitment at 3 d.p.i. upon PR8-HK4 infection.

A: Bodyweight loss of C57BL/6J WT *C3*^{-/-} or *C3*^{-/-} / *Daf*^{-/-} mice infected with 100 PFU of A/Puerto Rico/8/1934 with segment 4 from A/Hong Kong/1/68 (PR8-HK4) (Inf n = 14, n = 10, and n = 3, mock n = 4, n = 3 and n = 1 for WT, *C3*^{-/-} and *C3*^{-/-} / *Daf*^{-/-} respectively). Results are expressed as mean±sd. **B:** C3a levels in BALs of C57BL/6J WT or *Daf*^{-/-} mice 6 d.p.i. with 100 PFU of PR8-HK4 (n = 9 per group). Results are expressed as mean±sd. **C, D:** Analysis of neutrophils (**C**) and monocytes (**D**) levels in BALs of WT or *Daf*^{-/-} mice, 3 d.p.i. with 100 PFU PR8-HK4 (n = 6 per group). Results are expressed as mean±sd. **E, F, G, H:** Analysis of neutrophils (**E**), monocyte (**F**), CD4⁺ T cells (**G**) and CD8⁺ T cells (**H**) levels in BALs of WT or *Daf*^{-/-} mice, 6 d.p.i. with 100 PFU PR8-HK4 (n = 9 per group). Results are expressed as mean±sd. Statistical analysis detailed in materials and methods.

2.5 Discussion

This work highlights the importance of a balanced immune response to viral infections in order to clear the disease without causing immunopathology. The unexpected lower complement activation upon IAV infection is contrary to what is observed for autoimmune diseases, for which *Daf^{-/-}* mice have been widely used (53–55). These mice have increased disease severity coupled with high complement activation levels when compared to their WT counterparts, showing that *Daf^{-/-}* mice do not lack the ability to activate the complement.

Despite its intrinsic protective role, complement is a documented driver of immunopathology in severe viral infections such as IAV (32–34), SARS-CoV-2 (29–31) and MERS (28). In the context of IAV, inhibition of different components of the complement system such as C3a receptor and C5 decreased immune cell recruitment and activation leading to an ameliorated disease outcome (32–34). Our work is in accordance with these studies as *Daf^{-/-}* mice have less severe disease upon IAV infection, coupled with reduced C3a levels in BALs, and a lower number of immune cells recruited to the lungs (Fig. 2.4-A, B; 2.6-A, B; 2.8-A, B). However, C3 is essential in IAV infection. *C3^{-/-}* and *C3^{-/-} / Daf^{-/-}* mice had increased mortality when compared to the WT (Fig. 2.3-A; 2.6-A; 2.8-A) and *C3^{-/-}* mice presented increased lung inflammation and infiltration of immune cells upon IAV infection (50,56). These observations show the potential of regulating complement activation as a strategy to provide resilience to viral infections, without affecting pathogen clearance.

Interestingly, infection of *Cd59^{-/-}* mice and analysis of CDC in WT and *Daf^{-/-}* primary lung cells indicated that the last step of the complement cascade does not impact disease outcome in IAV infection (Fig. 2.2-E, F; 2.4-C; 2.S2-F, G). Rather, it suggests that earlier components of the complement cascade, such as anaphylatoxins C3a

and/or C5a have a modulatory role of IAV virulence. This hypothesis agrees with the function of C3a and C5a as recruiters and activators of the innate immune response, which can lead to immunopathology (32–34). Our results indicate that, in fact, and contrary to expected, in IAV infection, lack of DAF leads to reduced activation of complement, lower levels of C3a and decreased recruitment of monocytes and neutrophils, specifically (see model in Figure 2.9). The lower levels of C3a detected in the BALs of *Daf*^{-/-} mice could explain the lower numbers of innate immune cells recruited, and decreased tissue damage. However, compared to PR8-HK4,6, infection with PR8-HK6 altered recruitment of adaptive immune cells, and PR8-HK4 of innate immune cells, without changing the levels of C3a in *Daf*^{-/-} mice. These results indicate that complement is not the sole recruiter and activator of the immune response, and that a direct or indirect HA-DAF and/or NA-DAF interaction has additional roles to play in immune cell recruitment.

In fact, we found that HA-DAF interplay impacts recruitment of CD4⁺ and CD8⁺ T cells, both of which shown to be essential in the clearance of IAV (57). The lower levels of these cells in *Daf*^{-/-} mice might annul the beneficial effect of lower lung tissue damage observed at 6 d.p.i.. Indeed, upon PR8-HK6 challenge, mice bodyweight rapidly dropped at 7 d.p.i., whereas in infection with other viral strains loss of weight started around 4 d.p.i. and was more gradual, suggesting that the adaptive immune system is implicated in the process (10,58). Despite HA being amongst the most immunogenic proteins of IAV, and hence its involvement in adaptive immune response not surprising (58,59), our work shows for the first time a specific interaction of HA with DAF and the implications of this axis in T cell recruitment.

Ablation of neutrophils in IAV infections have been shown to prevent tissue damage without affecting viral loads (60–63). In fact, these cells have long been associated with acute respiratory distress syndrome (64), and extensive neutrophil infiltration and release of

neutrophil extracellular traps (NETs) have been linked to increased pneumonia severity in critical cases of COVID-19 (65–67). Despite these observations, neutrophils are important to the host response against IAV infection as neutrophil depletion resulted in exacerbated viral loads, lung damage and mortality in mice infected with PR8-HK4,6 (68,69). In addition to neutrophils, monocytes are readily recruited to sites of IAV challenge where they differentiate into macrophages or dendritic cells (DC) (70,71) that share many properties with their conventional counterparts (72) and have been studied upon IAV infection (72,73). Monocyte-derived macrophages contribute to the inflammation resolution by clearing apoptotic neutrophils and confer lasting protection against secondary bacterial infections (73,74). The interaction with apoptotic neutrophils has also been reported to increase differentiation of monocytes into DC, promoting adherence of CD8⁺ T cells (74). Conversely, monocyte and monocyte-derived cells may contribute to immunopathology, as their depletion decreased disease severity without altering viral loads (75–77). These studies show that both cell types are essential for IAV infection but can contribute to tissue damage, and support our hypothesis that increased immunopathology of WT mice upon IAV infection is mediated by excessive recruitment of neutrophils and monocytes.

Upon viral infection the immune response needs to be fine-tuned in order to clear the pathogen without promoting immunopathology. Therefore, the initial immune response may define the outcome of disease, and any deviations from the equilibrium may result in a poor disease outcome. We identified DAF as a novel virulence factor, and observed that its interaction with the viral proteins HA and NA modulates the immune response. The mechanism of interaction between DAF and NA will be addressed in the following chapter.

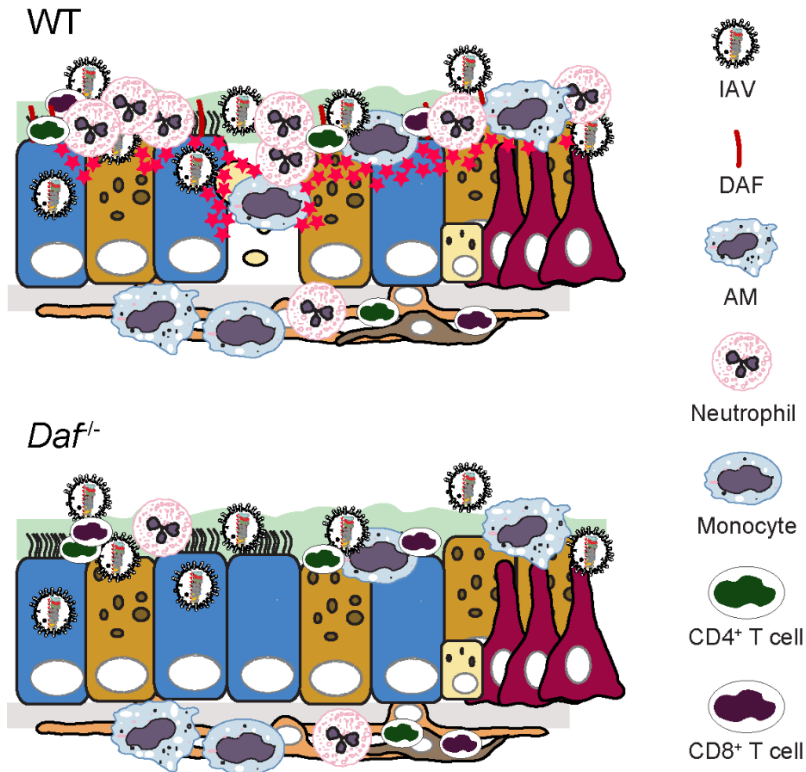


Fig. 2.9 – Proposed model for DAF as a virulence factor upon IAV infection (adapted from MJ Amorim).

DAF is a regulator of complement activation (RCA), and therefore inhibits non-specific activation of complement in steady state. However, we observed that, upon IAV challenge, DAF increases complement activation. Interestingly, complement-dependent cytotoxicity (CDC) is not affected, but instead there is an increase in C3a- (and likely C5a-)mediated immune cell recruitment. As illustrated, the amplified immune response in the presence of DAF (WT) does not contribute to viral clearance, but it promotes tissue damage and consequently worse disease outcome. Remarkably, the recruitment of the innate or adaptive immune system depends on the interaction of DAF with viral NA or HA, respectively, which will be explored in the following chapter. AM – alveolar macrophage.

2.6 Materials and methods

2.6.1 Statistical analyses

All statistical analyses were conducted using GraphPad Prism 6. Detailed statistics and number of replicates for all experiments can be found in the figure legends and/or in the main text. Bodyweight loss: Statistical significance represented as * $p < 0.05$, ** $p < 0.01$, *** $p < 0.001$, using two-way ANOVA followed by Holm-Sidak multiple comparisons test. Survival curves: Statistical significance compared with WT using Log-rank (Mantel-Cox) test. Compare two groups: Population normality assessed with D'Agostino & Pearson omnibus normality test. Statistical significance using unpaired t-test with Welch's correction for normal populations or Mann-Whitney test for populations whose normality was not proved. Multiple comparisons: Population normality assessed with D'Agostino & Pearson omnibus normality test. Kruskal-Wallis followed by Dunn's multiple comparisons test for populations whose normality was not proved.

2.6.2 Ethics statement

All animals were housed at IGC facilities under specific pathogen free conditions and fed *ad libitum*. Experimental animal procedures were previously approved by the IGC Animal Ethics Committee and licensed by the Portuguese General Directory of Veterinary (DGAV, Ministry of Agriculture, Rural Development and Fishing), with references A016/2013 and A013/2019. All animals were housed and handled according with good animal practice as defined by national authorities (DGAV, Law n^o1005/92 from 23rd October) and European legislation EEC/86/609. C57BL6/J wild-type (WT) mice were provided by the IGC animal facility. C57BL6/J *Daf*^{-/-} (*Daf*^{-/-}) and C57BL6/J *Cd59*^{-/-} (*Cd59*^{-/-}) were previously bred and genotyped in the IGC animal facility from C57BL6/J *Daf*^{-/-} / *Cd59a*^{-/-} mice (kindly provided by Prof. Wen-Chao

Song) crossed with WT mice from the IGC animal facility. C57BL6/J $C3^{-/-}$ / $Daf^{-/-}$ ($C3^{-/-}$ / $Daf^{-/-}$) and C57BL6/J $C3^{-/-}$ / $Cd59^{-/-}$ ($C3^{-/-}$ / $Cd59^{-/-}$) mice were previously bred and genotyped in the IGC animal facility from $Daf^{-/-}$ or $Cd59a^{-/-}$ mice crossed with C57BL6/J $C3^{-/-}$ mice from the IGC animal facility (kindly provided by Dr. Miguel Soares).

2.6.3 Mice infection

All experiments with animals were performed at IGC biosafety level 2 (BSL-2) animal facility. Under light anesthesia with isoflurane, 8-10 weeks old female mice were intranasally infected with a solution of 30 μ l of PBS containing the indicated viral doses. Mice were daily weighed for bodyweight assessment (Fig. 10-A) or sacrificed via CO₂ inhalation at the indicated timepoints for further analysis (Fig. 10-B).

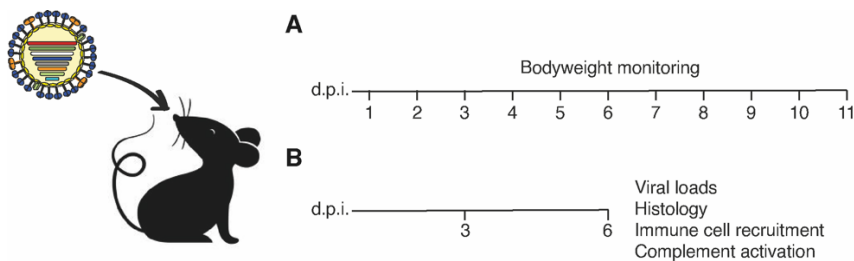


Fig. 2.10 – Experimental setup of mice infection.

Mice were intranasally infected with the indicated viral doses and were either monitored for bodyweight loss for 11 days (A) or sacrificed at 3 or 6 days post-infection (d.p.i.) for further analysis (B).

2.6.4 Viral loads

To determine viral loads, right lower lung lobes were aseptically collected and frozen immediately. Viruses were collected by grinding the lungs in Dulbecco's modified Eagle's medium (DMEM; Gibco®, 21969035) supplemented with 200mM L-glutamine (Life Technologies, 25030-024), 100U/ml penicillin and 10 μ g/ml streptomycin (Biowest, L0022-100) (serum-free DMEM), using tungsten carbide beads

(Qiagen, 69997) in a TissueLyser II (Qiagen) at 20Hz for 3min. After centrifugation at 2000g, 5min, 4°C, supernatants were collected and titrated.

2.6.5 Histology and Immunohistochemistry (IHC)

Left lung lobes were collected and fixed in 10% buffered formalin for 48h, then embedded in paraffin, divided into longitudinal sections (3µm thick) and stained with hematoxylin and eosin. To score lung inflammation and damage, lung samples were screened for the following parameters (Table S1): interstitial (alveolar septa) inflammation, alveolar inflammation, perivascular/peribronchial inflammation, bronchial exudates, bronchial epithelium hyperplasia, and edema. Each parameter was graded on a scale of 0–4 being 0, absent; 1, very mild; 2, mild; 3, moderate; and 4, severe. The total lung inflammation score was expressed as the sum of the scores for each parameter. Histological scoring was performed blindly by a pathologist.

For IHC, tissue sections were deparaffinized, rehydrated, and heated in citrate buffer (40mM sodium citrate dihydrate, 60mM citric acid, pH 6) and blocked with 1:50 Fc block reagent (rat anti-mouse CD16/CD32, IGC antibody facility, clone 2.4G2). Slides were then incubated with rabbit α-NP (78) 1:1000 for 16h at 4°C. After blocking of endogenous peroxidases with 3% (v/v) H₂O₂, sections were incubated with ImmPRESS® HRP Horse Anti-Rabbit IgG Polymer Detection Kit (Vector Laboratories, MP-7401-15) for 1h at RT and then with DAB substrate (Roche, 11718096001) according to manufacturer's instructions. Finally, lung sections were contrasted with Mayer Hematoxylin and images taken in a NanoZoomer-SQ Digital slide scanner (Hamamatsu Photonics). Visual inspection to assess the proportion of infected bronchioli was performed blindly.

2.6.6 Bronchoalveolar lavage (BAL)

After sacrifice by CO₂ inhalation, mice were dissected, exposing lungs and trachea. A small incision was performed in the upper trachea and a catheter (Braun, 4253329) carefully inserted until the base of the lungs. 1ml of sterile PBS was then pushed slowly into the lung with a 1ml syringe, and then retrieved. Samples were centrifuged 5min at 16000g, 4°C. Supernatants were collected and stored at -20°C and cells were analyzed by flow cytometry.

2.6.7 ELISA

BAL supernatants were thawed on ice and probed with Mouse C3a (TECOmedical, TE1038) or Mouse IFN- γ DuoSet ELISA (R&D Systems, DY485-05), following the manufacturer's instructions. Calibration curves and concentration interpolation were calculated using GraphPad Prism 6.

2.6.8 Flow cytometry

Cells from BAL were suspended in 100 μ l FC buffer (PBS supplemented with 2% FBS and 0.1% NaN₃) and transferred to a 96-well V-bottom plate (Thermo Scientific Nunc, 10580382).

Cells were centrifuged at 666g, 2min, 4°C and stained with 50 μ l primary antibodies (Table S2) for 20min, on ice, protected from light and with light rocking. Afterwards, cells were washed with PBS and stained with live-dead Zombie Aqua Fixable Viability Kit (BioLegend, 423101) according to manufacturer's instructions. Finally, cells were washed with PBS and fixed with IC fixation buffer (Life Technologies, 00-8222-49) following manufacturer's indications.

Cells were acquired in a BD LSRFortessa™ X-20 analyzer (BD Biosciences), equipped with BD FACSDiva™ 8 acquisition software (BD Biosciences). Results were analyzed using FlowJo 10 (BD Biosciences, version v10.6.2).

2.6.9 Immune cell depletion

Natural killer (NK) cells were depleted by intraperitoneal (IP) injection of 200µg α-NK1.1 (IGC antibody facility, clone PK136) in 200µl PBS every 72h, starting 72h before infection.

2.6.10 Primary mouse embryo fibroblasts (MEF) isolation

MEF cells were isolated from WT or *Daf^{-/-}* mice as previously described (79). Breedings were set up in a timed manner and embryos harvested at stages between E13.5 to E15.5. Embryos were carefully isolated from the yolk sac; the head, visceral tissues and blood clots removed, and the remaining tissue macerated using a scalpel blade. Macerated tissue was then transferred to a T75 flask containing DMEM supplemented with fetal bovine serum (FBS; Gibco®, S181i-500), 10% (v/v), 200 mM L-glutamine, 100 U/ml penicillin and 10 µg/ml streptomycin (complete DMEM) and incubated at 37°C, 5% CO₂ for 48h. Cells that grew from the tissue were harvested with trypsin-EDTA (Biowest, X0930-100), expanded to T150 flasks and, when 100% confluent, frozen in FBS with 10% DMSO and kept in liquid nitrogen until needed for experiments. This was performed by Zoé E Vaz da Silva.

2.6.11 Primary mouse lung cells isolation

Primary lung cells were isolated from WT or *Daf^{-/-}* mice adapted from (80). After sacrifice by CO₂ inhalation, mice were dissected, exposing lungs and trachea. Mice were exsanguinated by cutting the inferior vena cava and perfused with 20ml of PBS through the right ventricle. A small incision was performed in the upper trachea and a catheter (Braun, 4253329) carefully inserted until the base of the lungs. First, 1.5ml of sterile collagenase D (Roche, 11088858001) 0.5% (w/v) in PBS was pushed slowly into the lung with a 1ml syringe, followed by 0.5ml agarose (Lonza, 733-0829) 1% (w/v) in PBS. After 2min incubation, lungs were collected in one piece to 2ml of collagenase D

and incubated for 40min, at room temperature. Subsequently, lungs were transferred to a culture dish with 10ml of complete DMEM supplemented with 5U DNase I (NZYTech, MB13402) and lung tissue dissected and minced with a scalpel blade. Dissociated cells were filtered through a 100µm cell strainer, centrifuge at 650g, room temperature, for 5min, and resuspended in complete DMEM. Cells were counted and plated in a 6 well plate at $\sim 9 \times 10^5$ cells/well and incubated at 37°C, 5% CO₂ for 48h.

2.6.12 Cell culture

Madin-Darby canine kidney cells (MDCK), primary MEFs and primary murine lung cells were cultured in complete DMEM. Cells were kept in T50 flasks at 37°C, 5% CO₂ and sub-cultured every 3 to 4 days using trypsin-EDTA.

2.6.13 Influenza A virus strains

Reverse-genetics derived A/Puerto Rico/8/34 (PR8, H1N1) (kindly provided by Prof. Ron Fouchier) and A/X-31, a recombinant virus containing segments 4 and 6 from A/Hong Kong/01/1968 and the remaining from A/Puerto Rico/8/34 (47) (PR8-HK4,6, H3N2) (kindly provided by Prof. Paul Digard) were used as model viruses.

Viruses were grown in eggs as following: embryonated chicken eggs were incubated at 37°C for 10 days. After that, the egg shell was lightly sanded with a rotary tool and a hole was pierced with a sterile 27G needle on top of the egg and on the opposite side of the embryo. Through that hole, 100 PFU of virus diluted in 200µl PBS were injected into the allantoic fluid of the egg. Infected eggs were incubated at 37°C for 2-3 days, and then at -20°C for 2h. Viruses were collected by opening the eggs and carefully retrieving the allantoic fluid. After centrifugation at 3500g, 5min, 4°C to remove debris, the virus solution was aliquoted and kept at -80°C.

2.6.14 Reverse genetics

Reverse genetics production of PR8-HK4 and PR8-HK6 was conducted as previously described (81–83). pDual plasmids encoding PR8 segments were a kind gift from Prof. Ron Fouchier, (Erasmus MC, Netherlands). pDual plasmids encoding HK68 segments 4 and 6 were a kind gift from Prof. Paul Digard, (Roslin Institute, UK) Briefly, HEK293T cells were transfected in 6-well plates using Lipofectamine 2000 (ThermoFisher, 11668027) according to manufacturer's recommendations, with 250ng of each of the 8 pDual plasmids each encoding the corresponding viral segments. After 16h of incubation, culture medium was removed and added serum-free DMEM containing 1µg/ml Trypsin-TPCK and 0.14% (w/v) BSA. After further incubation for 48h at 37°C, 5% CO₂, cells were scraped to the medium and collected. After centrifugation at 800g, 5min, 4°C, supernatants were titrated and amplified in embryonated chicken eggs.

2.6.15 Virus titration by Plaque Assay

Plaque assays were conducted as previously described (84,85). Dissociated lung tissue samples were serially 10-fold diluted in serum-free DMEM, and used to infect MDCK cells plated at 80% confluence. After 45 min incubation at 37°C, cells were overlaid with an Avicel® solution (50% (v/v) Avicel® (FMC BioPolymer, CL-611F) / 50% (v/v) serum-free DMEM / 1µg/mL Trypsin-TPCK (Worthington, 39N11492) / 0.14% (v/v) bovine serum albumin (BSA; PAA, K45-00)) and incubated at 37°C, 5% CO₂ for 36-48h. Supernatant was then removed, cells washed with PBS, fixed and stained with a solution of 4% (v/v) paraformaldehyde (PFA; VWR 0493) / 0.2% (v/v) Toluidine Blue (Sigma-Aldrich, T3260) / pH = 7.4, overnight at room temperature. After washing the cells with tap water, plaques were counted by visual inspection.

2.6.16 Infections

Cells were seeded in culture plates at appropriate density and incubated overnight. For one-step infections, virus inoculum was added in serum-free DMEM at the MOI of 3 and incubated for 45min. Afterwards, samples were overlaid with serum-free DMEM supplemented with 0.14% (v/v) BSA. For multicycle infections, virus inoculum was added in serum-free DMEM at a MOI of 0.005 and incubated for 1h. After removing the inoculum, cells were overlaid with serum-free DMEM containing 0.14% (v/v) BSA and 1µg/mL Trypsin-TPCK. Cells were then incubated at 37°C, 5% CO₂ for the indicated times.

2.6.17 Complement-dependent cytotoxicity (CDC)

Primary lung cells isolated from WT or *Daf^{-/-}* mice were infected with PR8, PR8-HK4,6, PR8-HK4 or PR8-HK6. At 12h.p.i., supernatant was removed and cells were washed with PBS and then detached by incubation with 5mM EDTA (Sigma-Aldrich, 03690) in PBS for 10min, 37°C. Cells were then centrifuged at 666g, 4°C for 5min, resuspended in veronal buffer (CompTech, B100) and added to a 96-well V-bottom plate (Thermo Scientific Nunc, 10580382), adjusted to 10⁶ cells per well in 100µl. Serum obtained from WT mice or heat-inactivated serum (56°C, 30min) were added at a final concentration of 50%. Cells were incubated with serum for 1h at 37°C. Afterwards, cells were centrifuged and washed with 200µl PBS and stained with live-dead Zombie Aqua Fixable Viability Kit (BioLegend, 423101) according to manufacturer's instructions. Cells were centrifuged and washed as above and fixed with IC fixation buffer (Life Technologies, 00-8222-49) following manufacturer's instructions. Cells were then analyzed by flow cytometry.

2.7 References

1. Iwasaki A, Foxman EF, Molony RD. Early local immune defences in the respiratory tract. *Nat Rev Immunol*. 2017 Jan;17(1):7–20.
2. Iwasaki A, Pillai PS. Innate immunity to influenza virus infection. *Nat Rev Immunol*. 2014 May;14(5):315–28.
3. Gargaglioni LH, Marques DA. Let's talk about sex in the context of COVID-19. *J Appl Physiol Bethesda Md* 1985. 2020 Jun 1;128(6):1533–8.
4. Gebhard C, Regitz-Zagrosek V, Neuhauser HK, Morgan R, Klein SL. Impact of sex and gender on COVID-19 outcomes in Europe. *Biol Sex Differ*. 2020 May 25;11(1):29.
5. Haitao T, Vermunt JV, Abeykoon J, Ghamrawi R, Gunaratne M, Jayachandran M, et al. COVID-19 and Sex Differences: Mechanisms and Biomarkers. *Mayo Clin Proc*. 2020 Oct;95(10):2189–203.
6. Medzhitov R, Schneider DS, Soares MP. Disease tolerance as a defense strategy. *Science*. 2012 Feb 24;335(6071):936–41.
7. Sell S. Immunopathology. *Am J Pathol*. 1978 Jan;90(1):211–80.
8. WHO. Influenza (Seasonal) [Internet]. [cited 2021 Feb 9]. Available from: [https://www.who.int/en/news-room/fact-sheets/detail/influenza-\(seasonal\)](https://www.who.int/en/news-room/fact-sheets/detail/influenza-(seasonal))
9. He X, Lau EHY, Wu P, Deng X, Wang J, Hao X, et al. Temporal dynamics in viral shedding and transmissibility of COVID-19. *Nat Med*. 2020 May;26(5):672–5.
10. Krammer F, Smith GJD, Fouchier RAM, Peiris M, Kedzierska K, Doherty PC, et al. Influenza. *Nat Rev Dis Primer*. 2018 Jun 28;4(1):3.
11. Taubenberger JK, Morens DM. The pathology of influenza virus infections. *Annu Rev Pathol*. 2008;3:499–522.
12. Uyeki TM. High-risk Groups for Influenza Complications. *JAMA*. 2020 Dec 8;324(22):2334.
13. Taubenberger JK, Morens DM. 1918 Influenza: the mother of all pandemics. *Emerg Infect Dis*. 2006 Jan;12(1):15–22.
14. Melvin JA, Bomberger JM. Compromised Defenses: Exploitation of Epithelial Responses During Viral-Bacterial Co-Infection of the Respiratory Tract. *PLoS Pathog*. 2016 Sep;12(9):e1005797.
15. Rowe HM, Meliopoulos VA, Iverson A, Bomme P, Schultz-Cherry S, Rosch JW. Direct interactions with influenza promote bacterial adherence during respiratory infections. *Nat Microbiol*. 2019 Aug;4(8):1328–36.
16. Siegel SJ, Roche AM, Weiser JN. Influenza promotes pneumococcal growth during coinfection by providing host sialylated substrates as a nutrient source. *Cell Host Microbe*. 2014 Jul 9;16(1):55–67.
17. Talmi-Frank D, Altboum Z, Solomonov I, Udi Y, Jaitin DA, Klepfish M, et al. Extracellular Matrix Proteolysis by MT1-MMP Contributes to Influenza-Related Tissue Damage and Mortality. *Cell Host Microbe*. 2016 Oct 12;20(4):458–70.
18. Damjanovic D, Small C-L, Jeyanathan M, Jeyanathan M, McCormick S, Xing

Z. Immunopathology in influenza virus infection: uncoupling the friend from foe. *Clin Immunol Orlando Fla.* 2012 Jul;144(1):57–69.

19. Newton AH, Cardani A, Braciale TJ. The host immune response in respiratory virus infection: balancing virus clearance and immunopathology. *Semin Immunopathol.* 2016 Jul;38(4):471–82.

20. Arunachalam PS, Wimmers F, Mok CKP, Perera RAPM, Scott M, Hagan T, et al. Systems biological assessment of immunity to mild versus severe COVID-19 infection in humans. *Science.* 2020 Sep 4;369(6508):1210–20.

21. Hadjadj J, Yatim N, Barnabei L, Corneau A, Boussier J, Smith N, et al. Impaired type I interferon activity and inflammatory responses in severe COVID-19 patients. *Science.* 2020 Aug 7;369(6504):718–24.

22. Freeley S, Kemper C, Le Friec G. The “ins and outs” of complement-driven immune responses. *Immunol Rev.* 2016 Nov;274(1):16–32.

23. Merle NS, Church SE, Fremeaux-Bacchi V, Roumenina LT. Complement System Part I - Molecular Mechanisms of Activation and Regulation. *Front Immunol.* 2015;6:262.

24. Sarma JV, Ward PA. The complement system. *Cell Tissue Res.* 2011 Jan;343(1):227–35.

25. Radicioni G, Cao R, Carpenter J, Ford AA, Wang T, Li L, et al. The innate immune properties of airway mucosal surfaces are regulated by dynamic interactions between mucins and interacting proteins: the mucin interactome. *Mucosal Immunol.* 2016 Nov;9(6):1442–54.

26. Galinski LE, Sheahan TP, Morrison TE, Menachery VD, Jensen K, Leist SR, et al. Complement Activation Contributes to Severe Acute Respiratory Syndrome Coronavirus Pathogenesis. *mBio.* 2018 Oct 9;9(5).

27. Wang R, Xiao H, Guo R, Li Y, Shen B. The role of C5a in acute lung injury induced by highly pathogenic viral infections. *Emerg Microbes Infect.* 2015 May;4(5):e28.

28. Jiang Y, Zhao G, Song N, Li P, Chen Y, Guo Y, et al. Blockade of the C5a-C5aR axis alleviates lung damage in hDPP4-transgenic mice infected with MERS-CoV. *Emerg Microbes Infect.* 2018 Apr 24;7(1):77.

29. Fletcher-Sandersjö A, Bellander B-M. Is COVID-19 associated thrombosis caused by overactivation of the complement cascade? A literature review. *Thromb Res.* 2020 Oct;194:36–41.

30. Lo MW, Kemper C, Woodruff TM. COVID-19: Complement, Coagulation, and Collateral Damage. *J Immunol Baltim Md 1950.* 2020 Sep 15;205(6):1488–95.

31. Polycarpou A, Howard M, Farrar CA, Greenlaw R, Fanelli G, Wallis R, et al. Rationale for targeting complement in COVID-19. *EMBO Mol Med.* 2020 Aug 7;12(8):e12642.

32. Garcia CC, Weston-Davies W, Russo RC, Tavares LP, Rachid MA, Alves-Filho JC, et al. Complement C5 activation during influenza A infection in mice contributes to neutrophil recruitment and lung injury. *PloS One.* 2013;8(5):e64443.

33. Song N, Li P, Jiang Y, Sun H, Cui J, Zhao G, et al. C5a receptor1 inhibition alleviates influenza virus-induced acute lung injury. *Int Immunopharmacol.* 2018 Jun;59:12–20.

34. Sun S, Zhao G, Liu C, Wu X, Guo Y, Yu H, et al. Inhibition of complement activation alleviates acute lung injury induced by highly pathogenic avian influenza H5N1 virus infection. *Am J Respir Cell Mol Biol*. 2013 Aug;49(2):221–30.
35. Pandya PH, Fisher AJ, Mickler EA, Temm CJ, Lipking KP, Gracon A, et al. Hypoxia-Inducible Factor-1 α Regulates CD55 in Airway Epithelium. *Am J Respir Cell Mol Biol*. 2016 Dec;55(6):889–98.
36. Reddy P, Caras I, Krieger M. Effects of O-linked glycosylation on the cell surface expression and stability of decay-accelerating factor, a glycopospholipid-anchored membrane protein. *J Biol Chem*. 1989 Oct 15;264(29):17329–36.
37. Varsano S, Frolkis I, Ophir D. Expression and distribution of cell-membrane complement regulatory glycoproteins along the human respiratory tract. *Am J Respir Crit Care Med*. 1995 Sep;152(3):1087–93.
38. Hoffman EM. Inhibition of complement by a substance isolated from human erythrocytes. I. Extraction from human erythrocyte stromata. *Immunochemistry*. 1969 May;6(3):391–403.
39. Hoffmann EM. Inhibition of complement by a substance isolated from human erythrocytes. II. Studies on the site and mechanism of action. *Immunochemistry*. 1969 May;6(3):405–19.
40. Kim DD, Song W-C. Membrane complement regulatory proteins. *Clin Immunol Orlando Fla*. 2006 Mar;118(2–3):127–36.
41. Hillmen P, Lewis SM, Bessler M, Luzzatto L, Dacie JV. Natural history of paroxysmal nocturnal hemoglobinuria. *N Engl J Med*. 1995 Nov 9;333(19):1253–8.
42. Ozen A, Comrie WA, Ardy RC, Domínguez Conde C, Dalgic B, Beser ÖF, et al. CD55 Deficiency, Early-Onset Protein-Losing Enteropathy, and Thrombosis. *N Engl J Med*. 2017 Jul 6;377(1):52–61.
43. Hill A, DeZern AE, Kinoshita T, Brodsky RA. Paroxysmal nocturnal haemoglobinuria. *Nat Rev Dis Primer*. 2017 May 18;3:17028.
44. Socié G, Caby-Tosi M-P, Marantz JL, Cole A, Bedrosian CL, Gasteyer C, et al. Eculizumab in paroxysmal nocturnal haemoglobinuria and atypical haemolytic uraemic syndrome: 10-year pharmacovigilance analysis. *Br J Haematol*. 2019 Apr;185(2):297–310.
45. Lee N, Cao B, Ke C, Lu H, Hu Y, Tam CHT, et al. IFITM3, TLR3, and CD55 Gene SNPs and Cumulative Genetic Risks for Severe Outcomes in Chinese Patients With H7N9/H1N1pdm09 Influenza. *J Infect Dis*. 2017 Jul 1;216(1):97–104.
46. Zhou J, To KK-W, Dong H, Cheng Z-S, Lau CC-Y, Poon VKM, et al. A functional variation in CD55 increases the severity of 2009 pandemic H1N1 influenza A virus infection. *J Infect Dis*. 2012 Aug 15;206(4):495–503.
47. Kilbourne ED. Future influenza vaccines and the use of genetic recombinants. *Bull World Health Organ*. 1969;41(3):643–5.
48. Kash JC, Taubenberger JK. The role of viral, host, and secondary bacterial factors in influenza pathogenesis. *Am J Pathol*. 2015 Jun;185(6):1528–36.
49. Kopf M, Abel B, Gallimore A, Carroll M, Bachmann MF. Complement component C3 promotes T-cell priming and lung migration to control acute influenza virus infection. *Nat Med*. 2002 Apr;8(4):373–8.

50. O'Brien KB, Morrison TE, Dundore DY, Heise MT, Schultz-Cherry S. A protective role for complement C3 protein during pandemic 2009 H1N1 and H5N1 influenza A virus infection. *PLoS One*. 2011 Mar 9;6(3):e17377.
51. Ho AWS, Prabhu N, Betts RJ, Ge MQ, Dai X, Hutchinson PE, et al. Lung CD103+ dendritic cells efficiently transport influenza virus to the lymph node and load viral antigen onto MHC class I for presentation to CD8 T cells. *J Immunol Baltim Md* 1950. 2011 Dec 1;187(11):6011–21.
52. Califano D, Furuya Y, Roberts S, Avram D, McKenzie ANJ, Metzger DW. IFN- γ increases susceptibility to influenza A infection through suppression of group II innate lymphoid cells. *Mucosal Immunol*. 2018 Jan;11(1):209–19.
53. Miwa T, Maldonado MA, Zhou L, Yamada K, Gilkeson GS, Eisenberg RA, et al. Decay-accelerating factor ameliorates systemic autoimmune disease in MRL/lpr mice via both complement-dependent and -independent mechanisms. *Am J Pathol*. 2007 Apr;170(4):1258–66.
54. Miwa T, Maldonado MA, Zhou L, Sun X, Luo HY, Cai D, et al. Deletion of decay-accelerating factor (CD55) exacerbates autoimmune disease development in MRL/lpr mice. *Am J Pathol*. 2002 Sep;161(3):1077–86.
55. Soltys J, Halperin JA, Xuebin Q. DAF/CD55 and Protectin/CD59 modulate adaptive immunity and disease outcome in experimental autoimmune myasthenia gravis. *J Neuroimmunol*. 2012 Mar;244(1–2):63–9.
56. Kandasamy M, Ying PC, Ho AWS, Sumatoh HR, Schlitzer A, Hughes TR, et al. Complement mediated signaling on pulmonary CD103(+) dendritic cells is critical for their migratory function in response to influenza infection. *PLoS Pathog*. 2013 Jan;9(1):e1003115.
57. Topham DJ, Tripp RA, Doherty PC. CD8+ T cells clear influenza virus by perforin or Fas-dependent processes. *J Immunol Baltim Md* 1950. 1997 Dec 1;159(11):5197–200.
58. Chen X, Liu S, Goraya MU, Maarouf M, Huang S, Chen J-L. Host Immune Response to Influenza A Virus Infection. *Front Immunol*. 2018;9:320.
59. Krammer F. The human antibody response to influenza A virus infection and vaccination. *Nat Rev Immunol*. 2019 Jun;19(6):383–97.
60. Narasaraju T, Yang E, Samy RP, Ng HH, Poh WP, Liew A-A, et al. Excessive neutrophils and neutrophil extracellular traps contribute to acute lung injury of influenza pneumonitis. *Am J Pathol*. 2011 Jul;179(1):199–210.
61. Perrone LA, Plowden JK, García-Sastre A, Katz JM, Tumpey TM. H5N1 and 1918 pandemic influenza virus infection results in early and excessive infiltration of macrophages and neutrophils in the lungs of mice. *PLoS Pathog*. 2008 Aug 1;4(8):e1000115.
62. Sakai S, Kawamata H, Mantani N, Kogure T, Shimada Y, Terasawa K, et al. Therapeutic effect of anti-macrophage inflammatory protein 2 antibody on influenza virus-induced pneumonia in mice. *J Virol*. 2000 Mar;74(5):2472–6.
63. Zhu B, Zhang R, Li C, Jiang L, Xiang M, Ye Z, et al. BCL6 modulates tissue neutrophil survival and exacerbates pulmonary inflammation following influenza virus infection. *Proc Natl Acad Sci U S A*. 2019 Jun 11;116(24):11888–93.
64. Weiland JE, Davis WB, Holter JF, Mohammed JR, Dorinsky PM, Gadek JE.

Lung neutrophils in the adult respiratory distress syndrome. Clinical and pathophysiological significance. *Am Rev Respir Dis.* 1986 Feb;133(2):218–25.

65. Barnes BJ, Adrover JM, Baxter-Stoltzfus A, Borczuk A, Cools-Lartigue J, Crawford JM, et al. Targeting potential drivers of COVID-19: Neutrophil extracellular traps. *J Exp Med.* 2020 Jun 1;217(6).

66. Java A, Apicelli AJ, Liszewski MK, Coler-Reilly A, Atkinson JP, Kim AH, et al. The complement system in COVID-19: friend and foe? *JCI Insight.* 2020 Aug 6;5(15).

67. Zuo Y, Yalavarthi S, Shi H, Gockman K, Zuo M, Madison JA, et al. Neutrophil extracellular traps in COVID-19. *JCI Insight.* 2020 Jun 4;5(11).

68. Tate MD, Ioannidis LJ, Croker B, Brown LE, Brooks AG, Reading PC. The role of neutrophils during mild and severe influenza virus infections of mice. *PLoS One.* 2011 Mar 14;6(3):e17618.

69. Tate MD, Deng Y-M, Jones JE, Anderson GP, Brooks AG, Reading PC. Neutrophils ameliorate lung injury and the development of severe disease during influenza infection. *J Immunol Baltim Md 1950.* 2009 Dec 1;183(11):7441–50.

70. Williams M, Mildner A, Yona S. Developmental and Functional Heterogeneity of Monocytes. *Immunity.* 2018 Oct 16;49(4):595–613.

71. Short KR, Kroeze EJBV, Fouchier RAM, Kuiken T. Pathogenesis of influenza-induced acute respiratory distress syndrome. *Lancet Infect Dis.* 2014 Jan;14(1):57–69.

72. Coillard A, Segura E. In vivo Differentiation of Human Monocytes. *Front Immunol.* 2019;10:1907.

73. Duan M, Hibbs ML, Chen W. The contributions of lung macrophage and monocyte heterogeneity to influenza pathogenesis. *Immunol Cell Biol.* 2017 Mar;95(3):225–35.

74. Lim K, Kim T-H, Trzeciak A, Amitrano AM, Reilly EC, Prizant H, et al. In situ neutrophil efferocytosis shapes T cell immunity to influenza infection. *Nat Immunol.* 2020 Sep;21(9):1046–57.

75. Dawson TC, Beck MA, Kuziel WA, Henderson F, Maeda N. Contrasting effects of CCR5 and CCR2 deficiency in the pulmonary inflammatory response to influenza A virus. *Am J Pathol.* 2000 Jun;156(6):1951–9.

76. Herold S, Steinmueller M, von Wulffen W, Cakarova L, Pinto R, Pleschka S, et al. Lung epithelial apoptosis in influenza virus pneumonia: the role of macrophage-expressed TNF-related apoptosis-inducing ligand. *J Exp Med.* 2008 Dec 22;205(13):3065–77.

77. Lin KL, Suzuki Y, Nakano H, Ramsburg E, Gunn MD. CCR2+ monocyte-derived dendritic cells and exudate macrophages produce influenza-induced pulmonary immune pathology and mortality. *J Immunol Baltim Md 1950.* 2008 Feb 15;180(4):2562–72.

78. Amorim MJ, Bruce EA, Read EKC, Foeglein A, Mahen R, Stuart AD, et al. A Rab11- and microtubule-dependent mechanism for cytoplasmic transport of influenza A virus viral RNA. *J Virol.* 2011 May;85(9):4143–56.

79. Durkin ME, Qian X, Popescu NC, Lowy DR. Isolation of Mouse Embryo Fibroblasts. *Bio-Protoc.* 2013 Sep 20;3(18).

80. Pinto R, Herold S, Cakarova L, Hoegner K, Lohmeyer J, Planz O, et al.

Inhibition of influenza virus-induced NF-kappaB and Raf/MEK/ERK activation can reduce both virus titers and cytokine expression simultaneously in vitro and in vivo. *Antiviral Res.* 2011 Oct;92(1):45–56.

81. Hoffmann E, Neumann G, Kawaoka Y, Hobom G, Webster RG. A DNA transfection system for generation of influenza A virus from eight plasmids. *Proc Natl Acad Sci U S A.* 2000 May 23;97(11):6108–13.

82. de Wit E, Spronken MIJ, Bestebroer TM, Rimmelzwaan GF, Osterhaus ADME, Fouchier RAM. Efficient generation and growth of influenza virus A/PR/8/34 from eight cDNA fragments. *Virus Res.* 2004 Jul;103(1–2):155–61.

83. de Wit E, Spronken MIJ, Vervaet G, Rimmelzwaan GF, Osterhaus ADME, Fouchier RAM. A reverse-genetics system for Influenza A virus using T7 RNA polymerase. *J Gen Virol.* 2007 Apr;88(Pt 4):1281–7.

84. Gauth CR, Smith TF. Replication and plaque assay of influenza virus in an established line of canine kidney cells. *Appl Microbiol.* 1968 Apr;16(4):588–94.

85. Matrosovich M, Matrosovich T, Garten W, Klenk H-D. New low-viscosity overlay medium for viral plaque assays. *Virology.* 2006 Aug 31;349:63–68.

2.8 Acknowledgements

We acknowledge Dr. Jonathan Yewdell (NIAID, USA), Dr. Luís Moita (IGC, Portugal), Dr. Miguel Soares (IGC, Portugal), Prof. Paul Digard (Roslin Institute, UK), Prof. Ron Fouchier (Erasmus, Netherlands), Dr. Vera Martins and Prof. Wen-Chao Song (University of Pennsylvania, USA) for providing mice, cells and reagents. We are grateful to the Animal House Facility, Flow Cytometry Facility and Histopathology Unit at the IGC for technical support, sample processing and data collection. We thank André Barros (IGC, Portugal), Elsa Fonseca (IGC, Portugal) Dr. Gabriel Nuñez (University of Michigan, USA) and the members of CBV lab for helpful discussion. Financial support for this work was provided by Fundação Calouste Gulbenkian.

2.9 Supplementary material

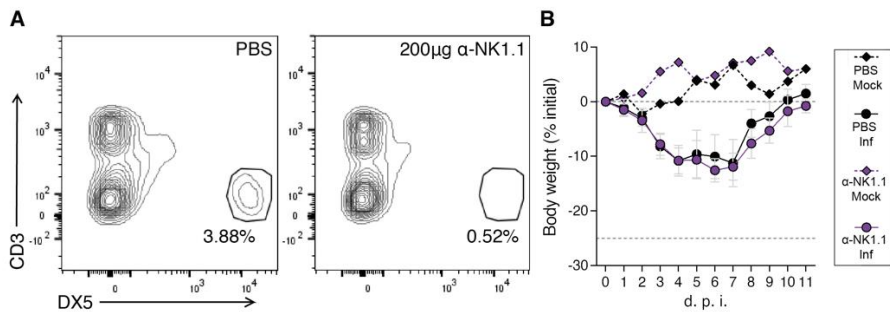


Fig. 2.S1 – NK cell depletion does not alter disease outcome.

A: Representative flow cytometry detection of NK cells (gated in CD45⁺ population) in C57BL/6J WT 72 hours after depletion via intraperitoneal (IP) injection of α-NK1.1. **B:** Bodyweight loss of C57BL/6J WT mice infected with 100 PFU of A/X-31 (PR8-HK4,6) and depleted of NK cells by IP injection of α-NK1.1 every 72 hours, starting 72 hours before infection (Inf n = 5 and mock n = 1 per group). Results are expressed as mean±sd. Statistical analysis detailed in materials and methods.

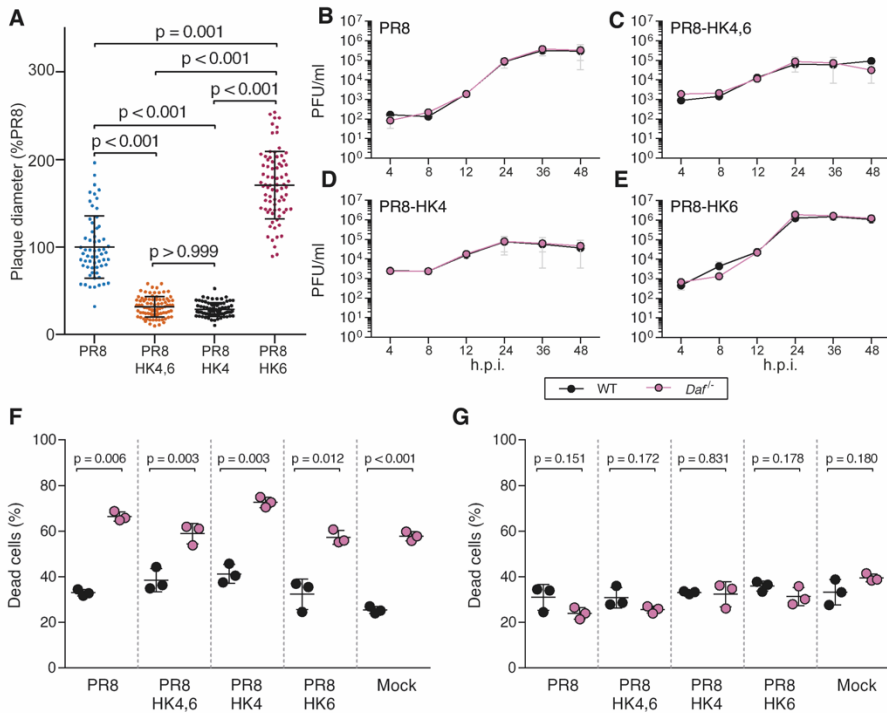


Fig. 2.S2 – DAF does not affect replication of PR8, PR8-HK4,6, PR8-HK4 and PR8-HK6.

A: Measurement of viral plaques diameter after infection of MDCK cells monolayers. Data shown as mean \pm sd of the total plaques from two independent experiments, each corresponding to six independent infections for each virus. Each point represents an individual plaque. **B-E:** Replication kinetics of A/Puerto Rico/8/1934 (PR8) (**B**), A/X-31 (PR8-HK4,6) (**C**), PR8 containing the segment 4 of A/Hong Kong/1/68 (HK68) (PR8-HK4) (**D**) and PR8 containing the segment 6 of HK68 (PR8-HK6) (**E**) in mouse embryonic fibroblasts (MEFs) derived from C57BL/6J WT or *Dafl^{-/-}* mice at multiplicity of infection (MOI) = 0.005. Data shown as mean \pm SEM, from two independent experiments. **F, G:** Percentage of cell death of murine lung primary cells after infection with the indicated viruses and treatment with serum (**F**) or heat-inactivated serum (**G**). Data shown as mean \pm sd of triplicates, representative of two independent experiments. Statistical analysis detailed in materials and methods.

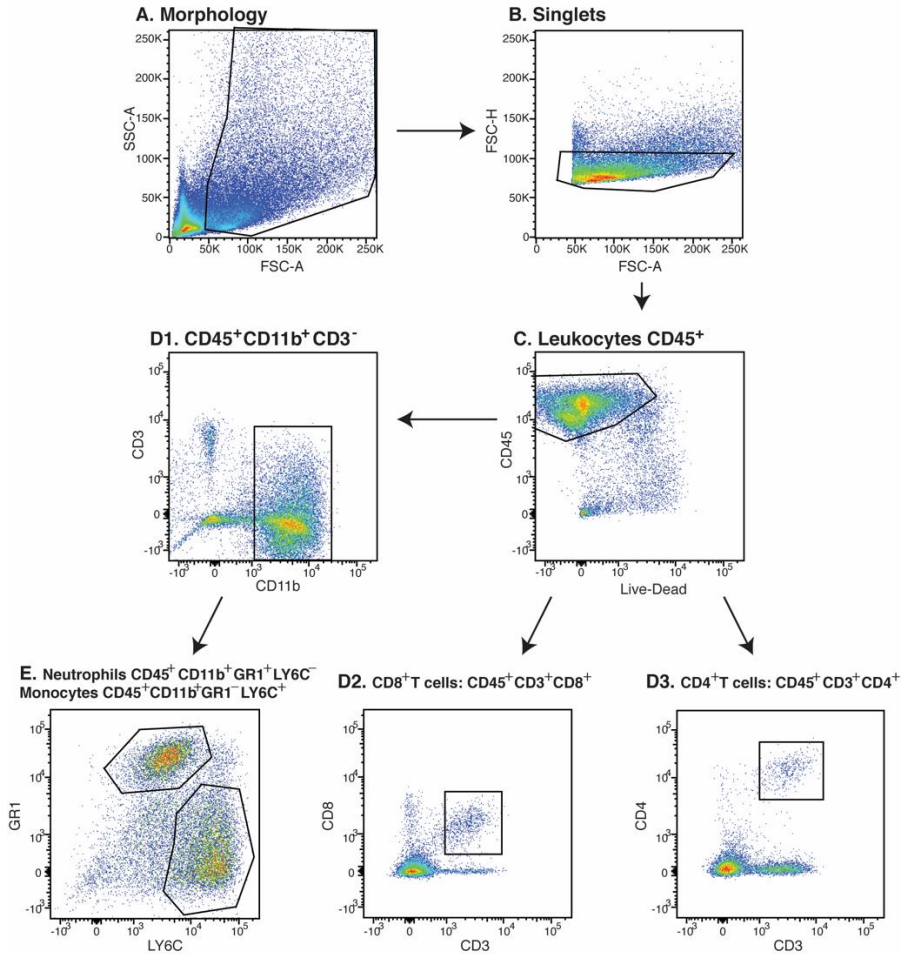


Fig. 2.S3 – Representative flow cytometry gating strategy
(adapted from Zoé E Vaz da Silva).

Table 2.S1 –Histological scoring parameters.

IAV	C57BL/6J	d.p.i.	Interstitial inflammation		Alveolar inflammation		Perivascular/peribronchial inflammation		Bronchial exsudates		Bronchial epithelium hyperplasia		Edema		
			median	IQR	median	IQR	median	IQR	median	IQR	median	IQR	median	IQR	
PR8	HK4,6	WT	3	1	0	0	1	2	0	2	2	0	0	0	0
		6	3	1	3	2	3	0	2	1	2	2	0	0	
PR8	HK4	WT	3	1	1	0	0	2	1	1	1	0	0	0	0
		6	2	1	2	1	3	0	2	1	2	1	0	0	
PR8	HK4	WT	3	0	0	0	0	1	1	1	0	0	0	0	0
		6	3	1	2	1	3	0	1	0	0	0	0	0	
PR8	HK6	WT	3	1	1	0	1	2	1	1	0	0	0	0	0
		6	4	1	4	1	3	2	2	2	2	0	0	0	
PR8	HK6	WT	3	1	1	0	0	3	2	1	0	0	0	0	0
		6	3	1	3	2	2	0	1	1	0	0	0	0	

Table 2.S2 – Antibodies used in flow cytometry.

	Target	Brand	Catalog	Clone	Host	Diluted 1:
CD11b/Mac1-BV605	Ms	IGC Antibody Facility	-	M1/70	Rt	100
GR1/Ly-6G-PE	Ms	BD Pharmingen	551461	1A8	Rt	200
Ly-6C-PerCPy5.5	Ms	eBioscience	45-5932-80	HK1.4	Rt	200
CD3-FITC	Ms	IGC Antibody Facility	-	AH	Rt	100
CD4-PE-Cy7	Ms	IGC Antibody Facility	-	GK1.5	Rt	100
CD8-Pacific Blue	Ms	IGC Antibody Facility	-	YTS169.4	Rt	100
CD45-APC	Ms	BioLegend	103112	30-F11	Rt	100
CD49b/DX5-PE	Ms	BioLegend	103506	HMA2	Ah	1600

Chapter 3 – Influenza A virus neuraminidase cleaves sialic acid from the complement decay-accelerating factor and activates complement

3.1 Author contributions

The experiments presented in this chapter were designed and planned by Nuno Brito Santos, Zoé E. Vaz da Silva and Maria João Amorim. Experiments for Fig. 3.4-A, B were performed by Zoé E Vaz da Silva. Primary mouse embryo fibroblasts (MEF) used for Fig. 3.4-C, D were collected by Zoé E Vaz da Silva. Experiments for Fig. 3.7 were performed by Nuno B Santos in collaboration with Catarina Gomes and Celso A Reis. All the remaining experiments were performed by Nuno B Santos. Nuno B Santos, Zoé E Vaz da Silva and Maria João Amorim wrote the manuscript. This chapter is part of a submitted manuscript, which can be assessed as a preprint: Santos NB, Vaz da Silva ZE, Gomes C, Reis CA, Amorim MJ. Complement Decay-Accelerating Factor is a modulator of influenza A virus lung immunopathology. *bioRxiv* **2021**, 10.1101/2021.02.16.431406, 2021.2002.2016.431406, doi:10.1101/2021.02.16.431406.

3.2 Summary

Sialic acid is a terminal sugar modification with essential roles in the regulation of biological functions, including the immune system. Unsurprisingly, challenges with pathogens that impose alterations in sialic acid levels are capable of modulating the immune response.

Influenza A virus (IAV) neuraminidase (NA), essential for viral egress, is an unspecific sialidase, able to remove sialic acid residues from heterologous proteins. In the previous chapter, we observed that the interaction between NA and complement decay-accelerating factor (CD55/DAF) is involved in IAV immunopathology, through alterations of innate immune cell recruitment.

Remarkably, DAF, which protects healthy cells from non-specific complement attack, is a heavily sialylated protein. Thus, we addressed if NA could cleave DAF sialic acid moieties, and what could be the biological impact of this interaction. We show that viral NA removes DAF sialic acid, exacerbating complement activation. We further dissected the cleavage mechanism, and propose it may have direct implications in zoonotic IAV transmissions.

3.3 Introduction

The complement system consists in a cascade of proteolytic interactions that lead to the direct killing of the pathogen or infected cell, as well as proinflammatory immune cell recruitment (1–3). C3 is found within the mucus barrier (4), which supports the role of complement in early immune response upon pathogen infection in the airways. Disease severity and mortality have been associated with both lack or excess of complement activation in several viral infections such as severe acute respiratory syndrome coronavirus (SARS-CoV) (5,6), middle eastern respiratory syndrome coronavirus (MERS-CoV) (7), severe acute respiratory syndrome coronavirus-2 SARS-CoV-2 (8–10), and influenza A virus (IAV) (11–13). However, it is still unclear how fine-tuning complement activation may impact in the development of disease severity.

Complement decay-accelerating factor (DAF/CD55) is a membrane-bound regulator of complement activation (RCA) which promotes the decay of C3 convertases, thus protecting healthy cells from non-specific complement attack, and inhibiting the release of pro-inflammatory anaphylatoxins (14–16). Remarkably, DAF is a heavily sialylated protein exposed at the surface of most cell types, including human and murine airways (17–24). In fact, removal of sialic acid has been proposed to induce DAF proteolytic cleavage (18), and to impair its function (21). Thus, it makes it an interesting host factor to consider upon IAV infection.

Sialic acid is an abundant terminal monosaccharide modification with multiple functional implications, including in the regulation of the immune response, (Fig. 3.1-A, B) (25–28).

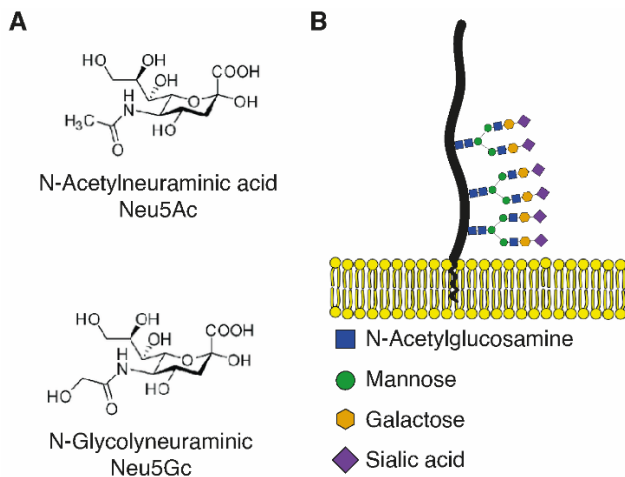


Fig. 3.1 – Sialic acid structure.

A: Sialic acids are composed of a nine-carbon structure, a carboxylic acid at the C1 position, and several α -glycosidic linkages to the underlying sugar chain from the C2 position. Numerous substitutions at the remaining positions, combined with linkage variability, produce a vast diversity of sialic acids in nature. The two most abundant types of sialic acid in mammals are N-acetylneuraminic acid (Neu5Ac) and N-glycolyneuraminic acid (Neu5Gc). Humans cannot produce Neu5Gc, therefore it presents a host restriction factor for IAV. **B:** Sialic acids are usually a terminal modification, linked to galactose residues in N- or O-linked glycans.

Specifically, sialic acid is involved in complement activation (29–31), self- vs. non self-recognition (32–34) and IgG regulation (35,36). Interestingly, desialylation mediated by host or microbial sialidases has been reported to activate neutrophils and monocytes, upon infections such as *Streptococcus pneumoniae*, *Escherichia coli*, *Klebsiella pneumoniae* or SARS-CoV-2 (37–39). Thus, viral-induced alterations in sialic acid levels may pose relevant physiological consequences in host defense.

IAV encodes a sialidase, neuraminidase (NA), whose main role is to release newly formed virions from the cell surface in the end of the viral cycle (40–43). Besides viral egress, described roles for NA include

aerosol transmission (44), mucus layer penetration (45–48) and cell entry (49–53). Of note, the type of sialic acid linkage is one of the described IAV host restriction factors, and therefore viral NAs exhibit receptor preference depending on the host species (54–57): while in avian-adapted IAV strains, NA has preference for α 2,3-, human-adapted IAVs cleave α 2,6-linked sialic acid moieties, as it is the dominant type of receptor in human upper airways (Fig. 3.2-A-C) (54,58–61).

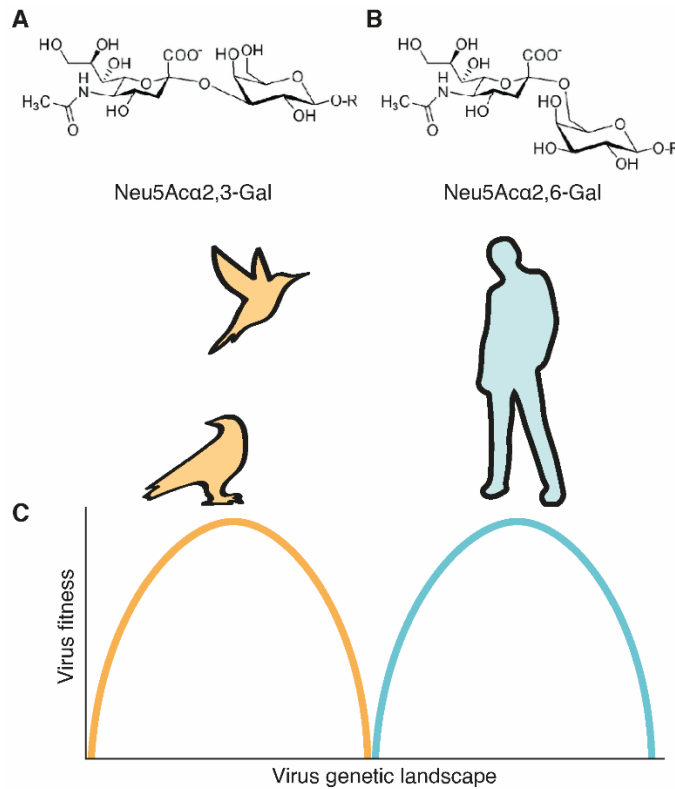


Fig. 3.2 – Influenza A virus sialic acid preference.

A: Hemagglutinin (HA) and Neuraminidase (NA) from avian-adapted IAV exhibit preference to bind and cleave, respectively, α 2,3-linked sialic acid. **B:** Conversely, human-adapted IAVs bind and cleave α 2,6-linked sialic acids, the dominant type of linkage in human upper airways. **C:** Consequently, a virus that is well adapted to avian hosts is not adapted to infect humans, and vice versa (adapted from (60)).

Nevertheless, NA is a relatively unspecific sialidase which has been shown to remove sialic acid from vesicular stomatitis virus (VSV) protein VSV-G, within the cell (62). Furthermore, NA have also been reported to cleave and activate LAP-TGF- β (63,64), suggesting potential new roles for NA in viral-induced pathogenesis.

In the previous chapter we reported that the interaction between DAF and the viral protein NA modulated the recruitment of cells from the innate immune system. Here, we investigate the underlying mechanism on how NA acts on DAF. We show that DAF acts on DAF in a strain-specific manner, removing α -2,6-linked sialic acids and propose that this may influence virulence upon IAV challenge in a DAF-dependent manner. Furthermore, as the recognition of different conformations of sialic acid by IAV is a key driver in intra- and interspecies transmission (56,57,61), our findings may have implications for IAV adaptation in host species jumps during zoonotic infections.

3.4 Results

3.4.1 IAV decreases DAF molecular weight in the timecourse of infection.

In the previous chapter we observed that different NAs elicit distinctive innate immune responses, and specifically NA-DAF interaction is responsible for the recruitment of innate immune cells. NA is an widely studied sialidase (43) and, as DAF is a highly sialylated protein, we hypothesized that the interaction between DAF and NA resided in the ability of NA to cleave DAF's sialic acid content. Sialic acids that reside on cell surface glycoproteins and glycolipids are the receptors for IAV, recognized by HA for viral entry and cleaved by NA for viral exit (41). In order to assess cleavage of DAF's sialic acid content, we infected a human alveolar cell line (A549) with A/California/7/2009 (Cal), A/England/195/2009 (Eng), A/Puerto Rico/8/1934 (PR8) or A/X-31 (PR8-HK4,6), and analyzed DAF content by western blot. We observed that in infected cells the band marked by the anti-DAF antibody was at a lower molecular weight (MW) than in mock-infected cells (Fig. 3.3-A). This difference in MW is of nearly 18 kDa, which corresponds to DAF sialic acid content (20) and suggests that infection leads to loss of said content. Quantification of this cleavage confirmed that it is dependent on infection and progressive over time. Interestingly, the extent of DAF cleavage is not identical in cells infected with different IAV strains, PR8 infected cells presenting the most drastic effect (Fig. 3.3-B).

Protein glycosylation type and levels may greatly vary between organisms (65). As previous results were obtained using human cell lines, we wanted to confirm that infection with the tested strains would remove the sialic acid content of murine DAF. For that purpose, we collected mouse embryonic fibroblasts (MEF) from WT mice and infected them with the laboratory adapted strains PR8 and PR8-HK4,6.

Similarly to what was shown in a human cell line infection, murine DAF in infected MEFs suffered a drop in MW, when compared to non-infected cells (Fig. 3.3-C). Moreover, the differences in cleavage efficacy between PR8 and PR8-HK4,6 were maintained (Fig. 3.3-D), showing that IAV is able to process murine DAF and giving an insight to what may be triggering complement activation *in vivo*.

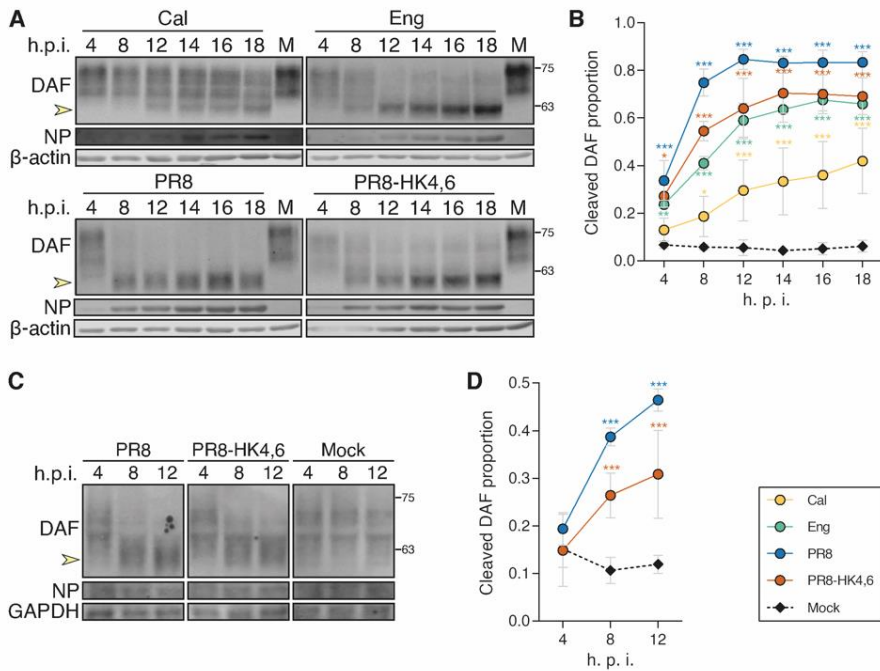


Fig. 3.3 – Influenza A virus decreases DAF molecular weight (MW) in the timecourse of the infection.

A: Western blot detection of complement decay-accelerating factor (DAF) in A549 cells upon infection with A/California/7/2009 (Cal), A/England/195/2009 (Eng), A/Puerto Rico/8/1934 (PR8) or A/X-31 (PR8-HK4,6) at a multiplicity of infection (MOI) of 5. **B:** The proportion of cleaved DAF was measured in each lane as the ratio of low molecular weight (MW) to total DAF pixel densitometry. **C:** Western blot detection of DAF in mouse embryonic fibroblasts (MEFs) derived from C57/BL6 WT or *Daf*^{-/-} mice upon infection with PR8 or PR8-HK4,6 at a MOI of 5. **D:** The proportion of cleaved DAF was measured in each lane as the ratio of low MW to total DAF pixel densitometry. (**B, D:** data shown as mean±sd, from three independent experiments). Yellow arrows indicate cleaved DAF. MW is indicated in kDa. Statistical analysis detailed in materials and methods.

3.4.2 NA removes DAF sialic acid, partially inside the cell.

To show that NA mediates processing of DAF and discard the involvement of other viral proteins, we transfected HEK293T cells with eight different plasmids, each encoding a different PR8 genomic segment (Fig. 3.4-A). As expected, cleavage only occurred when cells were transfected with segment 6, which encodes for NA, showing that NA is the only viral protein responsible for the reduction in DAF MW (Fig. 3.4-B). Furthermore, we excluded any role of the viral genome, in the form of viral ribonucleoproteins (vRNPs) in this process. Treatment with the antiviral drug nucleozin (66), which clusters vRNPs together and thus prevents their trafficking (Fig. 3.S1-A), did not impact DAF MW decrease (Fig. 3.S1-B, C).

To confirm that this drop in MW was indeed the result of direct enzymatic activity of NA, we introduced the mutation E229A in PR8 segment 6, which pronouncedly decreases NA enzymatic activity, while still sustaining a low level of viral replication (67). Using the RG technique as mentioned previously, we created a PR8 strain containing

the mutated NA: PR8 NA-E229A (Fig. 3.4-C). Analysis of DAF in cells transfected with the eight RG plasmids required for producing the passage 0 virus showed that, by impairing NA sialidase activity, DAF cleavage was prevented (Fig. 3.4-D). Taken together, these results confirm that DAF cleavage observed upon infection is due solely to NA sialidase activity.

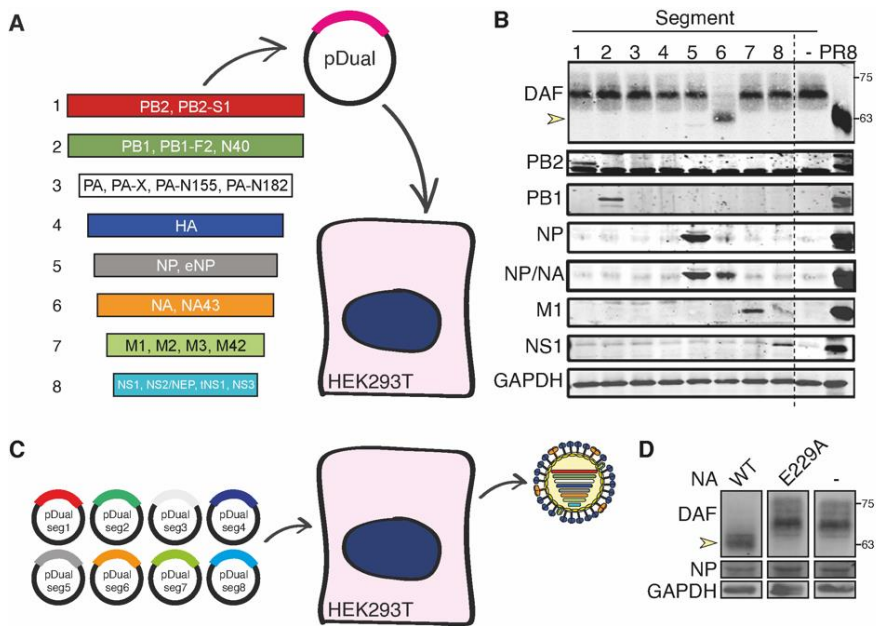


Fig. 3.4 – Influenza A virus neuraminidase cleaves DAF through its sialidase activity.

A: HEK293T cells were transfected with plasmids encoding the eight different A/Puerto Rico/8/1934 (PR8) viral segments. **B:** Western blot detection of DAF after transfection. **C:** HEK293T cells were transfected with eight plasmids encoding the eight different PR8 viral segments, in order to produce virions. Segment 6 was either the wild-type NA (WT) or the catalytically-impaired mutant NA-E229A (E229A). **D:** Western blot detection of DAF in cells used to produce the virions. Statistical analysis detailed in materials and methods.

As NA is a transmembrane protein with potential to cleave sialic acids at the cell surface, but also inside the cell while en route to the plasma membrane, we questioned where DAF cleavage was taking place. For that, PR8 infected A549 cells were treated with a non-permeable NA inhibitor, Zanamivir (Fig. 3.5-A). We observed that Zanamivir treatment reduced the proportion of cleaved DAF (0.60 vs. 0.75), showing that DAF cleavage happens in part at the cell membrane, and in part intracellularly (Fig. 3.5-B, C).

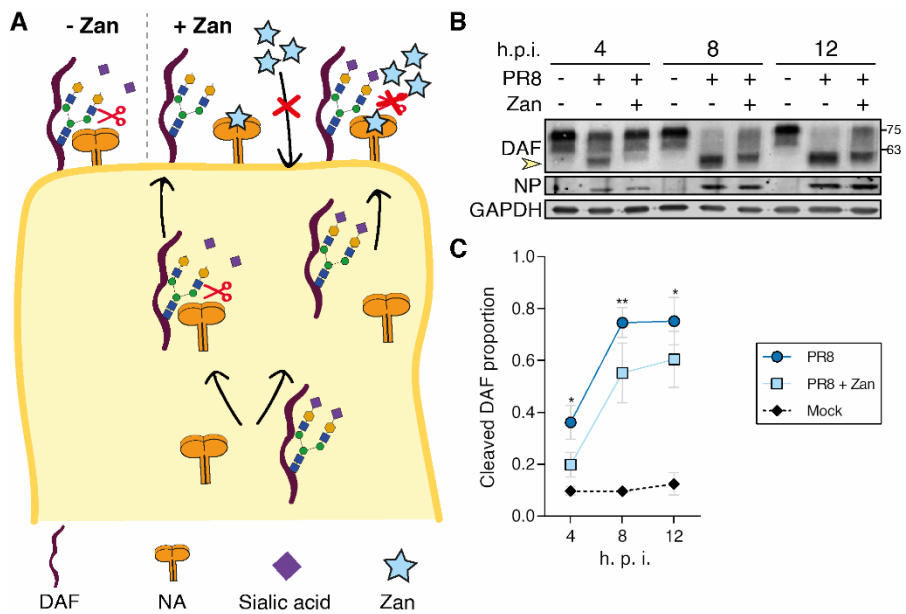


Fig. 3.5 – Influenza A virus neuraminidase cleaves DAF partially inside the cell.

A: Zanamivir (Zan) is a NA inhibitor, which is not cell permeable. Therefore, if DAF cleavage occurs at cell surface it will be prevented by Zan treatment. Alternatively, if cleavage occurs inside the cell, it will remain unaffected by Zan treatment. **B:** Western blot detection of DAF in A549 cells upon infection with A/Puerto Rico/8/1934 (PR8) at a MOI of 3, treated with Zan. **D:** The proportion of cleaved DAF was measured in each lane as the ratio of low MW to total DAF pixel densitometry (data shown as mean \pm sd, from four independent experiments). Yellow arrows indicate cleaved DAF. MW is indicated in kDa. Statistical analysis detailed in materials and methods.

3.4.3 NA removes DAF α 2,6-linked sialic acid and increases complement activation.

For IAV receptor recognition, the binding of sialic acid to the penultimate galactose residues of carbohydrate side chains is important, and different IAVs exhibit preference for Neu5Ac α (2,3)-Gal (hereafter α 2,3-) or Neu5Ac α (2,6)-Gal (hereafter α 2,6-) conformations (32,56). Interestingly, most avian IAVs bind preferentially to sialic acid joined to the sugar chain through an α 2,3-linkage, whereas human IAV preferentially use α 2,6-linked sialic acid as a cellular receptor (56,69). To assess which type of ligations were cleaved by NA, we infected A549 cells with PR8 and purified DAF by immunoprecipitation. Subsequently, we treated immunoprecipitated DAF with PNGaseF, which specifically removes N-glycans (Fig. 3.6-A), and probed DAF by western blot and lectin blot with *Sambucus nigra* agglutinin (SNA) or *Maackia amurensis* lectin (MAL), which detect α 2,6- or α 2,3-linked sialic acid, (Fig. 3.6-B). The cumulative effect in DAF MW decrease of PR8 infection and PNGaseF treatment, as well as loss of SNA staining only upon infection, indicates that PR8 infection specifically removes α 2,6-linked sialic acid from DAF O-glycans.

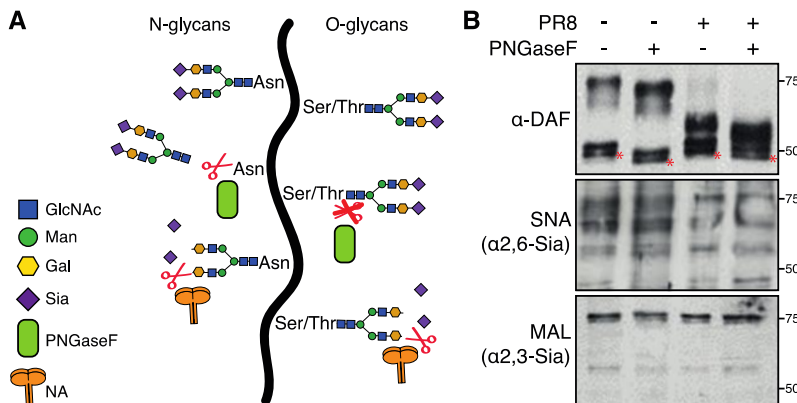


Fig. 3.6 – NA removes α 2,6-linked sialic acid from DAF O-glycans.

A: DAF was purified by immunoprecipitation from cell lysates of A549 cells infected with A/Puerto Rico/8/1934 (PR8) at 12 hours post-infection (h.p.i.), and treated with PNGaseF to remove N-glycans. **B:** DAF analysis by western blot or lectin blot with *Sambucus nigra* agglutinin (SNA) and *Maackia amurensis* lectin (MAL), which detect α 2,6- or α 2,3-linked sialic acid, respectively (* indicates IgGs from immunoprecipitation). Yellow arrows indicate cleaved DAF. MW is indicated in kDa. Results are representative of three independent experiments. Statistical analysis detailed in materials and methods. GlcNAc – N-acetylglucosamine; Man – mannose; Gal – galactose; Sia – sialic acid; Asn – asparagine; Ser/Thr – serine/threonine.

As DAF sialic acid residues are α 2,6-linked, opposed to the higher affinity of avian strains for α 2,3-linked sialic acids, we tested the ability of avian-derived NAs to cleave DAF (Fig. 3.7-A). In accordance with that, transfection of HEK293T cells with avian-adapted NAs did not impact DAF MW (Fig. 3.7-B). Remarkably, transfection with NAs from a H7N9 isolated from a human patient (A/Anhui/1/2013) and from a H5N6 isolated from a chicken (A/chicken/Jiangxi/02.05 YGYXG023-P/2015) caused a drop in DAF MW (Fig. 3.7-B). These two NAs are thus able to cleave α 2,6-linked sialic acid residues, indicating they are already

adapted to human sialic acid linkages and indeed both H7N9 (71,72) and H5N6 (73,74) strains have been shown to cause severe zoonotic disease. These results suggest that the pattern of host cells that are cleaved by NA may change during host adaptation in zoonotic events.

In order to confirm the link between NA-mediated DAF cleavage and complement exacerbation upon *in vivo* infection, we aimed to engineer recombinant mutant viruses composed of seven PR8 segments (segments 1-5, 7 and 8) and expressing segment 6 from viruses that do not cleave DAF. Supported by data in Fig. 3.7-B, we selected segment 6 from H5N2 and H5N8 avian IAVs to produce reverse genetics (RG) 7+1 PR8 reassortant viruses (Fig. 3.S2-A). After transfecting HEK293T cells with the eight plasmids to produce the P0 viruses, we observed that PR8 NA-H5N2 did not cleave DAF, as expected (Fig. 3.S2-B). However, PR8 NA-H5N8 viruses acquired the capacity to cleave DAF (Fig. 3.S2-B). For this reason, even though we amplified both viruses in eggs to avoid additional adaptation to host environment, we excluded the PR8 NA-H5N8 from further experiments as they cleaved DAF (Fig. 3.S2-C). The rescued PR8 NA-H5N2 in eggs (Fig. 3.S2-C), was then tested for its ability to infect and replicate in mammalian cells. Infection at low MOI in MDCK cells replicated effectively, with H5N2 growing almost to PR8 levels (Fig. 3.S2-D). However, when A549 cells were infected at an MOI of 3, PR8 NA-H5N2 cleaved DAF (Fig. 3.S2-E). These results strongly suggest that IAVs containing NAs from avian origin rapidly adapt to cleave DAF α 2,6-linked sialic acid, and could not be used to assess the link between DAF cleavage *in vitro* and pathogenicity upon mouse infection. Hence, to assess the effect of DAF sialic acid cleavage in complement activation and to overcome these mechanisms of fast adaptation, we have decided to perform an entirely *in vitro* experiment.

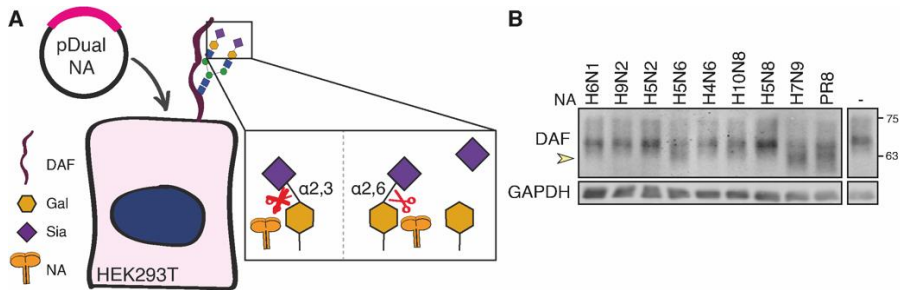


Fig. 3.7 – NA removes DAF α 2,6-linked sialic acid and increases complement activation.

A: Transfection of HEK293T cells with plasmids encoding NAs from the indicated avian IAVs: H6N1 A/chicken/Taiwan/67/2013, H9N2 A/chicken/Pakistan/UDL-01/08, H5N2 A/goose/Taiwan/01031/2015, H5N6 A/chicken/Jiangxi/02.05 YGYXG023-P/2015, H4N6 A/chicken/Hunan/S1267/2010, H10N8 A/chicken/Jiangxi/1204/2014, H5N8 A/scarlet ibis/Germany/Ar44-L01279/2015, H7N9 A/Anhui/1/2013. As DAF contains α 2,6-linked sialic acid, only NAs adapted to this type of ligation will cleave it. **B:** Western blot detection of DAF after transfection. Yellow arrows indicate cleaved DAF. MW is indicated in kDa. Gal – galactose; Sia – sialic acid.

NA unprecedented direct and pronounced effect on DAF strongly suggests a functional consequence. It has been proposed that DAF negatively charged sialic acids function as a spacer, which projects DAF RCA domains to the extracellular milieu (21). Additionally, sialic acid removal promotes DAF to be proteolytically shed (18). Therefore, we hypothesized that NA-mediated sialic acid cleavage would result in DAF loss/alteration of function, resulting in increased complement activity. To test this *in vitro*, we produced lentiviral vectors to deliver WT or E229A versions of PR8 NA fused to GFP. After transduction of A549 cells, we treated cells with normal human serum and stained for C5b-9 as a proxy for complement activation (Fig. 3.8-A). Transduction of cells with WT NA resulted in increased C5b-9 deposition when compared with cells transduced with E229A (1 ± 0.7 vs. 0.3 ± 0.2) (Fig. 3.8-B). Therefore, NA

removal of DAF sialic acid content does impair its complement regulator function, increasing complement activation.

DAF is a regulator of complement activation (RCA), which prevents unspecific complement activation in healthy cells (3,16,68). DAF specifically inhibits the C3 convertases, and thus prevents the activation of the remaining pathway (14–16). Results from the previous chapter suggested that DAF did not influence cell death, despite increased complement activation. After the observation that NA-mediated DAF cleavage increased C5b-9 deposition, we questioned if it would increase cell death. To test this hypothesis, we collected lung primary cells from WT or *Daf*^{-/-} mice, infected them for 12h and treated them with serum (Fig. 3.8-C). In mock-infected cells, as expected, DAF was required to confer protection from complement-dependent cytotoxicity (CDC). Infection with the RG viruses PR8, PR8-HK4,6, PR8-HK4 or PR8-HK6, which represent different combinations of HA and NA did not revert the increased cell death in *Daf*^{-/-} cells. Taken together, these results show that NA cleaves DAF promoting complement activation, however it is not reflected in cell death. Alternatively, DAF absence results in augmented cell death from CDC. Thus, absence of DAF and DAF cleavage should represent independent mechanisms of complement exacerbation. We propose that the removal of DAF sialic acid content triggers an exaggerated complement-dependent immune response that, in the context of the organism, poses more detrimental consequences than DAF depletion. This response is likely stimulated by the amplified generation of C3a and C5a anaphylatoxins, and not by C5b-9 deposition at target cells.

Our results show that the transfection of a fully catalytic competent NA increases C5b-9 deposition on A549 cells to a higher extent than a catalytically inactive NA. Despite not being conclusive, this experiment allowed us to raise the tempting hypothesis that sialic acid removal of DAF leads to increased complement activation *in vivo*. However, these

results need further experimental validation. Overall, we unveiled a widespread direct interaction between NA and DAF, with conceivable functional implications, which is an unprecedented way of a virus, via altering a host protein from within the infected cell, modulating the immune response.

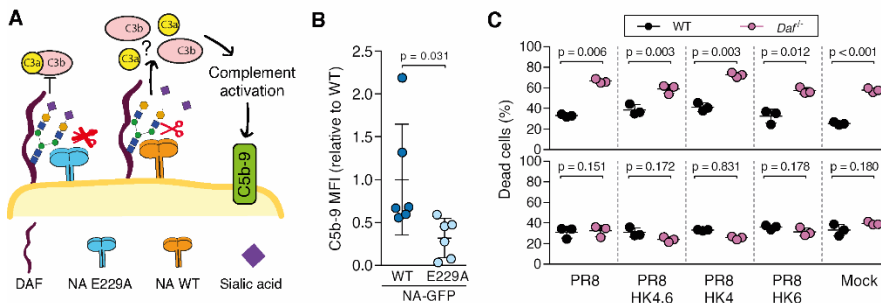


Fig. 3.8 – DAF protects from complement-dependent toxicity, but NA-mediated desialylation increases complement activation.

A: A549 cells were transduced with WT or catalytically-impaired mutant NA-E229A and treated with serum to activate complement. **B:** Flow cytometry detection of C5b-9 deposition, as a proxy for complement activation (data shown as mean \pm sd, from six independent experiments, each corresponding to a pool of five independent transductions. Each point represents the median fluorescence intensity (MFI) of a sample treated with serum minus its corresponding heat-inactivated control.). **C:** Percentage of cell death of murine lung primary cells after infection with the indicated viruses and treatment with serum (upper panel) or heat-inactivated serum (lower panel). Data shown as mean \pm sd of triplicates, representative of two independent experiments. (note: **C** is part of the supplementary material of Chapter 2 and was repeated here to highlight that increased C5b-9 deposition did not translate into more dead cells). Statistical analysis detailed in materials and methods.

3.5 Discussion

Our previous results demonstrated the potential of regulating complement activation as a strategy to provide resilience to viral infections, without affecting pathogen clearance. Unexpectedly, upon IAV infection, lack of DAF leads to reduced activation of complement. These results indicate that complement is not the sole recruiter and activator of the immune response, and that direct or indirect HA-DAF and/or NA-DAF interactions play additional roles in immune cell recruitment.

Previous examples of NA impacting the immune response include the activation of the NK cell sialylated receptors NKp44 and NKp46 by HA at the surface of infected cells, which is countered by NA-mediated desialylation (75,76). In the case of our work, it is known that apical delivery of NA to the cell surface is potentiated by HA (77) and during this transport (and also at the plasma membrane), NA would cleave DAF sialic acid giving rise to increased activation of complement. Indeed, we observed that IAV infection induces a drop in DAF MW over the course of infection both in human and murine cell lines (Fig. 3.3-A-D). Furthermore, this drop corresponds to described DAF sialic acid content, and NA is necessary and sufficient for this cleavage (Fig. 3.4-A-D).

Importantly, transduction of cells with NA and thus removal of DAF sialic acid content resulted in an increased C5b-9 deposition (Fig. 3.8-A, B). We propose that the removal of DAF sialic acid content would not lead to a loss of function, but instead trigger an exaggerated complement response. This is contrary to what is observed for autoimmune diseases, for which *Daf*^{-/-} mice have been widely used (78–80). These mice have increased disease severity coupled with higher complement activation levels when compared to their WT counterparts, showing that *Daf*^{-/-} mice do not lack the ability to activate the

complement and that the mechanism we now describe could be shared among viruses containing promiscuous NAs. As an alternative, NA-mediated DAF cleavage could result in the recruitment of innate immune cells by exposing “non-self” glycans at cell surface, which has been shown to activate complement via the lectin pathway (25). Besides complement, it could also be recognized by different PRRs (81). We propose that the removal of DAF sialic content would not lead to a loss of function, but instead trigger an exaggerated complement response. Thus, at the moment this hypothesis is speculative but raises concerns about using therapies, such as DAS181 (82), aiming at decreasing sialic acid levels at cell surface to prevent viral entry. Interestingly, our work indicates that NA cleavage of sialic acids does not happen solely at the cell surface, but also intracellularly, as treatment with Zanamivir did not completely abolish DAF cleavage (Fig. 3.5-A-C). To the best of our knowledge, this mechanism has not been reported before.

DAF cleavage provides a possible link between DAF-NA interaction and *in vivo* pathology that we provide in the model of Fig. 3.9. Given that our study shows that sialic acids cleaved by DAF are α 2,6-linked to O-glycans (Fig. 3.6-A, B), this mechanism may have implications in host species jumps, as for example, IAV adapted to birds exhibit preference for α 2,3-linked sialic acids. Interestingly, we present evidence that NAs derived from two avian-adapted strains, H5N6 and H7N9, were able to cleave human DAF (Fig. 3.7-A, B). As H7N9 and H5N6 outbreaks provoked severe infections in humans, associated with exacerbated immune response (71–73), hypothetically establishing DAF cleavage as a hallmark of virulence could be a useful tool to monitor viruses with pandemic potential.

In addition, many host proteins, including mucins, are decorated by sialic acids. Mucins form an important barrier at the cell surface preventing viral entry (83). These proteins are also heavily glycosylated, specifically at the terminal part of O-glycans (84), similarly to DAF,

indicating that they could be substrates of NA. As a consequence, the mechanism we describe could be used to manipulate the extracellular environment and facilitate viral cell-to-cell transmission. Identification of glycans exposed at the surface of infected cells and their interaction with viral proteins may help to understand the balance between viral entry and immune response targets and reveal disease resilience pathways prone to therapeutic intervention. The link we identified via NA, DAF and complement establishes a viral mediated mechanism for maintaining inflammation via increasing the recruitment of immune cells (Fig. 3.9).

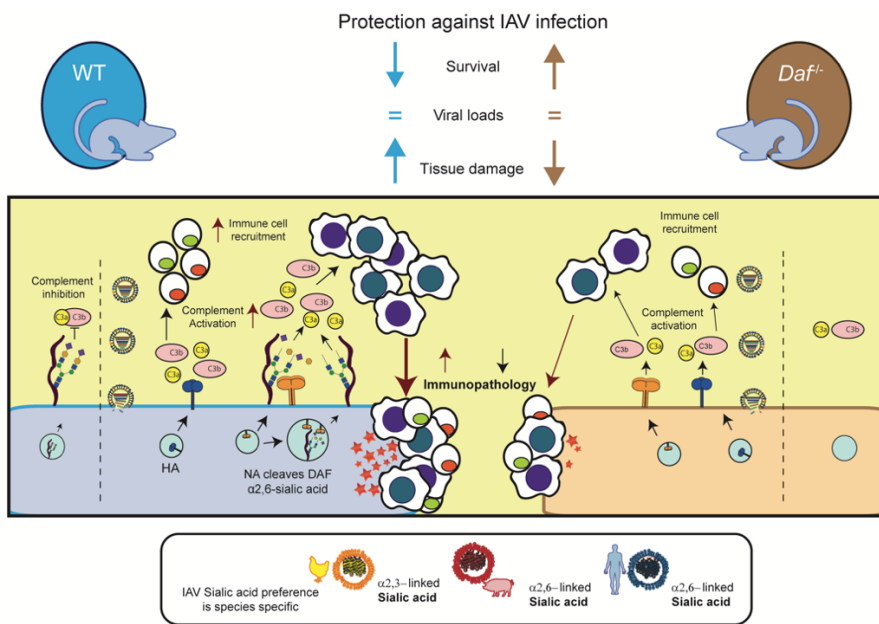


Fig. 3.9 – Proposed model for DAF-mediated immunopathology.

At steady state, DAF accelerates the decay of C3 convertases, inhibiting the formation of C3a and C3b and subsequent complement activation. Upon IAV infection, the cell will produce viral proteins, and in particular NA. NA is a potent sialidase that will remove the sialic acid content of DAF both inside the cell and at the surface. This processing of DAF by NA leads to DAF loss/alteration of function and hence overactivation of the complement pathway that will recruit innate immune cells. The excess of innate immune response leads to tissue damage and ultimately immunopathology, worsening disease outcome.

Taken together, results from this and the previous chapter revealed a novel host factor involved in pathology. Remarkably, DAF interaction with the viral proteins HA and NA controlled the viral-induced pathogenesis, either promoting immunopathology or disease tolerance (Fig. 3.10). In the next chapter, we will address the contribution of a viral protein, HA, to pathology, through a different mechanism that promotes disease resistance.

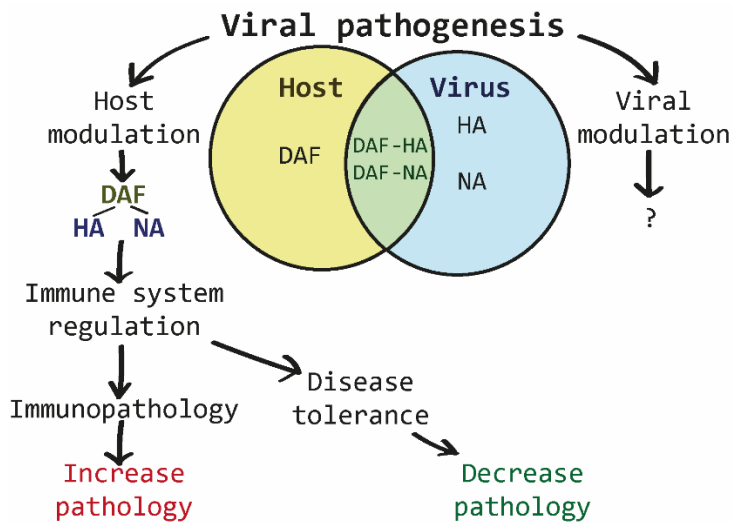


Fig. 3.10 – Summary of Chapters 2 and 3 contribution to viral pathogenesis.

The host protein DAF, via an interplay with viral HA and NA, promotes immunopathology, and thus a worse disease outcome. Modulation of this pathways could lead instead to disease tolerance, by controlling the immune response without altering the viral loads. In the next chapter, we will address the role of a viral factor in modulating viral pathogenesis through an independent mechanism.

3.6 Materials and methods

3.6.1 Statistical analyses

All statistical analyses were conducted using GraphPad Prism 6 (GraphPad, version 6.01). Detailed statistics and number of replicates for all experiments can be found in the figure legends and/or in the main text. DAF cleavage: Statistical significance represented as * $p < 0.05$, ** $p < 0.01$, *** $p < 0.001$, using two-way ANOVA followed by Holm-Sidak multiple comparisons test. C5b-9 deposition: Population normality was not proved using D'Agostino & Pearson omnibus normality test. Statistical significance tested using Wilcoxon matched-pairs signed rank test, as samples were paired.

3.6.2 Ethics statement

All animals were housed at IGC facilities under specific pathogen free conditions and fed *ad libitum*. Experimental animal procedures were previously approved by the IGC Animal Ethics Committee and licensed by the Portuguese General Directory of Veterinary (DGAV, Ministry of Agriculture, Rural Development and Fishing), with references A016/2013 and A013/2019. All animals were housed and handled according with good animal practice as defined by national authorities (DGAV, Law n^o1005/92 from 23rd October) and European legislation EEC/86/609. C57BL6/J wild-type (WT) mice were provided by the IGC animal facility. C57BL6/J *Daf*^{-/-} (*Daf*^{-/-}) were previously bred in the IGC animal facility from C57BL6/J *Daf*^{-/-} / *Cd59a*^{-/-} mice (kindly provided by Prof. Wen-Chao Song) crossed with WT mice from the IGC animal facility

3.6.3 Cell culture

Human basal alveolar epithelial cells (A549), Human embryonic kidney 293 cells expressing a mutant version of the SV40 large T

antigen (HEK293T) and mouse embryo fibroblasts (MEF) were cultured in Dulbecco's modified Eagle's medium (DMEM, Gibco®, 21969035) supplemented with fetal bovine serum (FBS, Gibco®, S181i-500), 10% (v/v), 200 mM L-glutamine (Life Technologies, 25030-024), 100 U/ml penicillin and 10 µg/ml streptomycin (Biowest, L0022-100) (complete DMEM). Cells were kept in T50 flasks at 37°C, 5% CO₂ and sub-cultured every 3 to 4 days using trypsin-EDTA (Biowest, X0930-100).

3.6.4 Primary MEF isolation

MEF cells were isolated from WT and mice as previously described (85). Breedings were set up in a timed manner and embryos harvested at stages between E13.5 to E15.5. Embryos were carefully isolated from the yolk sac; the head, visceral tissues and blood clots removed, and the remaining tissue macerated using a scalpel blade. Macerated tissue was then transferred to a T75 flask containing complete DMEM and incubated at 37°C, 5% CO₂ for 48h. Cells that grew from the tissue were harvested with trypsin, expanded to T150 flasks and, when 100% confluent, frozen in FBS with 10% DMSO and kept in liquid nitrogen until needed for experiments. This was performed by Zoé E Vaz da Silva.

3.6.5 Primary mouse lung cells isolation

Primary lung cells were isolated from WT or *Daf^{-/-}* mice adapted from (86). After sacrifice by CO₂ inhalation, mice were dissected, exposing lungs and trachea. Mice were exsanguinated by cutting the inferior vena cava and perfused with 20ml of PBS through the right ventricle. A small incision was performed in the upper trachea and a catheter (Braun, 4253329) carefully inserted until the base of the lungs. First, 1.5ml of sterile collagenase D (Roche, 11088858001) 0.5% (w/v) in PBS was pushed slowly into the lung with a 1ml syringe, followed by 0.5ml agarose (Lonza, 733-0829) 1% (w/v) in PBS. After 2min

incubation, lungs were collected in one piece to 2ml of collagenase D and incubated for 40min, at room temperature. Subsequently, lungs were transferred to a culture dish with 10ml of complete DMEM supplemented with 5U DNase I (NZYTech, MB13402) and lung tissue dissected and minced with a scalpel blade. Dissociated cells were filtered through a 100µm cell strainer, centrifuge at 650g, room temperature, for 5min, and resuspended in complete DMEM. Cells were counted and plated in a 6 well plate at $\sim 9 \times 10^5$ cells/well and incubated at 37°C, 5% CO₂ for 48h.

3.6.6 Influenza A virus strains

Reverse-genetics (RG) derived A/Puerto Rico/8/34 (PR8, H1N1) (kindly provided by Prof. Ron Fouchier) and A/X-31, a recombinant virus containing segments 4 and 6 from A/Hong Kong/01/1968 (HK68) and the remaining from A/Puerto Rico/8/34 (87) (PR8-HK4,6, H3N2) (kindly provided by Prof. Paul Digard) were used as model viruses. RG derived PR8 viruses containing segment 4 (PR8-HK4) or segment 6 from HK68 (PR8-HK6) were described in Chapter 2 and were used to assess the role of HA or NA proteins. RG derived PR8 NA-E229A was used as a control of impaired NA activity.

Viruses were grown in eggs as following: embryonated chicken eggs were incubated at 37°C for 10 days. After that, the egg shell was lightly sanded with a rotary tool and a hole was pierced with a sterile 27G needle on top of the egg and on the opposite side of the embryo. Through that hole, 100 PFU of virus diluted in 200µl PBS were injected into the allantoic fluid of the egg. Infected eggs were incubated at 37°C for 2-3 days, and then at -20°C for 2h. Viruses were collected by opening the eggs and carefully retrieving the allantoic fluid. After centrifugation at 3500g, 5min, 4°C to remove debris, the virus solution was aliquoted and kept at -80°C.

3.6.7 Reverse genetics

Reverse genetics virus production was conducted as previously described (88–90). pDual plasmids were a kind gift from Prof. Ron Fouchier, (Erasmus MC, Netherlands). Briefly, HEK293T cells were transfected as indicated below in 6-well plates with 250ng of each of the eight pDual plasmids each encoding the corresponding viral segments of PR8 or the indicated IAVs. After 16h of incubation, culture medium was removed and added DMEM supplemented with 100 U/ml penicillin, 10 µg/ml streptomycin and 200mM L-Glutamine (serum-free DMEM) containing 1µg/ml Trypsin-TPCK (Worthington, LS003750) and 0.14% (w/v) bovine serum albumin (BSA; PAA, K45-00). After further incubation for 48h at 37°C, 5% CO₂, cells were scraped to the medium and collected. After centrifugation at 800g, 5min, 4°C, cells were collected and analyzed by western blot while supernatants were titrated and amplified in embryonated chicken eggs.

3.6.8 Infections

Cells were seeded in culture plates at appropriate density and incubated overnight. Virus inoculum was added in serum-free DMEM at the MOI of 3 and incubated for 45min. Afterwards, cells were overlaid with complete DMEM and incubated at 37°C, 5% CO₂ for the indicated time. The drug nucleozin (66) was dissolved in DMSO and used at final concentration of 2µM. Zanamivir (Sigma, SML0492) was dissolved in H₂O and used at final concentration of 100mM.

3.6.9 Bacteria and cloning

All transformations for cloning or plasmid amplification were performed in *Escherichia coli* XL10 Gold (Agilent, 200314) according to manufacturer's instructions. Viral RNA (vRNA) was extracted from egg-grown viral stocks using QIAamp Viral RNA Mini Kit (Qiagen, 50952904) according to manufacturer's instructions. From purified vRNA, NA cDNA

was produced using NZY M-MuIV First-Strand cDNA Synthesis Kit (NZYTech, MB17302) with primer “NA_Fw_HindIII” following manufacturer’s recommendations. To produce pEGFP-N1::NA, NA was then amplified and cloned in HindIII-KpnI restriction sites of pEGFP-N1. To generate pLEX-MCS-1::NA-GFP, NA-GFP was amplified from pEGFP-N1::NA and cloned into NotI/XhoI sites of pLEX-MCS-1. pDual::seg6-E229A and pEGFP-N1::NA-E229A were generated by site directed mutagenesis of pDual::seg6 and pEGFP-N1::NA respectively, using the QuikChange Site-Directed Mutagenesis Kit (Agilent, 200518), according to manufacturer’s instructions. Primer sequences are indicated in Table S1.

3.6.10 Transfections

Transfection of HEK293T cells was performed using Lipofectamine 2000 (ThermoFisher, 11668027) according to manufacturer’s recommendations. Plasmids encoding NA genes from following strains were kindly provided by Dr. Holly Shelton (The Pirbright Institute, UK) and were synthesized by GeneArt (Invitrogen) and cloned into a pHW2000 vector (88): H6N1 A/chicken/Taiwan/67/2013 (GenBank accession no. KJ162862), H9N2 A/chicken/Pakistan/UDL-01/08 (91), H5N2 A/goose/Taiwan/01031/2015 (92), H5N6 A/chicken/Jiangxi/02.05 YGYXG023-P/2015 (92), H4N6 A/chicken/Hunan/S1267/2010 (GenBank accession no. KU160821), H10N8 A/chicken/Jiangxi/1204/2014 (GenBank accession no. KP285359), H5N8 A/scarlet ibis/Germany/Ar44-L01279/2015 (92), H7N9 A/Anhui/1/2013 (93).

3.6.11 Lentivirus production

Lentiviral vectors were produced in HEK293T cells transfected with the following plasmids (ThermoFisher, OHS4735): 6µg pLEX-MCS-1::NA-GFP WT/E229A, 4.2µg psPAX2, 1.8µg pMD2.G. 72h hours after

transfection, medium containing lentivirus was collected and stored at -80°C.

3.6.12 C5b-9 deposition

C5b-9 deposition measurement was adapted from (94). A549 cells were seeded in 24-well plates. 24h later, lentiviral vectors encoding either WT or E229A NA-GFP were added in complete DMEM supplemented with 8µg/ml of polybrene (Sigma-Aldrich, H9268). After 36h, cells were washed with PBS and then detached by incubation with 5mM EDTA (Sigma-Aldrich, 03690) in PBS for 10min, 37°C. For each condition, 5 individually transduced wells were pooled and centrifuged at 666g, 5min, 4°C. Cells were then resuspended in veronal buffer (CompTech, B100) and added to a 96-well V-bottom plate (Thermo Scientific Nunc, 10580382), adjusted to 10⁶ cells per well in 100µl. Non-transduced cells were used as unstained control. Normal human serum (Sigma-Aldrich, H4522) or heat-inactivated serum (56°C, 30min) were added at a final concentration of 50%. Cells were incubated with serum for 15min at 37°C. Afterwards, cells were centrifuged and washed with 200µl PBS. Primary staining was made with a mouse α-C5b-9 (Abcam, ab55811, clone aE11) diluted 1:100 in PBS. As a single-stained control, mouse α-DAF (Merck-Millipore, CBL511, clone BRIC 216) was used diluted 1:100 in PBS. Cells were incubated for 20min, 4°C in the dark and then centrifuged and washed as above. Secondary staining was performed with donkey α-Mouse-Alexa Fluor 647 (Invitrogen, A31571) diluted 1:1000 in PBS for 20min, 4°C in the dark. Cells were centrifuged and washed as above and fixed with IC fixation buffer (Life Technologies, 00-8222-49) according to manufacturer's instructions.

3.6.13 Complement-dependent cytotoxicity (CDC)

Primary lung cells isolated from WT or *Daf*^{-/-} mice were infected with PR8, PR8-HK4,6, PR8-HK4 or PR8-HK6. At 12h.p.i., supernatant

was removed and cells were washed with PBS and then detached by incubation with 5mM EDTA (Sigma-Aldrich, 03690) in PBS for 10min, 37°C. Cells were then centrifuged at 666g, 4°C for 5min, resuspended in veronal buffer (CompTech, B100) and added to a 96-well V-bottom plate (Thermo Scientific Nunc, 10580382), adjusted to 10⁶ cells per well in 100µl. Serum obtained from WT mice or heat-inactivated serum (56°C, 30min) were added at a final concentration of 50%. Cells were incubated with serum for 1h at 37°C. Afterwards, cells were centrifuged and washed with 200µl PBS and stained with live-dead Zombie Aqua Fixable Viability Kit (BioLegend, 423101) according to manufacturer's instructions. Cells were centrifuged and washed as above and fixed with IC fixation buffer (Life Technologies, 00-8222-49) following manufacturer's instructions. Cells were then analyzed by flow cytometry.

3.6.14 DAF glycosylation

A549 cells were infected with PR8 as described above. After 12h of infection, cells were lysed with lysis buffer 17 (R&D Systems, 895943) and protein quantified using bicinchoninic acid protein assay (BCA) (Pierce™, 23225). Protein G Sepharose 4 Fast flow beads (GE Healthcare, GE17-0618-01) were incubated with α-DAF (Abcam, ab133684) for 5h and then Protein G-DAF complexes were crosslinked using bis(sulfosuccinimidyl)suberate (BS³) (Sigma, S5799). Protein from total cell extracts (100 µg) were then added to the antibody Protein G complex and incubated 16h at 4°C in a rotator mixer. Washing steps were performed with PBS and samples used for downstream analysis. After DAF immunoprecipitation, removal of N-glycans was performed by digestion with PNGaseF (New England Biolabs, P0704S), according to manufacturer's instructions. For blotting experiments gels were transferred onto nitrocellulose and unspecific binding blocked using 5% BSA and 2% polyvinylpyrrolidone (PVP) for blot detection with α-DAF or biotinylated *Sambucus nigra* agglutinin (SNA) (Vector Laboratories B-

1305-2), respectively. DAF was detected with HRP-conjugated goat anti-rabbit (Jackson ImmunoResearch, 111-035-144) and SNA with Vectastain Avidin/Biotin Complex (Vector Laboratories, PK-4000) incubation. Detection was performed by enhanced chemiluminescence (ECL) (GE Healthcare, RPN2232) and film sheet exposure. After cell infection and collection, this was performed by Catarina Gomes.

3.6.15 Western blotting

Samples were collected in Laemmli's sample buffer (20% (v/v) glycerol (Sigma-Aldrich, 1.04093) / 2% (v/v) SDS (NZYtech, MB01501) / 100 μ M DTT (NZYtech, MB03101) / 24 μ M Tris-HCl (VWR, 28.811.295) pH 6.8 / 0.04% (w/v) Xylene Cyanol FF (Sigma-Aldrich, X4126) / 0.04% (w/v) Bromophenol Blue (Sigma-Aldrich, B0126)) and denatured by heating at 95°C for 10min. Exceptionally, when indicated samples were collected in non-reducing Laemmli's sample buffer, without DTT. Protein samples were loaded into a resolving gel containing 9% (v/v) acrylamide (GRiSP, GB16.3037) with a 4.3% (v/v) acrylamide stacking gel and ran in PAGE buffer (0.25M Tris / 0.192M Glycine (PanReac AppliChem, A1067) / 1% (v/v) SDS) at 150V in a Mini-PROTEAN Tetra Vertical Electrophoresis Cell (BioRad). Proteins were transferred to a 0.45 μ m nitrocellulose blotting membrane (GE Healthcare, 10600003) using a Trans-Blot SD Semi-Dry Electrophoretic Transfer Cell (Bio-Rad, 1703940). Membranes were blocked overnight at 4°C in 5% (w/v) dried non-fat milk (Nestlé, Molico) in PBS-T (0.1% (v/v) Tween-20 (Sigma-Aldrich, P1379) in PBS), followed by washing with PBS-T. Subsequently, membranes were stained with primary antibodies for 1h at room temperature, with rocking. After incubation, membranes were washed with PBS-T, and incubated with secondary antibodies for 45 min at room temperature, with rocking. Membranes were then washed again with PBS-T and PBS and visualized on a LI-COR Biosciences Odyssey near-infrared platform (LI-COR, 9120). Red and green channels were

split and converted to gray scale using ImageJ (NIH, version 1.51h). Corrections were made to improve visualization by adjusting brightness and contrast of the entire image. All antibodies were diluted in PBS-T and are indicated in Table S2.

3.6.16 Immunofluorescence

Cells were seeded at appropriate densities on coverslips and incubated overnight prior to infection. After infection, at the indicated time points supernatant was removed and cells fixed with 4% (v/v) PFA in PBS. Cells were washed three times with 1% (v/v) newborn calf serum (NCS) in PBS and then permeabilized by incubation with 0.2% (v/v) Triton X-100 (Sigma-Aldrich, X-100) in PBS for 7min, at room temperature. After three more washes, cells were incubated with rabbit polyclonal α -NP (kind gift from Prof. Paul Digard, Roslin Institute, UK) diluted 1:1000 in 1% (v/v) NCS in PBS for 1h at room temperature. After three washes, cells were incubated with donkey α -rabbit conjugated to Alexa Fluor 488nm (Life Technologies, A21206) and Hoechst (Sigma, H6024), both diluted 1:1000 in 1% (v/v) NCS in PBS for 45 min at room temperature. After three washes with PBS, slides were mounted with Faramount Mounting Medium (Dako, S302580-2). Single optical sections were imaged with a Leica SP5 live confocal microscope, using a 63x 1.3NA oil immersion objective, the 488nm laser line, and spectral detection adjusted for the emission of the Alexa 488 fluorochromes, using HyD detectors in Standard Mode/Photon Counting Mode. Primary antibodies. Image channels were split using ImageJ (NIH, version 1.51h).

3.7 References

1. Freeley S, Kemper C, Le Friec G. The “ins and outs” of complement-driven immune responses. *Immunol Rev.* 2016 Nov;274(1):16–32.
2. Merle NS, Church SE, Fremeaux-Bacchi V, Roumenina LT. Complement System Part I - Molecular Mechanisms of Activation and Regulation. *Front Immunol.* 2015;6:262.
3. Sarma JV, Ward PA. The complement system. *Cell Tissue Res.* 2011 Jan;343(1):227–35.
4. Radicioni G, Cao R, Carpenter J, Ford AA, Wang T, Li L, et al. The innate immune properties of airway mucosal surfaces are regulated by dynamic interactions between mucins and interacting proteins: the mucin interactome. *Mucosal Immunol.* 2016 Nov;9(6):1442–54.
5. Gralinski LE, Sheahan TP, Morrison TE, Menachery VD, Jensen K, Leist SR, et al. Complement Activation Contributes to Severe Acute Respiratory Syndrome Coronavirus Pathogenesis. *mBio.* 2018 Oct 9;9(5).
6. Wang R, Xiao H, Guo R, Li Y, Shen B. The role of C5a in acute lung injury induced by highly pathogenic viral infections. *Emerg Microbes Infect.* 2015 May;4(5):e28.
7. Jiang Y, Zhao G, Song N, Li P, Chen Y, Guo Y, et al. Blockade of the C5a-C5aR axis alleviates lung damage in hDPP4-transgenic mice infected with MERS-CoV. *Emerg Microbes Infect.* 2018 Apr 24;7(1):77.
8. Fletcher-Sandersjö A, Bellander B-M. Is COVID-19 associated thrombosis caused by overactivation of the complement cascade? A literature review. *Thromb Res.* 2020 Oct;194:36–41.
9. Lo MW, Kemper C, Woodruff TM. COVID-19: Complement, Coagulation, and Collateral Damage. *J Immunol Baltim Md 1950.* 2020 Sep 15;205(6):1488–95.
10. Polycarpou A, Howard M, Farrar CA, Greenlaw R, Fanelli G, Wallis R, et al. Rationale for targeting complement in COVID-19. *EMBO Mol Med.* 2020 Aug 7;12(8):e12642.
11. Garcia CC, Weston-Davies W, Russo RC, Tavares LP, Rachid MA, Alves-Filho JC, et al. Complement C5 activation during influenza A infection in mice contributes to neutrophil recruitment and lung injury. *PLoS One.* 2013;8(5):e64443.
12. Song N, Li P, Jiang Y, Sun H, Cui J, Zhao G, et al. C5a receptor1 inhibition alleviates influenza virus-induced acute lung injury. *Int Immunopharmacol.* 2018 Jun;59:12–20.
13. Sun S, Zhao G, Liu C, Wu X, Guo Y, Yu H, et al. Inhibition of complement activation alleviates acute lung injury induced by highly pathogenic avian influenza H5N1 virus infection. *Am J Respir Cell Mol Biol.* 2013 Aug;49(2):221–30.
14. Hoffman EM. Inhibition of complement by a substance isolated from human erythrocytes. I. Extraction from human erythrocyte stromata. *Immunochemistry.* 1969 May;6(3):391–403.
15. Hoffmann EM. Inhibition of complement by a substance isolated from human erythrocytes. II. Studies on the site and mechanism of action. *Immunochemistry.* 1969

May;6(3):405–19.

16. Kim DD, Song W-C. Membrane complement regulatory proteins. *Clin Immunol Orlando Fla.* 2006 Mar;118(2–3):127–36.
17. Pandya PH, Fisher AJ, Mickler EA, Temm CJ, Lipking KP, Gracon A, et al. Hypoxia-Inducible Factor-1 α Regulates CD55 in Airway Epithelium. *Am J Respir Cell Mol Biol.* 2016 Dec;55(6):889–98.
18. Reddy P, Caras I, Krieger M. Effects of O-linked glycosylation on the cell surface expression and stability of decay-accelerating factor, a glycopospholipid-anchored membrane protein. *J Biol Chem.* 1989 Oct 15;264(29):17329–36.
19. Varsano S, Frolkis I, Ophir D. Expression and distribution of cell-membrane complement regulatory glycoproteins along the human respiratory tract. *Am J Respir Crit Care Med.* 1995 Sep;152(3):1087–93.
20. Lublin DM, Krsek-Staples J, Pangburn MK, Atkinson JP. Biosynthesis and glycosylation of the human complement regulatory protein decay-accelerating factor. *J Immunol Baltim Md* 1950. 1986 Sep 1;137(5):1629–35.
21. Coyne KE, Hall SE, Thompson S, Arce MA, Kinoshita T, Fujita T, et al. Mapping of epitopes, glycosylation sites, and complement regulatory domains in human decay accelerating factor. *J Immunol Baltim Md* 1950. 1992 Nov 1;149(9):2906–13.
22. Medof ME, Kinoshita T, Nussenzweig V. Inhibition of complement activation on the surface of cells after incorporation of decay-accelerating factor (DAF) into their membranes. *J Exp Med.* 1984 Nov 1;160(5):1558–78.
23. Medof ME, Walter EI, Rutgers JL, Knowles DM, Nussenzweig V. Identification of the complement decay-accelerating factor (DAF) on epithelium and glandular cells and in body fluids. *J Exp Med.* 1987 Mar 1;165(3):848–64.
24. Lukacik P, Roversi P, White J, Esser D, Smith GP, Billington J, et al. Complement regulation at the molecular level: the structure of decay-accelerating factor. *Proc Natl Acad Sci U S A.* 2004 Feb 3;101(5):1279–84.
25. Varki A, Gagneux P. Multifarious roles of sialic acids in immunity. *Ann N Y Acad Sci.* 2012 Apr;1253:16–36.
26. Varki A. Sialic acids in human health and disease. *Trends Mol Med.* 2008 Aug;14(8):351–60.
27. Varki NM, Varki A. Diversity in cell surface sialic acid presentations: implications for biology and disease. *Lab Investig J Tech Methods Pathol.* 2007 Sep;87(9):851–7.
28. Pshezhetsky AV, Ashmarina LI. Desialylation of surface receptors as a new dimension in cell signaling. *Biochem Biokhimiia.* 2013 Jul;78(7):736–45.
29. Langford-Smith A, Day AJ, Bishop PN, Clark SJ. Complementing the Sugar Code: Role of GAGs and Sialic Acid in Complement Regulation. *Front Immunol.* 2015;6:25.
30. Oerlemans MMP, Moons SJ, Heming JJA, Boltje TJ, de Jonge MI, Langereis JD. Uptake of Sialic Acid by Nontypeable *Haemophilus influenzae* Increases Complement Resistance through Decreasing IgM-Dependent Complement Activation. *Infect Immun.* 2019 Jun;87(6).
31. Abeln M, Albers I, Peters-Bernard U, Flächsig-Schulz K, Kats E, Kispert A, et

- al. Sialic acid is a critical fetal defense against maternal complement attack. *J Clin Invest*. 2019 Jan 2;129(1):422–36.
32. Bhide GP, Colley KJ. Sialylation of N-glycans: mechanism, cellular compartmentalization and function. *Histochem Cell Biol*. 2017 Feb;147(2):149–74.
33. Khan N, de Manuel M, Peyregne S, Do R, Pruffer K, Marques-Bonet T, et al. Multiple Genomic Events Altering Hominin SIGLEC Biology and Innate Immunity Predated the Common Ancestor of Humans and Archaic Hominins. *Genome Biol Evol*. 2020 Jul 1;12(7):1040–50.
34. Macauley MS, Crocker PR, Paulson JC. Siglec-mediated regulation of immune cell function in disease. *Nat Rev Immunol*. 2014 Oct;14(10):653–66.
35. Pagan JD, Kitaoka M, Anthony RM. Engineered Sialylation of Pathogenic Antibodies In Vivo Attenuates Autoimmune Disease. *Cell*. 2018 Jan 25;172(3):564-577.e13.
36. van de Bovenkamp FS, Derksen NIL, Ooijevaar-de Heer P, van Schie KA, Kruithof S, Berkowska MA, et al. Adaptive antibody diversification through N-linked glycosylation of the immunoglobulin variable region. *Proc Natl Acad Sci U S A*. 2018 Feb 20;115(8):1901–6.
37. Formiga RO, Amaral FC, Souza CF, Mendes DAGB, Wanderley CWS, Lorenzini CB, et al. Neuraminidase inhibitors rewire neutrophil function in murine sepsis and COVID-19 patient cells. *BioRxiv Prepr Serv Biol*. 2020 Nov 12;
38. Suzuki H, Kurita T, Kakinuma K. Effects of neuraminidase on O₂ consumption and release of O₂ and H₂O₂ from phagocytosing human polymorphonuclear leukocytes. *Blood*. 1982 Aug;60(2):446–53.
39. Chang Y-C, Uchiyama S, Varki A, Nizet V. Leukocyte inflammatory responses provoked by pneumococcal sialidase. *mBio*. 2012;3(1).
40. Hirst GK. ADSORPTION OF INFLUENZA VIRUS ON CELLS OF THE RESPIRATORY TRACT. *J Exp Med*. 1943 Aug 1;78(2):99–109.
41. Hutchinson EC, Yamauchi Y. Understanding Influenza. *Methods Mol Biol Clifton NJ*. 2018;1836:1–21.
42. Krammer F, Smith GJD, Fouchier RAM, Peiris M, Kedzierska K, Doherty PC, et al. Influenza. *Nat Rev Dis Primer*. 2018 Jun 28;4(1):3.
43. McAuley JL, Gilbertson BP, Trifkovic S, Brown LE, McKimm-Breschkin JL. Influenza Virus Neuraminidase Structure and Functions. *Front Microbiol*. 2019;10:39.
44. Zanin M, Marathe B, Wong S-S, Yoon S-W, Collin E, Oshansky C, et al. Pandemic Swine H1N1 Influenza Viruses with Almost Undetectable Neuraminidase Activity Are Not Transmitted via Aerosols in Ferrets and Are Inhibited by Human Mucus but Not Swine Mucus. *J Virol*. 2015 Jun;89(11):5935–48.
45. Matrosovich MN, Matrosovich TY, Gray T, Roberts NA, Klenk H-D. Neuraminidase is important for the initiation of influenza virus infection in human airway epithelium. *J Virol*. 2004 Nov;78(22):12665–7.
46. Yang X, Steukers L, Forier K, Xiong R, Braeckmans K, Van Reeth K, et al. A beneficiary role for neuraminidase in influenza virus penetration through the respiratory mucus. *PLoS One*. 2014;9(10):e110026.
47. Vahey MD, Fletcher DA. Influenza A virus surface proteins are organized to

help penetrate host mucus. *eLife*. 2019 May 14;8.

48. Cohen M, Zhang X-Q, Senaati HP, Chen H-W, Varki NM, Schooley RT, et al. Influenza A penetrates host mucus by cleaving sialic acids with neuraminidase. *Viol J*. 2013 Nov 22;10:321.

49. Ohuchi M, Asaoka N, Sakai T, Ohuchi R. Roles of neuraminidase in the initial stage of influenza virus infection. *Microbes Infect*. 2006 Apr;8(5):1287–93.

50. Sakai T, Nishimura SI, Naito T, Saito M. Influenza A virus hemagglutinin and neuraminidase act as novel motile machinery. *Sci Rep*. 2017 Mar 27;7:45043.

51. Sakai T, Takagi H, Muraki Y, Saito M. Unique Directional Motility of Influenza C Virus Controlled by Its Filamentous Morphology and Short-Range Motions. *J Virol*. 2018 Jan 15;92(2).

52. Guo H, Rabouw H, Slomp A, Dai M, van der Vegt F, van Lent JWM, et al. Kinetic analysis of the influenza A virus HA/NA balance reveals contribution of NA to virus-receptor binding and NA-dependent rolling on receptor-containing surfaces. *PLoS Pathog*. 2018 Aug;14(8):e1007233.

53. Yang J, Liu S, Du L, Jiang S. A new role of neuraminidase (NA) in the influenza virus life cycle: implication for developing NA inhibitors with novel mechanism of action. *Rev Med Virol*. 2016 Jul;26(4):242–50.

54. Long JS, Mistry B, Haslam SM, Barclay WS. Host and viral determinants of influenza A virus species specificity. *Nat Rev Microbiol*. 2019 Jan;17(2):67–81.

55. Gamblin SJ, Vachieri SG, Xiong X, Zhang J, Martin SR, Skehel JJ. Hemagglutinin Structure and Activities. *Cold Spring Harb Perspect Med*. 2020 Jun 8;

56. Joseph U, Su YCF, Vijaykrishna D, Smith GJD. The ecology and adaptive evolution of influenza A interspecies transmission. *Influenza Other Respir Viruses*. 2017 Jan;11(1):74–84.

57. Wille M, Holmes EC. The Ecology and Evolution of Influenza Viruses. *Cold Spring Harb Perspect Med*. 2020 Jul 1;10(7).

58. Thompson AJ, Paulson JC. Adaptation of Influenza Viruses to Human Airway Receptors. *J Biol Chem*. 2020 Nov 3;

59. Wang D, Zhu W, Yang L, Shu Y. The Epidemiology, Virology, and Pathogenicity of Human Infections with Avian Influenza Viruses. *Cold Spring Harb Perspect Med*. 2020 Jan 21;

60. Byrd-Leotis L, Cummings RD, Steinhauer DA. The Interplay between the Host Receptor and Influenza Virus Hemagglutinin and Neuraminidase. *Int J Mol Sci*. 2017 Jul 17;18(7).

61. Kuchipudi SV, Nelli RK, Gontu A, Satyakumar R, Surendran Nair M, Subbiah M. Sialic Acid Receptors: The Key to Solving the Enigma of Zoonotic Virus Spillover. *Viruses*. 2021 Feb 8;13(2).

62. Fuller SD, Bravo R, Simons K. An enzymatic assay reveals that proteins destined for the apical or basolateral domains of an epithelial cell line share the same late Golgi compartments. *EMBO J*. 1985 Feb;4(2):297–307.

63. Schultz-Cherry S, Hinshaw VS. Influenza virus neuraminidase activates latent transforming growth factor beta. *J Virol*. 1996 Dec;70(12):8624–9.

64. Carlson CM, Turpin EA, Moser LA, O'Brien KB, Cline TD, Jones JC, et al. Transforming growth factor- β : activation by neuraminidase and role in highly pathogenic H5N1 influenza pathogenesis. *PLoS Pathog*. 2010 Oct 7;6(10):e1001136.
65. Gagneux P, Aebi M, Varki A. Evolution of Glycan Diversity. In: Varki A, Cummings RD, Esko JD, Stanley P, Hart GW, Aebi M, et al., editors. *Essentials of Glycobiology* [Internet]. 3rd ed. Cold Spring Harbor (NY): Cold Spring Harbor Laboratory Press; 2015 [cited 2021 Feb 9]. Available from: <http://www.ncbi.nlm.nih.gov/books/NBK453067/>
66. Kao RY, Yang D, Lau L-S, Tsui WHW, Hu L, Dai J, et al. Identification of influenza A nucleoprotein as an antiviral target. *Nat Biotechnol*. 2010 Jun;28(6):600–5.
67. Doyle TM, Jaentschke B, Van Domselaar G, Hashem AM, Farnsworth A, Forbes NE, et al. The universal epitope of influenza A viral neuraminidase fundamentally contributes to enzyme activity and viral replication. *J Biol Chem*. 2013 Jun 21;288(25):18283–9.
68. Gadjeva M. The complement system. Overview. *Methods Mol Biol Clifton NJ*. 2014;1100:1–9.
69. Rogers GN, Paulson JC. Receptor determinants of human and animal influenza virus isolates: differences in receptor specificity of the H3 hemagglutinin based on species of origin. *Virology*. 1983 Jun;127(2):361–73.
70. Yoon S-W, Webby RJ, Webster RG. Evolution and ecology of influenza A viruses. *Curr Top Microbiol Immunol*. 2014;385:359–75.
71. Wu X, Xiao L, Li L. Research progress on human infection with avian influenza H7N9. *Front Med*. 2020 Feb;14(1):8–20.
72. Zhou J, Wang D, Gao R, Zhao B, Song J, Qi X, et al. Biological features of novel avian influenza A (H7N9) virus. *Nature*. 2013 Jul 25;499(7459):500–3.
73. Bi Y, Tan S, Yang Y, Wong G, Zhao M, Zhang Q, et al. Clinical and Immunological Characteristics of Human Infections With H5N6 Avian Influenza Virus. *Clin Infect Dis Off Publ Infect Dis Soc Am*. 2019 Mar 19;68(7):1100–9.
74. Bonilla-Aldana DK, Aguirre-Florez M, Villamizar-Peña R, Gutiérrez-Ocampo E, Henao-Martínez JF, Cvetkovic-Vega A, et al. After SARS-CoV-2, will H5N6 and other influenza viruses follow the pandemic path? *Infez Med*. 2020 Dec 1;28(4):475–85.
75. Bar-On Y, Seidel E, Tsukerman P, Mandelboim M, Mandelboim O. Influenza virus uses its neuraminidase protein to evade the recognition of two activating NK cell receptors. *J Infect Dis*. 2014 Aug 1;210(3):410–8.
76. Duev-Cohen A, Bar-On Y, Glasner A, Berhani O, Ophir Y, Levi-Schaffer F, et al. The human 2B4 and NTB-A receptors bind the influenza viral hemagglutinin and co-stimulate NK cell cytotoxicity. *Oncotarget*. 2016 Mar 15;7(11):13093–105.
77. Ohkura T, Momose F, Ichikawa R, Takeuchi K, Morikawa Y. Influenza A virus hemagglutinin and neuraminidase mutually accelerate their apical targeting through clustering of lipid rafts. *J Virol*. 2014 Sep 1;88(17):10039–55.
78. Miwa T, Maldonado MA, Zhou L, Yamada K, Gilkeson GS, Eisenberg RA, et al. Decay-accelerating factor ameliorates systemic autoimmune disease in MRL/lpr mice via both complement-dependent and -independent mechanisms. *Am J Pathol*. 2007 Apr;170(4):1258–66.
79. Miwa T, Maldonado MA, Zhou L, Sun X, Luo HY, Cai D, et al. Deletion of decay-

accelerating factor (CD55) exacerbates autoimmune disease development in MRL/lpr mice. *Am J Pathol*. 2002 Sep;161(3):1077–86.

80. Soltys J, Halperin JA, Xuebin Q. DAF/CD55 and Protectin/CD59 modulate adaptive immunity and disease outcome in experimental autoimmune myasthenia gravis. *J Neuroimmunol*. 2012 Mar;244(1–2):63–9.

81. Patel MC, Shirey KA, Boukhvalova MS, Vogel SN, Blanco JCG. Serum High-Mobility-Group Box 1 as a Biomarker and a Therapeutic Target during Respiratory Virus Infections. *mBio*. 2018 Mar 13;9(2).

82. Marjuki H, Mishin VP, Chesnokov AP, De La Cruz JA, Fry AM, Villanueva J, et al. An investigational antiviral drug, DAS181, effectively inhibits replication of zoonotic influenza A virus subtype H7N9 and protects mice from lethality. *J Infect Dis*. 2014 Aug 1;210(3):435–40.

83. Hariri BM, Cohen NA. New insights into upper airway innate immunity. *Am J Rhinol Allergy*. 2016 Sep;30(5):319–23.

84. Zanin M, Baviskar P, Webster R, Webby R. The Interaction between Respiratory Pathogens and Mucus. *Cell Host Microbe*. 2016 Feb 10;19(2):159–68.

85. Durkin ME, Qian X, Popescu NC, Lowy DR. Isolation of Mouse Embryo Fibroblasts. *Bio-Protoc*. 2013 Sep 20;3(18).

86. Pinto R, Herold S, Cakarova L, Hoegner K, Lohmeyer J, Planz O, et al. Inhibition of influenza virus-induced NF-kappaB and Raf/MEK/ERK activation can reduce both virus titers and cytokine expression simultaneously in vitro and in vivo. *Antiviral Res*. 2011 Oct;92(1):45–56.

87. Kilbourne ED. Future influenza vaccines and the use of genetic recombinants. *Bull World Health Organ*. 1969;41(3):643–5.

88. Hoffmann E, Neumann G, Kawaoka Y, Hobom G, Webster RG. A DNA transfection system for generation of influenza A virus from eight plasmids. *Proc Natl Acad Sci U S A*. 2000 May 23;97(11):6108–13.

89. de Wit E, Spronken MIJ, Bestebroer TM, Rimmelzwaan GF, Osterhaus ADME, Fouchier RAM. Efficient generation and growth of influenza virus A/PR/8/34 from eight cDNA fragments. *Virus Res*. 2004 Jul;103(1–2):155–61.

90. de Wit E, Spronken MIJ, Vervaet G, Rimmelzwaan GF, Osterhaus ADME, Fouchier RAM. A reverse-genetics system for Influenza A virus using T7 RNA polymerase. *J Gen Virol*. 2007 Apr;88(Pt 4):1281–7.

91. James J, Howard W, Iqbal M, Nair VK, Barclay WS, Shelton H. Influenza A virus PB1-F2 protein prolongs viral shedding in chickens lengthening the transmission window. *J Gen Virol*. 2016 Oct;97(10):2516–27.

92. Bialy D, Shelton H. Functional neuraminidase inhibitor resistance motifs in avian influenza A(H5Nx) viruses. *Antiviral Res*. 2020 Oct;182:104886.

93. Chang P, Sealy JE, Sadeyen J-R, Bhat S, Lukosaityte D, Sun Y, et al. Immune Escape Adaptive Mutations in the H7N9 Avian Influenza Hemagglutinin Protein Increase Virus Replication Fitness and Decrease Pandemic Potential. *J Virol*. 2020 Sep 15;94(19).

94. Moskovich O, Fishelson Z. Quantification of complement C5b-9 binding to cells by flow cytometry. *Methods Mol Biol Clifton NJ*. 2014;1100:103–8.

3.8 Acknowledgements

We acknowledge Dr. Colin Adrain (IGC, Portugal), Dr. Jonathan Yewdell (NIAID, USA), Prof. Paul Digard (Roslin Institute, UK) and Dr. Ron Fouchier (Erasmus, Netherlands) for providing cells and reagents. We are grateful to the Animal House, Imaging and Flow Cytometry Facilities at the IGC for technical support, sample processing and data collection. We thank Dr. Edward Hutchinson (University of Glasgow, Scotland) and the members of CBV lab for helpful discussion. Financial support for this work was provided by Fundação Calouste Gulbenkian.

3.9 Supplementary material

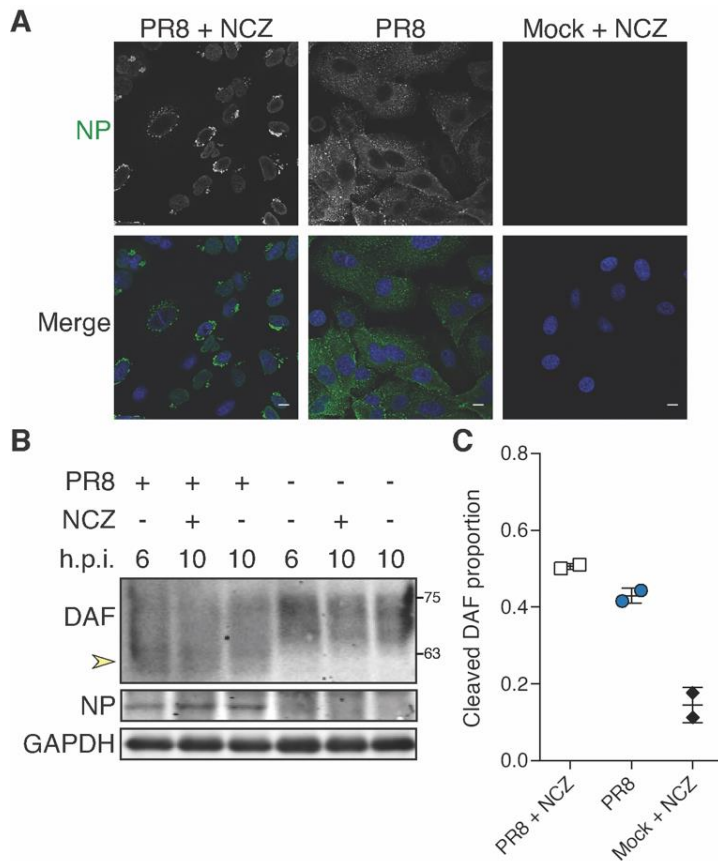


Fig. 3.S1 – vRNPs are not involved in DAF cleavage.

A549 cells were infected with A/Puerto Rico/8/34 (PR8) at a multiplicity of infection (MOI) of 3. At 6 hours post-infection (h.p.i.), 2 μ M of nucleozin (NCZ) were added to prevent viral ribonucleoprotein (vRNP) trafficking. **A:** Viral nucleoprotein (NP) detection at 10 h.p.i.. NP (green), merged with Hoechst (blue). Scale bars, 10 μ m. **B:** Western blot detection of DAF. Yellow arrows indicate cleaved DAF. MW is indicated in kDa. **D:** The proportion of cleaved DAF was measured in each lane as the ratio of low MW to total DAF pixel densitometry (data shown as mean \pm sd, from two independent experiments).

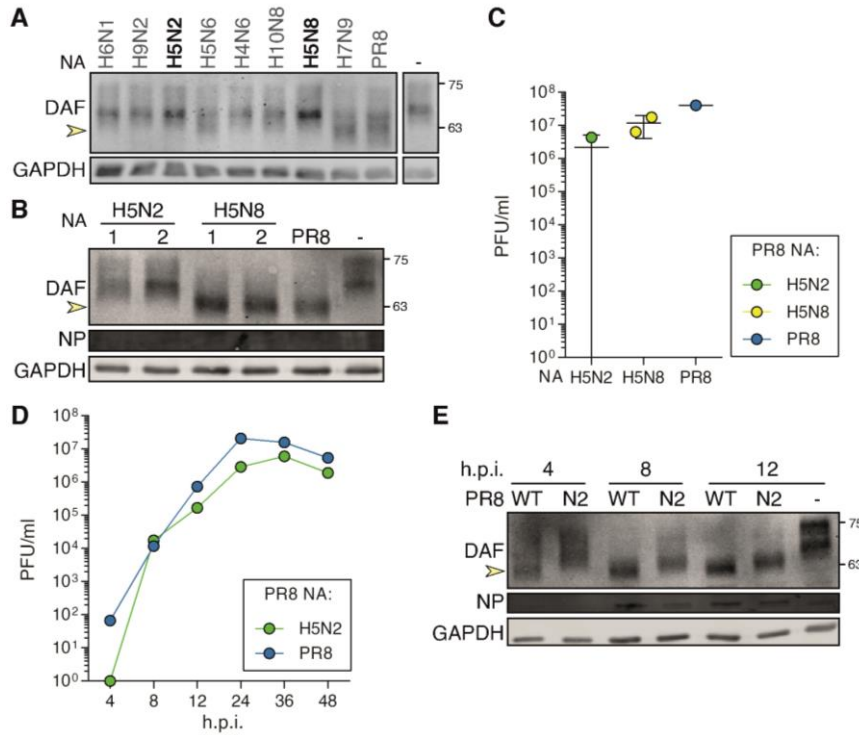


Fig. 3.S2 – Influenza A viruses with avian NA promptly adapt to cleave DAF.

A: As showed in Fig. 3.7-B, HEK293T cells were transfected with eight different avian derived NAs. **B:** To produce reverse genetics (RG) reassortant A/Puerto Rico/8/34 (PR8) viruses, HEK293T cells were transfected with seven plasmids encoding segments 1-5, 7 and 8 from PR8, and the segment 6, which encodes NA, from the indicated viruses. **C:** After one round of amplification in embryonated chicken eggs, recovered viruses were titrated. **D:** MDCK cells were infected with PR8 NA-H5N2 at a multiplicity of infection (MOI) of 0.005 and samples collected at the indicated timepoints and released virions titrated. **E:** A549 cells were infected with PR8 NA-H5N2 at an MOI of 3 and samples collected at the indicated timepoints to analyze by western blot.

Table 3.S1 – Primers used in cloning and site-directed mutagenesis.

Primer	Sequence	For	Insert	Vector	RE
NA E229A_fw	GAGGACACAAGAGTCTGCATGTGCCTGTGTAATG	SDM	NA	-	-
NA E229A_rv	CATTTACACAGGCACATGCAGACTCTTGTCCTC	SDM	NA	-	-
NA_Fw_HindIII	GCGCAAGCTTATGAATCCAAACAAAAGAT	Cloning	NA	to pEGFP-N1	HindIII
NA_Rv_KpnI_pEGFP-N1	GCGCGGTACCGTCTTGTCATGGTAAATGGC	Cloning	NA	to pEGFP-N1	KpnI
PR8_NA_NotI_fw	GCGCGCGCGCCGCATGAATCCAAATCAGAAA	Cloning	NA	from pEGFP-N1 to pLEX	NotI
GFP_XhoI_rv	TCAGCTCGAGTTACTTGTACAGCTCGTCCATGC	Cloning	GFP	from pEGFP-N1 to pLEX	XhoI

Table 3.S2 – Antibodies used in western blot.

	Target	Brand	Catalog	Clone	Host	Diluted 1:
WB - Primary antibodies						
DAF	Ms	R&D Systems	AF5376	Poly	Sh	200
DAF	Hu	Abcam	ab133684	EPR6689	Rb	2000
GAPDH	Hu/Ms	Sicgen	AB0049	Poly	Gt	2000
β-actin	Hu	Sigma-Aldrich	A5441	AC-15	Ms	2000
GFP	-	Sicgen	AB0020	Poly	Gt	2000
M1	IAV	Abcam	ab20910	Poly	Gt	500
NA	IAV	R&D Systems	AF4858	Poly	Sh	500
NP	IAV	Homemade*	-	Poly	Rb	2000
NS1	IAV	Homemade*	-	Poly	Rb	500
PA	IAV	Homemade*	-	Poly	Rb	1000
PB1	IAV	Homemade*	-	Poly	Rb	500
PB2	IAV	Homemade*	-	Poly	Rb	200
WB - Secondary antibodies						
Goat IRDye 680RD	Gt	LI-COR Biosciences	926-68074	-	Dk	10.000
Goat IRDye 800CW	Gt	LI-COR Biosciences	926-32214	-	Dk	10.000
Mouse IRDye 680RD	Ms	LI-COR Biosciences	926-68072	-	Dk	10.000
Mouse IRDye 800CW	Ms	LI-COR Biosciences	926-32212	-	Dk	10.000
Rabbit IRDye 800CW	Rb	LI-COR Biosciences	926-32213	-	Dk	10.000
Rabbit IRDye 680RD	Rb	LI-COR Biosciences	926-68073	-	Dk	10.000
Sheep Dylight™ 800	Sh	Rockland	613-445-002	-	Rb	10.000

*hybridomas and homemade antibodies were provided by Dr. Jonathan Yewdell and Prof. Paul Digard, respectively

**Chapter 4 – Mutation S110L of H1N1 influenza A virus
hemagglutinin: a potent determinant of attenuation**

4.1 Author contributions

This chapter includes part of the published manuscript Nieto A, Vasilijevic J, Santos NB, Zamarreño N, López P, Amorim MJ, Falcon A. Mutation S110L of H1N1 Influenza Virus Hemagglutinin: A Potent Determinant of Attenuation in the Mouse Model. *Front Immunol.* **2019**;10:132. doi: 10.3389/fimmu.2019.00132.

Amelia Nieto designed the research studies, conducted databases research and wrote the manuscript. Jasmina Vasilijevic designed the research studies, analyzed the data, and conducted experiments. Nuno B Santos designed the research studies, analyzed the data and conducted experiments. Noelia Zamarreño and Pablo López conducted experiments. Maria João Amorim designed the research studies, analyzed the data and wrote the manuscript. Ana Falcon designed the research studies, conducted the experiments, analyzed the data and wrote the manuscript.

4.2 Summary

In 2009, a new pandemic influenza A virus (IAV) emerged. While the majority of infected people only displayed mild symptoms, numerous individuals suffered severe infection, which suggested the existence of viral strains with increased virulence.

Characterization of a virus isolated from a fatal infection (F-IAV) revealed three mutations when compared to a virus isolated from a mild patient (PB2 A221T, PA D529N and HA S110L), which could potentially determine the higher virulence of this strain. Previous work showed that both polymerase mutations inserted in A/California/04/09 (CAL) backbone increased pathogenicity, but the contribution of the HA mutation remained to be elucidated.

Here, we have evaluated the contribution of HA S110L to F-IAV pathogenicity, through introduction of this point mutation in CAL virus (HA mut). When compared with the WT protein, HA S110L protein had similar pH stability, comparable mobility, and entry properties. However, characterization of the lungs of HA mut infected animals showed reduced lung damage. Accordingly, lower virus replication, decreased presence in bronchioli and parenchyma, and diminished numbers of infected leukocytes and epithelial cells were found in the lungs of HA mut-infected animals. Our results indicate that HA S110L mutation constitutes a determinant of attenuation, and suggest that its interaction with components of the respiratory tract, such as mucus and lectins, may prevent the infection of the target cells, thus compromising the infection outcome. As a consequence, viruses containing HA S110L alone or in combination with polymerase mutations were considerably attenuated in infected mice, elucidating the potential of HA in modulating pathology.

4.3 Introduction

In the previous chapters, we focused on the contribution of a host factor to viral-induced disease regulated by the viral proteins HA and NA, in a mechanism that prevented immunopathology, but did not alter viral loads. In this chapter, we explore an alternative mechanism, based on the impact of a mutation in a viral protein that limits viral pathogenesis by reducing viral burden in the lungs.

Influenza A virus (IAV) recurrently provokes pandemic outbreaks, associated with zoonotic events, which lead to significant higher mortality than seasonal epidemics (1). The 1918 Spanish influenza, for example, caused up to 50 million deaths, making it the deadliest viral outbreak ever recorded (2,3). Severe infections may result in hemorrhagic bronchitis, pneumonia (primary viral or secondary bacterial), and death (4–7). Remarkably, complications usually derive from an exacerbated immune response leading to tissue damage (8,9).

In 2009, a novel reassortant H1N1 influenza A virus, composed of segments from avian, human, and swine origin, was responsible for the first pandemic of the twenty-first century (10–12). Despite resulting mainly in mild infections, there was a considerable number of occurrences of severe disease amongst previously healthy patients, which suggested the possibility of co-circulation of strains with higher virulence (13). Indeed, *in vitro* and *in vivo* characterization of a viral isolate derived from a fatal infection (F-IAV) confirmed this proposition, as it exhibited superior pathogenicity when compared to an isolate from a patient who suffered mild infection (M-IAV) (13). Remarkably, the F-IAV presented three amino acids alterations, which could be accountable for its higher virulence (13). Two of the mutations were mapped to the viral polymerase subunits PB2 (PB2 A221T) and PA (PA D529N), and one to the hemagglutinin (HA) protein (S110L, considering HA1 sequence without the signal peptide) (13). Interestingly, the

mutation S110L corresponds to a region in the globular head of HA that has not been previously linked to any functional implications (Fig. 4.1-A) (14).

To analyze the contribution of each mutation to the F-IAV phenotype, these were individually introduced in the backbone of the A/California/04/09 (CAL) using reverse genetics (15). Subsequently, a comprehensive characterization addressing the influence of polymerase mutations on the augmented virulence of the F-IAV virus revealed that PA D529N had the most pronounced impact in its higher pathogenicity, by decreasing the extent of defective viral genomes (16). However, the role of the mutation HA S110L remained to be elucidated.

As introduced in the previous chapters, HA has a critical role in IAV replication in the host. Not only the receptor binding specificity of the HA is one of the key factors in viral host tropism, virulence and transmission (17,18), but also HA is the most immunogenic viral protein (19,20). For viral entry, HA attaches to sialic acids residues conjugated to galactose on glycoproteins exposed at host cell surface (18). However, HA is synthesized as a precursor that forms non-covalent associated homotrimers (HA0) upon removal of the signal peptide (18). Activation of HA fusion ability, and therefore viral infectivity, requires proteolytic cleavage of each HA0 monomer in the disulfide-linked subunits, originating HA1 and HA2 (21,22). After being internalized, IAV progresses through the endosomal network, where it is subjected to pH reduction (23). This endosomal acidification induces conformational changes in HA that expose its fusion peptide and trigger the fusion of viral and endosomal membranes (24–27).

Accordingly, mutations in HA would be expected to impact the outcome of the disease, by impacting viral entry and/or recognition by the host immune system. In fact, A/California/04/09 bearing the HA S110L mutation (HA mut) was more efficiently neutralized by monoclonal and polyclonal antibodies against the WT virus, suggesting

it could be more efficiently recognized by the immune system (Fig. 4.1-B-C). However, HA S110L did not impact HA glycosylation levels (Fig. 4.2-C) nor acid stability (Fig. 4.2-D), indicating that this mutation does not affect HA function.

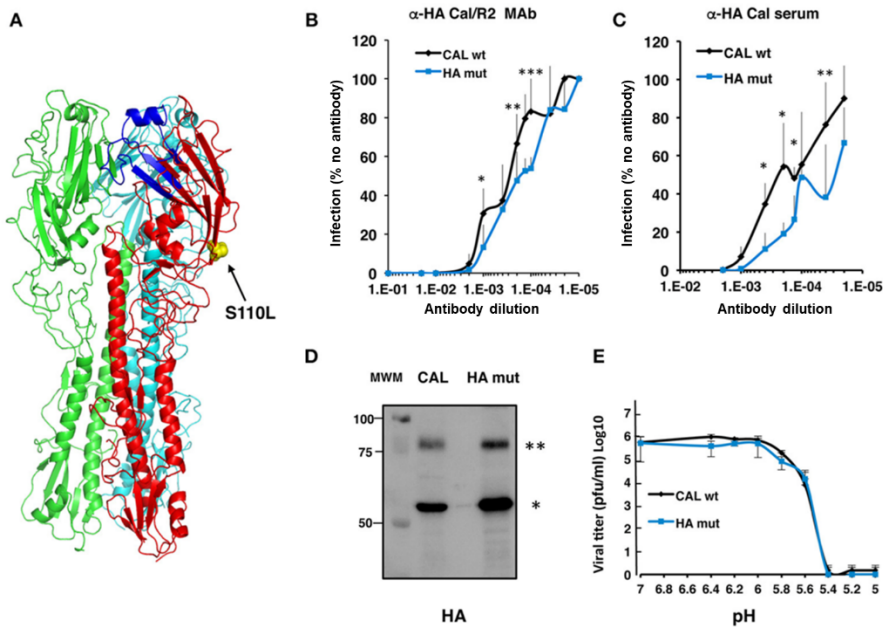


Fig. 4.1 – HA S110L mutation increases neutralization, but does not affect glycosylation and acid stability (14).

A: Representation of HA S110L mutation in HA structure and impact in antibody recognition. **B, C:** A/California/04/09 WT (CAL wt) or HA S110L (HA mut) were preincubated with monoclonal antibody α -HA/Cal/2 (**B**) or polyclonal antibody raised against HA from A/California/07/09 (**C**) and then infection capability was measured in MDCK cells (data shown as mean \pm sd, from two independent experiments using six viral doses; * $p < 0.05$; ** $p < 0.01$; *** $p < 0.001$). **D:** Western blot detection of HA using α -HA/Cal/2 monoclonal antibody. (**) denotes HA0, and (*) HA1. **E:** CAL and HA mut viruses were incubated at the indicated pHs for 15 minutes and then replication capability was measured in MDCK cells data shown as mean \pm sd, from triplicates).

HA is a crucial player in viral tropism due to its receptor binding preference. Nevertheless, HA mut retained the ability to enter human and murine cell lines, as this virus was affected by chloroquine, which inhibits IAV endocytosis, similarly to CAL (Fig. 4.2-A, B). Moreover, the ability to efficiently undergo successive cycles of replication in a human cell line was preserved (Fig. 4.2-C).

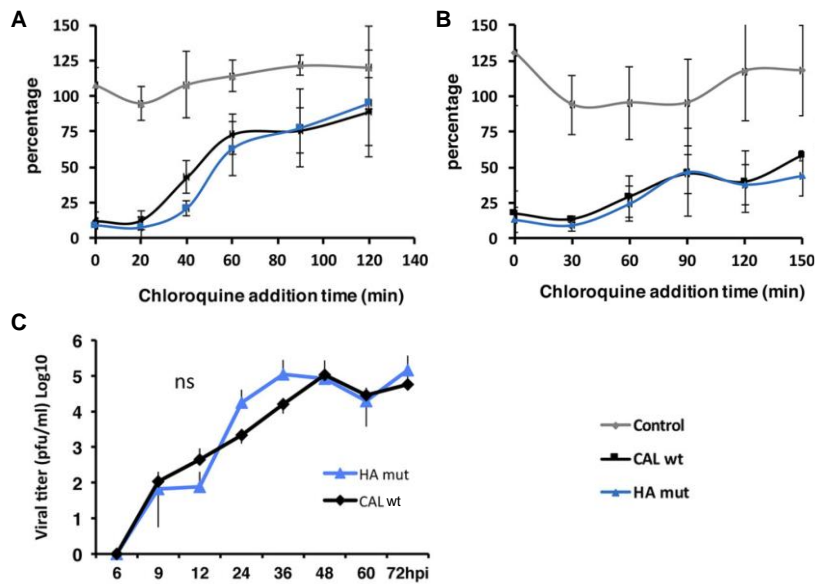


Fig. 4.2 – HA S110L mutation does not affect cell entry nor replication (adapted from (14)).

A, B: A/California/04/09 WT (CAL wt) or HA S110L (HA mut) entry in A549 (**A**) or NIH3T3 (**B**) cells. Cells were infected at a multiplicity of infection (MOI) of 3 and treated with 75 or 25 μ M chloroquine, respectively, added at the indicated times, for 2 hours. Chloroquine was then removed, and cells collected at 8 hours post-infection (h.p.i.). Results are shown as percentage of NP in relation to GAPDH accumulation, measured by western blot. **C:** A549 cells were infected at a MOI of 0.001, and released virions were titrated at the indicated time points.

Remarkably, HA S110L mutation elicited a significant attenuation *in vivo*, even in combination with the other pathogenic mutations found

in the viral polymerase subunits of the F-IAV (Fig. 4.3-A). Additionally, when compared to CAL, HA mut replicated to a lower extent in murine lungs (Fig. 4.3-B).

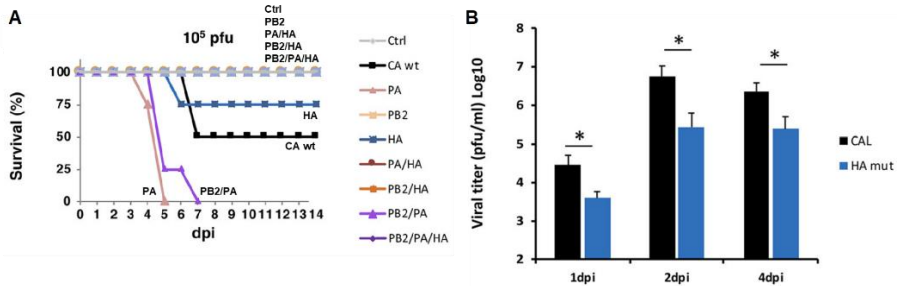


Fig. 4.3 – HA S110L confers protection from infection *in vivo* (adapted from (14)).

A: BALB/c mice were infected with 10^5 PFU of the indicated viruses, and survival measured in the course of infection. **B:** at the indicated time points, lungs were collected to measure viral loads. * $p < 0.05$.

The detailed mechanism of attenuation of HA S110L remained to be elucidated. In this work, we have explored the attenuation triggered by HA S110L, despite the increased pathogenicity of the F-IAV. We observed that HA S110L limits viral presence in bronchioli and parenchyma, as well as decreases levels of infection in lung leukocytes and epithelial cells. Therefore, we describe a mechanism of pathology modulated by viral HA, associated with a decrease in viral loads.

4.4 Results

4.4.1 HA S110L induces lower lung histological damage than CAL

Despite being identified in a fatal case of IAV infection (F-IAV), the mutation HA S110L was shown to cause a reduction on virus pathogenicity (14). This discrepancy could not be explained by differences in protein glycosylation, cell entry or viral replication *in vitro* (14). Therefore, we aimed to explore possible reasons that could explain this phenotype *in vivo*.

HA S110L virus replicated to lower viral titers in the lungs of infected mice when compared with CAL (Fig. 4.3-B). (14). To address if decreased viral loads were associated with decreased tissue damage, we infected BALB/c mice with a sublethal dose of CAL or HA S110L, and collected samples at 1, 2 and 3 days post-infection (d.p.i.) for further analyses. We started by assessing the tissue damage in histological preparations of lungs of CAL- and HA S110L-infected mice (Fig. 4.4-A, B). The overall lung histological score for each virus is depicted in Fig. 4.4-C, represented as the sum of the different assessed parameters (Fig. 4.4-D-G; 4.S1-A-I).

Accordingly, at 2 d.p.i., which corresponds to the peak of viral replication (Fig. 4.3-B) (14), HA S110L virus presented significantly lower histological damage (Fig. 4.4-C). Specifically, peribronchial infiltration (2 d.p.i.) and bronchial exudates (3 d.p.i.) were decreased in the lungs of HA S110L-infected mice (Fig. 4.4-D, E). Additionally, at 2 d.p.i., edema was observed in CAL-infected mice and absent upon HA S110L infection (Fig. 4.4-F). These results indicate that decreased viral loads are associated with lower lung tissue damage, and thus support the attenuation observed with the HA S110L mutation.

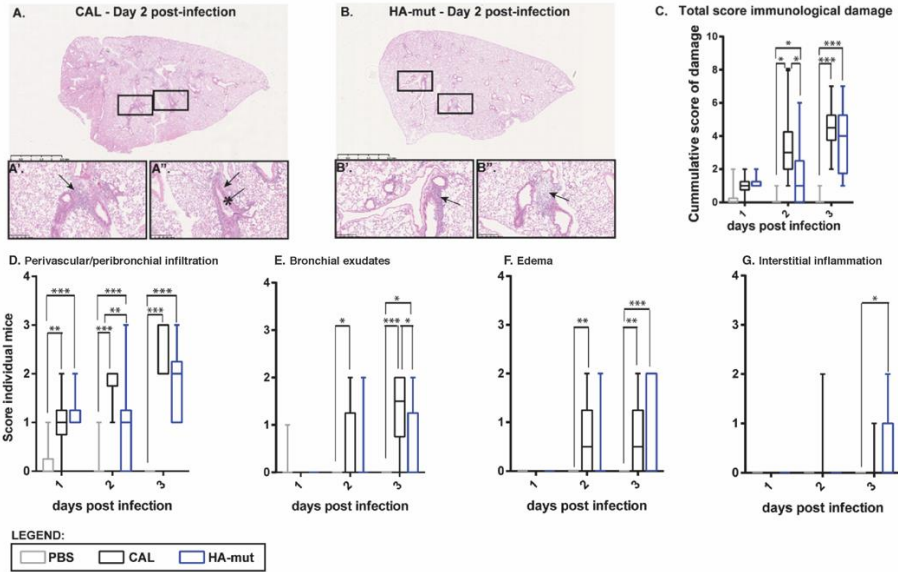


Fig. 4.4 – HA S110L mutation decreases lung histological damage (adapted from (14)).

Five BALB/c female mice per condition were infected with 1000 PFU of A/California/04/09 WT (CAL) or HA S110L (HA mut). At 1, 2, and 3 days post-infection (d.p.i.) lungs were collected. **A, B:** representative lung histological analyses, after hematoxylin and eosin (H&E) staining. Lungs at 1.25x amplification at 2 d.p.i., where higher differences were detected. Inlets are areas 10x amplified where specific damage (or its absence) is observed. (→ Perivascular/peribronchial infiltrates; →* Bronchial exudates). **C:** Total score immunological is expressed as the sum of the scores for each parameter detailed in **D-G:** different inflammation and damage parameters were graded on a scale 0–4 (0, absent; 1, very mild; 2, mild; 3, moderate; and 4, severe). (plotted as box and whiskers from min to max with the line representing the median). Statistical analyses were done using two-way ANOVA and are indicated as * $p < 0.05$; ** $p < 0.01$, *** $p < 0.001$ where significant differences were found. The experiment was performed twice. Representative histological images are in Fig. 4.S1.

In vitro results suggested that HA S110L did not impact viral replication, however *in vivo* infection showed otherwise (Fig. 4.2-C; 4.3-B). Therefore, the difference in viral loads should not be caused by limitations in cell entry process *per se*, instead it suggests distinctive interactions with the different cell types within the lung tissue. To address this hypothesis, we performed immunohistochemical (IHC) analyses to detect the presence of viruses in different airway structures. Bronchioli are some of the smallest airways in the respiratory tract, and lead directly to the alveolar canals, which contain the alveoli, where gas exchange with the blood occurs (28). Lung parenchyma encompasses a large number of thin-walled alveoli, which support efficient gas exchange (28). Therefore, these structures will be exposed to an inhaled pathogen, such as IAV.

Detection of the viral nucleoprotein (NP) in lung sections of infected mice was used to assess viral localization in bronchioli and lung parenchyma (Fig. 4.5-A, B; 4.S2-A-I). Overall, the cumulative NP score, resulting of the parameters analyzed in Fig. 4.5-D-F, showed a significant reduction of HA S110L presence in the lungs of infected animals at 2 d.p.i. (Fig. 4.5-C), which is in agreement with the decreased viral loads (Fig. 4.3-B). In detail, at 1 and 2 d.p.i., HA S110L-infected mice showed a decreased number of infected bronchioli when compared with CAL-infected mice (Fig. 4.5-D). Of note, the percentage of infection within each bronchioli did not differ between HA S110L- and CAL-infected mice (Fig. 4.5-E). In addition, despite the absence of significant differences in viral presence in lung parenchyma between HA S110L and CAL, significant infected parenchyma was found in CAL-infected mice when compared with mock-infected animals, but not in HA S110L-infected mice (Fig. 4.5-F). Remarkably, the observed differences upon HA S110L infection as early as 1 d.p.i. suggest this mutation prevents the virus to reach the lungs at higher levels.

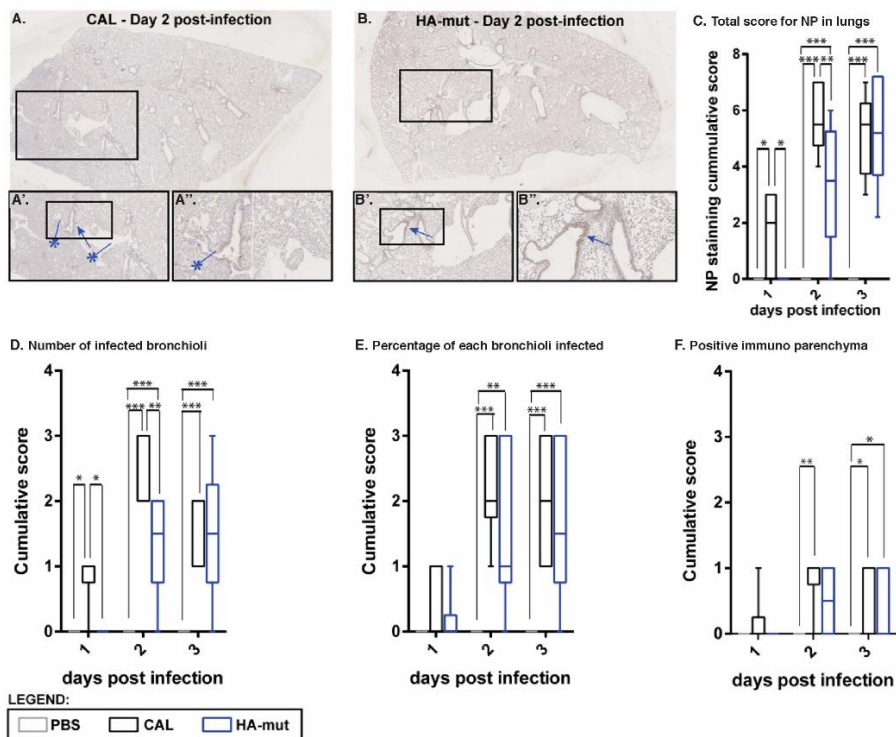


Fig. 4.5 – HA S110L mutation decreases NP expression in the airways (14).

Five BALB/c female mice per condition were infected with 1000 PFU of A/California/04/09 WT (CAL) or HA S110L (HA mut). At 1, 2, and 3 days post-infection (d.p.i.), lungs were collected and lung sections were processed for NP staining. **A, B:** representative lung immunohistochemical (IHC) analysis. Lungs at 1.25x amplification at 2 d.p.i.. Inlets are areas 5–20x amplified where staining (or its absence) is observed. Perivascular/peribronchial infected areas; parenchyma areas infected). **C:** NP expression in lungs was scored for all parameters detailed in **D-F:** NP expression in lungs was scored for the number and areas of infected bronchioli as follows: 1, 0–25% infected cells; 2, 25–50% infected cells; 3, 50–75% infected cells; 4, 75–100% infected cells. NP expression was also scored as present/absent, infection foci on alveoli were scored 0 when absent or 1 if present (plotted as a box and whiskers from min to max with the line representing the median). Statistical analyses were done using two-way ANOVA and are indicated as * $p < 0.05$; ** $p < 0.01$, *** $p < 0.001$ where

significant differences were found. The experiment was performed twice. Representative IHC images are in Fig. 4.S2.

4.4.2 HA mut infection affects a lower proportion of lung epithelial cells and leukocytes.

Virus-induced pathology depends on viral and host factors, as well as an adequate immune response (9,29). Previous results showed increased tissue damage inflicted by CAL infection, when compared with HA S110L. As leukocytes are the cells surveilling the lungs for pathogen detection to trigger the immune response, we assessed their levels, and their infection permission upon challenge with CAL or HA S110L. Particularly, we monitored by flow cytometry the infection of lung leukocytes, as well as epithelial cells, at 1, 2 and 3 d.p.i.. Lung cell suspensions were stained with antibodies to recognize the viral protein NP, epithelial cellular adhesion molecule (EpCAM) and the leukocyte marker CD45 (Fig. 4.6-A-D).

In accord with decreased viral loads (Fig. 4.3-B), the proportion of total infected cells was significant decreased upon HA mut infection in all tested d.p.i. (Fig. 4.6-E). Remarkably, that decrease corresponded to a reduced percentage of infected epithelial cells (Fig. 4.6-F), as well as leukocytes (Fig. 4.6-G). However, global leukocyte recruitment was not altered upon HA S110L infection, when compared with CAL (Fig. 4.6-H).

Additionally, analysis of neutrophils and alveolar macrophages (AMs) revealed distinct patterns: while HA S110L elicited a trend of decreased neutrophil recruitment upon infection, there was apparently higher presence of AMs (14). Although not statistically significant, these differences agree with the observed increase in infected leukocytes upon CAL infection, which are very likely eliminated at 2 and 3 d.p.i.. Importantly, lower neutrophil infiltration and increased AM presence, partially observed upon HA S110L infection, have been described as

important factors for attenuated IAV infections (30,31), which is in agreement with the observed role of HA S110L.

Taken together, these results indicated that the attenuated phenotype of the recombinant HA S110L virus results from a lower infection of the target cells in the mice airways, despite its unaltered ability to efficiently replicate and enter in cultured cells.

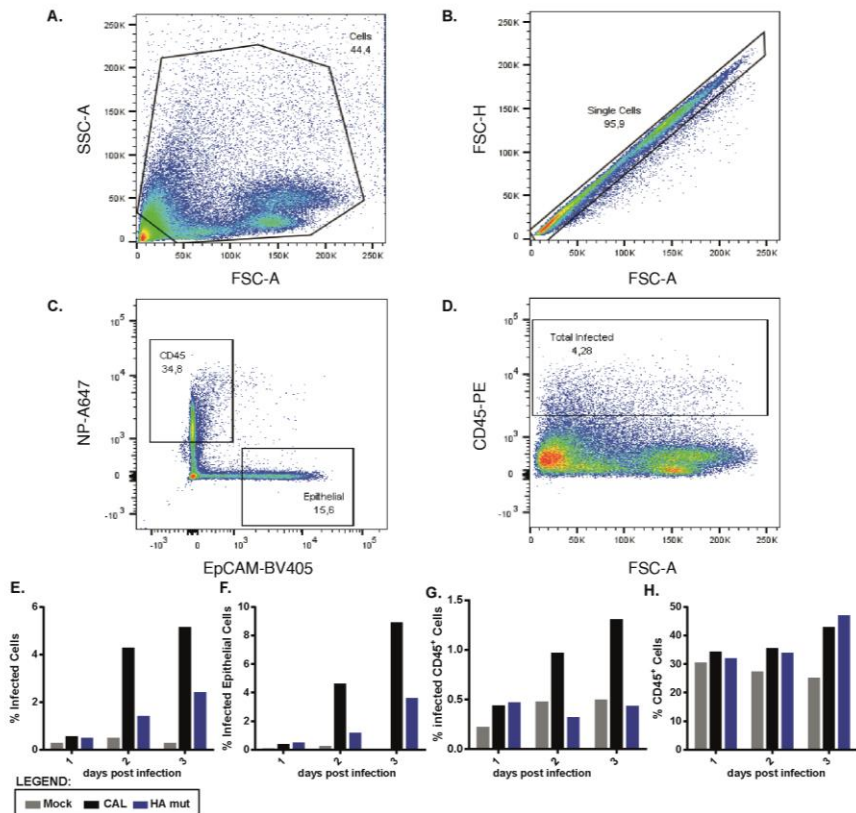


Fig. 4.6 – Lung cells are differentially infected by CAL and HA mut viruses (adapted from (14)).

Five BALB/c female mice per condition were infected with 1000 PFU of A/California/04/09 WT (CAL) or HA S110L (HA mut). At 1, 2, and 3 days post-infection (d.p.i.) lungs were collected, and processed for flow cytometry. Lungs from the same condition were pooled. Single cell suspensions were stained with antibodies against NP, EpCAM and CD45, to detect infected

cells, epithelial cells and leukocytes, respectively. **A-D**: representative flow cytometry plots showing gating strategy. **E**: percentage of infected cells in relation to total cells. **F**: percentage of infected cells in relation to the total number of epithelial cells. **G**: percentage of infected cells in relation to the total number of CD45 leukocytes. **H**: percentage of CD45 leukocytes in relation to total cells. The experiment was performed twice. Flow cytometry data was acquired with the help of Dr. Vera Martins (IGC, Portugal).

4.5 Discussion

Throughout the 2009 IAV pandemic, there were reports of viral isolates with exacerbated pathogenicity, such as the one that was isolated from a fatal infection case (F-IAV). The isolated virus contained three point mutations: PA D529N, PB2 A221T and HA S110L (13). Interestingly, individual characterization of these mutations defined PB2 A221T as a determinant of attenuation, conversely to PA D529N, which was an extremely high pathogenicity determinant (16). In this study we have addressed the potential contribution of HA S110L mutation to the higher pathogenicity of F-IAV virus. Remarkably, we observed that this HA mutation is a strong attenuation determinant.

Viral attenuation deserves substantial attention, as the mechanisms governing it may include distinct stages in the viral replication cycle, as well as interactions with the host defenses. Moreover, the most effective available viral vaccines are based on live attenuated viruses (19,32). Particularly, mechanisms of attenuation involving the viral protein HA are of unique interest, as it is the principal antigen displayed to the host immune system (19,20), and HA has been reported as a critical element in IAV virulence (18,33). Thus, using engineered viruses to explore attenuation from a genetic level provided the identification of a new determinant of attenuation in HA.

In the beginning of the viral replication cycle, HA is involved in the attachment to sialylated receptors, which in turn triggers cell entry (18,34). Therefore, HA properties define which cells could be infected, depending on receptor binding ability, previous activation through cleavage by host proteases and glycosylation (18,22,35). However, the mutation HA S110L was not shown to affect these properties (14). Subsequently, when the virus is internalized in the endosome it undergoes a pH drop, which provokes a conformational change in HA protein, exposing its fusion peptide, which then fuses the viral and

endosome membranes to release the viral genomic material into the cytoplasm (18,36,37). Nevertheless, HA S110L did not alter HA acidic stability, indicating this mutation does impact the ability of the virus to enter the cell (14).

IAV low fidelity polymerase promotes amino acid variation, that could be selected for immune evasion in a process named antigenic drift (34,38). Consequently, this poses a fundamental challenge to long-lasting immunity and vaccine strategies. HA S110L localizes to the exposed globular head of the protein (Fig. 4.1-A), which suggests it could alter its structure, and consequently its antigenicity. Interestingly, inhibition by monoclonal and polyclonal antibodies against the HA protein of A/California/07/09 was increased in the HA S110L virus, proposing it could be more efficiently targeted by the immune system *in vivo* (Fig. 4.1-B, C) (14). Hence, improved immune detection may explain the attenuation by preventing the HA S110L virus from reaching the lungs in higher numbers and/or by limiting initial viral replication.

Remarkably, mice infection clearly showed that HA S110L confers attenuation. Infection with 10^6 PFU of CAL virus resulted in 100% lethality, while all mice survived to the same dose of HA S110L virus (14). Furthermore, HA S110L combined with PB2 A221T and PA D529N, individually or together, elicited attenuation (14), revealing the potential of this mutation in modulating IAV virulence. This observation was unexpected, since these three mutations were proposed to be responsible for the increased virulence of the F-IAV when compared with the M-IAV. However, this could be explained by the differences between humans and the mouse model.

In agreement with the attenuated phenotype of HA S110L, histological analysis of infected mice showed decreased lung tissue damage and inflammation in the HA S110L- when compared with CAL-infected mice (Fig. 4.4-C). This reduction in lung damage appears to be caused by the a lower capacity of HA S110L virus to reach the bronchioli

and lung parenchyma (Fig. 4.5-D-F), and accordingly, it revealed an overall reduction on viral replication in the lungs, when compared with CAL (14). Lastly, this limited replication of the HA S110L virus in the lungs was also reflected in the infection of leukocytes, which was also decreased (Fig. 4.6-A-C). Taken together, *in vivo* data indicated that the mutation HA S110L modifies HA protein, probably inducing a conformational change, reducing its capability to reach the target cells in the murine airways. Therefore, it suggests that the attenuation mechanism might be related with viral ability to reach the lungs.

Host-pathogen co-evolution selects strategies of defense and invasion, respectively. When IAV reaches the airways, it encounters the mucus barrier, a biophysical barrier composed of mucins, highly sialylated proteins that trap the incoming virions by binding to HA (39,40). This defense mechanism, in turn, is countered by viral neuraminidase (NA), which cleaves sialic acid residues and allows the incoming virions to penetrate through the mucus barrier and reach the epithelium (41–43). As CAL and HA S110L viruses did not evidence disparities in viral entry (Fig. 4.2-A, B), it suggests that HA S110L did not alter sialic acid preference. Nevertheless, as the CAL and HA S110L viruses contain the same NA protein, different HA ability to bind mucins could result in different efficiency to reach the epithelial surface.

Other host factors may impact the success of a virus to penetrate the airway epithelium, and thus contribute to the attenuation of HA S110L. Building evidence suggests that HA glycosylation, and thus how HA is detected by lectins, is important upon IAV infection. Specifically, it has been reported that HA glycans are bound by surfactant protein D (SP-D) in airway secretions (44–46) and to mannose-binding lectin (MBL) present in serum (47). Then, SP-D and MBL neutralize IAV through diverse mechanisms, such as hindrance of the HA receptor-binding site, viral aggregation and modulation of complement-dependent pathways (48,49). Besides the mucus layer, mucosal

epithelium also contains immunoglobulins, such as IgA, able to confer innate protection by neutralizing IAV at cell surface (50,51). As HA is a viral surface protein and is exposed to numerous components of the respiratory tract, it is plausible that subtle alterations in its conformation, such as HA S110L, might affect the interaction with these host defense mechanisms. Infections of IgA deficient mice, for example, could be useful to clarify the role of this immunoglobulin.

HA has a well-documented role in viral tropism, based on its receptor preference, protease sensitivity and glycosylation (18,22,33,35,52). HA S110L virus infects and spreads less in the murine lungs, which could immediately indicate impaired penetration in the respiratory tract. Alternatively, it could also be a downstream consequence of attenuation. Remarkably, it has been suggested that IAV could infect different cell types, including immune cells, in a strain-specific manner, with opposing effects in their survival (53–55). These differences could then influence the immune response, and thus future experiments should address if CAL and HA S110L infect distinctive cell populations within the airways.

Furthermore, HA has also been linked to cell autonomous response. Precisely, stress pathways in the ER sense viral proteins and trigger innate immunity pathways (56). Additionally, ER stress may induce the unfolded protein response (UPR), increasing the presence of high-mannose at cell surface, which in turn activates the complement pathway and aggravates disease pathology (57).

Taken together, our data suggest that HA S110L attenuation depends on mechanisms related with viral tropism and/or recognition by the host innate immune sensors. Then, disparities, even if not pronounced, in the number of virions that reach the airways epithelium and establish infection may strongly condition the extent of the disease, penetration of the virus in the respiratory tract and eventually define its ultimate outcome (Fig. 4.7).

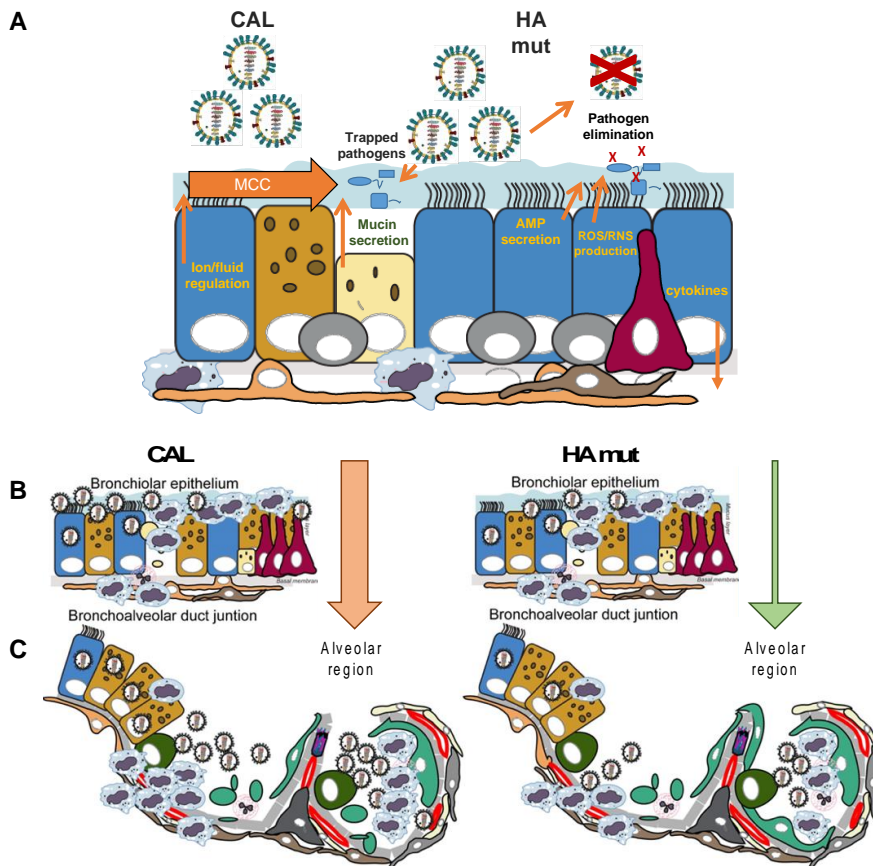


Fig. 4.7 – Proposed model for HA mut attenuation (adapted from MJ Amorim).

A: Despite invading with the same initial dose, Ha mut is more inactivated

on its way through the airways by host innate defense mechanisms such as lectins, IgA and mucins in the mucus barrier. **B, C:** Therefore, it reaches the bronchioli (**B**) and alveoli (**C**) in reduced numbers, replicating to a lower extent. This will finally result in less immune cell recruitment, and decreased lung tissue damage and inflammation, inducing a less severe pathology than CAL.

4.6 Materials and methods

4.6.1 Statistical analyses

All statistical analyses were conducted using GraphPad Prism 6. Detailed statistics and number of replicates for all experiments can be found in the figure legends and/or in the main text.

4.6.2 Ethics statement

All animals were housed at IGC facilities under specific pathogen free conditions and fed *ad libitum*. Experimental animal procedures were previously approved by the IGC Animal Ethics Committee and licensed by the Portuguese General Directory of Veterinary (DGAV, Ministry of Agriculture, Rural Development and Fishing), with reference A016/2013. All animals were housed and handled according with good animal practice as defined by national authorities (DGAV, Law n^o1005/92 from 23rd October) and European legislation EEC/86/609. BALB/c mice were provided by the IGC animal facility.

4.6.3 Mice infection

All experiments with animals were performed at IGC biosafety level 2 (BSL-2) animal facility. Under light anesthesia with isoflurane, 6-9 weeks old female mice were intranasally infected with a solution of 30µl of PBS containing the indicated viral doses. Mice were sacrificed via CO₂ inhalation at the indicated timepoints for further analysis.

4.6.4 Histology

Left lung lobes were collected and fixed in 10% buffered formalin for 48h, then embedded in paraffin, divided into longitudinal sections (3µm thick) and stained with hematoxylin and eosin. To score lung inflammation and damage, lung samples were screened for the following parameters: interstitial (alveolar septa) inflammation, alveolar

inflammation, perivascular/peribronchial inflammation, bronchial exudates, bronchial epithelium hyperplasia, and edema. Each parameter was graded on a scale of 0–4 being 0, absent; 1, very mild; 2, mild; 3, moderate; and 4, severe. The total lung inflammation score was expressed as the sum of the scores for each parameter. Histological scoring was performed blindly by a pathologist.

4.6.5 Immunohistochemistry

The previously described formalin-fixed, paraffin-embedded tissue specimens were divided into tissue sections (3 μ m thick) and processed for immunohistochemical analysis. After deparaffinization of tissue, slides were incubated in sodium citrate buffer, pH 6 at 95 $^{\circ}$ C for 20 min. Sections were permeabilized with PBS supplemented with 0.1% triton X- 100 for 7min, at room temperature and blocked with 2.5% BSA and Fc-block (purified rat anti-mouse CD16/CD32, IGC antibody facility, clone 2.4G2). Infected cells were discriminated by the presence of the viral nucleoprotein (NP) with rabbit α -NP (58) diluted 1:1000 for 16h, at 4 $^{\circ}$ C. Endogenous peroxidases were quenched by treating tissue sections with 3% H₂O₂ for 15min, at room temperature. NP positive cells were detected with ImmPRESS HRP Anti-Rabbit IgG (Vector, MP-7401-15), followed by color developing with diaminobenzidine (DAB) substrate (Roche, 11718096001), both according to manufacturer's instructions. Sections were counterstained with Mayer Hematoxylin before analysis. Tissue sections were observed using a Leica DMLB2 microscope (Leica) and images were captured using NanoZoomer-SQ Digital slide scanner (Hamamatsu). NP expression around bronchioli was scored as: 1, 0–25% infected cells; 2, 25–50% infected cells; 3, 50–75% infected cells; 4, 75–100% infected cells. NP expression was also scored as present/absent infection foci on alveoli. Histological scoring was performed blindly by a pathologist.

4.6.6 Flow cytometry

Mice lungs were collected to 1ml FC buffer (PBS supplemented with 2% FBS and 0.1% NaN₃), minced with a scalpel, incubated with 0.5mg/ml Collagenase D (Roche, 1108885801), 50U/ml DNase I (Zymo Research, E1010) in PBS for 1h, 37°C, passed through a 100µm cell strainer (Falcon, 352360), centrifuged at 666g, 5min, 4°C. The pellet was treated with ACK buffer for 4min, at RT. After this incubation, the lung cell suspension was centrifuged and then resuspended in FC buffer. Cells were counted in each condition and 10⁶ cells transferred to a V-bottom 96 well plate (Thermo Scientific, 249570). Unspecific staining was minimized with Fc-Blocking (purified rat anti-mouse CD16/CD32, IGC antibody facility, clone 2.4G2) for 15 min, at 4°C. Surface staining was performed with α-EpCAM-BV421 (BioLegend, clone G8.8) and α-CD45.2-PE (IGC antibody facility, clone 104.2) diluted 1:100 for 30min, at 4°C, in the dark. Cells were fixed with IC fixation buffer (Thermo Fisher, 00-8222-49) according to manufacturer's instructions. Fixed cells were washed with permeabilization buffer (0.1% triton X-100 in PBS) and intracellular viral nucleoprotein (NP) detected with rabbit α-NP (58) diluted 1:100 in the same buffer, for 30min, at 4°C in the dark. Secondary staining was performed with a chicken α-rabbit IgG conjugated with Alexa Fluor 647 (Life Technologies, A-21443) diluted 1:1000 in permeabilization buffer for 30min, at 4°C in the dark. Cells were acquired in a BD LSRFortessa™ X-20 (BD Biosciences) analyzer, equipped with BD FACSDiva™ 8 acquisition software (BD Biosciences). Populations were gated using fluorescence minus one (FMO) controls and results analyzed using FlowJo 10 (BD Biosciences, version v10.6.2).

4.6.7 Influenza A virus strains

Generation of recombinant HA Mut viruses was performed in (14). Specific mutations were engineered in pHH plasmids derived from the

A/California/04/2009 (CAL) strain using the QuickChange site-directed mutagenesis kit (Stratagene) as recommended by the manufacturer. These materials were developed using the licensed technology (Ref. Kawaoka-P99264US Recombinant Influenza viruses for vaccines and gene therapy). The mutations were rescued into infectious virus by standard techniques as described (15). The identity of rescued mutant viruses was ascertained by sequencing of DNAs derived from viral segments by reverse transcription-PCR amplification.

4.7 References

1. Wang D, Zhu W, Yang L, Shu Y. The Epidemiology, Virology, and Pathogenicity of Human Infections with Avian Influenza Viruses. *Cold Spring Harb Perspect Med.* 2020 Jan 21;
2. Taubenberger JK, Morens DM. 1918 Influenza: the mother of all pandemics. *Emerg Infect Dis.* 2006 Jan;12(1):15–22.
3. Taubenberger JK, Morens DM. The 1918 Influenza Pandemic and Its Legacy. *Cold Spring Harb Perspect Med.* 2020 Oct;10(10):a038695.
4. Melvin JA, Bomberger JM. Compromised Defenses: Exploitation of Epithelial Responses During Viral-Bacterial Co-Infection of the Respiratory Tract. *PLoS Pathog.* 2016 Sep;12(9):e1005797.
5. Rowe HM, Meliopoulos VA, Iverson A, Bomme P, Schultz-Cherry S, Rosch JW. Direct interactions with influenza promote bacterial adherence during respiratory infections. *Nat Microbiol.* 2019 Aug;4(8):1328–36.
6. Siegel SJ, Roche AM, Weiser JN. Influenza promotes pneumococcal growth during coinfection by providing host sialylated substrates as a nutrient source. *Cell Host Microbe.* 2014 Jul 9;16(1):55–67.
7. Talmi-Frank D, Altboum Z, Solomonov I, Udi Y, Jaitin DA, Klepfish M, et al. Extracellular Matrix Proteolysis by MT1-MMP Contributes to Influenza-Related Tissue Damage and Mortality. *Cell Host Microbe.* 2016 Oct 12;20(4):458–70.
8. Sell S. Immunopathology. *Am J Pathol.* 1978 Jan;90(1):211–80.
9. Medzhitov R, Schneider DS, Soares MP. Disease tolerance as a defense strategy. *Science.* 2012 Feb 24;335(6071):936–41.
10. Garten RJ, Davis CT, Russell CA, Shu B, Lindstrom S, Balish A, et al. Antigenic and genetic characteristics of swine-origin 2009 A(H1N1) influenza viruses circulating in humans. *Science.* 2009 Jul 10;325(5937):197–201.
11. Smith GJD, Vijaykrishna D, Bahl J, Lycett SJ, Worobey M, Pybus OG, et al. Origins and evolutionary genomics of the 2009 swine-origin H1N1 influenza A epidemic. *Nature.* 2009 Jun 25;459(7250):1122–5.
12. Neumann G, Noda T, Kawaoka Y. Emergence and pandemic potential of swine-origin H1N1 influenza virus. *Nature.* 2009 Jun 18;459(7249):931–9.
13. Rodriguez A, Falcon A, Cuevas MT, Pozo F, Guerra S, García-Barreno B, et al. Characterization in vitro and in vivo of a pandemic H1N1 influenza virus from a fatal case. *PLoS One.* 2013;8(1):e53515.
14. Nieto A, Vasilijevic J, Santos NB, Zamarreño N, López P, Amorim MJ, et al. Mutation S110L of H1N1 Influenza Virus Hemagglutinin: A Potent Determinant of Attenuation in the Mouse Model. *Front Immunol.* 2019;10:132.
15. Hoffmann E, Neumann G, Kawaoka Y, Hobom G, Webster RG. A DNA transfection system for generation of influenza A virus from eight plasmids. *Proc Natl Acad Sci U S A.* 2000 May 23;97(11):6108–13.
16. Vasilijevic J, Zamarreño N, Oliveros JC, Rodriguez-Frandsen A, Gómez G, Rodriguez G, et al. Reduced accumulation of defective viral genomes contributes to

severe outcome in influenza virus infected patients. *PLoS Pathog.* 2017 Oct;13(10):e1006650.

17. Joseph U, Su YCF, Vijaykrishna D, Smith GJD. The ecology and adaptive evolution of influenza A interspecies transmission. *Influenza Other Respir Viruses.* 2017 Jan;11(1):74–84.

18. Gamblin SJ, Vachieri SG, Xiong X, Zhang J, Martin SR, Skehel JJ. Hemagglutinin Structure and Activities. *Cold Spring Harb Perspect Med.* 2020 Jun 8;

19. Krammer F. The human antibody response to influenza A virus infection and vaccination. *Nat Rev Immunol.* 2019 Jun;19(6):383–97.

20. Topham DJ, DeDiego ML, Nogales A, Sangster MY, Sant A. Immunity to Influenza Infection in Humans. *Cold Spring Harb Perspect Med.* 2019 Dec 30;

21. Klenk HD, Rott R, Orlich M, Blödorn J. Activation of influenza A viruses by trypsin treatment. *Virology.* 1975 Dec;68(2):426–39.

22. Böttcher E, Matrosovich T, Beyerle M, Klenk H-D, Garten W, Matrosovich M. Proteolytic activation of influenza viruses by serine proteases TMPRSS2 and HAT from human airway epithelium. *J Virol.* 2006 Oct;80(19):9896–8.

23. Yoshimura A, Ohnishi S. Uncoating of influenza virus in endosomes. *J Virol.* 1984 Aug;51(2):497–504.

24. Bullough PA, Hughson FM, Skehel JJ, Wiley DC. Structure of influenza haemagglutinin at the pH of membrane fusion. *Nature.* 1994 Sep 1;371(6492):37–43.

25. Chen J, Skehel JJ, Wiley DC. A polar octapeptide fused to the N-terminal fusion peptide solubilizes the influenza virus HA2 subunit ectodomain. *Biochemistry.* 1998 Sep 29;37(39):13643–9.

26. Huang RT, Rott R, Klenk HD. Influenza viruses cause hemolysis and fusion of cells. *Virology.* 1981 Apr 15;110(1):243–7.

27. Maeda T, Ohnishi S. Activation of influenza virus by acidic media causes hemolysis and fusion of erythrocytes. *FEBS Lett.* 1980 Dec 29;122(2):283–7.

28. Guillot L, Nathan N, Tabary O, Thouvenin G, Le Rouzic P, Corvol H, et al. Alveolar epithelial cells: master regulators of lung homeostasis. *Int J Biochem Cell Biol.* 2013 Nov;45(11):2568–73.

29. Iwasaki A, Pillai PS. Innate immunity to influenza virus infection. *Nat Rev Immunol.* 2014 May;14(5):315–28.

30. Brandes M, Klauschen F, Kuchen S, Germain RN. A systems analysis identifies a feedforward inflammatory circuit leading to lethal influenza infection. *Cell.* 2013 Jul 3;154(1):197–212.

31. Schneider C, Nobs SP, Heer AK, Kurrer M, Klinke G, van Rooijen N, et al. Alveolar macrophages are essential for protection from respiratory failure and associated morbidity following influenza virus infection. *PLoS Pathog.* 2014 Apr;10(4):e1004053.

32. Nogales A, DeDiego ML, Topham DJ, Martínez-Sobrido L. Rearrangement of Influenza Virus Spliced Segments for the Development of Live-Attenuated Vaccines. *J Virol.* 2016 Jul 15;90(14):6291–302.

33. Goto H, Kawaoka Y. A novel mechanism for the acquisition of virulence by a

- human influenza A virus. *Proc Natl Acad Sci U S A*. 1998 Aug 18;95(17):10224–8.
34. Hutchinson EC, Yamauchi Y. Understanding Influenza. *Methods Mol Biol Clifton NJ*. 2018;1836:1–21.
 35. York IA, Stevens J, Alymova IV. Influenza virus N-linked glycosylation and innate immunity. *Biosci Rep*. 2019 Jan 31;39(1).
 36. Harrison SC. Viral membrane fusion. *Virology*. 2015 May;479–480:498–507.
 37. Huotari J, Helenius A. Endosome maturation. *EMBO J*. 2011 Aug 31;30(17):3481–500.
 38. Krammer F, Smith GJD, Fouchier RAM, Peiris M, Kedzierska K, Doherty PC, et al. Influenza. *Nat Rev Dis Primer*. 2018 Jun 28;4(1):3.
 39. Zanin M, Baviskar P, Webster R, Webby R. The Interaction between Respiratory Pathogens and Mucus. *Cell Host Microbe*. 2016 Feb 10;19(2):159–68.
 40. Lai SK, Wang Y-Y, Wirtz D, Hanes J. Micro- and macrorheology of mucus. *Adv Drug Deliv Rev*. 2009 Feb 27;61(2):86–100.
 41. Cohen M, Zhang X-Q, Senaati HP, Chen H-W, Varki NM, Schooley RT, et al. Influenza A penetrates host mucus by cleaving sialic acids with neuraminidase. *Virology*. 2013 Nov 22;463(1):321.
 42. Vahey MD, Fletcher DA. Influenza A virus surface proteins are organized to help penetrate host mucus. *eLife*. 2019 May 14;8.
 43. Matrosovich MN, Matrosovich TY, Gray T, Roberts NA, Klenk H-D. Neuraminidase is important for the initiation of influenza virus infection in human airway epithelium. *J Virol*. 2004 Nov;78(22):12665–7.
 44. Hillaire MLB, Haagsman HP, Osterhaus ADME, Rimmelzwaan GF, van Eijk M. Pulmonary surfactant protein D in first-line innate defence against influenza A virus infections. *J Innate Immun*. 2013;5(3):197–208.
 45. Reading PC, Tate MD, Pickett DL, Brooks AG. Glycosylation as a target for recognition of influenza viruses by the innate immune system. *Adv Exp Med Biol*. 2007;598:279–92.
 46. Hartshorn KL. Role of surfactant protein A and D (SP-A and SP-D) in human antiviral host defense. *Front Biosci Sch Ed*. 2010 Jan 1;2:527–46.
 47. Tate MD, Brooks AG, Reading PC. Inhibition of lectin-mediated innate host defences in vivo modulates disease severity during influenza virus infection. *Immunol Cell Biol*. 2011 Mar;89(3):482–91.
 48. Sarma JV, Ward PA. The complement system. *Cell Tissue Res*. 2011 Jan;343(1):227–35.
 49. Gadjeva M. The complement system. Overview. *Methods Mol Biol Clifton NJ*. 2014;1100:1–9.
 50. Mazanec MB, Coudret CL, Fletcher DR. Intracellular neutralization of influenza virus by immunoglobulin A anti-hemagglutinin monoclonal antibodies. *J Virol*. 1995 Feb;69(2):1339–43.
 51. Chen X, Liu S, Goraya MU, Maarouf M, Huang S, Chen J-L. Host Immune Response to Influenza A Virus Infection. *Front Immunol*. 2018;9:320.

52. Wille M, Holmes EC. The Ecology and Evolution of Influenza Viruses. *Cold Spring Harb Perspect Med*. 2020 Jul 1;10(7).
53. Hartmann BM, Albrecht RA, Zaslavsky E, Nudelman G, Pincas H, Marjanovic N, et al. Pandemic H1N1 influenza A viruses suppress immunogenic RIPK3-driven dendritic cell death. *Nat Commun*. 2017 Dec 5;8(1):1931.
54. Meischel T, Villalon-Letelier F, Saunders PM, Reading PC, Londrigan SL. Influenza A virus interactions with macrophages: Lessons from epithelial cells. *Cell Microbiol*. 2020 May;22(5):e13170.
55. Short KR, Kroeze EJBV, Fouchier RAM, Kuiken T. Pathogenesis of influenza-induced acute respiratory distress syndrome. *Lancet Infect Dis*. 2014 Jan;14(1):57–69.
56. Frabutt DA, Wang B, Riaz S, Schwartz RC, Zheng Y-H. Innate Sensing of Influenza A Virus Hemagglutinin Glycoproteins by the Host Endoplasmic Reticulum (ER) Stress Pathway Triggers a Potent Antiviral Response via ER-Associated Protein Degradation. *J Virol*. 2018 Jan 1;92(1).
57. Heindel DW, Koppolu S, Zhang Y, Kasper B, Meche L, Vaiana CA, et al. Glycomic analysis of host response reveals high mannose as a key mediator of influenza severity. *Proc Natl Acad Sci U S A*. 2020 Oct 27;117(43):26926–35.
58. Jorba N, Coloma R, Ortín J. Genetic trans-complementation establishes a new model for influenza virus RNA transcription and replication. *PLoS Pathog*. 2009 May;5(5):e1000462.

4.8 Acknowledgements

This chapter is part of a publication (14), and we therefore acknowledge all the other authors. In addition, we are indebted to Pedro Faísca at the Histopathology Unit of the IGC for his helpful contribution to the histopathology analysis. We are grateful to Jose Antonio Melero, John Skehel, Juan Ortín, and Pablo Gastaminza for their suggestions to the experimental work. We acknowledge Marta Alenquer and Silvia Vale Costa for their help in sample collection. We acknowledge Dr. Vera Martins (IGC, Portugal) for her help in flow cytometry data acquisition and for providing reagents. We are grateful to the Animal House Facility, Flow Cytometry Facility and Histopathology Unit at the IGC for technical support, sample processing and data collection. We thank Marta Monteiro (IGC, Portugal), Rafael Paiva (IGC, Portugal) and the members of CBV lab for helpful discussion.

4.9 Supplementary material

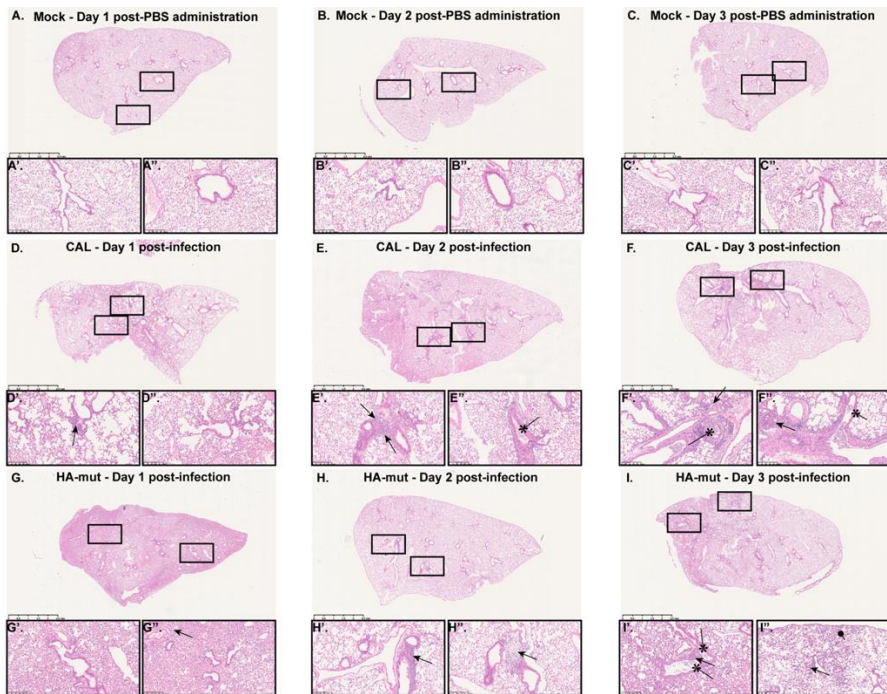


Fig. 4.S1 – Immunological damage in lungs of CAL and HA mut-infected mice (14).

Five BALB/c female mice/condition were infected with 1000 PFU of A/California/04/09 WT (CAL) or HA S110L (HA mut). At 1, 2, and 3 days post-infection (d.p.i.) lungs were collected. **A-I:** representative lung histological analyses, after hematoxylin and eosin (H&E) staining. Lungs at 1.25x amplification at 2 d.p.i., where higher differences were detected. Inlets are areas 10x amplified where specific damage (or its absence) is observed Perivascular/peribronchial infiltrates; →* Bronchial exudates). Histological scoring is presented in Fig. 4.4.

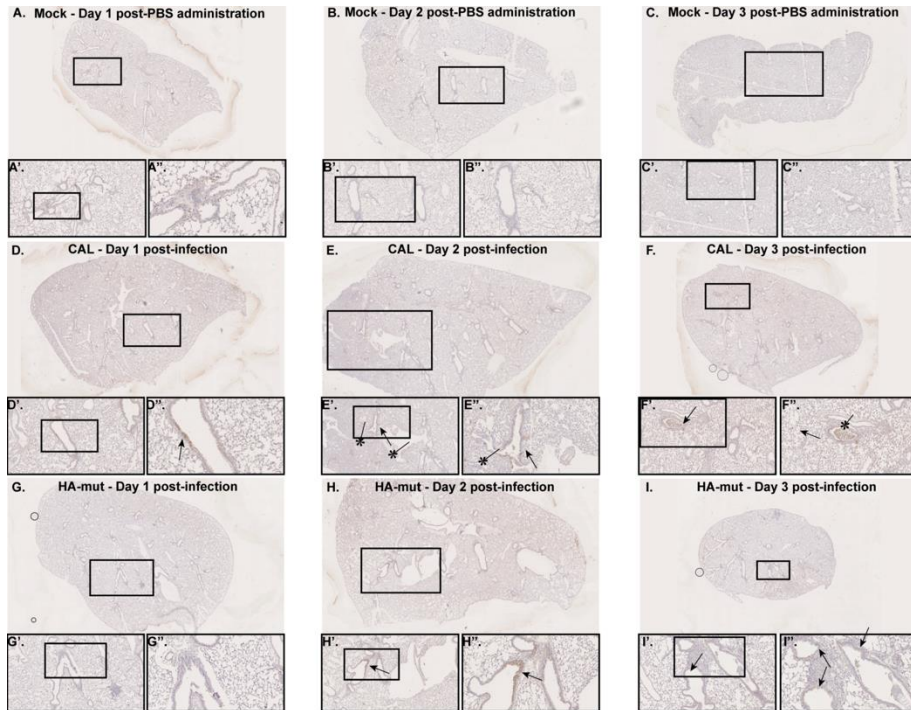


Fig. 4.S2 – NP expression in lungs of CAL and HA mut-infected mice (14).

Five BALB/c female mice/condition were infected with 1000 PFU of A/California/04/09 WT (CAL) or HA S110L (HA mut). At 1, 2, and 3 days post-infection (d.p.i.) lungs were collected and processed for NP staining. **A-I:** representative lung immunohistochemical analysis. Lungs at 1.25x amplification at 2 d.p.i.. Inlets are areas 5–20x amplified where staining (or its absence) is observed. (→ Perivascular/peribronchial infected areas; →* parenchyma areas infected). NP scoring is presented in Fig. 4.5.

Chapter 5 – General discussion

5.1 General discussion

The current pandemic outbreak of coronavirus disease 2019 (COVID-19) forced us to experience first-hand the health care problems associated with uncontrolled viral infections. In addition, the heterogenous disease spectra provoked by severe acute respiratory syndrome coronavirus 2 (SARS-CoV-2) infection highlighted the relevance of better understanding the mechanisms associated with host susceptibility. The host reacts to a viral infection by mounting an immune response aiming at clearing the invading virus from the organism. The immune system is, however, a two-edged sword as it may clear the infection but also inflict damage to the organism during the process (1). Two different options have for long been recognized as modulators of viral infection and organism homeostasis restoration: one is to recognize the virus and clear it rapidly (disease resistance) and the other is to equip the organism with features that make it more resilient to infection, without clearing the virus quickly (disease tolerance) (2,3). Therefore, the balance between viral clearance and viral-induced pathology results from an intricate interplay between host and viral factors.

Throughout this work, we explored different perspectives of this interaction (Fig. 5.1): in chapters 2 and 3, we uncovered a host virulence factor and its mechanism to modulate virally-induced immunopathology, without interfering with viral load and penetrance. In chapter 4, we assessed how simple mutations in a virus can lead to improved recognition and elimination by the immune system, looking at a point mutation in a viral factor, HA S110L, and its role in viral attenuation. Overall, this work will contribute to the understanding of the processes governing viral pathogenesis, and hint on strategies to modulate them.

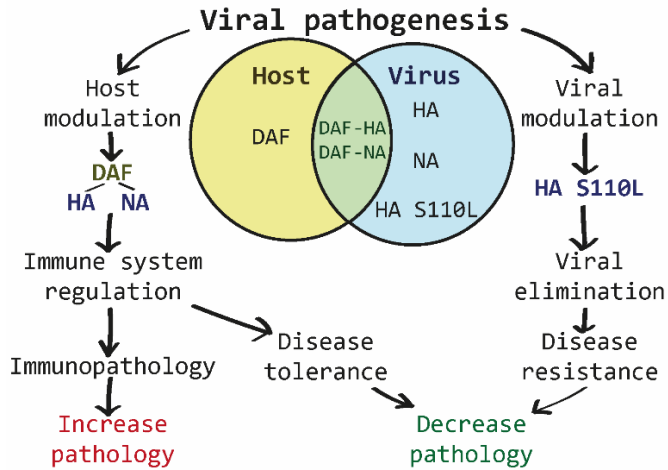


Fig. 5.1 – Summary of the contribution of host and viral factors to pathogenesis.

Our results demonstrated that DAF is a new host virulence factor and identified two viral factors, HA and NA, that are implicated in DAF-mediated virulence. The host immune system comprises complex networks of interactions, feedback mechanisms and redundancies (3–6), therefore, it is challenging to isolate the individual contribution of each player. Interestingly, DAF promoted immunopathology through increased complement activation, associated with excessive immune cell recruitment. In the future, a thorough characterization of the recruited cell types, as well as their activation states, will help to improve the comprehension of the detrimental effect of DAF upon IAV infection.

Based on our evidence, we can speculate that DAF and HA interaction could be impacting adaptive immune cell recruitment, however this requires experimental confirmation by assessing the levels of HA-specific T cells recruited in WT or *Daf*^{-/-} mice. It would not be surprising if HA, one of the major antigenic viral proteins, impacted the recognition by the adaptive immune system in a passive way. This is illustrated by the mutation HA S110L, with a predicted minimal impact in protein structure, being more prone to neutralization by monoclonal and

polyclonal antibodies against the circulating WT strain (7). Nevertheless, it would be unexpected that the HA impact on the adaptive immune system depended on DAF. This suggests that DAF could somehow contribute to expose HA to incoming immune cells. Alternatively, HA-DAF interaction could actively modulate immune cell recruitment through a more complex mechanism. In any case, both hypotheses could be associated to DAF binding affinity to CD97 in leukocytes (8,9). Additionally, HA binding of DAF sialic acid would be an attractive hypothesis in this model, as it attaches to sialic acid residues on host proteins. Interestingly, different viral strains have distinct preference for the sialic acid linkage. For instance, avian influenza viruses primarily bind to α 2,3-linked sialic acid, whereas human influenza viruses preferentially bind to α 2,6-linked sialic acid (10–12). Therefore, we hypothesized that HA could bind to DAF sialic acid moieties in a strain-specific manner, conditioning disease outcome. However, we could not detect a direct interaction between DAF and HA, despite several attempts of co-immunoprecipitation (data not shown). We can speculate that DAF-HA interaction is weak/transient and/or that it requires a third party. Alternatively, it is possible that HA-DAF binding follows the same principles of the NK cell receptors NKp44 and NKp46, which have been reported to be bound by IAV HA, and released by NA desialylation (13). As we performed DAF pulldown after 12 hours of infection, it is possible that we could not detect DAF-HA binding because DAF is already completely desialylated at this timepoint. Therefore, further experiments with individual transfection and/or different timepoints of infection should be conducted in order to test this hypothesis.

As HA is involved in cell entry, we would expect that, if DAF directly interacted with HA, DAF's absence should impact viral loads. Nevertheless, we did not observe differences in viral replication or clearance in DAF depleted mice compared to WT, as well as in viral replication *in vitro*. In this context, DAF is a definitive virulence factor, as

its absence does not affect the virus, but its presence is detrimental to the host. Importantly, viruses are prone to exploit host factors and induce alterations in their function. This is well illustrated by the numerous pathways the host evolved to detect viral infection and activate antiviral responses, and the abundant means viruses developed to counteract all of them (14). Hypothetically, one could think that interactions that are detrimental for the host and unnecessary for the virus, as it appears to be the case of IAV and DAF, would tend to be eliminated. Within this framework, it is counterintuitive that IAV-DAF interaction would be shared by many viral strains, suggesting its preservation, despite seemingly detrimental for the host and negligible for the virus. However, we analyzed infection within an individual for a limited period of time, so we cannot exclude that the virus could be benefiting outside of this context, for example in transmission capability. Still, this would not be straightforward, as viral loads were not affected. An alternative explanation could be that this feature resulted from a stronger selection in other hosts (e.g. avian) where the virus is better adapted. This hypothesis is supported by the fact that birds are the major reservoir for IAV (11,15–18). Thus, it would be interesting to evaluate the role of DAF upon IAV infection in other species.

Our data also highlighted a novel interaction between DAF and NA that modulates innate immune cell recruitment. Particularly, DAF-NA interplay promoted the excessive recruitment of neutrophils, which are known drivers of immunopathology upon IAV infection (19–23), but also other infections such as respiratory syncytial virus (RSV) and SARS-CoV-2 (24–28). Furthermore, we provided evidence supporting a mechanism of enhanced complement activation via NA-mediated cleavage of DAF sialic acid. The direct link between DAF desialylation and increased complement activation we propose is based on modest *in vitro* evidence, and requires further experimental validation. But this is a plausible explanation, supported by the extensive data on how

changes in sialic acid content affect several arms of immunity, such as complement regulation, antibody modulation, lectin recognition and innate immune cell activation (29–35). Taken together, these data reveal a novel way of IAV to control the host immune response.

Remarkably, we observed that *Daf^{-/-}* mice protection was stronger with a lethal dose of PR8-HK4 (250 PFU) than with a sublethal one (100 PFU). As expected, a higher viral dose inflicts further bodyweight loss in WT mice (Fig. S1-A). Surprisingly, the extent of bodyweight loss upon DAF depletion was similar between 100 and 250 PFU (Fig. 5.S1-B). This result suggests a role for DAF in sensing the viral infection, and contributing to mount the initial immune response in a dose-dependent manner. In agreement with *in vitro* results, PR8-HK4 would extensively cleave DAF, promoting augmented complement activation and innate immune cell recruitment. An initial higher viral load would inflict a faster DAF cleavage, and therefore a stronger immune response, resulting in increased immunopathology and poorer prognosis, as observed in WT mice. Conversely, in *Daf^{-/-}* mice there cannot be DAF cleavage. Therefore, the immune response would be similar upon high or low viral doses, and the disease outcome would be identical, as we observed in *Daf^{-/-}* mice. This should be confirmed by analyzing the immune response in *Daf^{-/-}* mice infected with increasing doses of PR8-HK4, as it would contribute to further comprehend DAF virulence mechanism.

DAF cleavage by NA was observed in different human and murine cell lines, which indicates it may be a widespread feature of IAV infection. At the moment, there are effective antivirals to treat IAV infection, but their usage has to be restricted to serious disease outcomes, to avoid emergence of resistant viruses (15,36,37). It has always been an attractive hypothesis to develop antiviral therapies focusing on host factors as they are less likely to induce viral resistance. However, this is not straightforward, as compounds targeting the host may be toxic, as is the case of chloroquine or leptomycin B (38–40).

Ideally, therapies should specifically aim at the infected cells. IAV alters the surface glycosylation of infected cells, as demonstrated by NA-mediated DAF cleavage, hence an interesting option would be to define and develop drugs specifically targeting the newly exposed glycans. Despite the quite distinct mechanisms, a similar approach has been proposed for malaria, as antibodies targeting Gal α 1-3Gal β 1-4GlcNAc-R (α -Gal), in mice depleted from this glycan, protected from *Plasmodium* infection (41). Due to scarcity of efficient antivirals, vaccination is the best available strategy to control seasonal IAV epidemics, nevertheless current vaccines efficacy is still far from ideal (42,43). To elicit a stronger response, NA-mediated DAF cleavage and modulation of complement activation and immune cell recruitment could be an alternative target to be explored upon vaccine design.

Within the tested viruses, PR8 was the most virulent in mice, as well as the one that cleaved DAF to a further extent. Remarkably, we did not observe any protection from PR8 infection in DAF-depleted mice. It is possible that the complete removal of DAF sialic acid would render DAF inert; however, at this moment we cannot discard that PR8 intrinsic virulence could overpower DAF effect. A thorough characterization of PR8 infection in *Daf*^{-/-} mice would be required to shed some light into these hypotheses: if PR8 action on DAF hinders its function, *Daf*^{-/-} mice will present the same immunopathology as their WT counterparts; alternatively, if *Daf*^{-/-} mice exhibit reduced lung tissue damage, complement activation and immune cell recruitment, as we observed upon the remaining viruses' infection, it will show that PR8 increased virulence (e.g. faster replication, immune evasion or systemic effects) is overcoming DAF depletion effect.

As mentioned above, receptor preference is one of the best described inter-species barriers, and implies that adaptation from an avian to a human host requires adaption of HA and NA (11,17,18,44). Thus, monitoring avian circulating viruses for the acquisition of ability to

cleave α 2,6-linked sialic acid is essential to anticipate emerging zoonosis. Potentially, DAF cleavage could be explored as a new tool to determine viral adaptation to human hosts. Furthermore, the type of DAF glycosylation is common to other proteins, such as mucins (45–48), which suggests that NA-mediated cleavage of sialic acids may be necessary to modulate infection in a broader sense than we explored here.

Besides exploring the host part of the infection, we also assessed the contribution of a viral factor to pathology. HA is involved in cell entry and is the major viral antigenic protein, consequently it is crucial to successfully establish an infection (10,42). In order to avoid the immune system, HA tends to accumulate mutations, which could have implications in viral fitness, and therefore in virulence. We analyzed the effect of the point mutation HA S110L in a circulating strain isolated from a fatal infection upon 2009 pandemic (49). Surprisingly, HA S110L conferred a strong attenuation, despite no obvious differences in protein structure nor infection ability *in vitro*. Nevertheless this mutation markedly impaired viral replication and penetration in murine airways (7). Conversely to what we observed in the first two chapters, these results elucidated a new mutation that promotes viral elimination by the host. Nevertheless, in both cases, the outcome is decreased pathology.

Viral pathogenesis results from an interplay of viral and host factors. The COVID-19 pandemic reinforced the need to study host-pathogen interaction pathways and how could we modulate them to prevent severe disease. The most immediate idea to confer protection is to clear the pathogen, promoting disease resistance (2,3). However, immunopathology is a consequence of an excessive immune response, and a major cause of complications upon infection (1,2,50). In fact, most available and prospective antiviral drugs target the virus, making them more effective early in the infection, as in humans IAV replication peaks around 2 days post-infection. (15,36,51–53). An interesting therapeutic

alternative would be to target host pathways that limit immunopathology, and therefore promote disease tolerance (2,3,54). Targeting host factors upon viral infection is not novel, as it has been explored in infections with human immunodeficiency virus (HIV), hepatitis B virus (HBV) or hepatitis C virus (HCV) (55–57). Host-directed therapies for IAV have also been proposed, such as the antagonists of TLR4 and CXCR2, eritoran and danirixin, respectively, aiming to decrease excessive inflammation (57–59). This type of approach would provide significant benefits, such as decreased proneness to develop resistance, broad-spectrum activity against respiratory viral infections and increased efficiency later in infection. This is particularly relevant in infections such as SARS-CoV-2, which are characterized by a longer period between infection and symptom onset (53). Nevertheless, immunosuppressive strategies must be carefully designed, as opportunistic bacteria may establish severe secondary infections, which were a major cause of death upon the Spanish flu pandemic (50,60–62). As an example, complement inhibition therapy in patients suffering from its excessive intrinsic activation, using the clinically approved α -C5 monoclonal antibody eculizumab, was associated with increased risk of bacterial infections (63). Currently, more than twenty drug candidates ranging different steps of the complement cascade are at clinical development stage (64–66), which could be assessed in the future for their ability to prevent immunopathology without compromising host defense upon infection.

It is imperative to understand in detail which pathways may lead to disease tolerance or immunopathology. In summary, our results reveal DAF as a novel virulence factor and suggest it operates via complement, which is, in turn, the major driver of immunopathology. Complement-dependent cytotoxicity is not the major cause of tissue damage but, instead, the excessive recruitment of neutrophils and monocytes via C3a, and likely C5a. Remarkably, we observed that viral

NA directly cleaved DAF sialic acid moieties, increasing complement activation *in vitro*, which provides a possible link to immunopathology (Fig 5.2).

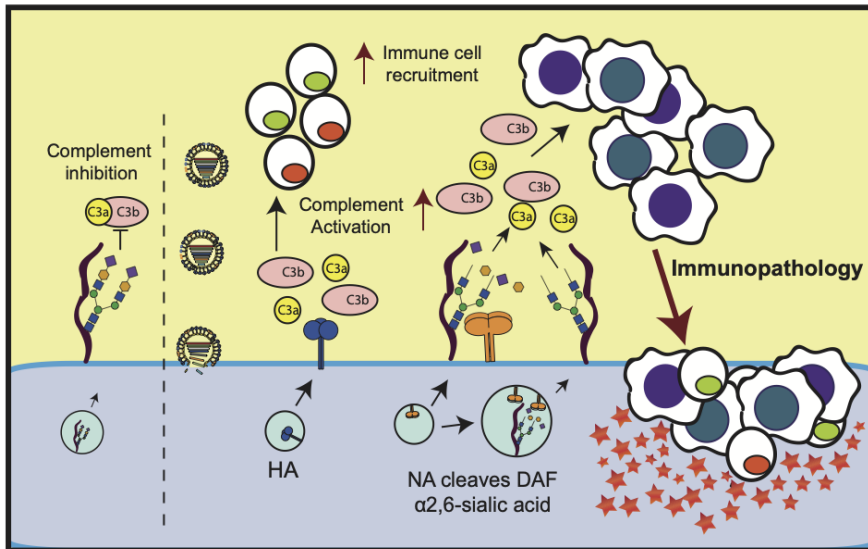


Fig. 5.2 – Proposed model for DAF-mediated immunopathology.

At steady state, DAF accelerates the decay of C3 convertases, inhibiting the formation of C3a and C3b and subsequent complement activation. Upon IAV infection, the cell will produce viral proteins, and in particular NA. NA is a potent sialidase that will remove the sialic acid content of DAF both in the cytoplasm and at the surface. This processing of DAF by NA leads to DAF loss/alteration of function and hence overactivation of the complement pathway that will recruit innate immune cells. The excess of innate immune response leads to tissue damage and ultimately immunopathology, worsening disease outcome.

5.2 Future perspectives

Overall, this work contributed to the understanding of viral pathogenesis. Ultimately, only a solid comprehension of the processes governing it will support the prospective development of new strategies to modulate viral-induced pathology. Hence, future work should aim at exploring these mechanisms in-depth.

The host immune response is intricate, and therefore it would be valuable to pinpoint which immune cell populations are responsible for IAV-associated immunopathology. At the moment, the major candidate cells are neutrophils, for their timing in the immune response and previous reports of provoking immunopathology upon viral infection. Thus, in order to address this, neutrophils should be depleted in WT mice, to levels that resemble their *Daf*^{-/-} counterparts, and assess if they acquire protection from IAV infection. Moreover, a complementary and unbiased approach would be to compare the transcriptomic/proteomic profiles of different cell populations upon DAF depletion.

Complement system provides a potent and expeditious response, which may lead to immunopathology when excessive. Assessment of the levels of complement activation in the course of infection would offer insight on its detailed impact at different stages, and how it could be connected to immunopathology.

Type I IFN delivers the first reaction to infection, and deviations from an equilibrated response have been associated with severe viral infections. Our evidence did not hint any role of IFN signaling early in infection of *Daf*^{-/-} mice, as we did not observe disparities in viral loads. Nevertheless, IFN levels should be measured to test a hypothetical participation of IFN in immunopathology via DAF.

Our results indicated that DAF interacts with HA and NA, with distinct implications. Particularly, DAF-HA interaction suggested an impact in adaptive immunity. To confirm this, it would be then essential

to define the mechanistic interaction between DAF and HA, and to test the recruited T cells for their specificity to target HA. Whilst the DAF-NA interaction was better defined, it would be also important to analyze NAs from different viral strains, and relate their contribution to infection *in vivo* with their ability to cleave DAF and activate complement *in vitro*. Furthermore, it would be interesting to assess if DAF-HA and/or DAF-NA interactions could somehow impact immune cell attachment and recruitment, independently of complement.

DAF shares the typical mucin glycosylation, in which sialic acid residues are attached to O-glycans. Analysis of specific mucins present in the airways would reveal if NA-mediated sialic acid cleavage could be extended to other proteins. As the mucus barrier is essential to protect from IAV, it would be noteworthy to assess if a hypothetical mucin desialylation could induce local immunosuppression. Moreover, it is key to evaluate the overall impact of NA in glycosylation. This could be achieved by labeling of sialic acid and subsequent analysis of its linked proteomic content. Comparing this in steady-state and infection would hint proteins that lose sialic acid upon infection due to NA effect. Remarkably, other viruses, such as paramyxovirus, possess sialidases, and therefore the exploitation of host sialic acid removal could unveil a new layer of understanding to host-pathogen interactions.

5.3 References

1. Sell S. Immunopathology. *Am J Pathol.* 1978 Jan;90(1):211–80.
2. Medzhitov R, Schneider DS, Soares MP. Disease tolerance as a defense strategy. *Science.* 2012 Feb 24;335(6071):936–41.
3. Iwasaki A, Pillai PS. Innate immunity to influenza virus infection. *Nat Rev Immunol.* 2014 May;14(5):315–28.
4. Chen X, Liu S, Goraya MU, Maarouf M, Huang S, Chen J-L. Host Immune Response to Influenza A Virus Infection. *Front Immunol.* 2018;9:320.
5. Iwasaki A, Medzhitov R. Control of adaptive immunity by the innate immune system. *Nat Immunol.* 2015 Apr;16(4):343–53.
6. Hartl D, Tirouvanziam R, Laval J, Greene CM, Habel D, Sharma L, et al. Innate Immunity of the Lung: From Basic Mechanisms to Translational Medicine. *J Innate Immun.* 2018;10(5–6):487–501.
7. Nieto A, Vasilijevic J, Santos NB, Zamarreño N, López P, Amorim MJ, et al. Mutation S110L of H1N1 Influenza Virus Hemagglutinin: A Potent Determinant of Attenuation in the Mouse Model. *Front Immunol.* 2019;10:132.
8. Hamann J, Vogel B, van Schijndel GM, van Lier RA. The seven-span transmembrane receptor CD97 has a cellular ligand (CD55, DAF). *J Exp Med.* 1996 Sep 1;184(3):1185–9.
9. Dho SH, Lim JC, Kim LK. Beyond the Role of CD55 as a Complement Component. *Immune Netw.* 2018 Feb;18(1):e11.
10. Gamblin SJ, Vachieri SG, Xiong X, Zhang J, Martin SR, Skehel JJ. Hemagglutinin Structure and Activities. *Cold Spring Harb Perspect Med.* 2020 Jun 8;
11. Wille M, Holmes EC. The Ecology and Evolution of Influenza Viruses. *Cold Spring Harb Perspect Med.* 2020 Jul 1;10(7).
12. Wang D, Zhu W, Yang L, Shu Y. The Epidemiology, Virology, and Pathogenicity of Human Infections with Avian Influenza Viruses. *Cold Spring Harb Perspect Med.* 2020 Jan 21;
13. Bar-On Y, Seidel E, Tsukerman P, Mandelboim M, Mandelboim O. Influenza virus uses its neuraminidase protein to evade the recognition of two activating NK cell receptors. *J Infect Dis.* 2014 Aug 1;210(3):410–8.
14. Muñoz-Moreno R, Martínez-Romero C, García-Sastre A. Induction and Evasion of Type-I Interferon Responses during Influenza A Virus Infection. *Cold Spring Harb Perspect Med.* 2020 Jul 6;
15. Krammer F, Smith GJD, Fouchier RAM, Peiris M, Kedzierska K, Doherty PC, et al. Influenza. *Nat Rev Dis Primer.* 2018 Jun 28;4(1):3.
16. Webster RG, Bean WJ, Gorman OT, Chambers TM, Kawaoka Y. Evolution and ecology of influenza A viruses. *Microbiol Rev.* 1992 Mar;56(1):152–79.
17. Joseph U, Su YCF, Vijaykrishna D, Smith GJD. The ecology and adaptive evolution of influenza A interspecies transmission. *Influenza Other Respir Viruses.* 2017 Jan;11(1):74–84.

18. Yoon S-W, Webby RJ, Webster RG. Evolution and ecology of influenza A viruses. *Curr Top Microbiol Immunol*. 2014;385:359–75.
19. Oda T, Akaike T, Hamamoto T, Suzuki F, Hirano T, Maeda H. Oxygen radicals in influenza-induced pathogenesis and treatment with pyran polymer-conjugated SOD. *Science*. 1989 May 26;244(4907):974–6.
20. Narasaraju T, Yang E, Samy RP, Ng HH, Poh WP, Liew A-A, et al. Excessive neutrophils and neutrophil extracellular traps contribute to acute lung injury of influenza pneumonitis. *Am J Pathol*. 2011 Jul;179(1):199–210.
21. Sakai S, Kawamata H, Mantani N, Kogure T, Shimada Y, Terasawa K, et al. Therapeutic effect of anti-macrophage inflammatory protein 2 antibody on influenza virus-induced pneumonia in mice. *J Virol*. 2000 Mar;74(5):2472–6.
22. Zhu B, Zhang R, Li C, Jiang L, Xiang M, Ye Z, et al. BCL6 modulates tissue neutrophil survival and exacerbates pulmonary inflammation following influenza virus infection. *Proc Natl Acad Sci U S A*. 2019 Jun 11;116(24):11888–93.
23. Perrone LA, Plowden JK, García-Sastre A, Katz JM, Tumpey TM. H5N1 and 1918 pandemic influenza virus infection results in early and excessive infiltration of macrophages and neutrophils in the lungs of mice. *PLoS Pathog*. 2008 Aug 1;4(8):e1000115.
24. Wu Z, McGoogan JM. Characteristics of and Important Lessons From the Coronavirus Disease 2019 (COVID-19) Outbreak in China: Summary of a Report of 72 314 Cases From the Chinese Center for Disease Control and Prevention. *JAMA*. 2020 Apr 7;323(13):1239–42.
25. Barnes BJ, Adrover JM, Baxter-Stoltzfus A, Borczuk A, Cools-Lartigue J, Crawford JM, et al. Targeting potential drivers of COVID-19: Neutrophil extracellular traps. *J Exp Med*. 2020 Jun 1;217(6).
26. Java A, Apicelli AJ, Liszewski MK, Coler-Reilly A, Atkinson JP, Kim AH, et al. The complement system in COVID-19: friend and foe? *JCI Insight*. 2020 Aug 6;5(15).
27. Zuo Y, Yalavarthi S, Shi H, Gockman K, Zuo M, Madison JA, et al. Neutrophil extracellular traps in COVID-19. *JCI Insight*. 2020 Jun 4;5(11).
28. Habibi MS, Thwaites RS, Chang M, Jozwik A, Paras A, Kirsebom F, et al. Neutrophilic inflammation in the respiratory mucosa predisposes to RSV infection. *Science*. 2020 Oct 9;370(6513).
29. Varki A, Gagneux P. Multifarious roles of sialic acids in immunity. *Ann NY Acad Sci*. 2012 Apr;1253:16–36.
30. Schauer R, Srinivasan GV, Coddeville B, Zanetta J-P, Guérardel Y. Low incidence of N-glycolylneuraminic acid in birds and reptiles and its absence in the platypus. *Carbohydr Res*. 2009 Aug 17;344(12):1494–500.
31. Varki A. Sialic acids in human health and disease. *Trends Mol Med*. 2008 Aug;14(8):351–60.
32. Formiga RO, Amaral FC, Souza CF, Mendes DAGB, Wanderley CWS, Lorenzini CB, et al. Neuraminidase inhibitors rewire neutrophil function in murine sepsis and COVID-19 patient cells. *BioRxiv Prepr Serv Biol*. 2020 Nov 12;
33. Abeln M, Albers I, Peters-Bernard U, Flächsig-Schulz K, Kats E, Kispert A, et al. Sialic acid is a critical fetal defense against maternal complement attack. *J Clin Invest*. 2019 Jan 2;129(1):422–36.

34. Khan N, de Manuel M, Peyregne S, Do R, Prufer K, Marques-Bonet T, et al. Multiple Genomic Events Altering Hominin SIGLEC Biology and Innate Immunity Predated the Common Ancestor of Humans and Archaic Hominins. *Genome Biol Evol*. 2020 Jul 1;12(7):1040–50.
35. Pagan JD, Kitaoka M, Anthony RM. Engineered Sialylation of Pathogenic Antibodies In Vivo Attenuates Autoimmune Disease. *Cell*. 2018 Jan 25;172(3):564-577.e13.
36. Hurt AC, Chotpitayasunondh T, Cox NJ, Daniels R, Fry AM, Gubareva LV, et al. Antiviral resistance during the 2009 influenza A H1N1 pandemic: public health, laboratory, and clinical perspectives. *Lancet Infect Dis*. 2012 Mar;12(3):240–8.
37. Whitley RJ, Boucher CA, Lina B, Nguyen-Van-Tam JS, Osterhaus A, Schutten M, et al. Global assessment of resistance to neuraminidase inhibitors, 2008–2011: the Influenza Resistance Information Study (IRIS). *Clin Infect Dis Off Publ Infect Dis Soc Am*. 2013 May;56(9):1197–205.
38. Akpovwa H. Chloroquine could be used for the treatment of filoviral infections and other viral infections that emerge or emerged from viruses requiring an acidic pH for infectivity. *Cell Biochem Funct*. 2016 Jun;34(4):191–6.
39. Newlands ES, Rustin GJ, Brampton MH. Phase I trial of elactocin. *Br J Cancer*. 1996 Aug;74(4):648–9.
40. Watanabe K, Takizawa N, Katoh M, Hoshida K, Kobayashi N, Nagata K. Inhibition of nuclear export of ribonucleoprotein complexes of influenza virus by leptomycin B. *Virus Res*. 2001 Sep;77(1):31–42.
41. Yilmaz B, Portugal S, Tran TM, Gozzelino R, Ramos S, Gomes J, et al. Gut microbiota elicits a protective immune response against malaria transmission. *Cell*. 2014 Dec 4;159(6):1277–89.
42. Krammer F. The human antibody response to influenza A virus infection and vaccination. *Nat Rev Immunol*. 2019 Jun;19(6):383–97.
43. WHO. Influenza (Seasonal) [Internet]. [cited 2021 Feb 9]. Available from: [https://www.who.int/en/news-room/fact-sheets/detail/influenza-\(seasonal\)](https://www.who.int/en/news-room/fact-sheets/detail/influenza-(seasonal))
44. Thompson AJ, Paulson JC. Adaptation of Influenza Viruses to Human Airway Receptors. *J Biol Chem*. 2020 Nov 3;
45. Zanin M, Baviskar P, Webster R, Webby R. The Interaction between Respiratory Pathogens and Mucus. *Cell Host Microbe*. 2016 Feb 10;19(2):159–68.
46. Cohen M, Zhang X-Q, Senaati HP, Chen H-W, Varki NM, Schooley RT, et al. Influenza A penetrates host mucus by cleaving sialic acids with neuraminidase. *Virology*. 2013 Nov 22;10:321.
47. Button B, Cai L-H, Ehre C, Kesimer M, Hill DB, Sheehan JK, et al. A periciliary brush promotes the lung health by separating the mucus layer from airway epithelia. *Science*. 2012 Aug 24;337(6097):937–41.
48. Lai SK, Wang Y-Y, Wirtz D, Hanes J. Micro- and macrorheology of mucus. *Adv Drug Deliv Rev*. 2009 Feb 27;61(2):86–100.
49. Rodriguez A, Falcon A, Cuevas MT, Pozo F, Guerra S, García-Barreno B, et al. Characterization in vitro and in vivo of a pandemic H1N1 influenza virus from a fatal case. *PLoS One*. 2013;8(1):e53515.

50. Kash JC, Taubenberger JK. The role of viral, host, and secondary bacterial factors in influenza pathogenesis. *Am J Pathol.* 2015 Jun;185(6):1528–36.
51. Baker J, Block SL, Matharu B, Burleigh Macutkiewicz L, Wildum S, Dimonaco S, et al. Baloxavir Marboxil Single-dose Treatment in Influenza-infected Children: A Randomized, Double-blind, Active Controlled Phase 3 Safety and Efficacy Trial (miniSTONE-2). *Pediatr Infect Dis J.* 2020 Aug;39(8):700–5.
52. Finberg RW, Lanno R, Anderson D, Fleischhackl R, van Duijnhoven W, Kauffman RS, et al. Phase 2b Study of Pimodivir (JNJ-63623872) as Monotherapy or in Combination With Oseltamivir for Treatment of Acute Uncomplicated Seasonal Influenza A: TOPAZ Trial. *J Infect Dis.* 2019 Mar 15;219(7):1026–34.
53. He X, Lau EHY, Wu P, Deng X, Wang J, Hao X, et al. Temporal dynamics in viral shedding and transmissibility of COVID-19. *Nat Med.* 2020 May;26(5):672–5.
54. Velho TR, Santos I, Póvoa P, Moita LF. Sepsis: the need for tolerance not complacency. *Swiss Med Wkly.* 2016;146:w14276.
55. Weydert C, De Rijck J, Christ F, Debyser Z. Targeting Virus-host Interactions of HIV Replication. *Curr Top Med Chem.* 2016;16(10):1167–90.
56. Puhl AC, Garzino Demo A, Makarov VA, Ekins S. New targets for HIV drug discovery. *Drug Discov Today.* 2019 May;24(5):1139–47.
57. Kaufmann SHE, Dorhoi A, Hotchkiss RS, Bartenschlager R. Host-directed therapies for bacterial and viral infections. *Nat Rev Drug Discov.* 2018 Jan;17(1):35–56.
58. Madan A, Chen S, Yates P, Washburn ML, Roberts G, Peat AJ, et al. Efficacy and Safety of Danirixin (GSK1325756) Co-administered With Standard-of-Care Antiviral (Oseltamivir): A Phase 2b, Global, Randomized Study of Adults Hospitalized With Influenza. *Open Forum Infect Dis.* 2019 Apr;6(4):ofz163.
59. Shirey KA, Lai W, Scott AJ, Lipsky M, Mistry P, Pletneva LM, et al. The TLR4 antagonist Eritoran protects mice from lethal influenza infection. *Nature.* 2013 May 23;497(7450):498–502.
60. Taubenberger JK, Morens DM. The pathology of influenza virus infections. *Annu Rev Pathol.* 2008;3:499–522.
61. Taubenberger JK, Morens DM. 1918 Influenza: the mother of all pandemics. *Emerg Infect Dis.* 2006 Jan;12(1):15–22.
62. Morens DM, Taubenberger JK, Fauci AS. Predominant role of bacterial pneumonia as a cause of death in pandemic influenza: implications for pandemic influenza preparedness. *J Infect Dis.* 2008 Oct 1;198(7):962–70.
63. Socié G, Caby-Tosi M-P, Marantz JL, Cole A, Bedrosian CL, Gasteyger C, et al. Eculizumab in paroxysmal nocturnal haemoglobinuria and atypical haemolytic uraemic syndrome: 10-year pharmacovigilance analysis. *Br J Haematol.* 2019 Apr;185(2):297–310.
64. Ricklin D, Mastellos DC, Reis ES, Lambris JD. The renaissance of complement therapeutics. *Nat Rev Nephrol.* 2018 Jan;14(1):26–47.
65. Zelek WM, Xie L, Morgan BP, Harris CL. Compendium of current complement therapeutics. *Mol Immunol.* 2019 Oct;114:341–52.
66. Risitano AM, Marotta S, Ricci P, Marano L, Frieri C, Cacace F, et al. Anti-complement Treatment for Paroxysmal Nocturnal Hemoglobinuria: Time for Proximal

Complement Inhibition? A Position Paper From the SAAWP of the EBMT. *Front Immunol.* 2019 Jun 14;10:1157.

5.4 Supplementary material

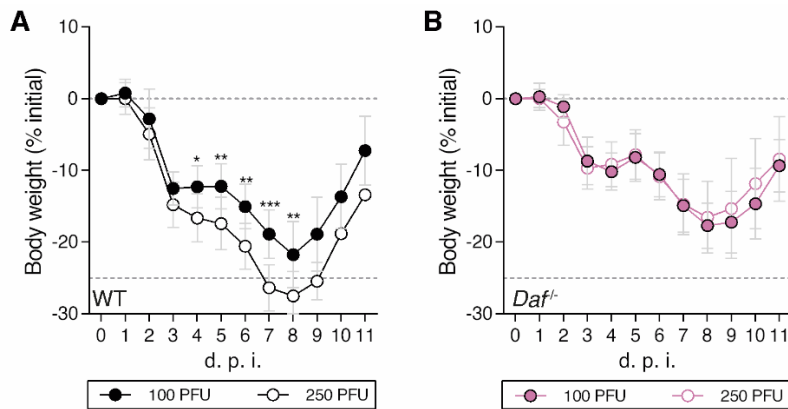


Fig. 5.S1 – Complement decay-accelerating factor is required for dose-dependent pathology.

A, B: Bodyweight loss of C57BL/6J WT (**A**) or *Daf*^{-/-} (**B**) mice infected with the indicated doses of A/Puerto Rico/8/1934 with segment 4 from A/Hong Kong/1/68 (PR8-HK4). (**A**: 100 PFU n = 14, 250 PFU n = 8; **B**: 100 PFU n = 10, 250 PFU n = 8). Results are expressed as mean±sd. Statistical significance analyzed with two-way ANOVA followed by Holm-Sidak multiple comparisons test.

ITQB-UNL | Av. da República, 2780-157 Oeiras, Portugal
Tel (+351) 214 469 100 | Fax (+351) 214 411 277

www.itqb.unl.pt